AFFDL-TR-67-6

SELF-REGULATED OXYGEN CONCENTRATOR

G. L. Mrava

R. A. Wynveen

FOREWORD

This report was prepared by the TRW Equipment Laboratories, TRW Inc., 23555 Euclid Avenue, Cleveland, Ohio 44117 under USAF Contract No. AF 33(615)-3392. This contract was initiated under Project No. 6146, "Atmosphere and Thermal Control," Task 614614, "Supply of Atmospheric Gases."

The program was administered under the direction of the Air Force Flight Dynamics Laboratory, Research and Technology Division, Mr. David A. Geiger, FDFE Task Engineer.

This report covers research completed between January 1966 and January 1967, inclusive.

Dr. Richard A. Wynveen, Section Manager, Mr. Gene L. Mrava, Principal Engineer, and Mr. Keith M. Montgomery, Engineer, were the principal project engineers for TRW Inc.

The authors acknowledge the assistance of the following TRW consultants: Mr. Russ Englehaupt and Mr. Steve Gittinger, Designers; Mr. Warren F. Wade and Mr. Richard G. Huebscher, Principal Engineers; and Mr. C. Nelson Hoedt, Technician; all of the TRW Equipment Laboratories.

The manuscript was submitted by the authors in February, 1967 for publication as an RTD technical report. Report number ER-7043 was assigned to the report by the contractor, prior to Government approval.

The distribution of this report or its abstract is limited because it covers an area of technology that is embargoed under the Department of State International Traffic in Arms Regulations and U. S. Export Control Act of 1949.

This technical report has been reviewed and is approved.

W. C. Savage
Chief, Environmental Control Branch
Vehicle Equipment Division

ABSTRACT

A program to design, fabricate and test a model of an oxygen concentrator employing a method of control termed "self regulation" was successfully conducted. The stack assembly consists of three cells, wherein oxygen is electrochemically separated from the air, sandwiched between two humidifier chambers. Self-regulation of the unit results from the thermal equilibrium that exists between the heat generated in the electrochemical cells during the O_2 concentrating process and the evaporative cooling in the humidifiers due to the air humidification process. This mode of operation eliminates external humidifiers and associated thermal controls previously used on apparatus of this type. As a laboratory model, the three-cell unit demonstrated oxygen delivery rates up to 0.045 lb/hr while displaying oxygen purities at a level of 100%. Wide-range parametric testing conducted on the unit covered cell operating temperatures of 100-175F, air inlet pressures from 5-90 psia, air flow rates from 2-5 times theoretical, and current densities up to 166 amps/ft^2. The program was culminated with two test runs totaling 201 hours, which successfully demonstrated the self-regulating characteristics of the unit. As a final conclusion, the data and analyses were used to specify an advanced 0.2-lb/hr oxygen concentrator utilizing self-regulation in addition to size optimization. With additional development the design will be capable of being incorporated into an aviator's oxygen supply system.

*** Export controls have been removed ***

TABLE OF CONTENTS

LIST OF ILLUSTRATIONS

LIST OF ILLUSTRATIONS (CON'T.)

LIST OF TABLES

*** Export controls have been removed ***

SECTION I

INTRODUCTION

1. BACKGROUND

The requirement to provide a reliable source of breathing oxygen for aviators flying at high altitudes has traditionally been met by placing a sufficient amount of oxygen on board each flight prior to takeoff. Provisions for the production, storage and transportation of aircraft oxygen at air bases levy a significant cost in servicing, maintenance and personnel training. Storage and maintenance of quantities of high-pressure or cryogenic oxygen on board aircraft result in logistic and safety problems.

A technique has been developed at TRW that extracts oxygen directly from atmospheric air at the time and place it is needed. This technique seems well-suited to aircraft application in that the source of oxygen could be cabin air, and the logistics and servicing associated with the pressurized gas or cryogen liquid systems would be avoided.

The concept is based upon electrochemical technology. It utilizes a design that is inherently lightweight and compact, and its operation is independent of orientational or gravitational forces. Applying electrical power to the device as air is being fed into it results in the separation of oxygen from the inert gases (nitrogen, argon, etc.) and impurities found in the air.

A program to design, fabricate, test and deliver a laboratory or experimental model of the oxygen concentrator was successfully conducted under Air Force Contract AF 33(615)-1856. The model has a 0.2-lb/hr oxygen capacity rating. It consists of 26 series-connected cells and could, for short time periods, operate at three times the normal rated capacity. It was shown to function over an air feed pressure of 6.5 - 15.5 psia. The percentage of oxygen removed from the air passing through the device ranged from 20 to 50%. The oxygen purity was shown to exceed 99.5%.

Associated with the experimental model delivered under AF 33(615)-1856 was a test rig used to characterize the model's performance over a range of operating parameters. A separate humidifier and cooling system were used to allow for independent control of the air conditioning process and to control the operating temperature of the device. Such independent regulation allowed for greater versatility in evaluating the response of the device to changes in operating parameters. It did not, however, make use of the evaporative cooling which occurs in the humidifier to remove heat generated during the oxygen concentrating process.

2. OBJECTIVE

A program was initiated under Air Force Contract AF 33(615)-3392 for the design, fabrication, and test of an electrochemical oxygen concentrating unit which employs

self-regulated internal humidification and evaporative cooling. The primary technical objective was to demonstrate that the controls and the electrical power and cooling air requirements associated with the external humidifier and air-cooled fins employed on the concentrator defined in reference 1 could be eliminated.

Secondly, size and weight were to be minimized and performance was to be improved by design changes which reduced cell voltage, increased current density, and increased the percentage of oxygen concentrated from the inlet air.

3. APPROACH

A three-cell self-regulating oxygen concentrator was designed, fabricated and tested. The unit consisted of three cells sandwiched between humidifier compartments. Electrode areas were 20 square inches each.

Testing of the device was completed to demonstrate the principle of self-regulation and to obtain additional data on variations in the concentrator's power requirements as a function of operating parameters. The self-regulating concept was demonstrated to be feasible, with performance following the pattern predicted by the design calculations.

The cell size and weight were reduced by minimizing flange dimensions, reducing bipolar plate thickness, and optimizing the end plate configuration. Additional reduction in design size and weight of a unit with a given oxygen output was effected as a result of improvement in cell performance. This was realized through (a) reduced cell voltage at a given current density, (b) increased current density at a given voltage, and/or (c) an increased percentage of oxygen concentrated from the incoming air stream.

SECTION II

SELF-REGULATING OXYGEN CONCENTRATOR

In the oxygen concentrating system delivered under AF 33(615)-1856, independent humidification and cooling system controls were provided to allow for broader experimental evaluation of operating parameters.[1] It was recognized, however, that these controls would not be required on a flight unit. It appeared that a simple and compact control system could result if the humidifier were integrated with the concentrator itself. In this way, the heat used to evaporate the water during air humidification would be provided by the heat produced in the process of generating the oxygen. By carrying this idea one step further it seemed possible, under certain conditions, to remove the entire heat load of the concentrator by the evaporative cooling produced during the air humidification process. In such cases the temperature of the concentrator would increase until the heat input was balanced by heat losses, with the majority of the cooling resulting from evaporation of water for air humidification.

1. PRINCIPLES USED IN SELF-REGULATION

The heat input to the concentrator is a function of the operating current and voltage. The heat loss, in turn, is the sum of the heat loss to the surroundings, heat loss to the gases, and evaporative cooling during humidification of the inlet air. The self-regulated concentrator design that allows for the simplest controls is based upon the concept that the concentrator temperature will rise until the heat input is just balanced by the heat losses. The operating environment expected for an aircraft oxygen system is one where the temperature of the surroundings and the temperature of the air inlet feed can vary over a wide range. The importance of basing the control concept on a technique that is effective, in spite of such changes, is significant.

2. SELF-REGULATING CONDITIONS

The equilibrium temperature attained by the self-regulating oxygen concentrator is dependent upon inlet air flow rates, operating current densities, cell voltages, and inlet air pressures. The expressions used to relate these parameters, while the concentrator is operating in the mode of self-regulation, are detailed in Appendix I.

Considering a typical single-cell potential of 1.0 volt allows the computation of predicted data for various air multiples of stoichiometric requirements, pressures, and equilibrium temperatures. The results are presented in Figure 1, the Theoretical Equilibrium Map. This map indicates the predicted temperature equilibrium that will result under self-regulation when the unit is operating at the pressure and air flow multiples specified by the coordinates. This plot serves to focus on the fact that self-regulation is a low-pressure process. While operating at an air flow of five times stoichiometric (denoted as 5T) or less, increases in pressure beyond 25 psia would be expected to result in equilibrium temperatures in excess of 200F. Should this level

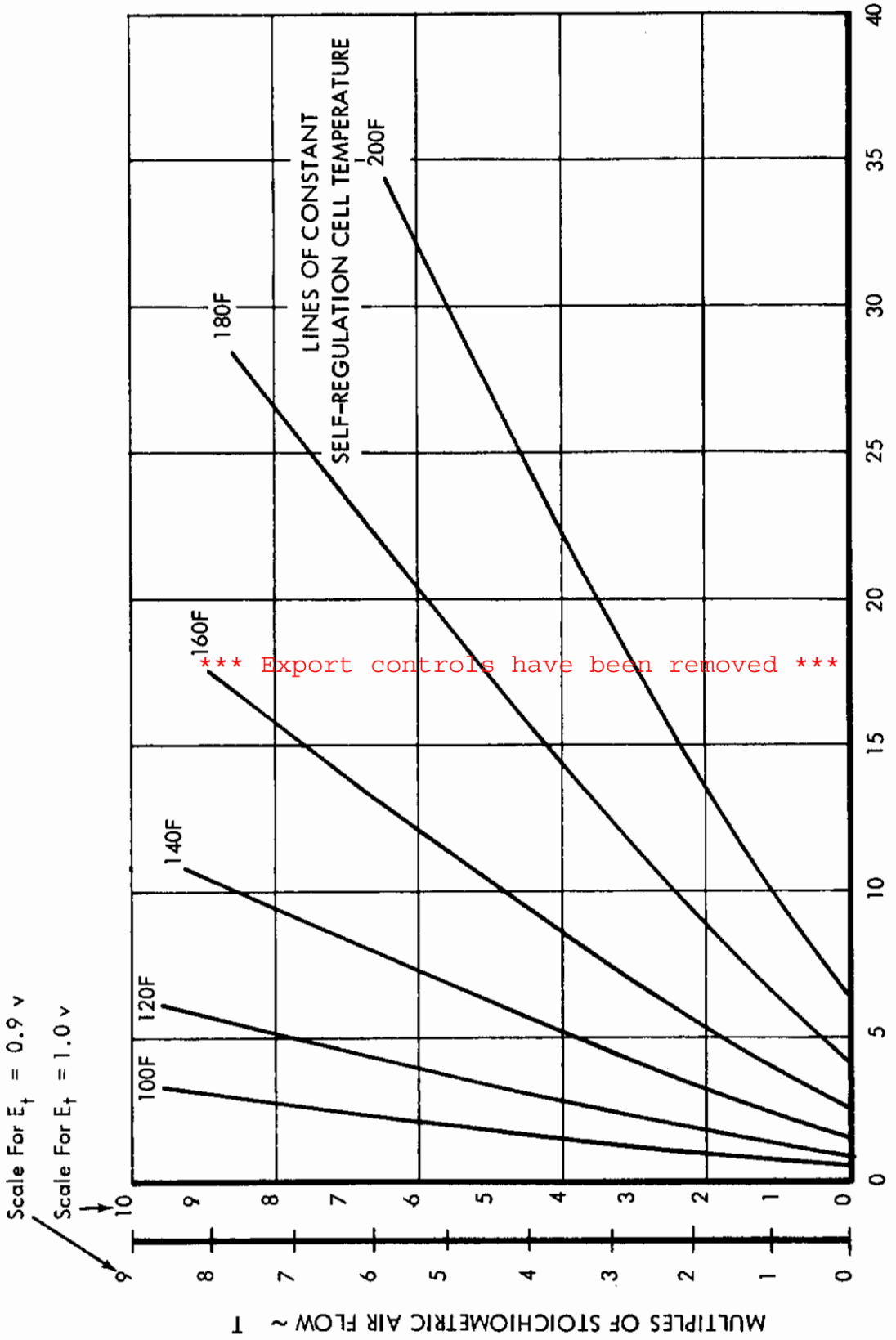

Figure 1 Theoretical Equilibrium Map

of pressure be desirable, auxiliary cooling would be needed to minimize material constraints which might be imposed by increased temperatures. Figure 1 serves as a design guide when considering the effect of parameter variations.

3. VARIATION OF PARAMETERS

The Theoretical Equilibrium Map has been plotted with scales corresponding to single cell potentials of 0.9 and 1.0 volt. If, however, parameters are varied such that a voltage different from these is needed to deliver a given oxygen flow rate, the ordinate scale is modified merely by multiplying it by the actual voltage. For example, if the cell voltage requirement to deliver a specified amount of oxygen decreases from 1.0 to 0.8 volt, the ordinate scale at 1.0 volt is multiplied by 0.8. A 5T flow now becomes 4T, thus indicating a 20% reduction in flow rate necessary to maintain an equivalent cell temperature at a specified pressure. If the flow is adjusted back to 5T, at the same pressure, one traverses up the ordinate to this point (originally 6.25T on the scale corresponding to 1.0 volt) and finds that the cell equilibrium temperature has decreased. Within the assumptions set forth in Appendix I, this map will hold true for any desired oxygen flow rate. To quantitatively evaluate the ordinate in pounds of air per hour, simply specify an oxygen requirement and solve equation (10) in Appendix I.

SECTION III

DESIGN AND FABRICATION

1. CONCENTRATOR STACK DESIGN

A self-regulating oxygen concentrator featuring internal humidification eliminates the need for elaborate system controls, an external humidifier and an externals means of cooling the cell assembly. Based on heat and moisture balance calculations, using performance data obtained with cells and humidifiers previously operated at TRW, the concentrator was designed to consist of three cells with humidifiers on each side. Numerous cell-humidifier groupings were evaluated before arriving at the 3:1 ratio; including 5:1, 4:1, and 2:1. The temperature differential existing between the center cell and the humidifier at the end with the 5:1 and 4:1 configurations would be too large to allow attaining a satisfactory moisture tolerance. In addition, the 5:1 configuration would overload the wicking rate capacity of the humidifier. With the 2:1 ratio, the number of humidifiers would increase beyond those actually necessary for humidifying the air and removing the heat load, resulting in extra weight because of the overdesigned humidifier capacity.

The experimental model for the program was designed and built to have a "half" humidifier on each side. In an actual prototype concentrator, each humidifier will handle the heat load from three cells, meaning 1-1/2 cells on each side. Since the model was designed to have only three cells, the humidifiers on the outside only had to handle the heat load from 1-1/2 cells. Figure 2 is a schematic of the model design illustrating the configuration and gas and water flow paths.

The water fed to the humidifiers was designed to be transferred to the individual wicks in much the same manner as was used with the external humidifier delivered under contract AF 33(615)-1856. This configuration allows for operation independent of gravitational fields. Automatic water control is provided by the wicking system which transports only the required make-up water to maintain a stable system under the operating conditions. Wicking principles ensure there will be no flooding problem under steady-state operation; the wicks will transport water to only those areas that become less than saturated.

The feed air passes through the humidifiers into the concentrator air compartments, and exhausts from the unit. Once outside the concentrator, the gases pass through a condenser where the water is removed. In actual application, this reclaimed water would be returned to the humidifier feed system. This method duplicates the approach that could be used to transfer the concentrator's heat load to the aircraft cooling system. The operating design parameters for the three-cell unit are presented in Table I.

The cell size and weight were optimized by minimizing flange dimensions, reducing the bipolar plate thickness 25% below that used in the model delivered under AF 33(615)-

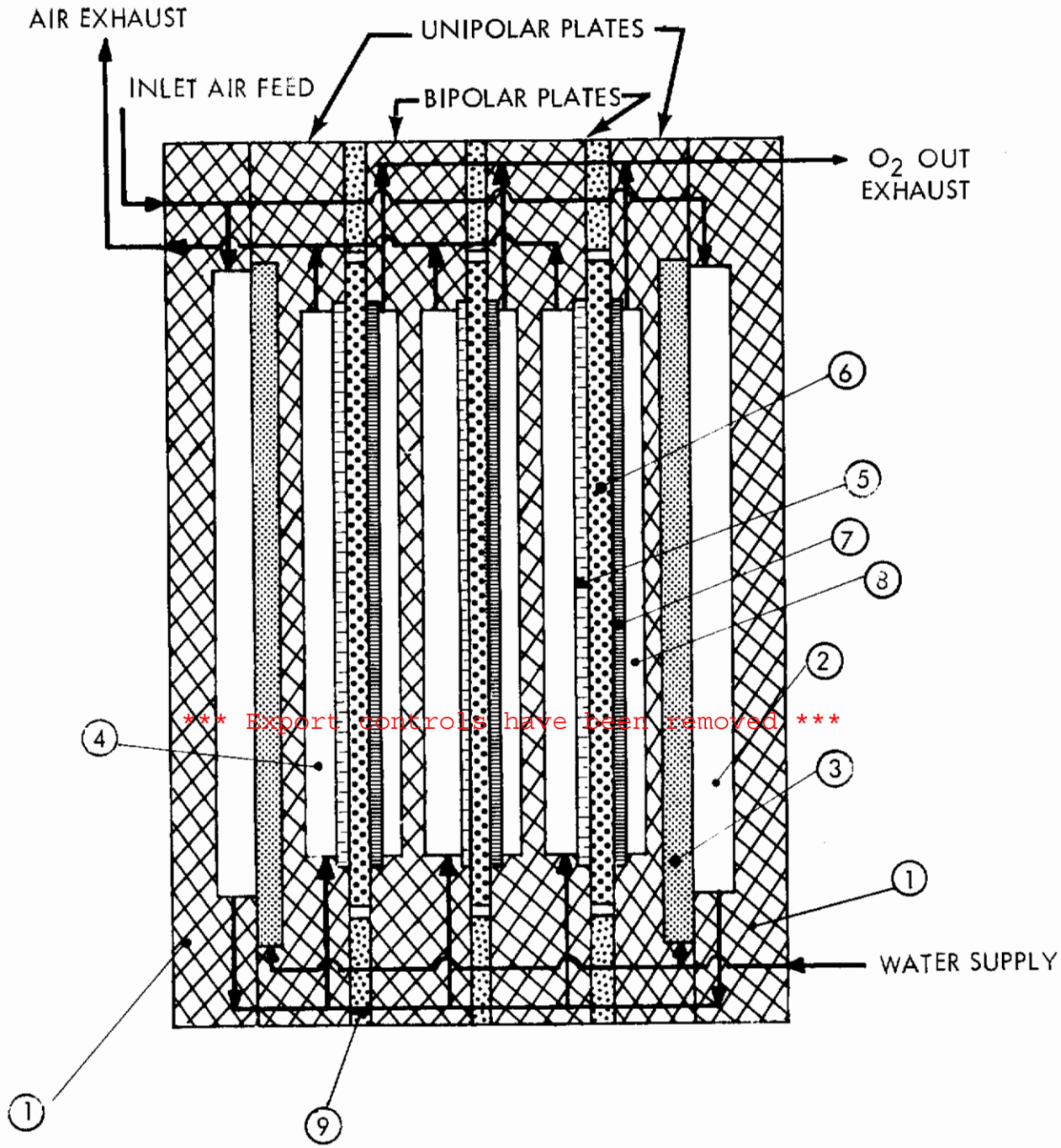

(1) WICK PLATES
(2) HUMIDIFICATION COMPARTMENT
(3) HUMIDIFIER WICK
(4) AIR COMPARTMENT
(5) CATHODE
(6) MATRIX HELD ELECTROLYTE
(7) ANODE
(8) O_2 COMPARTMENT
(9) GASKET

Figure 2 Three-Cell Self-Regulating Model

Table I Operating Design Parameters for the Three-Cell Unit

Current Density Range, ASF *	to 100		
Effective Electrode Area, ft^2	0.14 (3.5 x 5.8 in.)		
Current, amps *	to 14		
Number of Cells, Series Connected	3		
Voltage per Cell, volts	0.9 @ 40 ASF		
Concentrator Temperature, F	70 to 200		
Air Pressure, psia	2.5 to 90		
Air Feed Flow Rate **,	lb/hr	SCFM	SLPM
Theoretical, lb	0.119	0.0246	0.70
2 x Theoretical (2T)	0.238	0.0493	1.40
3 x Theoretical (3T)	0.357	0.0739	2.09
4 x Theoretical (4T)	0.476	0.0985	2.79
5 x Theoretical (5T)	0.595	0.123	3.49
Oxygen Output Flow Rate*	0.0275	0.0051	0.144

*During testing, unit was actually operated at current densities as high as 166 ASF, with the corresponding increase in current. See Section IV for discussion of these results.

**At 100 ASF in units of pound/hour, standard cubic feet/minute (SCFM) and standard liter/minute (SLPM), dry.

1856 (see page 23). Optimizing and weight-saving techniques were used in the design only to the point where performance, along with sound structural characteristics, was not sacrificed for further weight savings. Table II presents a summary of the geometrical parameters of the design. The design point was 40 ASF at 0.9 volt with 25% of the oxygen in the cathode compartment air being concentrated. This represented an improvement over the AF 33(615)-1856 design, where the nominal performance level was 35 ASF at 1.0 volt, with only 20% of the oxygen being separated.

A difficult problem in designing the self-regulating oxygen concentrator was the need for a configuration capable of demonstrating the self-regulation concept. At the same time, the concentrator design had to be sufficiently flexible to enable measuring the effect of changes in the configuration and operating parameters. The change in configuration encompassed a threefold change in matrix thickness. The anticipated variations in control operating parameters included temperatures ranging from room temperature to 200F, pressures from 2.5 to 90 psia, and current densities to beyond 100 ASF at air flow rates of 2 to 5T.

2. CONCENTRATOR CELL DESIGN

a. Air Distribution

Configurations I through V shown in Figure 3 were considered in designing the mode of air distribution to be used in the cathode compartment. Designs I and III assured uniform gas distribution across the field but, because of the number and size of the gas entrance ducts required, the pressure drop through the ducts was too high. These designs are satisfactory, however, when high pressure air is available. Design IV adds excess weight in the flange area because ports on both ends of the field necessitate wide flanges at both ends.

Design V considers the fact that air entering the field is high in oxygen concentration but is depleted in oxygen content when leaving the field. By making each successive baffle pass smaller, the Reynolds number in each compartment of the field is increased. The higher the Reynolds number, the more turbulent the gas flow, and more gas mixing is experienced in the compartment. This increased mixing tends to reduce nitrogen stagnation layer build-up on the electrode surface. However, the flow rates necessary to achieve turbulance (Reynolds numbers > 2000) within the gas compartments are in excess of 100 times the theoretical air flow. This is in contrast to the desired maximum of 5 times theoretical air flow.

b. Baffles

Concentrator assemblies in reference 1 used baffles consisting of Teflon spaghetti tubing inserted between rows of pins on the bipolar plates. Subsequent evaluation of baffle effectiveness, after the plates were in use, indicated that air leaked under the baffles thereby reducing the amount of active electrode area exposed to the air stream. To prevent this from happening, the baffles in the self-regulated concentrator consisted

Table II Geometrical Design Parameters for the Three-Cell Unit

Cell Matrices	
Material	Johns Manville Fuel Cell Asbestos
Area Dimensions, in	4.1 x 6.4
Uncompressed Thickness, mil	10, 20, 30
Electrolyte	
Weight % KOH	32
Loading, g/g dry matrix	1.0 to 2.25
Electrodes*	
Type	American Cyanamid AB-1
Area Dimensions, in	3.7 x 6.0
Effective Area Dimensions, in	3.5 x 5.8
Bipolar Plates	
Material	Magnesium ZE-10
Plating Thickness, mil	
Nickel	1.3
Gold	0.03
Area Dimensions, in	5.38 x 8.62
Pin Height, in	
Air Compartment	0.052
Oxygen Compartment	0.052
Duct Diameter, in	0.042
Total Thickness, in	0.140
Insulating Gaskets	
Material	Neoprene, Fairprene
Thickness, in	0.009 with 10 mil matrices 0.016 with 20 mil matrices 0.030 with 30 mil matrices
O-Rings	
Material	Ethylene-Propylene
Wicks	
Material	Polypropylene
Uncompressed Thickness, in	0.030
Electrolyte, wt % KOH	23

* See Table XI for details on electrodes

Table II Geometrical Design Parameters for the Three-Cell Unit (cont.)

Support Screens	
Material	Nickel
Thickness, in	0.005
Three Cell Assembly	
Weight, dry, lb	
End plates, 2, including fittings	4.57
Wick plates, 2	0.88
Unipolar plates, 2	0.66
Bipolar plates, 2	0.65
30 mil matrices w/2 electrodes each, 3 sets	0.13
Wicks and support screens, 2 sets	0.05
Fasteners, set	0.33
Gaskets, O-rings, set	0.13
Total	7.40
External Dimensions, in	2.25 x 5.38 x 8.62
Volume, in^3	104

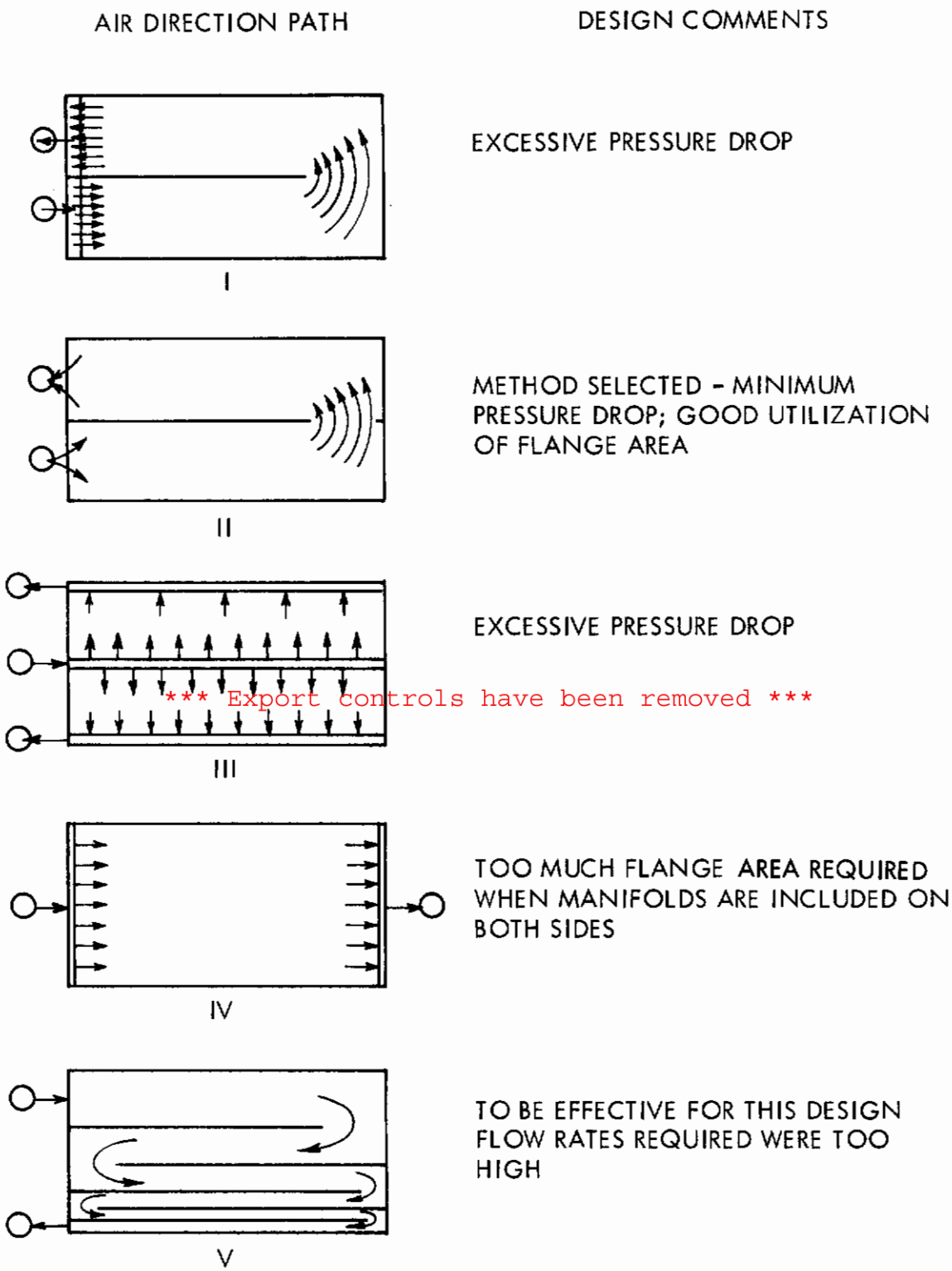

Figure 3 Air Direction Paths Across Electrode Field

of cut rubber O-rings fitted in linear grooves to provide improved sealing and better air distribution.

c. Gas Ports and Ducts

All port and duct passages were designed to resist clogging and maintain a uniform gas flow throughout the entire system. This was accomplished by specifying that the pressure drop down a duct passage be one hundred times or more than the pressure drop down the accompanying port passage.[2] It was decided that external duct cleanouts should not be included since duct clogging had not been a problem in concentrator operation. Also, it would be virtually impossible to seal the cleanout holes against internal pressures several times that of atmospheric. The ports were 3/8 inch diameter, while the ducts were 0.042 inch diameter.

d. Electrode Support

The face of each plate was in the form of a pin pattern to supply sufficient area for heat transfer, electrical current paths, and necessary electrode support while incorporating the required gas cavity. Pins 1/16 inch square located on 1/4 inch centers were used.

e. Plating

The self-regulating concentrator design was initially prepared using 120-mil bipolar plates, 42-mil gas compartment heights and ducts 32 mils in diameter. Prior to commencing fabrication of the unit, the plating subcontractor's ability to plate inside the 32-mil ducts was questioned. The plating subcontractor was reluctant to guarantee the thickness of the plate inside ducts of this size. They recommended a sample be tried first since their experience indicated the results would be marginal. A special drill was required to prepare a sample plate containing several 32-mil diameter holes which, after plating, could be cross-sectioned to determine the resulting plate thickness inside the ducts. This special drill was not immediately available. Because of the wait required for the drill and for the sample plating, it was decided that the design would proceed using 140-mil magnesium (42-mil ducts) for the bipolar plate. In addition, it was decided that when the drill was received, the sample plate containing several 32-mil ducts would still be submitted to the plater for evaluation. This sample plate would then be cross-sectioned to determine if the 32-mil diameter ducts could be used in future designs.

A 13% saving in weight results if the 120-mil model of the self-regulated concentrator is used instead of the 140-mil model. It was subsequently determined, from cross-sectioning of the test sample, that 32-mil gas ducts can be successfully plated inside. A complete description of the sample analysis is included in Appendix II. The design recommendations presented later (page 111) in Table X utilize the 120-mil plates with either 32-mil ducts or rectangular slots.

3. CONCENTRATOR FABRICATION

A basic concentrator cell consists of two porous electrodes separated by an electrolyte solution of aqueous potassium hydroxide. The electrolyte is held in an absorbent porous matrix designed to prevent the solution from leaking through the porous electrodes and to serve as a gas impermeable barrier between the air and the pure oxygen that is generated. Bipolar plates separate the individual cells in the series.

A photograph of the components used to make up an individual cell is shown in Figure 4 and illustrates the manner in which a cell is assembled. First, the insulating rubber gasket and anode electrode are placed on top of the bipolar plate. Next, the matrix is positioned. It is then handloaded with electrolyte. On this the cathode electrode is located, and then the next bipolar plate is placed on the top of this assembly. This procedure is repeated for as many cells as are required in the concentrator stack.

a. Electrodes

The three-cell assembly was fabricated with electrodes having an effective area of 20 square inches (3.5 x 5.8 inches). The actual geometrical dimensions were 3.7 x 6.0 inches which allowed for a 0.1-inch overlap at the cell edges. The final dimensions were selected to comply with the desire to retain a reasonable height for the wicks in the humidifier. The difficulty in wicking increases rapidly with height. Prior experience with humidifier designs has shown that a practical height limitation is four inches. Beyond that height, the effectiveness of the wick becomes questionable.

The electrodes consisted of a porous layer of platinum black and waterproofing agent supported by a 100-mesh nickel screen using 2-mil wire. The electrode thickness is 4-5 mils and designated as an American Cyanamid Type AB-1 electrode.

b. Electrolyte and Electrolyte Holding Matrix

The electrolyte used was a 32-weight percent aqueous solution of potassium hydroxide. The concentrator was designed so that 10, 20 and 30-mil electrolyte absorbent matrices could be used. This versatility required that the design be able to handle various gasketing thicknesses. The porous matrix used to contain the electrolyte between the cell electrodes is a high-purity form of asbestos. It provided a separation of the electrode and held the electrolyte in proper contact with the electrodes regardless of their orientation relative to gravity or acceleration. Previous experimental studies showed that decreasing the matrix thickness decreased the cell internal resistance; however, the change is not linear with change in thickness. For example, the difference in measured resistance between a 30- and 20-mil matrix is more than the resistance change measured in going from a 20- to a 10-mil matrix. Resistance, however, is only one aspect of the design which varied with change in matrix thickness. Other changes which occurred and affected cell performance included the stability to pressure differentials and the ratio of electrolyte held in the electrodes to that held in the matrix (see Section IV).

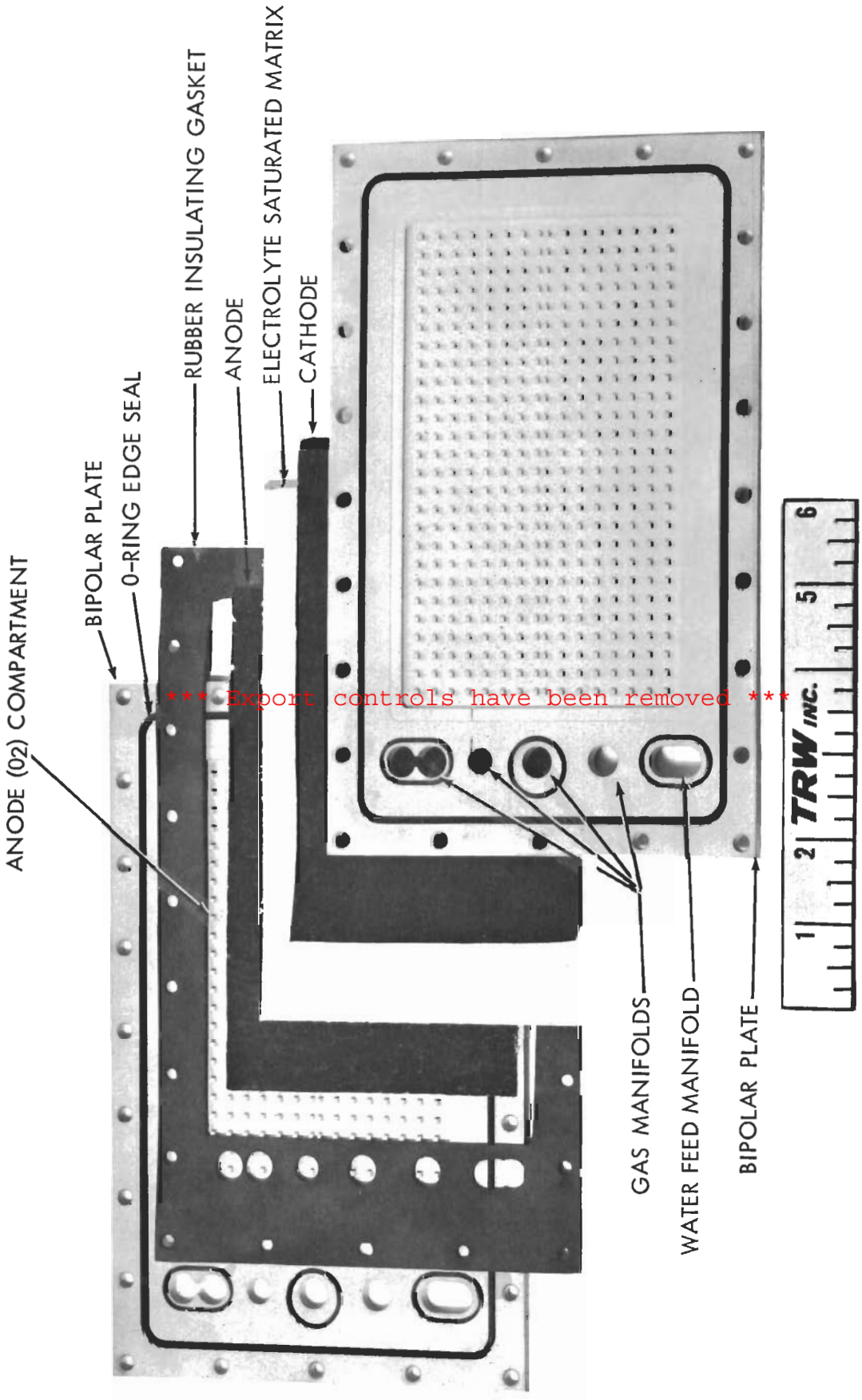

Figure 4 Concentrator Cell Components

c. Bipolar and Unipolar Plates

The material chosen for fabrication of the bipolar and unipolar plates was Dow ZE-10 magnesium. The plate thickness was 140 mils with 52-mil gas compartment heights on both the air and oxygen sides. Following machining of the plates, they were plated first with 1.3-mil nickel and then with 0.03-mil gold to prevent corrosion.[3] A 3-mil recess in the flange area on the air and oxygen sides was used to retain the cell electrodes.

Pictures of the cathode and anode sides of a bipolar plate are shown in Figures 5 and 6, respectively. The manner in which a section of an O-ring was made to serve as a gas baffle in the cathode is shown in Figure 5. A baffle is not required in the anode, or oxygen, side. Both photographs show the O-rings in place. The O-rings prevent gas leakage in the individual manifolding compartments, as well as exterior leakage from the electrode field to the outside of the cell. The gas ports and ducts are also indicated.

The term "unipolar plate" is used to describe those plates of the three-cell stack that have a humidification compartment on one side. The other side of the plate is either the anode or cathode gas compartment for a single cell of the three-cell assembly. Figure 7 is a photograph of the unipolar plates showing the sides that face the electrochemical cell electrodes. The plate on the left shows the oxygen, or anode, compartment. The plate on the right shows the air, or cathode, compartment. The backs of these plates fit against the wick contained in the wick plates shown in Figure 9 described below.

d. Seals and Insulation

Ethylene-propylene O-rings were used to seal the concentrator from external leaks under the anticipated operating pressures of 2.5 and 90 psia. Materially similar O-rings were used to seal the ports in the bi- and unipolar plates. A rubber gasket framed the matrix, thereby serving to control the matrix compression. The gasketing was made from either Neoprene or Fairprene, a Buna N-nylon combination. The Fairprene, although not as resistant to the electrolyte as Neoprene, was selected to be used in the assembly when testing the 10-mil matrix, since Neoprene of the required thickness was not available to fit the program scheduling.

e. Humidification and Self-Regulation

A continuous water feed mechanism using wicking principles was built into the self-regulated design. As shown in Figure 2, a humidification section is located at each end of the three-cell unit. The air entering the cell is manifolded in a manner that divides the air, with half flowing through each humidifier compartment. Previously completed experimental work demonstrated that the water transport mechanism using the wicking process does work. Each wicking compartment was 72 mils thick. This was to allow future experimental versatility in that a range of wicking materials and thicknesses can be tested.

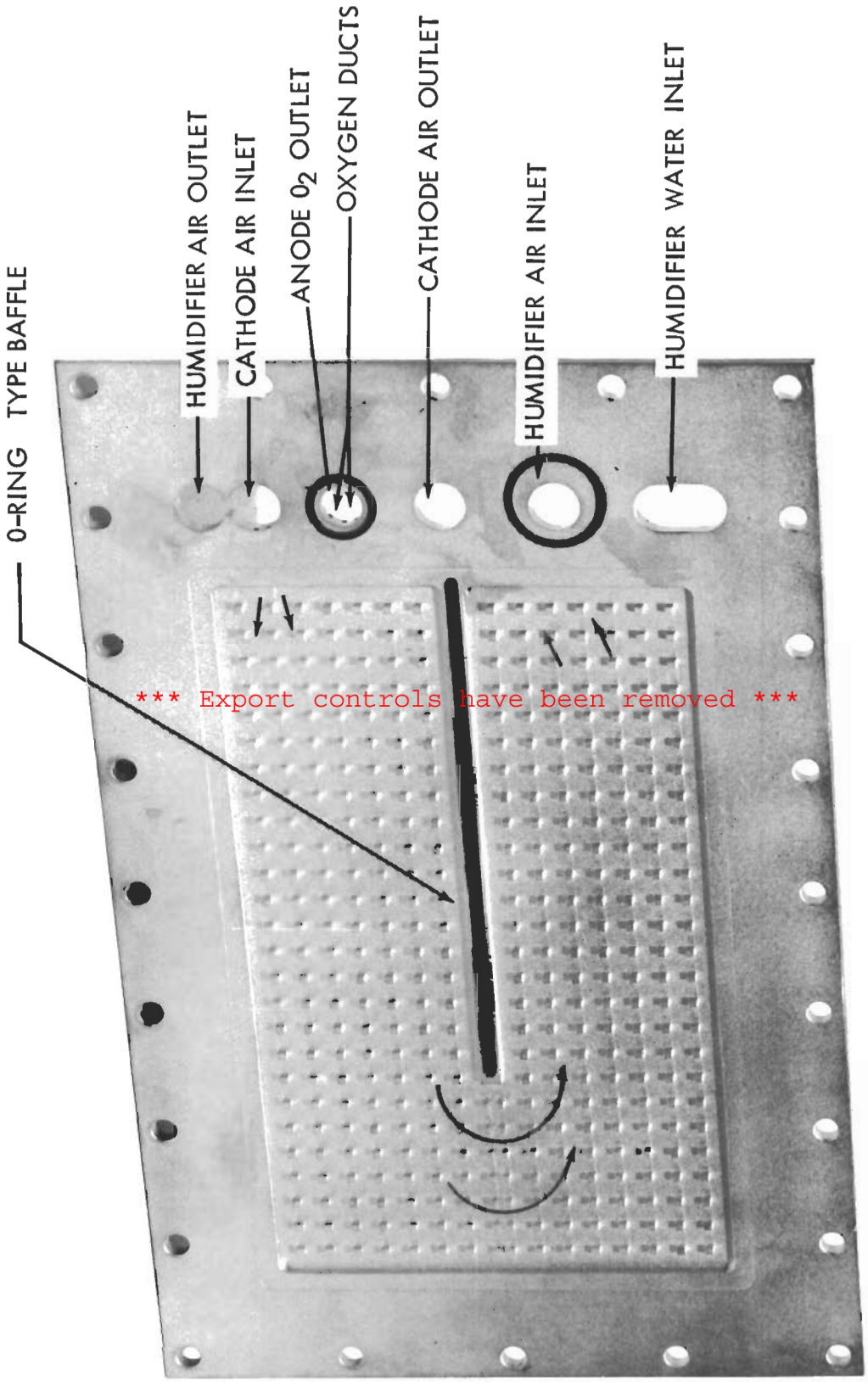

Figure 5 Concentrator Bipolar Plate (Cathode Side)

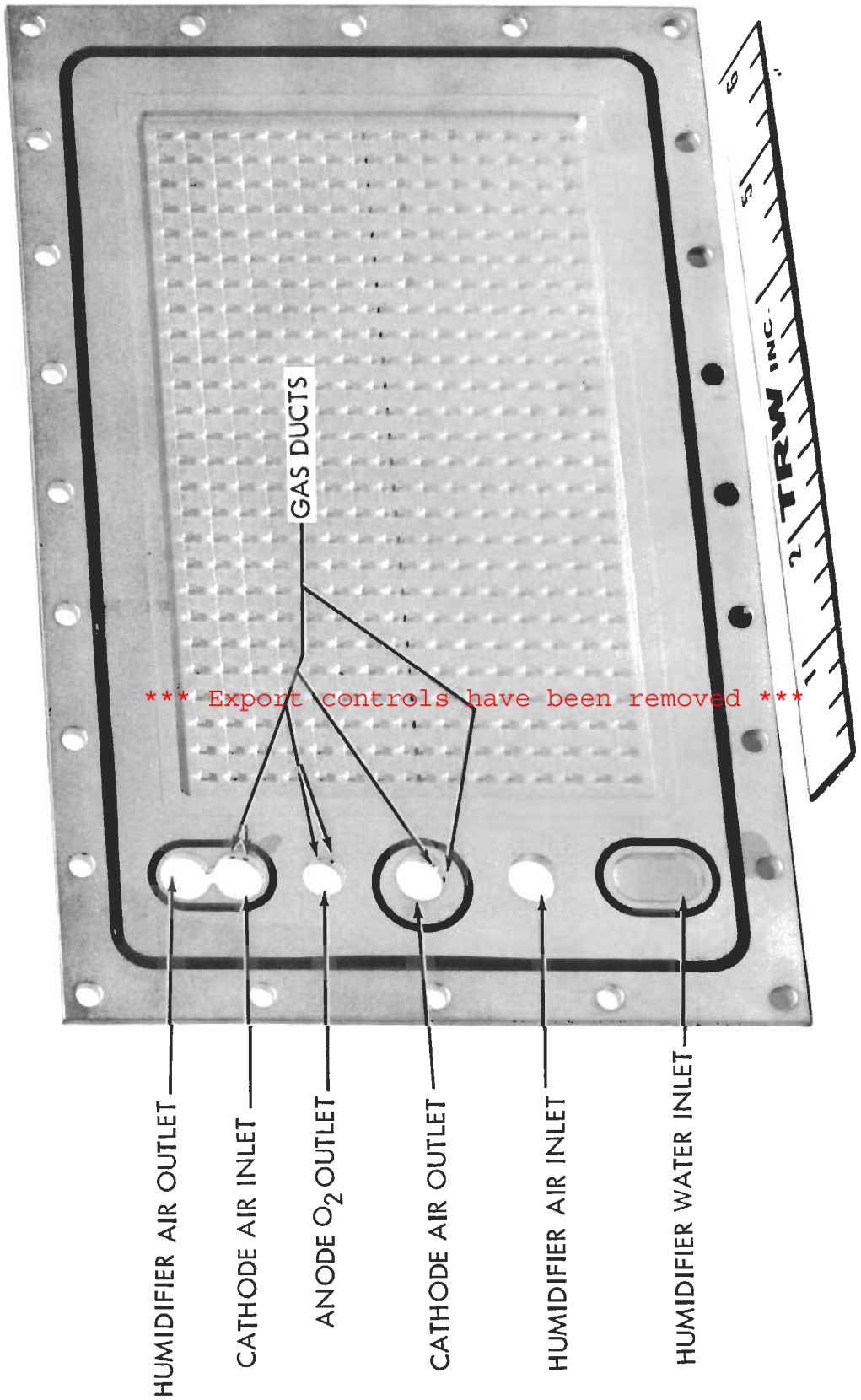

Figure 6 Concentrator Bipolar Plate (Anode Side)

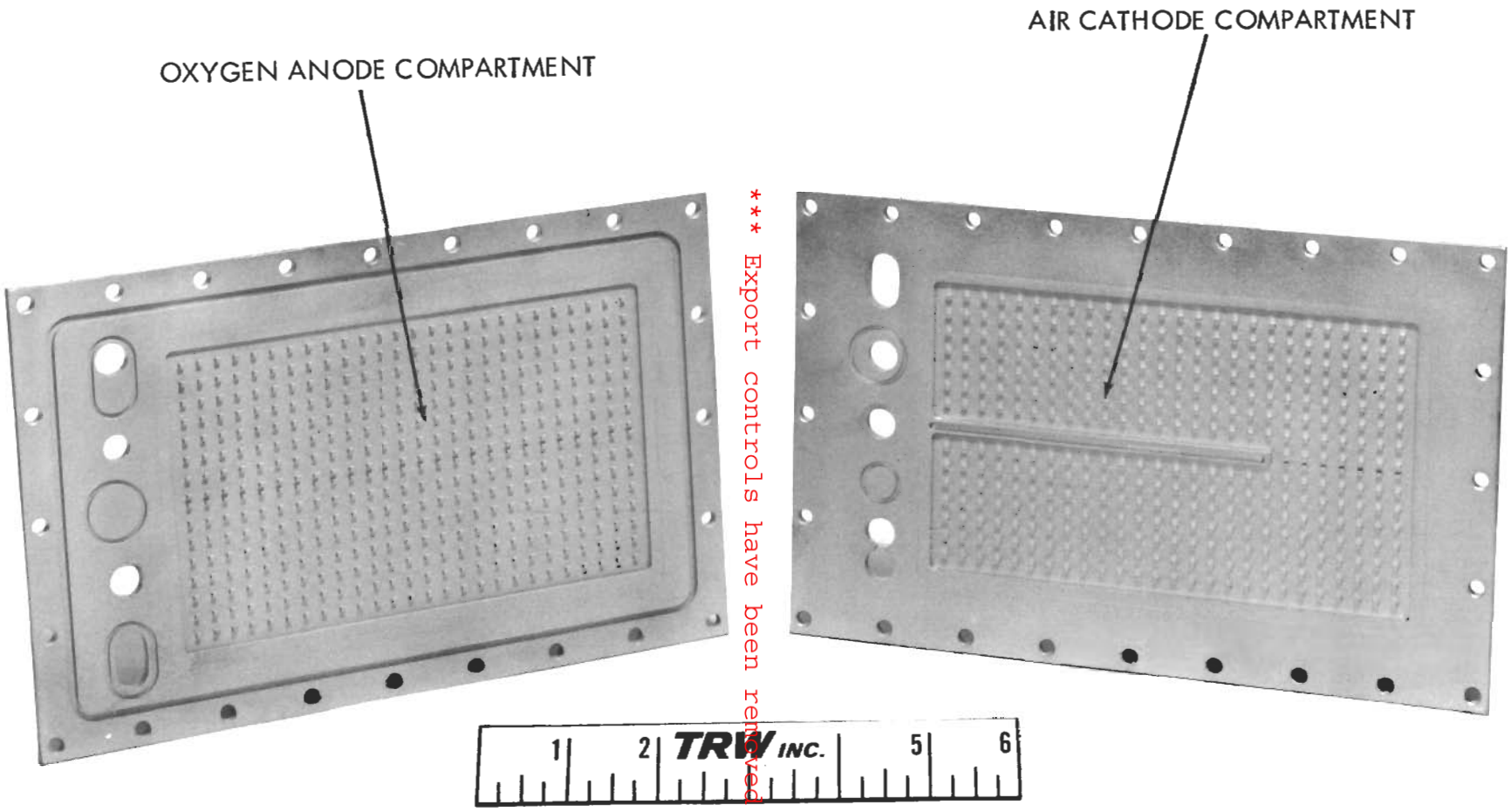

Note: Manifolding is the same as that for corresponding compartments of bi-polar plates as shown in Figures 5 and 6.

Figure 7 Concentrator Unipolar Plates

A thermal analysis was conducted to predict cell equilibrium temperature profiles under self-regulating conditions. Effects of various air pressures and flows were predicted. This allowed the specification of the vapor pressure requirement in the humidifier compartments. The result indicated compartments that were some ten-to-fifteen Fahrenheit degrees cooler than the operating cell temperatures. Since the partial pressure of water within the humidifier must be equal to that of the cell, the solution chosen to saturate the wicks had to have a vapor pressure characteristic correspondingly higher than the 32% KOH used in the matrix. A reduced percentage solution of KOH meets these requirements. However, the Dacron wicking material, which has proven successful in previous water transport schemes, was not compatible with KOH.

For this reason, initial self-regulation tests were conducted with Dacron wicks saturated with a 25% Na_2SO_4 solution. Later, a polypropylene wicking material, compatible with KOH and possessing similar water transport properties, was substituted for the Dacron. With this, a 23% KOH solution was used for the humidification solution. The relationships of vapor pressure versus temperature of various solutions are shown in Figure 8.

The wick plates are shown in Figure 9. These cavities were recessed so that both the wick and an expanded nickel metal screen could be placed into the compartment. The screen was necessary to compact the wick and keep it from completely filling the cavity and blocking the gas flow path in the accompanying unipolar plate. The backs of the wick plates are flat and made to fit flush against the cooling water cavities of the end plates.

In the external humidifier delivered under AF 33(615)-1856, a reservoir of Solka-Floc saturated with water was built into the bottom of the assembly. In the self-regulated model, water is transported directly to the wicking surface through a side port rather than to a reservoir under the cell stack. This resulted in a considerable weight savings since a water-saturated Solka-Floc compartment does not have to run under the entire unit. It was anticipated, however, that the technique might limit the wicking rate into the humidifier. For this reason, an additional fitting was incorporated into the middle of each end plate, whereby auxiliary water could be supplied to the two half-humidifiers (see Figure 9).

One additional feature was incorporated into the self-regulated model design but was never actually used. It consisted of a porting system in the humidifier compartment whereby the humidifier fluid could be made to flow behind the wick materials. This technique was included in the initial design to allow for the possibilities of better water distribution throughout the wick material and supplemental cooling of the humidifier fluid.

f. End Plates and Bolts

The series stack, of three cells and two humidifiers, shown in Figure 2 was sandwiched between two structural end plates. Calculations were made to determine an optimum

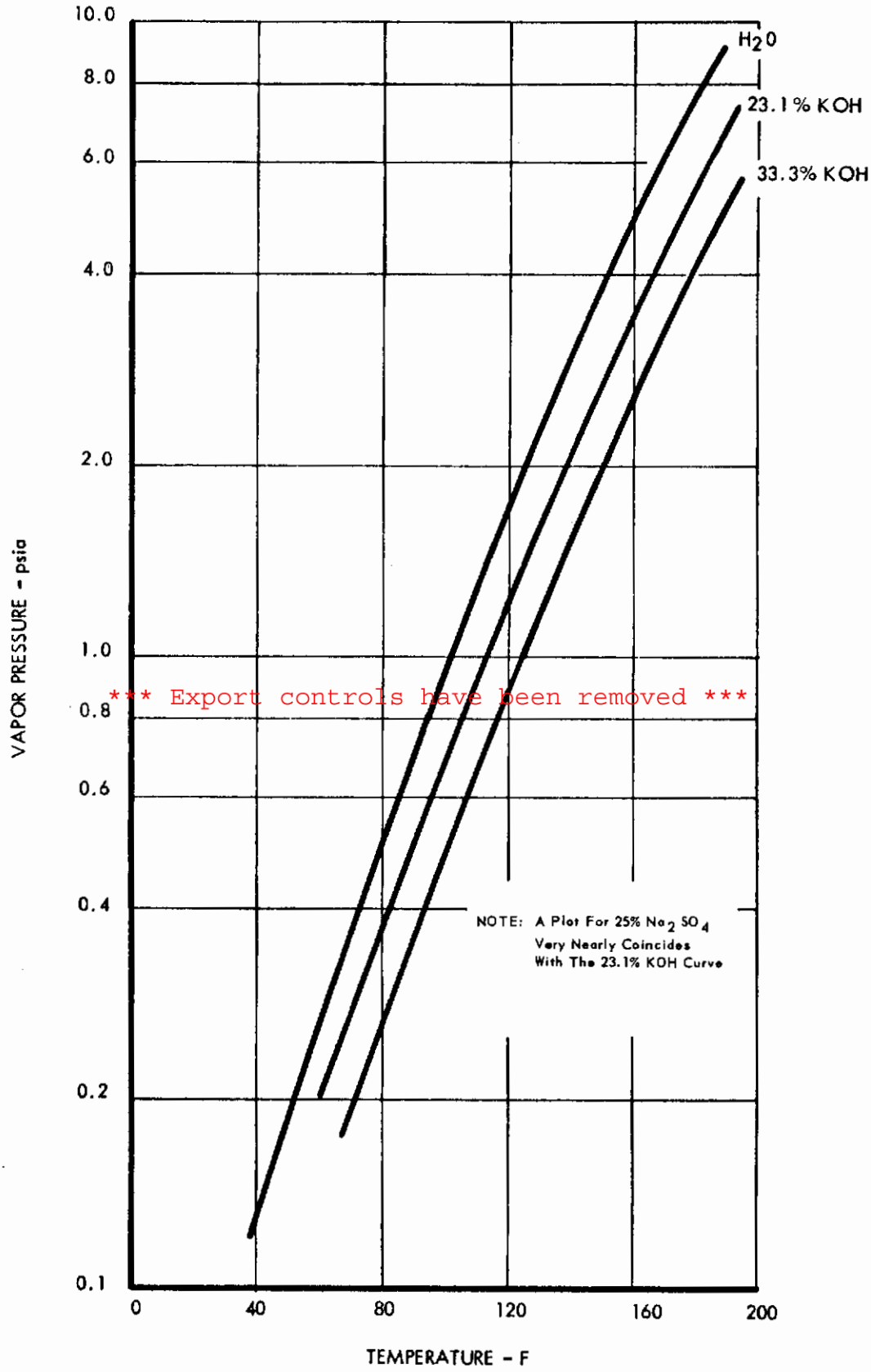

Figure 8 Temperature Versus Vapor Pressure

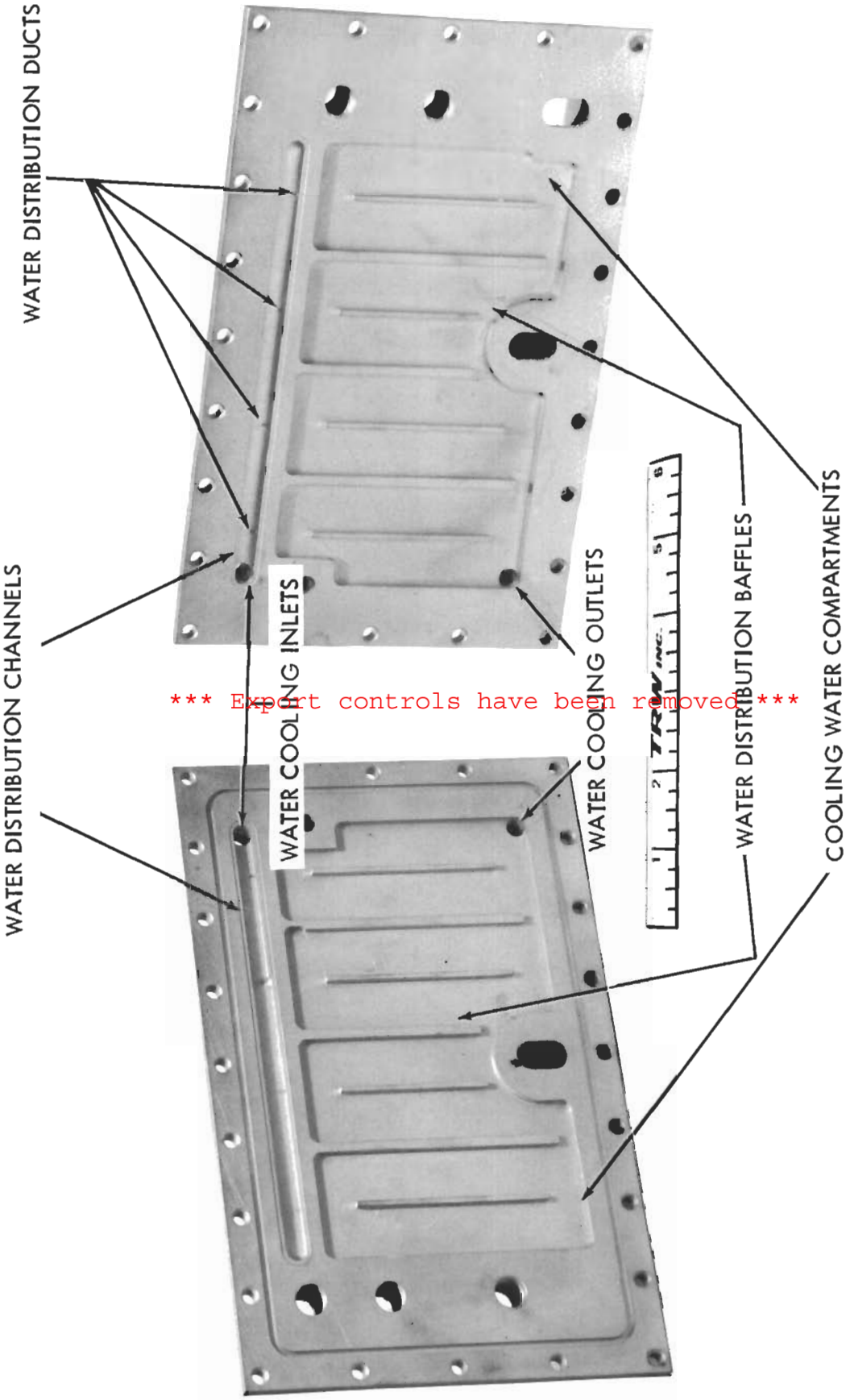

Figure 12 Concentrator End Plates

thickness and shape of the end plates. To withstand a 90 psia internal pressure, a 3/8 inch thick slab with a rectangular cross-section was necessary. Rather than use this configuration, a ribbed end plate of the cross-section shown in Figure 10 was selected. The ribs extended the width of the plate, not along the longitudinal direction.

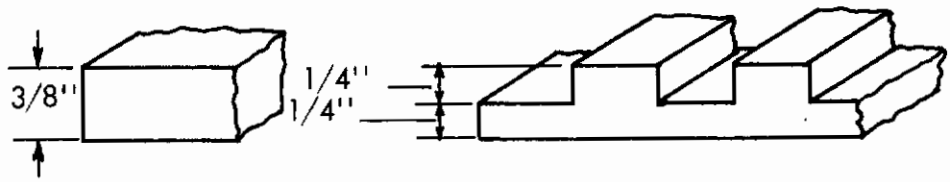

Figure 10 End Plate Cross-Section

This geometry resulted in an end plate that was 7% less in weight but had the same rigidity characteristics as the 3/8 inch rectangular cross-sectional piece. Further optimizations, by extending the ribs in both the length and breadth dimensions or by using geometrical configurations other than ribs, could be accomplished. An optimization study of this nature should be performed on prototypic units. A photograph of the actual self-regulating concentrator is shown in Figure 11. It clearly indicates the ribbed structure used to provide rigidity.

The design calculations indicated that twelve 8-32 stainless steel bolts would supply sufficient strength to prevent leakage when the assembled cells were internally stressed with 90 psia pressure. Twelve bolts were used in the assembly as shown in Figure 11, although a contingency factor was incorporated by making provisions for twenty-four bolts. Helicoil thread inserts were built into one end plate eliminating the need for nuts. Additional weight savings and optimization of the end plate could have resulted by cutting away excess metal between the bolt holes.

g. Supplemental Heating and Cooling

Since a wide range of conditions were to be tested, supplementary cooling and heating subsystems had to be included to allow parametric studies at nonequilibrium points of operation. These were used only as testing tools and would not be required on a prototype unit. The eventual choice for cooling the concentrator stack was to circulate cooling water through the end plates. The cooling water sides of both end plates are shown in Figure 12. Cooling water enters the top channel of the plate and is distributed evenly into each of the ribbed cooling channels by means of orifice ducts leading from

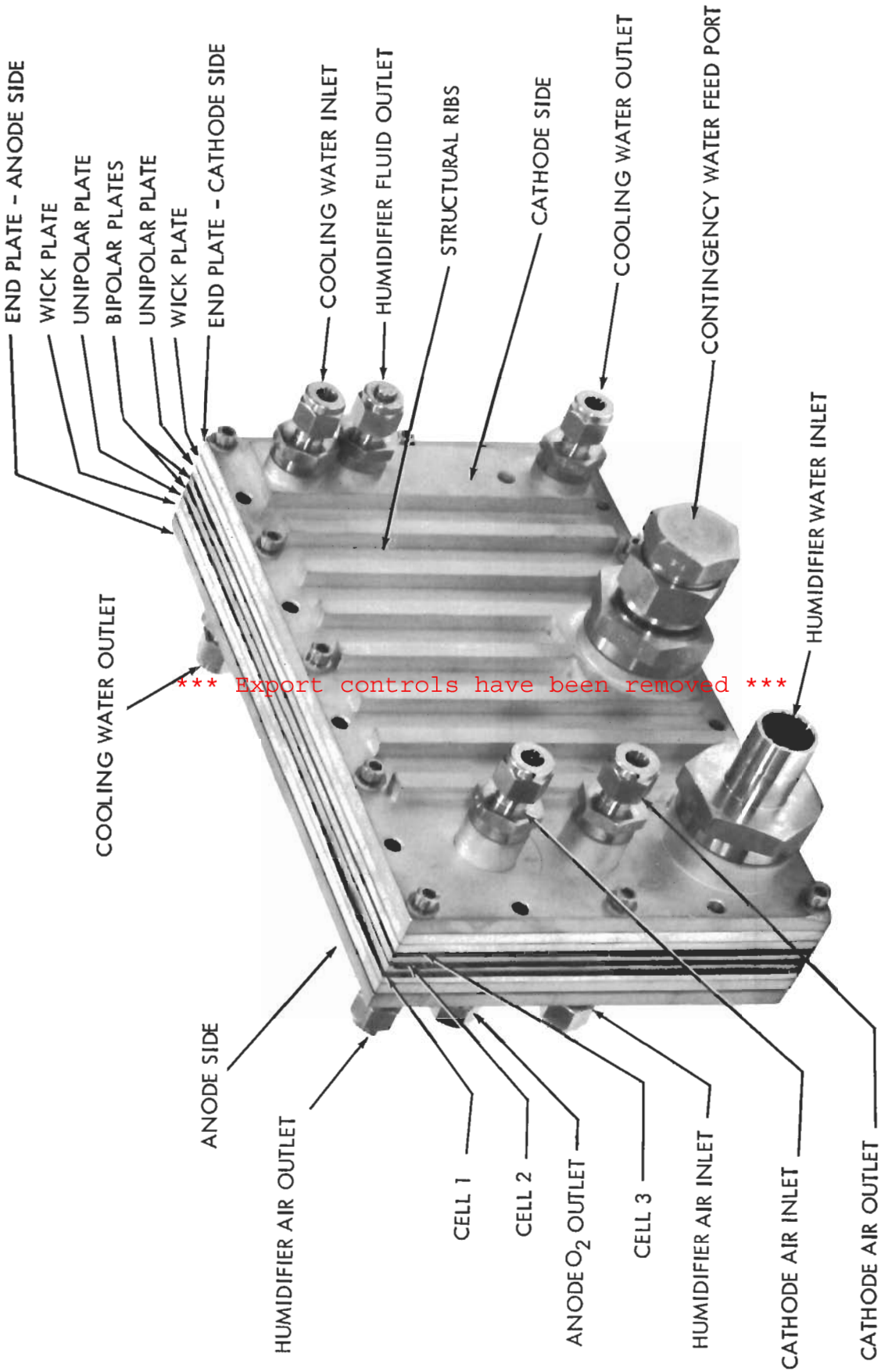

Figure 11 Assembled Self-Regulating Oxygen Concentrator

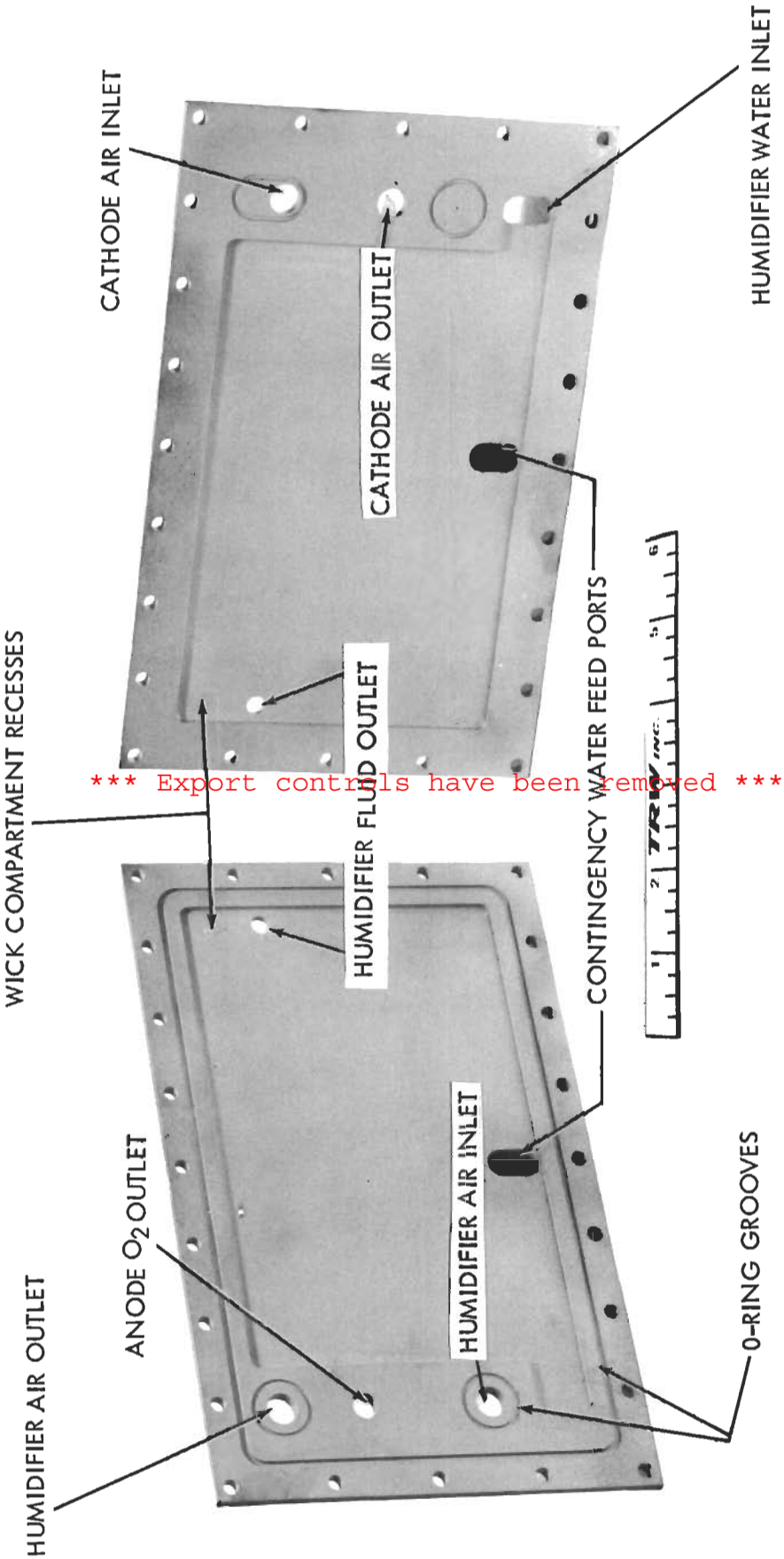

Figure 9 Humidifier Wick Plates

the top channel. The openings in the bottom corner of the cooling fields are drains that direct the water out of the cell. The large opening in the corner of the right end plate is the water inlet port leading to the humidifiers. The openings in the lower center of the plates are the contingency water feed ports.

SECTION IV

EXPERIMENTAL RESULTS

During the fabrication, assembly and initial evaluation of the three-cell concentrator, several checks were made to verify certain aspects of the design. These included verifying the structural integrity of the unit and its ability to hold internal pressures with no gas leakage, verifying water manifold effectiveness and wicking capabilities, establishing that the humidifier compartments and cells themselves presented minimal pressure drops, and evaluating plating techniques (see Appendix II). The cell stack was subjected to a series of tests to provide relationship of performance to such parameters as current density, air flow rates, cell temperature, gas compartment pressures, pressure differential across the matrix, matrix thickness, and matrix compression. Finally, the ability of the unit to operate under self-regulation was established.

The test time on the unit totaled approximately 235 hours. The breakout was some 34 hours for parametric runs which included a mixture of three-cell and single cell operation, and two (59-hour and 142-hour) continuous three-cell, self-regulation runs totaling 201 hours.

1. TEST RIG

A photograph of the test rig panel is shown in Figure 13. The assembly has the capability of monitoring and regulating gas pressures in both the anode and cathode compartments. A fifteen-point thermocouple temperature selection system was also available to monitor temperatures of the cells, humidifiers, and auxiliary components. Air flow rates to five times the theoretical stoichiometric quantity could be controlled and monitored at current densities up to 200 ASF over an inlet pressure range of 2.5 to 90 psia. A cell temperature controller with two set points for ON-OFF temperature control, a band temperature control, or a limiting ON-OFF temperature control was also included. By using a Kordesch-Marko Bridge, cell voltage relationships could be measured both with and without internal resistance.[4, 5] This data is presented in Table V and Figures 30, 31 and 64 and is discussed under Parametric Testing and Results of this section. Not shown in the photograph, but included as a portion of the test rig, was the supplementary external humidification equipment. The cell temperature control loop and humidification equipment were necessary because of the wide range parametric data requirement. A characteristic of self-regulation is that the cell will seek some equilibrium temperature, dependent upon the other variables of the system. To keep the cell temperature constant while changing other parameters, which would be a point of non-equilibrium, a heating-cooling temperature control loop was required for the stack. It was decided, therefore, to include an external humidifier to facilitate parametric testing over the wide range of conditions.

During the testing phase, the apparatus successfully operated at current densities up to 166 ASF, cell temperatures to 175F, air and oxygen pressures ranging from 5 to 90

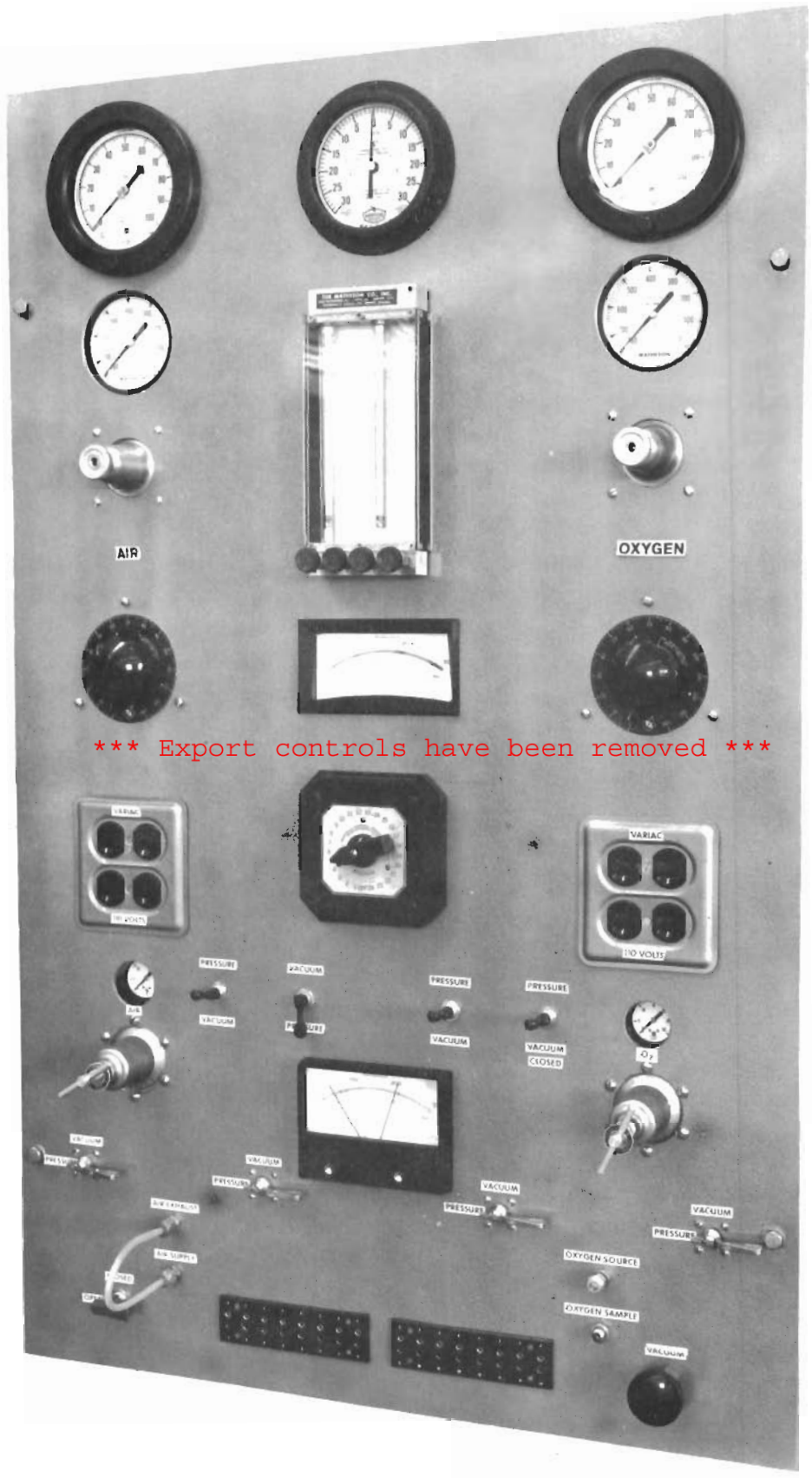

Figure 13 TRW Test Rig Panel

psia, and pressure differentials of 5 psia, in either direction, across the matrices. The range of parameters covered during the testing is fully discussed in the Parametric Testing and Results section and tabulated in Table III.

2. PRELIMINARY EVALUATIONS AND CONSIDERATIONS

a. Concentrator Performance

The three-cell stack was assembled and given a brief trial run prior to establishment of a detailed test program. It further served as a check on the test rig itself. This evaluation was conducted with a three-cell stack, but with external humidification of the inlet air. The internal humidifiers were not used at this time. The data taken is tabulated in Appendix III under points PE-1 to PE-23. The set of curves resulting from this initial effort are presented in Figures 14 through 16. The performance of Cells 1, 2, and 3 was nearly identical over the current density range studied at the flow rate of five times stoichiometric. In addition, Cells 1 and 2 were very nearly equal at flow rates of two, three, and four times stoichiometric. Cell 3, however, was sensitive to flow rates less than five times theoretical. The apparent reason for this difference was insufficient air flowing through the cathode compartment of Cell 3 when the flow rate decreased below 5T. When the unit was disassembled the gas ducts leading to Cell 3 were cleaned out. Some minor particles were found; however, no gross blockage was in evidence at the time of disassembly.

It is possible that the poor performance of Cell 3 was due to improper moisture balance. Data taken on a smaller oxygen concentrating cell is included in Figure 17 to show the effect of an improper cell moisture balance upon performance and thereby illustrate the importance of correct moisture balance. Curves 1 through 5 were taken sequentially on the same cell. Curve 1 was the initial performance obtained while the cell had proper moisture balance. Curve 2 was obtained after the cell had been desiccated, i. e., the cell had been run for some length of time with the water content of the incoming air less than that required to match the vapor pressure of the electrolyte. Curves 3, 4 and 5 illustrate the improvement in cell performance as the cell was brought back to its initial moisture conditions. It is evident from these curves that for a cell to attain its best performance, the moisture balance must be optimum. Otherwise, as shown, the cell voltage requirement will increase, especially at higher current densities.

b. Pressure Drop Measurements

The data presented in Figure 18 represents the measured pressure difference between the air entrance and air exhaust when:

1) air was passed only through the humidifier compartments of the concentrator, and

2) air was passed through both the humidifier compartments and the three cells of the concentrator.

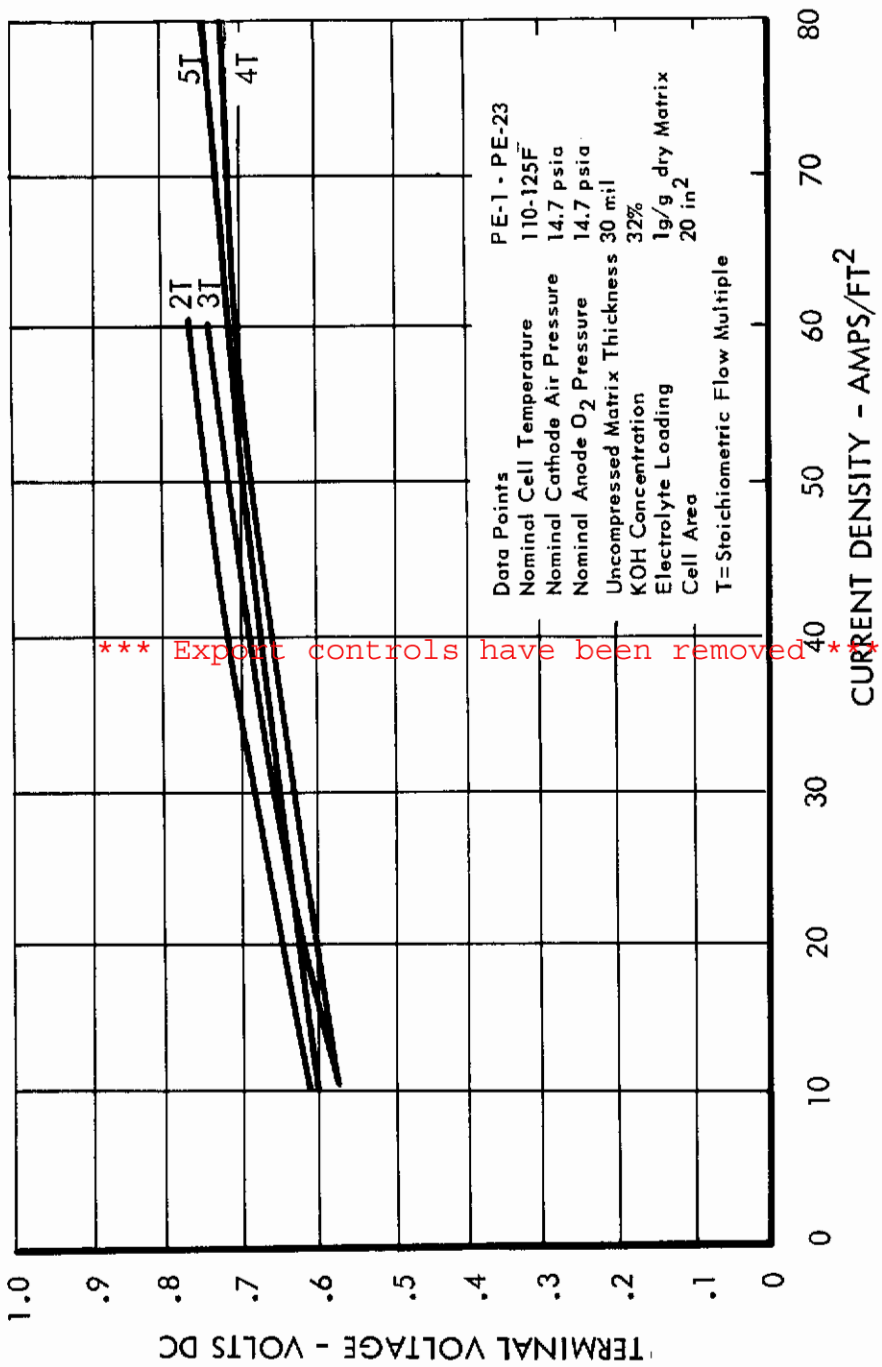

Figure 14 Cell 1 Performance in Three-Cell Unit - Preliminary Evaluation

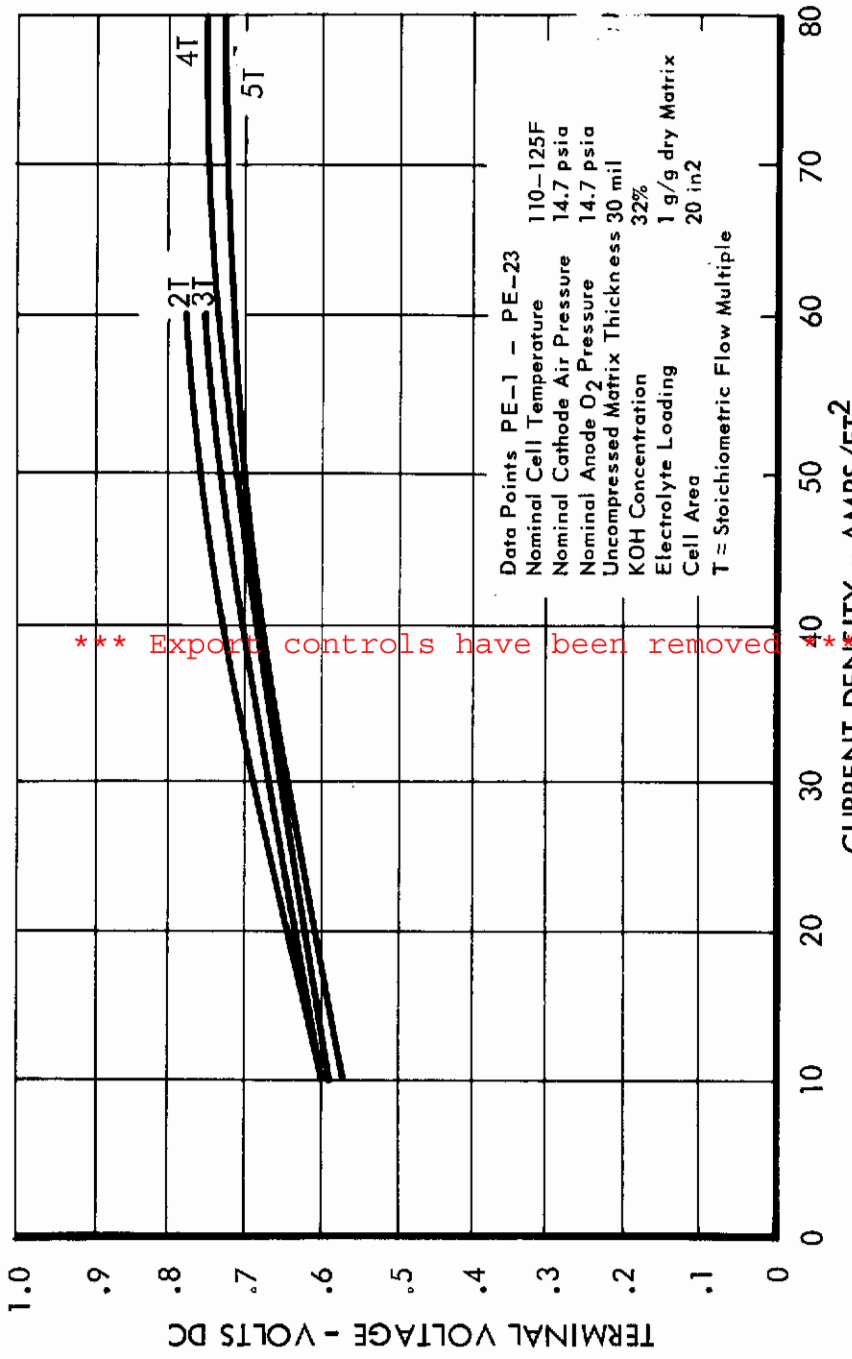

Figure 15 Cell 2 Performance in Three-Cell Unit-Preliminary Evaluation

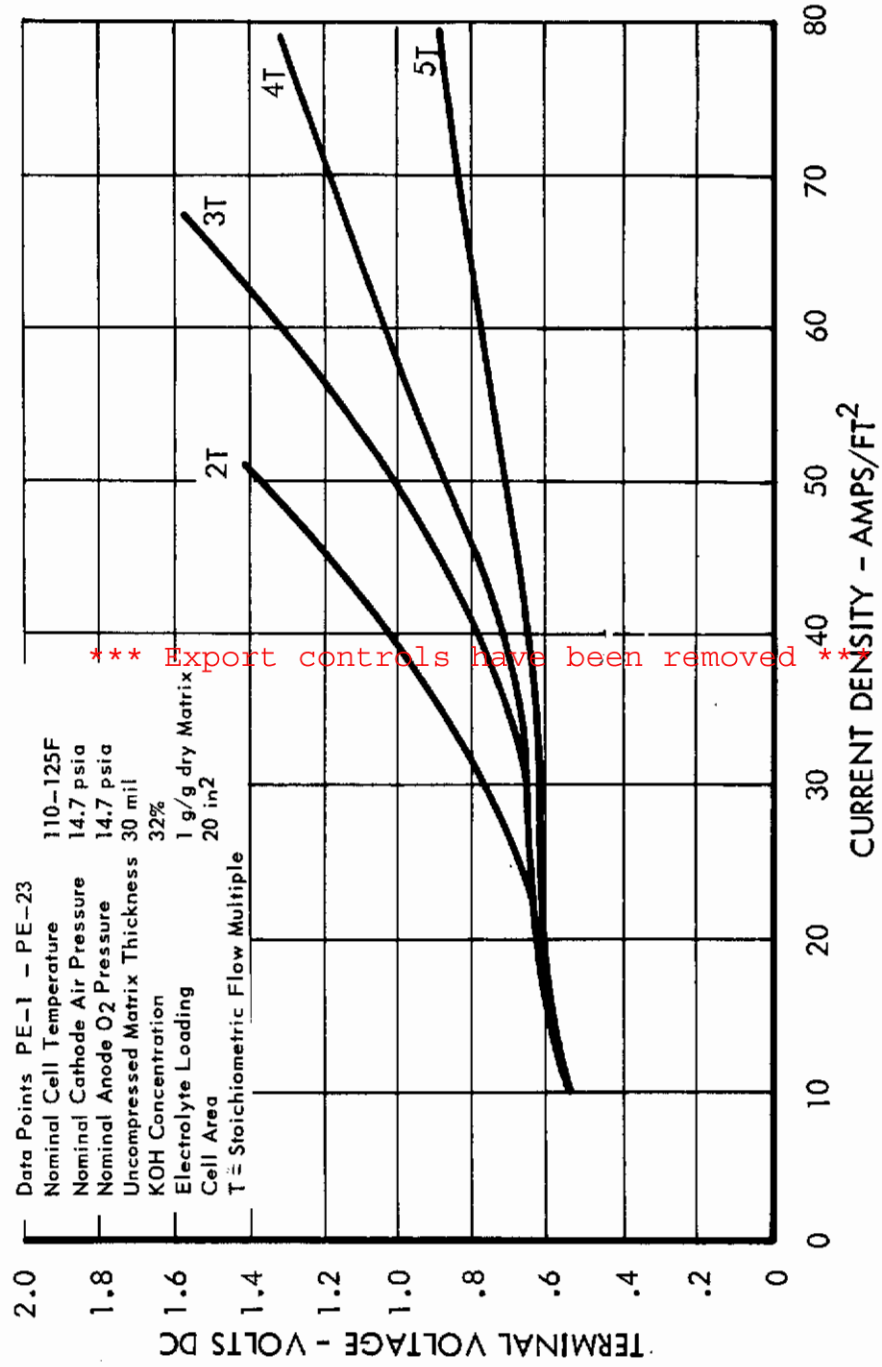

Figure 16 Cell 3 Performance in Three-Cell Unit - Preliminary Evaluation

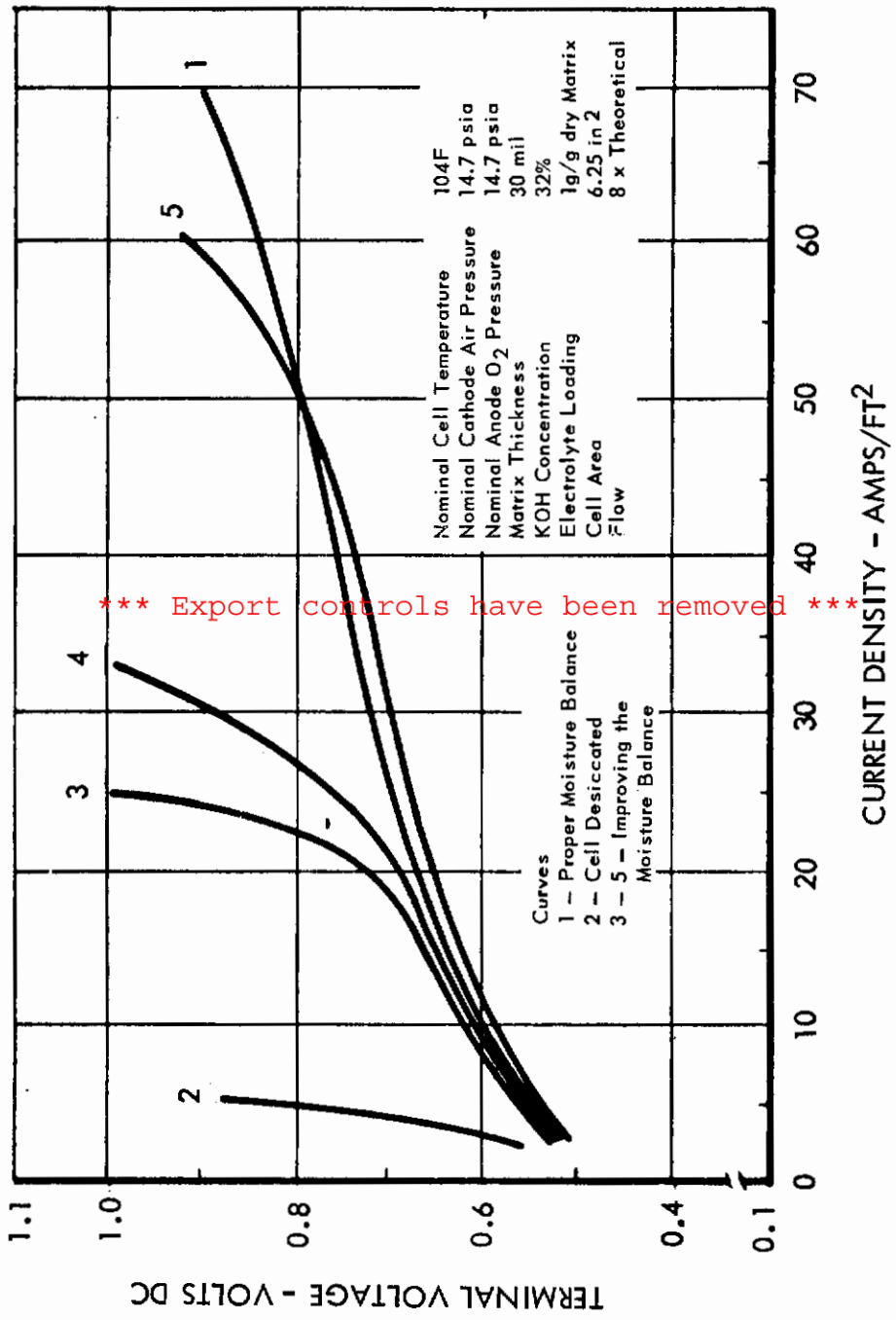

Figure 17 Effect of Cell Moisture Balance

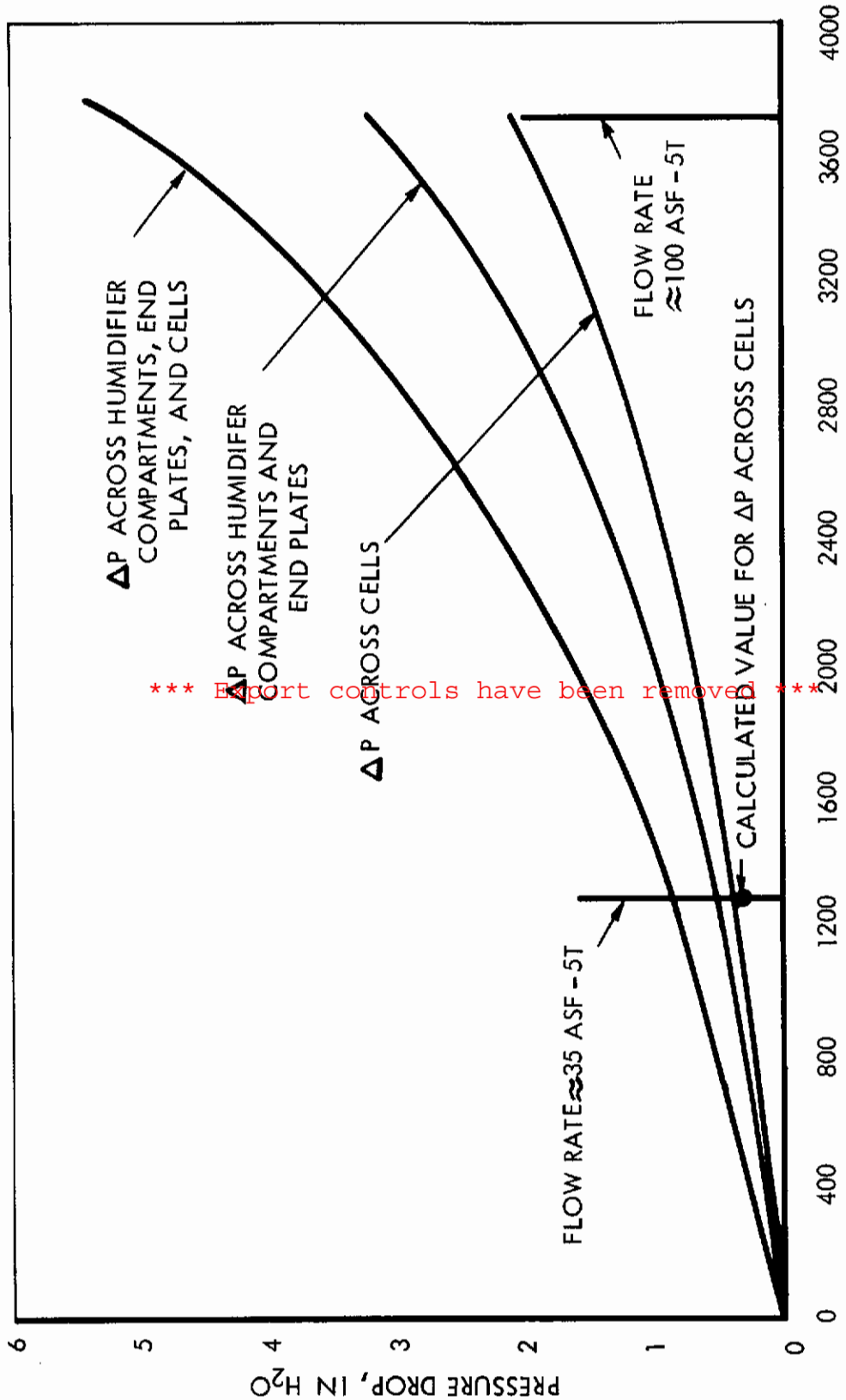

Figure 18 Measured Pressure Drop Across Self-Regulated Oxygen Concentrator

The difference between items (1) and (2) is the pressure drop across the cells in the concentrator. To better explain this, the flow pattern is presented schematically in Figure 19.

At an air flow rate of 1300 cc per minute, corresponding to a 5T flow at 35 ASF, a pressure drop across the cells of 0.38 inch of water was experimentally measured. The calculated pressure drop for the same air flow rate and temperature was 0.32 inch of water. The close agreement between the two numbers indicates that the gas flowing through the concentrator does so according to predictable fluid calculations. Further, the low pressure drop experienced indicates an attractive characteristic of both the humidifier and cell, and allows projection of these configurations to units of larger capacity without undue air compression requirements.

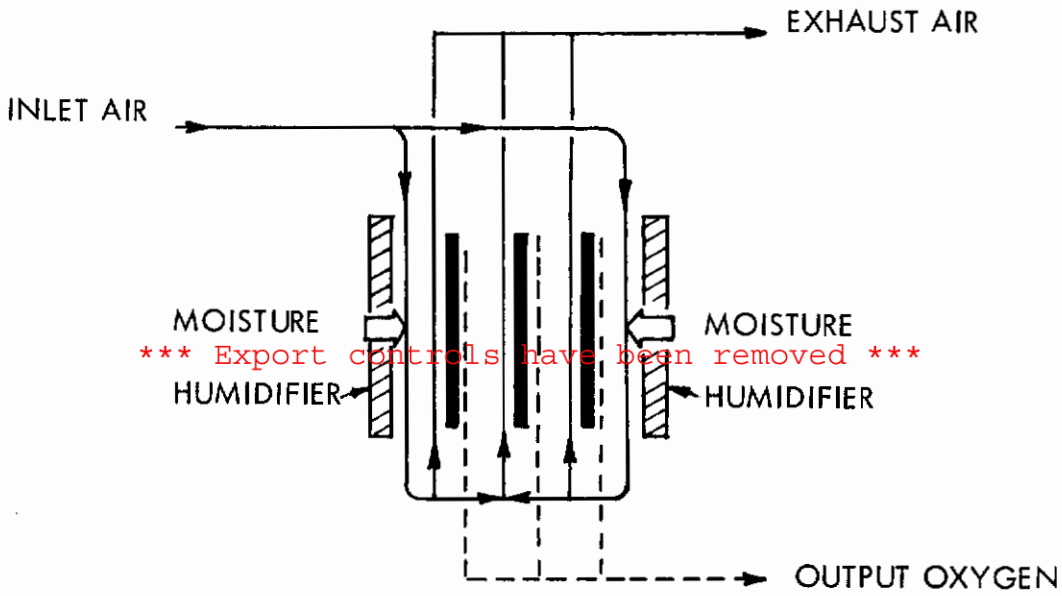

Figure 19 Flow Pattern

c. Pressure Differential Stability

During structural integrity tests, the cathode side of the 30-mil matrix was pressurized to 10 psig, and a line from the anode side was immersed in water to determine if gas leakage was occurring across the membrane separating the two compartments. No leaks were observed. This result was in agreement with earlier studies which indicated that the bubble pressure was around 19 psig for the 30-mil matrix. During the early phases of parametric testing, the corrosion (discussed under Atmosphere Performance) that took place as a result of a cooling water leak reduced the unit's ability to support similar pressure differentials. During subsequent testing, therefore, pressure differentials could not be increased above 5 psi without experiencing intercell leakage.

3. PARAMETRIC TESTING AND RESULTS

Following the initial check points, a detailed five-phase test program was prepared, which was designed to evaluate the effects of current density, air flow rate, temperature, pressure and differential pressure, matrix thickness, and self-regulation characteristics. This program is delineated in Table III. The testing was conducted in such a manner that the initial and final portions were run with a three-cell stack, while a single cell was used for some of the parametric testing. This is noted in Table III.

The reason for conducting the testing in this manner was twofold. First, an attempt was made to prevent compromise of the results by corrosion damage which occurred during the preparations for the first phase of parametric testing. The details of that damage are discussed in the Atmospheric Performance section. A second benefit of using only one cell was the reduced time for assembly and disassembly when changing matrices. As shown in Table III, the first four phases of testing, being parametric in nature and corresponding to thermal nonequilibrium with respect to self-regulation, were conducted with external, rather than internal, humidification. During the fifth phase, which resulted in over 200 hours of self-regulating operation, the unit was allowed to perform without external constraints, utilizing its internal humidifiers, and to attain the corresponding thermal equilibrium.

The tabulation of data taken appears in Appendix III. This information was then converted to Figures 21-66 for comparison of the various parameters. To aid in interpreting this series of plots, Table IV, A Tabular Guide to Reduced Data Plots, is included. This table reveals the relationship between the basic test program, data points plotted, and the range of parameters covered by each plot. The discussion of these figures appears in the corresponding test section.

a. Atmospheric Performance

During initial setup for atmospheric testing, the complete three-cell stack, gas compartments included, became flooded with water. Assessment of the problem indicated a cooling water leak. Upon opening the unit, it was observed that corrosion had taken place in the end plates and adjacent wick plates, thus allowing leakage of cooling water into the gas passages. Specifically, water was allowed to leak from the coolant passages through corroded O-ring grooves in the contingency water feed ports (see Figure 9 for location of these ports) and fill the humidifier chambers. From there, the water eventually flooded the entire three-cell stack through the gas ducts and ports. Some of the gas ports displayed corrosion to the point of affecting the O-ring grooves. No corrosion was observed in any of the anode or cathode compartments where KOH was in intimate contact with the gold- and nickel-plated magnesium structure. Experience related by the plating subcontractor indicated that similar problems had been encountered where gold-plated magnesium was in contact with water. The corroded areas were coated with an epoxy adhesive to prevent further damage to the exposed magnesium areas. This was done after the Preliminary Evaluation previously discussed, but before any of the data points listed in Table III were obtained. The three-cell stack was reassembled and data points 1-64 were taken.

Table III Oxygen Concentrator Test Program

Test Phase	Data Point Nos.	Matrix Thickness Mils	Electrolyte Loading g/g dry matrix	No. Of Cells	Cell Temp. F	Cell Pressure Cathode/Anode psia	Current Density - ASF @ Flow-xT	Run Time Hrs.
Atmospheric Performance	1-64	30	1.25	3	100 125 150 175	14.7/14.7	10, 20, 40, 60, 80, 100 @ 3T and 5T 20, 60, 80, 100 @ 2T	6.6
	565-580	30	1.75	1 (No. 1)	125	14.7/14.7	35, 65, 100, 150 @ 2T, 3T, 4T, 5T	0.6
Matrix Comparisons	65-136	20 10	1.25	1 (No. 3)	125	14.7/14.7 10.0/14.7 14.7/10.0	15, 35, 50, 65, 80, 100 @ 5T 15, 35, 65, @ 2T and 3T	6.1
Vacuum Operation	137-172	30	1.25	1 (No. 3)	125	5.0/5.0 7.5/7.5 10.0/10.0	15, 35, 50, 65, 80, 100 @ 5T 15, 35, 65, @ 2T and 3T	3.3
	137A-160A	30	1.25	1 (No. 3)	125	5.0/5.0 7.5/7.5	15, 35, 50, 65, 80, 100 @ 5T 15, 35, 65, @ 2T and 3T	1.9
	553-564	30	1.75	1 (No. 1)	125	7.5/7.5 10.0/10.0	15, 35, 50, 65, 80, 100 @ 5T	1.1
Pressure and Pressure Differential Operation	173-352	30	1.25	1 (No. 3)	125	10.0/14.7 14.7/10.0 14.7/14.7 30.0/25.0 30.0/30.0 30.0/35.0 45.0/40.0 45.0/45.0 45.0/50.0 60.0/55.0 60.0/60.0 60.0/65.0 75.0/70.0 75.0/75.0 75.0/80.0	15, 35, 50, 65, 80, 100 @ 5T 15, 35, 65, @ 2T and 3T	12.5

*** Export controls have been removed ***

Table III Oxygen Concentrator Test Program (cont.)

Test Phase	Data Point Nos.	Matrix Thickness Mils	Electrolyte Loading g/g dry matrix	No. Of Cells	Cell Temp. F	Cell Pressure Cathode/Anode psia	Current Density - ASF @ Flow-xT	Run Time Hrs.
Pressure and Pressure Differential Operation	526-543; 552	30	2.25	1 (No. 1)	125	14.7/14.7 20.0/14.7 20.0/20.0 30.0/30.0 45.0/45.0 60.0/55.0 60.0/60.0 60.0/65.0 75.0/70.0 75.0/75.0 75.0/80.0 90.0/85.0 90.0/90.0	60 @ 4T	1.5
	544-551	30	2.25	1 (No. 1)	125	30.0/25.0	15, 35, 60, 100, 144, 166 @ 4T	1.1
Self-Regulation	353-525 59-hr. run	30	1.25	3	Not Controlled	10.0/10.0	Variable to 35 @ 5T Nominal	59
	581-636 142-hr. run	30	1.75	3	Not Controlled	14.7/14.7	Variable to 60 @ 4T Nominal	142

Table IV A Tabular Guide to Reduced Data Plots

Figure No.	Test Phase	Data Pts. Plotted	Matrix;	Electrolyte Loading;	Range of Pertinent Parameters No. of Cells; Temp.; Flow; Cathode Pressure/Anode Pressure
21	Atmospheric Pressure	1-6	30 Mil;	1.25 g/g dry matrix;	Three-Cell Performance; 100F; 5T; 14.7 psia/14.7 psia
22	"	17-22	" ;	" ;	" ; 125F; " ; "
23	"	33-38	" ;	" ;	" ; 150F; " ; "
24	"	49-54	" ;	" ;	" ; 175F; " ; "
25	"	1-16	" ;	" ;	Cell 2 Performance ; 100F; 2T, 3T, 5T; 14.7 psia/14.7 psia
26	"	17-32	" ;	" ;	" ; 125F; " "
27	"	33-48	" ;	" ;	" ; 150F; " "
28	"	49-64	" ;	" ;	" ; 175F; " "
29	"	1-6; 17-22; 33-38;49-54	" ;	" ;	" ; 100F, 125F, 150F, 175F;5T; 14.7 psia/14.7 psia
30	"	33-38	" ;	" ;	" ; 150F; 5T; 14.7 psia/14.7 psia Terminal & IR Free Voltage
31	"	565-568; 577-580	" ;	1.75 g/g dry matrix;	Cell 1 Performance ; 125F; 2T, 5T; 14.7 psia/14.7 psia; Terminal & IR Free Voltage
32	Matrix Comparisons	65-76	20 Mil;	1.25 g/g dry matrix;	Cell 3 Performance ; 125F; 2T, 3T, 5T; 14.7 psia/14.7 psia
33	"	77-88	" ;	" ;	" ; " ; " ; 10.0 psia/14.7 psia
34	"	89-100	" ;	" ;	" ; " ; " ; 14.7 psia/10.0 psia
35	"	65-70;77-82	" ;	" ;	" ; " ; 5T; 14.7 psia/14.7 psia, 10.0 psia/ ; 14.7 psia, 14.7 psia/10.0 psia
36	"	101-112	10 Mil ;	" ;	" ; " ; 2T, 3T, 5T; 14.7 psia/14.7 psia
37	"	125-136	" ;	" ;	" ; " ; " ; 14.7 psia/10.0 psia
38	"	101-106; 125-130	" ;	" ;	" ; " ; 5T; 14.7 psia/14.7 psia, 14.7 psia/10.0 psia
39	"	17-22;65-70; 101-106	10, 20, 30 Mil;	1.25 g/g dry matrix;	" ; " ; "; 14.7 psia/14.7 psia
40	Vacuum Operation	137-148	30 Mil;	1.25 g/g dry matrix ;	Cell 3 Performance ; 125F; 2T, 3T, 5T; 5.0 psia/5.0 psia
41	"	149-160	" ;	" ;	" ; " ; " ; 7.5 psia/7.5 psia
42	"	161-172	" ;	" ;	" ; " ; " ; 10.0 psia/10.0 psia
43	"	137A-148A	" ;	" ;	" ; " ; " ; 5.0 psia/5.0 psia
44	"	149A-160A	" ;	" ;	" ; " ; " ; 7.5 psia/7.5 psia
45	"	553-556	" ;	1.75 g/g dry matrix ;	Cell 1 Performance ; " ; 5T; 7.5 psia/7.5 psia
46	"	559-563	" ;	" ;	" ; " ; " ; 10.0 psia/10.0 psia

Table IV A Tabular Guide to Reduced Data Plots (cont.)

Figure No.	Test Phase	Data Pts. Plotted	Matrix	Electrolyte Loading	Range of Pertinent Parameters: No. of Cells; Temp.; Flow; Cathode Pressure/Anode Pressure
47	Pressure & Pressure Differential Operation	209-220	30 Mil	1.25 g/g dry matrix	Cell 3 Performance; 125F; 2T, 3T, 5T; 30.0 psia/25.0 psia
48	"	221-232	"	"	" ; " ; " ; " ; 30.0 psia/30.0 psia
49	"	233-244	"	"	" ; " ; " ; " ; 30.0 psia/35.0 psia
50	"	209-214 221-226 233-238	"	"	" ; " ; 5T; 30.0 psia/25.0 psia/30.0 psia/ 30.0 psia, 30.0 psia/ 35.0 psia
51	"	245-256	"	"	" ; " ; 2T, 3T, 5T; 45.0 psia/40.0 psia
52	"	257-268	"	"	" ; " ; " ; " ; 45.0 psia/45.0 psia
53	"	269-280	"	"	" ; " ; " 45.0 psia/50.0 psia
54	"	245-250 257-262 269-274	"	"	" ; " ; 5T; 45.0 psia/40.0 psia, 45.0 psia/ 45.0 psia, 45.0 psia/50.0 psia
55	"	281-292	"	"	" ; " ; 2T, 3T, 5T; 60.0 psia/55.0 psia
56	"	293-304	"	"	" ; " ; " ; " ; 60.0 psia/60.0 psia
57	"	305-316	"	"	" ; " ; " ; " ; 60.0 psia/65.0 psia
58	"	281-286 293-298 305-310	"	"	" ; " ; 5T; 60.0 psia/55.0 psia, 60.0 psia/ 60.0 psia, 60.0 psia/65.0 psia
59	"	317-328	"	"	" ; " ; 2T, 3T, 5T; 75.0 psia/70.0 psia
60	"	329-340	"	"	" ; " ; " ; " ; 75.0 psia/75.0 psia
61	"	341-352	"	"	" ; " ; " ; " ; 75.0 psia/80.0 psia
62	"	317-322 329-334 341-346	"	"	" ; " ; 5T; 75.0 psia/70.0 psia, 75.0 psia/ 75.0 psia, 75.0 psia/75.0 psia
63	"	17-22 209-353	"	"	Single-Cell Performance Bands; 125F; 5T; 14.7-75.0 psia/14.7-80.0 psia
64	"	545-551	"	2.25 g/g dry matrix	Cell 1 Performance; 125F; 4T; 30.0 psia/25.0 psia; Terminal & IR Free Voltage
65	Self-Regulation (59-hour run)	353-525	30 Mil	1.25 g/g dry matrix	Three-Cell Performance; Variable; Nominal 5T; 10.0 psia/10.0 psia
66	Self-Regulation (142-hour run)	581-636	"	1.75 g/g dry matrix	" ; " ; 4T, 5T; 14.7 psia/14.7 psia

*** Export controls have been removed ***

This phase of testing shows the variation of performance with respect to cell temperature while operating under atmospheric conditions. Figures 21-24 indicate the performance of all three cells at a flow five times stoichiometric (5T) as a function of temperature. Cell 3 did not perform as well as either of the other cells. The gas ducts were checked both before and after testing and found to be clear, indicating correct air flow. Cell 2 was selected for individual cell comparisons as a function of flow and temperature. These are shown in Figures 25-29. Clearly indicated in Figure 29 is the fact that the cell voltage requirements are reduced as temperature is increased. The internal resistance of the cell as a function of current density is shown in Figure 30. Finally, in a single-cell test conducted on Cell 1 with a higher electrolyte loading (1.75 g 32% KOH/g dry matrix as opposed to 1.25 g 32% KOH/g dry matrix) improved performance is indicated to current densities of 150 ASF. This is shown in Figure 31. Note that the internal resistance is less than that displayed in Figure 30. This would seem to indicate that electrolyte loadings above the minimum of 1.0 g/g dry matrix as quoted[6] are required for improved performance.

In Table V are presented the IR voltage losses for the three cells taken as a function of temperature and air flow at 100 ASF (data points 1-64). As would be expected, the IR loss is essentially independent of flow rate since it is concerned with the electrolyte and its conductivity.[7] Note that the IR loss increases with temperature. This is contrary to normal expectations since the electrolyte conductivity increases with temperature.[8] Cells 1 and 2 display nearly equal characteristics, while Cell 3 shows an abnormally high internal resistance. As mentioned, it appears that high cell resistances may have been caused by matrices that were on the low boundary of recommended electrolyte loadings.[6]

b. Matrix Comparisons

Since it was felt that 125F represented a likely possibility for eventual cell operation under the self-regulation mode, it was selected as the operating temperature at which the comparison of other parameters would be made. It was under this condition that the performance of a single cell with 20-mil matrix was assessed. As noted in Table III, the cell was operated at atmospheric pressure with nearly a 5 psia differential in each direction. The results are presented in Figures 32-35. Figure 35 indicates that the cell operated best when no pressure differential was present. This effect would be expected of the cells operating at low levels of electrolyte loading. At low loading levels the effect of pressure differential would be to shift the limited amount of electrolyte from the electrode on the high pressure side to the low pressure side. This would, in turn, cause excessive electrode polarization.

In a manner similar to the previous test, a cell containing a 10-mil matrix was evaluated. Due to internal cell leakage, data points 113-124 were not obtained. The leak was apparently caused by undue gasketing constraints which did not allow the matrix to be compressed to the desired degree. Figure 38 again indicates that cell performance was somewhat better with no pressure differential present across the matrix. In the matrix comparison, Figure 39, it can be seen that the cell performed best with a 20-mil matrix.

Table V Cell IR Loss and Resistance x Area

Cell	Temp. F	IR Loss @ 100 ASF - volts, Air Flow 2T	3T	5T	Avg.	Avg. ohm-cm^{2}**
1	100	0.125	0.12	(0.15)*	0.122	1.13
	125	0.11	0.13	0.13	0.123	1.14
	150	0.13	0.14	0.125	0.132	1.23
	175	0.20	0.20	0.182	0.194	1.80
2	100	0.11	0.11	0.14	0.120	1.11
	125	0.10	0.12	0.11	0.110	1.00
	150	0.135	0.14	0.135	0.137	1.27
	175	0.19	0.19	0.18	0.187	1.74
3	100	0.10	0.11	0.14	0.117	1.09
	125	0.165	0.15	0.12	0.145	1.35
	150	0.19	0.19	0.19	0.183	1.70
	175	(0.27)*	0.33	0.325	0.327	3.04

Taken From Data Points 1-64

Nominal Cathode Air Pressure	-	14.7 psia
Nominal Anode O_2 Pressure	-	14.7 psia
Uncompressed Matrix Thickness	-	30 mil
KOH Concentration	-	32%
Electrolyte Loading	-	1.25 g/g dry matrix

*These data points not used in computing average IR loss.

**This is equal to the average IR loss/current density, and hence becomes a measure of cell internal resistance which is independent of current density.

Normally, due to lower internal resistances, it would be expected that the 10-mil matrix would provide superior results. However, it is possible that the same factors which resulted in internal leakage tended to impair cell performance as well. Further, since a thinner matrix offers reduced reservoir action in relation to moisture balance, this also may have been a performance deterrent.

c. Vacuum Operation

The data taken during this phase served to focus upon the more difficult water management problem at reduced pressures. At low pressures, the specific humidity (mass of water vapor/mass of air) required to keep the cell in proper moisture balance is higher than at elevated pressures. For example, attempting to run at a total inlet pressure of 2.5 psia at a 125F cell temperature would result in over two-thirds of the total flow consisting of water vapor. With the air flow rates required, this water requirement was beyond the capabilities of the external humidifier.

During the first attempt at data points 137-172, a malfunction of the temperature control loop allowed the cell to overheat and the matrix to dry out. During an attempted rerun (points 137A-160A), a line between the external humidifier and the cell was insufficiently heated, thus causing moisture condensation from inlet air before it reached the cell, resulting in cell desiccation. Therefore, data points 137-172 and 137A-160A, which resulted in Figures 40-44, are not representative of cell performance under balanced humidity conditions. Contained in these figures is the cell desiccation variance with time. Shown in Figures 45 and 46 are the results of a third and more successful attempt (data points 553-564) at vacuum operation. These were taken at a higher electrolyte loading (1.75 g/g dry matrix) which served as a deterrent to rapid desiccation. However, at the higher current densities the voltage again showed a tendency to rise. Since the external humidifier was being taxed beyond its capacity, it was obvious that prolonged operation under these conditions would have resulted in performance similar to data points 137-172.

d. Pressure and Pressure Differential Operation

Conversion of the test rig for pressure operation included the replacement of the heretofore glass humidifier by a smaller stainless steel container. A flow separator was placed at the inlet to allow dispersion of the entering air and a screen at the outlet to eliminate unwanted liquid carryover due to violent bubbling. The assembly and all lines were carefully wrapped with heater tapes and insulated. After having run through the first few data points (209-232), it became apparent that the humidifier was not saturating the air passing through it. This was indicated by the low dew point of the exhaust air stream - a sign that the cell was beginning to desiccate.

From data points 233-352,therefore, the procedure was to heat the humidifier considerably above the normal saturation temperature in an effort to allow the partial saturation to increase the specific humidity to more acceptable levels. This resulted in an increased downstream dew point reading more in keeping with that in earlier successful

testing. Particular trends are difficult to ascertain from this phase of testing. The cell required its lowest voltage when the cathode/anode pressures were nominally 60.0 psia/55.0 psia and its highest voltage when they were 45.0 psia/40.0 psia. During both the 30.0 and 45.0 psia testing, the cell operated best with no pressure differential, while a differential pressure of 5 psia (cathode > anode) provided the lowest voltage requirement during 60.0 and 75.0 psia testing. Figures 47-62 cover the results.

Since at increased cathode air pressures the partial pressure of oxygen is increased, it was expected that cell performance would show improvement at elevated pressures. This was not experienced, however. Figure 63 shows a comparison of the spread in data obtained with Cell 3 at points 209-352 (125F), and the performance obtained under atmospheric conditions with Cells 1 and 2 (125F). The performance demonstrated by both Cells 1 and 2 is superior to the best pressure data for Cell 3. As mentioned, this is contrary to expected operation. A later single-cell test using Cell 1 (data points 526-552) indicated performance superior to that previously obtained with Cell 3 (points 209-352). It should be noted that the heavier electrolyte loading (2.25 g/g dry matrix) was used at this time. During assembly, this seemed excessively moist. Once more, no significant performance improvement was realized as a function of increased cathode air pressure (up to 90 psia). However, cell voltage requirement was always less when the cathode air pressure exceeded the anode oxygen pressure (see data points 526-552, Appendix III). An extended current density plot taken during this run is shown in Figure 64.

e. Self-Regulation

Consideration of the response times of temperatures and voltages, while operating in the self-regulation mode, ruled out complete wide-range performance evaluation. Several long-term runs would be required to obtain wide-range performance data. The equilibrium temperature attained by the concentrator is dependent upon air flow rate and pressure, current density, and voltage.

The analysis of thermal equilibrium previously described in Section II was used as a basis for selecting the operating pressure for the first self-regulation run. The desire was to keep the pressure high enough to minimize water consumption rates, yet low enough to maintain reasonable cell temperatures, while operating with no supplementary cooling. Based upon these considerations, a pressure of 10 psia was chosen. To establish the required vapor pressure during preliminary evaluation of the self-regulation principle, Dacron wicking material saturated with a solution of 25% Na_2SO_4 was used. The Na_2SO_4 was necessitated because of Dacron's incompatibility with KOH. Ideally, the required vapor pressure would be established by humidifier wicks saturated with KOH solution of lower concentration than that used in the cell matrix. Since it seemed advisable not to have a two-chemical system, the wicking material was later changed to polypropylene, which is compatible with KOH. Therefore during the long-term, self-regulation test, the wicks were saturated with a 23% KOH solution.

An important point to note is the manner in which the wicks were installed in the stack. One side of the polypropylene is somewhat softer than the other side. In order to

evaluate any difference in performance, dependent on method of wick installation, the wicks were installed as illustrated in Figure 20.

It later became apparent that the wick installed adjacent to Cell 1 provided superior operation. Figure 65 covers the running information of selected parameters during the testing which lasted 59 hours. Data points 353-525, included in Appendix III, provide all data taken during the run. Also included in this data log are notations which indicate adjustments made during the run.

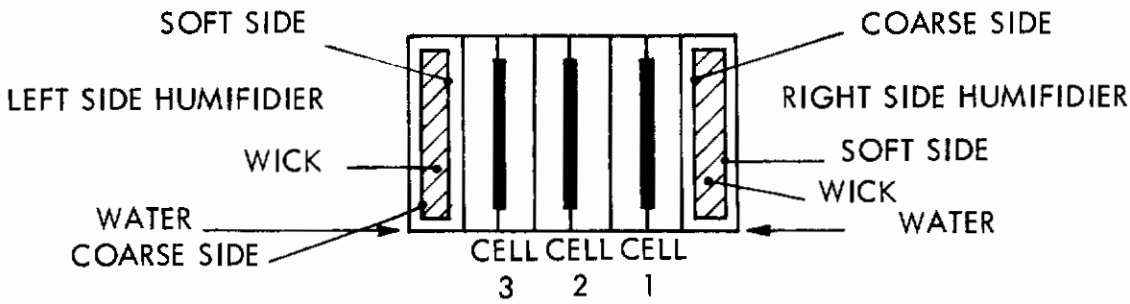

Figure 20 Wick Installation

The run proved that the principle of self-regulation does work. When held in proper moisture balance, the cells performed quite well. Note from Figure 65, that between the running hours 9-13 and 26-45 several extended stable periods were displayed by the cells. Two problems, both centering on moisture introduction, were encountered leading to eventual shutdown of the stack. The first problem was due to the method of water transport from a reservoir to the internal humidifiers. (This was needed to replenish the water vapor carried overboard in the exhaust air. In a final application, water would be condensed from the air, collected and returned to the humidifiers, thus replacing the reservoir.) The second problem encountered during testing was the inability to maintain a consistent reference pressure on the water's surface, so that the required rate of water could be fed to the humidifiers.

Several pressure references were tried before starting the long-term test, but none appeared to have fail-safe characteristics. An increase of the reference would cause the humidifier to flood with water, while a decrease would allow the air to flow out of the humidifier water feed port rather than through the cell. Finally, it was decided to inject water periodically by allowing atmospheric pressure to force water from the reservoir into the 10-psia humidifiers. The need for water was detected by monitoring the dew point of the exhaust air.

The humidifier adjacent to Cell 1 appeared to function properly, but the humidifier adjacent to Cell 3 did not accept water correctly. The water appeared to flow too freely

through this humidifier, without correct wicking, and flowed into the Cell 3 cathode compartment. As a result, Cell 3 became very sensitive to moisture balance. Figure 65 shows several times where all three cells, particularly Cell 3, experienced various degrees of overwet conditions. This resulted in high cell voltages. The introduction of excessively large amounts of water eventually would also affect Cell 2; this can be noted in the plot. From these results, it was concluded that the wicks are best installed with the soft side facing the water entrance port.

When flooding of the cell (or cells) occurred, air flow was increased to aid in lowering the moisture content. This usually resulted in lowering the voltage requirements. After traversing through alternate cycles of drying and flooding, as a result of periodic water injection, Cell 3 failed to recover. At this point, Cell 3 was removed from the electrical circuit. But prior to this, namely during running hours 9-13, the entire three-cell stack operated quite stably under self-regulation. Coincident with the latter hours of testing, a micrometer valve was calibrated and inserted in the water line between the reservoir and humidifiers, thereby allowing make-up water to be fed at selected rates. The valve was successfully integrated near the cessation of testing. By this time however, Cells 2 and 1, having gone through several wet and dry cycles, did not respond to recovery techniques intended to restore the proper moisture content to the matrices. Shortly after 59 hours of continuous running, the unit was shut down. Several periods of stable, self-regulated operation, however, had been experienced. Upon cell disassembly, it was discovered that the packs were quite dry. In fact, electrolyte crystallization was present over some portions of the electrode which tended to minimize the effective area. This crystallization was very likely progressive in nature as a function of alternate wetting and drying and eventually responsible for the unit's inability to recover to previous performance levels. The bipolar plates appeared almost as clean as when originally assembled.

A second attempt at operation under the self-regulation mode proved a good deal more successful. The three cell stack was operated for 142 continuous hours which culminated the testing program of over 235 hours (see Table III). During this run, current densities of 60 ASF were achieved, with all cells requiring less than 0.9 volts terminal voltage. The results of the run are plotted in Figure 66 (three cell voltages with representative temperatures) with the complete data being covered by points 581-636 in Appendix III. Note the very stable voltages displayed in Figure 66. Two items made this test more successful than the 59-hour run. First, an improved, although far from optimum, water feed system was installed which allowed continuous, rather than periodic, water injection to the humidifiers. Second, the wicks were installed in the manner that appeared optimum based on the 59-hour test, that is, the soft side facing the water inlet port. A third item which may have contributed to the success was the fact that the electrolyte loading was 1.75 g/g dry matrix. However, it is felt that insufficient data has been accumulated to allow this judgment.

Although the water feed was improved, it was not prototype in nature, and its inadequacies resulted in both over and under water feed at various times. This led to eventual stack shutdown and is so noted on Figure 66. Generally, the problems that were

encountered took place during unattended operation when hourly data were not taken and adjustments could not be made, or when pressure transients apparently occurred in the shop air supply (used to supply the cathode)causing varying water feed. This is noted at the seventh hour of operation when a decrease in supply pressure allowed excessive water to enter the humidifier chambers. Such transients have apparently permanent deleterious effects. However, in spite of testing difficulties, the successful display of self-regulation lends substance to the projected design of the 0.2-lb O_2/hr unit discussed in Section V.

Upon disassembly of the unit, it was found that the packs were quite moist. Cell 1 anode showed signs of having been flooded with liquid, which occurred during the last unattended operation (see Figure 66). These signs included some small, but rather wet, coagulations of platinum separated from the electrode, and a pack that was overly wet compared to Cells 2 and 3. In general, the other plates appeared as they had prior to assembly, except that one area in a wick plate which had been previously corroded and repaired with epoxy showed signs of shedding its epoxy patch. Although the principle of self-regulation has been established, it is recommended that this same hardware be subjected to several additional long-term self-regulation tests to amplify life data while providing more insight into the design and operation of a prototype water system.

f. Test Conclusions

The desired result of a parametric test program of the nature undertaken is that sufficient evidence is gathered which gives guidance to allow projection of the hardware design into the next phase of performance. This includes establishing the strong points of the design, opening areas for possible additional investigation, as well as identifying the pitfalls which should be avoided. It is believed that these goals have been achieved. It is felt that the principle of self-regulation has been shown to be feasible and a foundation for a higher capacity unit incorporating this design feature has been laid. Specifically, the test program served to indicate the distinct performance improvement with temperature; the difficulties of water management when high specific humidities are required; the lack of performance improvement with increasing pressure, pointing to a possible limit in cell performance to be found elsewhere, as yet unidentified; the care that will have to be taken in designing a water feed device for the self-regulated concept; the possibility of additional electrolyte loading investigation; and finally, the desirability of more life testing while operating under self-regulation.

4. CELL COMPRESSION

During the initial assembly of the concentrator, the thickness of the eight-piece stack was measured after successive tightenings of the bolts from 6-to 30-lb-in torque. At 6-lb-in torque, a bowing of the assembly was observed, evidenced by the fact that the thickness of the stack was 1.584 inches along the ends and 1.627 inches at the center. After tightening the bolts to 30-lb-in torque, the end thickness was 1.565 inches and the middle thickness was 1.573 inches. The degree of bowing had been reduced from 43 mils to 8 mils.

Leak tests made at different torque loadings on the bolts showed that the cell assembly was leak-free at the low-torque as well as at the high-torque loadings. A major result from the increased torque on the bolts was a lowering of the ohmic resistance of the individual cells. Specifically, the three cell stack resistance decreased from 4.3 to 3.1 ohm square centimeters when increasing the stack bolt torques from 20 to 30 lb-in. The net effect is a 28% power reduction during cell operation.

In Table VI are summarized the cell thickness measurements as taken at various stations throughout the test program. Note that the cell stack was always thickest at station F. This station is in line with the porting arrangement and associated O-rings of the stack, and the extra thickness at this station is probably due to compressive resistance of the O-rings.

During the final compression measurements taken on the three-cell assembly used for data points 526-552 (see Table VI) a "clay plug" gasket compression measurement was also conducted. Small holes of 1/16-inch diameter were punched in one of the gaskets between each bolt hold (24 holes in all). During assembly a small clay plug was inserted in each hole. The object was that the plugs would deform to match the gasket compression during assembly and could be measured upon disassembly to determine operating compressions. The sketch in Table VI indicates the location of the plugs. Starting in the upper left corner and traveling clockwise, they were numbered 1-24. Upon disassembly, it was found that plugs 1-22 measured in the range of 25-29 mils, with the majority being 26 and 27 mils, thus indicating a 3 to 4-mil compression. However, plugs 23 and 24 measured 32 and 31 mils, respectively, which indicated no compression in this area. This coincides with the largest outside dimension readings at stations F and G. If such assemblies had been consistent throughout the test program, this may have contributed to the inability to consistently hold pressure differentials above 5 psia. Future concentrator designs must consider this aspect carefully.

5. OXYGEN PURITY

Initial oxygen purity measurements were made by performing Coulomb balances. By measuring the current used to power the concentrator, and the time over which the current was applied, theoretical oxygen output was calculated with the aid of Faraday's Laws. Comparing this number to the experimentally measured volume of oxygen generated during this time is a measure of the purity of the generated gas. Typical results of these measurements are presented in Table VII. Moisture, temperature, and pressure corrections were made in the measured data.

The difference in the calculated and measured volumes is approximately 1%. This indicates that the generated gas is only oxygen and that impurities, either from leaks through the membrane or generation of gases other than oxygen, probably had not occurred. These initial measurements were later supplemented with analyses from a Beckman E-2 analyzer. For example, during an initial one-and-one-half hour test run, after a cell reassembly, six data points indicated a gradual increase in output stream oxygen purities ranging from 99.11 to 100.00%. The collected and calculated volumes

Table VI Compression Data

Station	1.* 1-64 2. 3 3. 30/30 4. 13/40	1. 65-100 2. 1 (3) 3. 20/16 4. 19/40	1. 101-136 2. 1 (3) 3. 10/9 4. 18/30	1. 137-172 2. 1 (3) 3. 30/30 4. 18/35-40	1. 173-352 2. 1 (3) 3. 30/25 4. 18/34	1. 353-525 2. 3 3. 30/30 4. 22/30	1. 526-552 2. 1 (1) 3. 30/30 4. 22/30
	Assembled Stack - Outside Dimensions (in)						
A	1.553	0.818	0.808	0.830	0.825	1.556	0.833
B	1.540	0.816	0.806	0.819	0.812	1.550	0.820
C	1.562	0.823	0.817	0.827	0.824	1.560	0.836
D	1.552	0.824	0.812	0.831	0.824	1.552	0.836
E	1.557	0.823	0.812	0.831	0.822	1.553	0.836
F	1.567	0.826	0.818	0.839	0.830	1.564	0.832
G	1.556	0.825	0.817	0.833	0.829	1.558	0.837

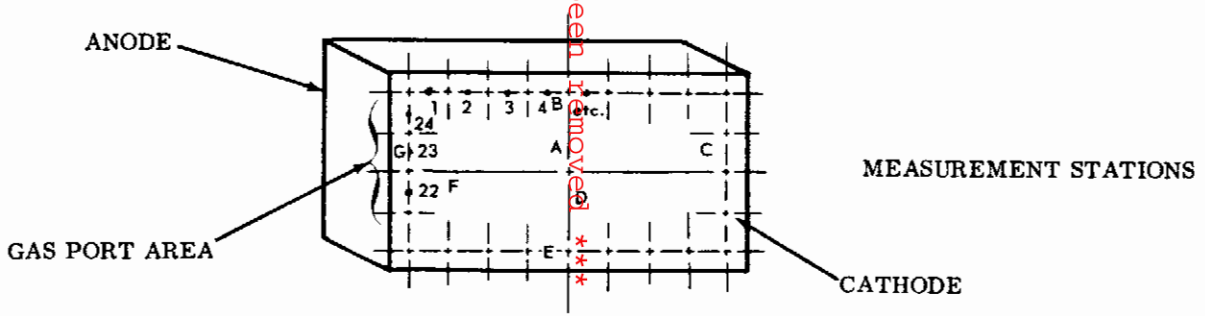

1.* Test data points covered with stack assembly
2. Number of cells in stack (Cell No.)
3. Uncompressed matrix thickness (mils)/uncompressed gasket thickness (mils)
4. Number of bolts/Bolt torque (lb-in)

Table VII Coulomb Measurements of Oxygen Purity

Applied Current (Amps)	Collection Time (Seconds)	Experimental Collected Volume (cc)	Calculated Volume (cc)
5	300	305	308
2	600	250	247

of oxygen generated within this same time period agreed within 0.1% of the other. Repeated measurements taken during initial trials showed that the output stream always had an oxygen purity greater than 99%. Following the corrosion problem encountered during the parametric testing, the oxygen purity readings became erratic as a result of intercell leakage and thus failed to provide meaningful data.

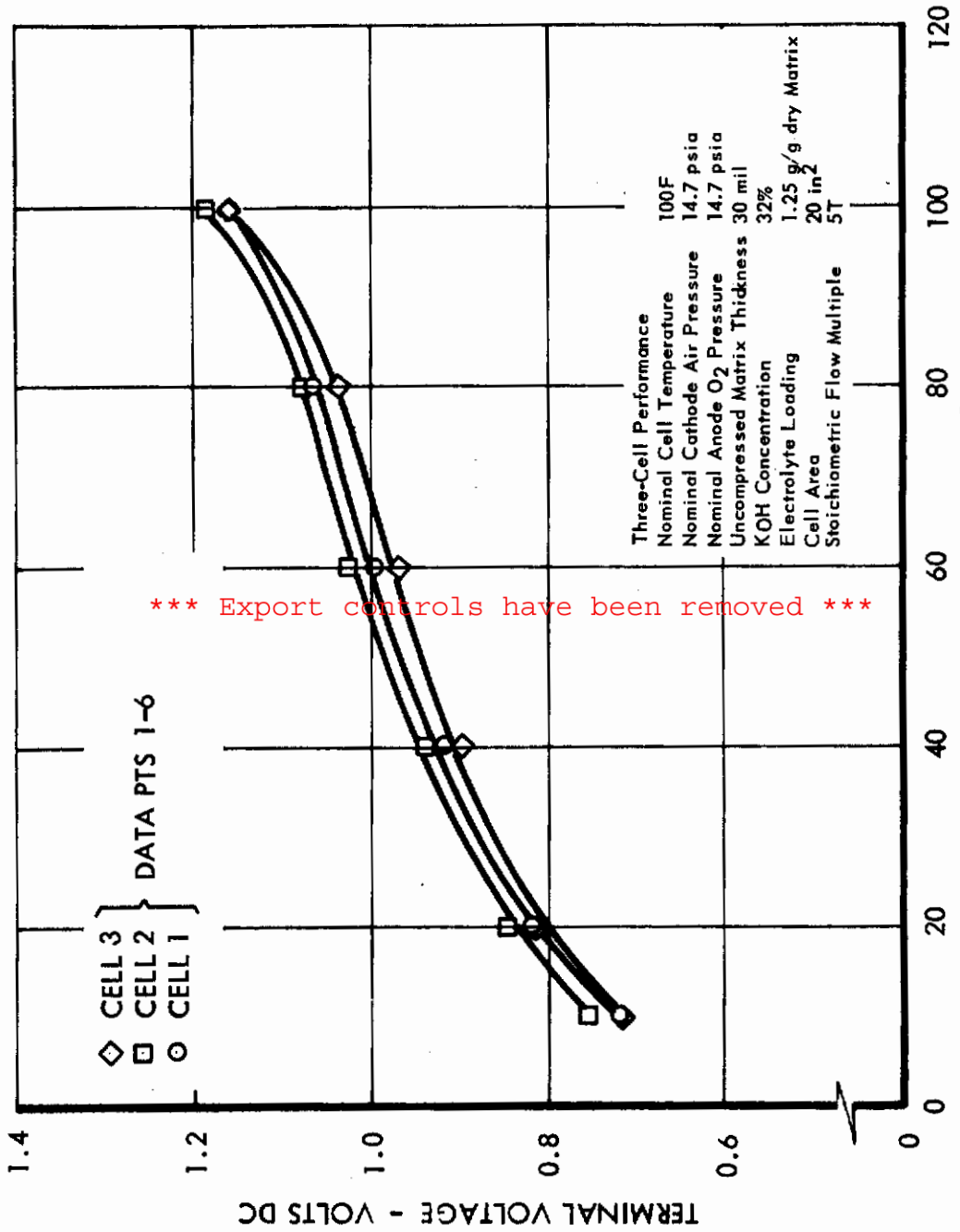

Figure 21 Reduced Data Plot

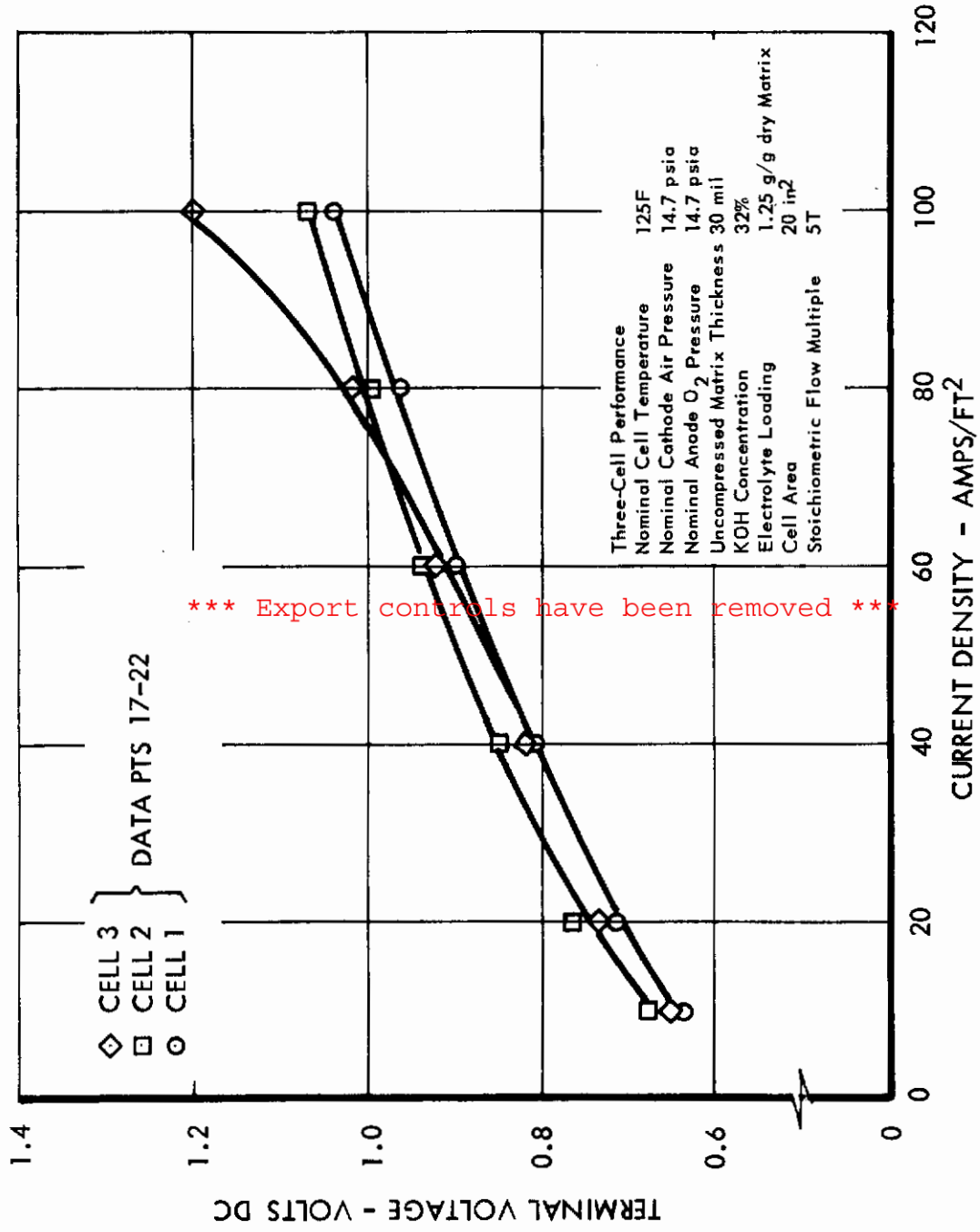

Figure 22 Reduced Data Point

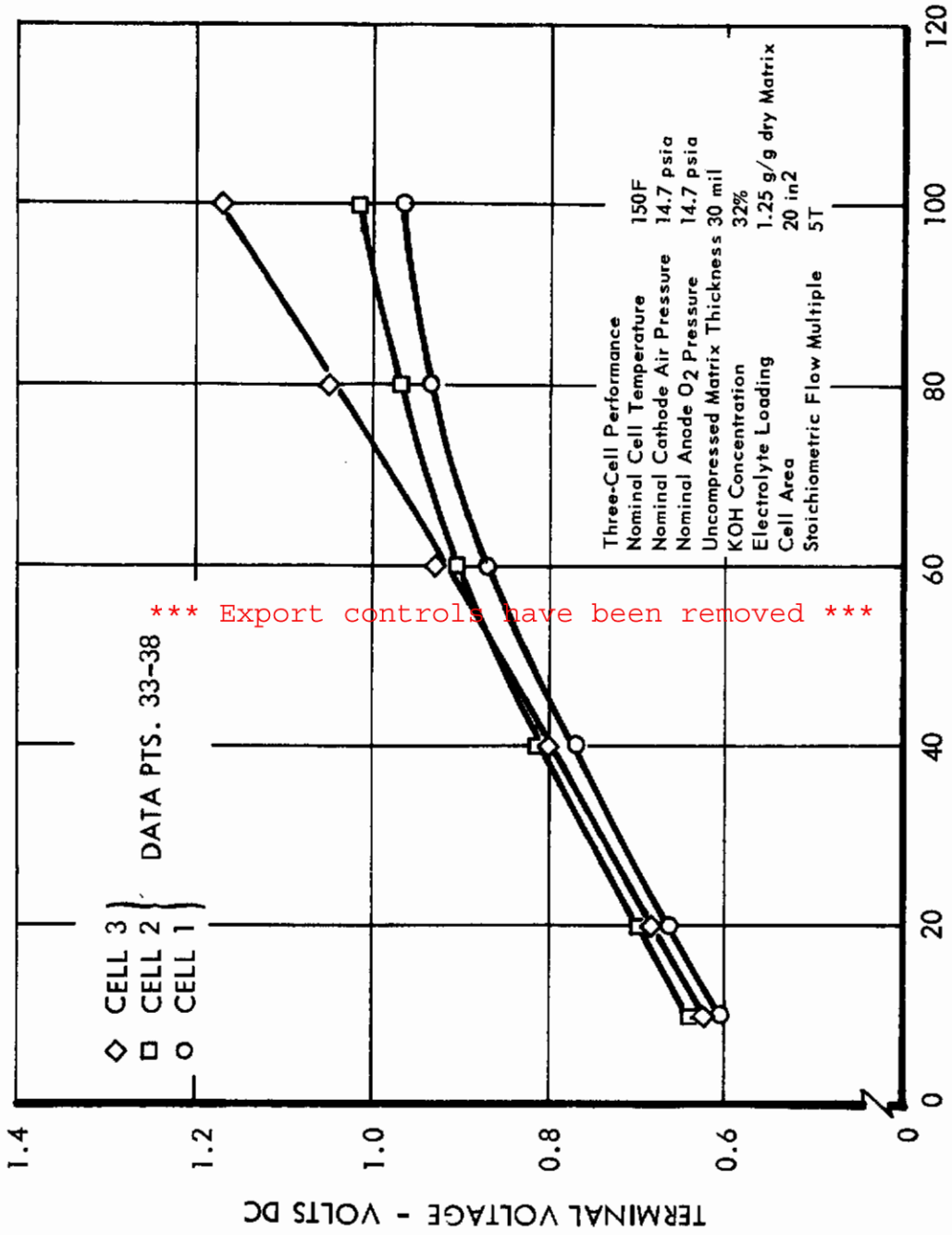

Figure 23 Reduced Data Plot

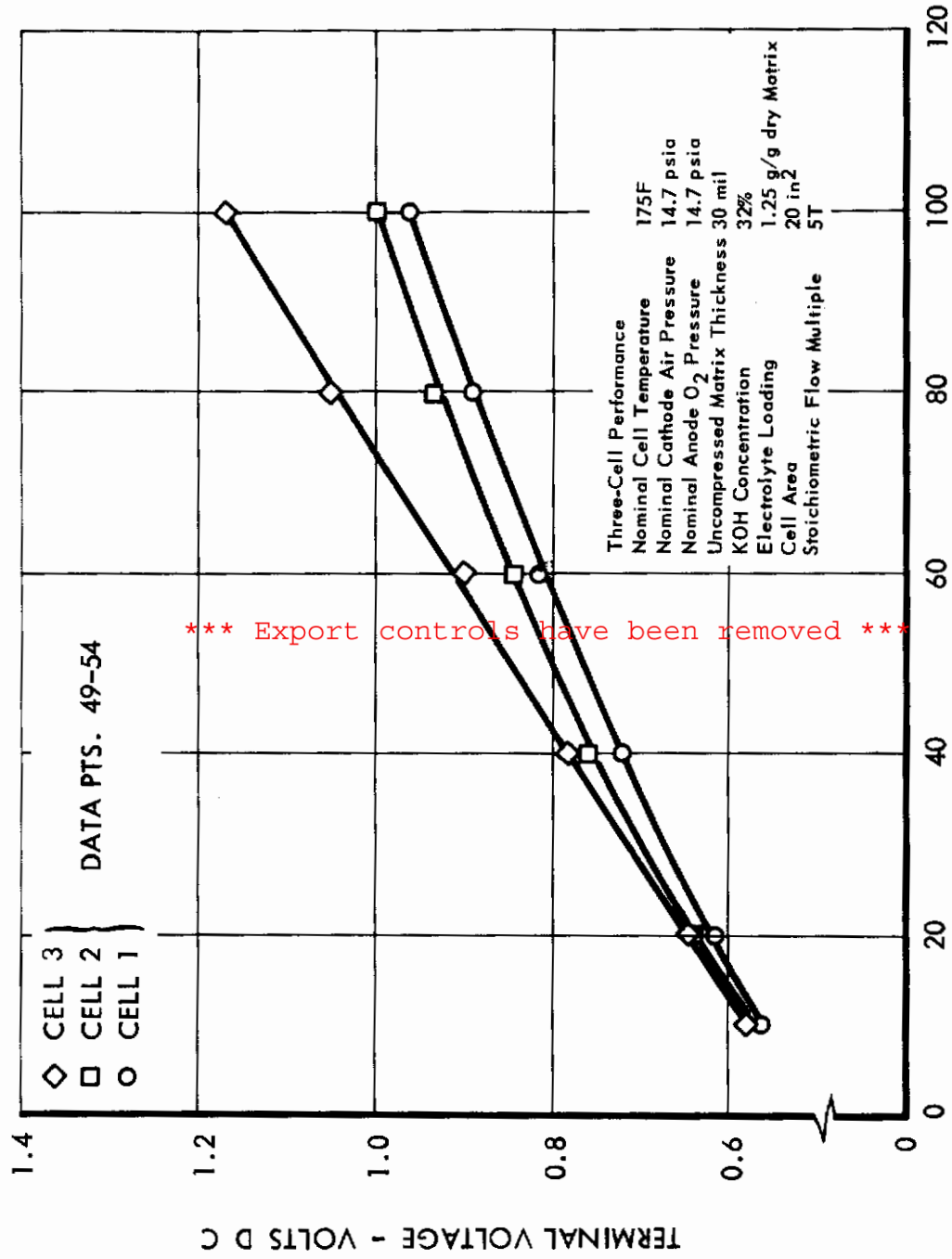

Figure 24 Reduced Data Plot

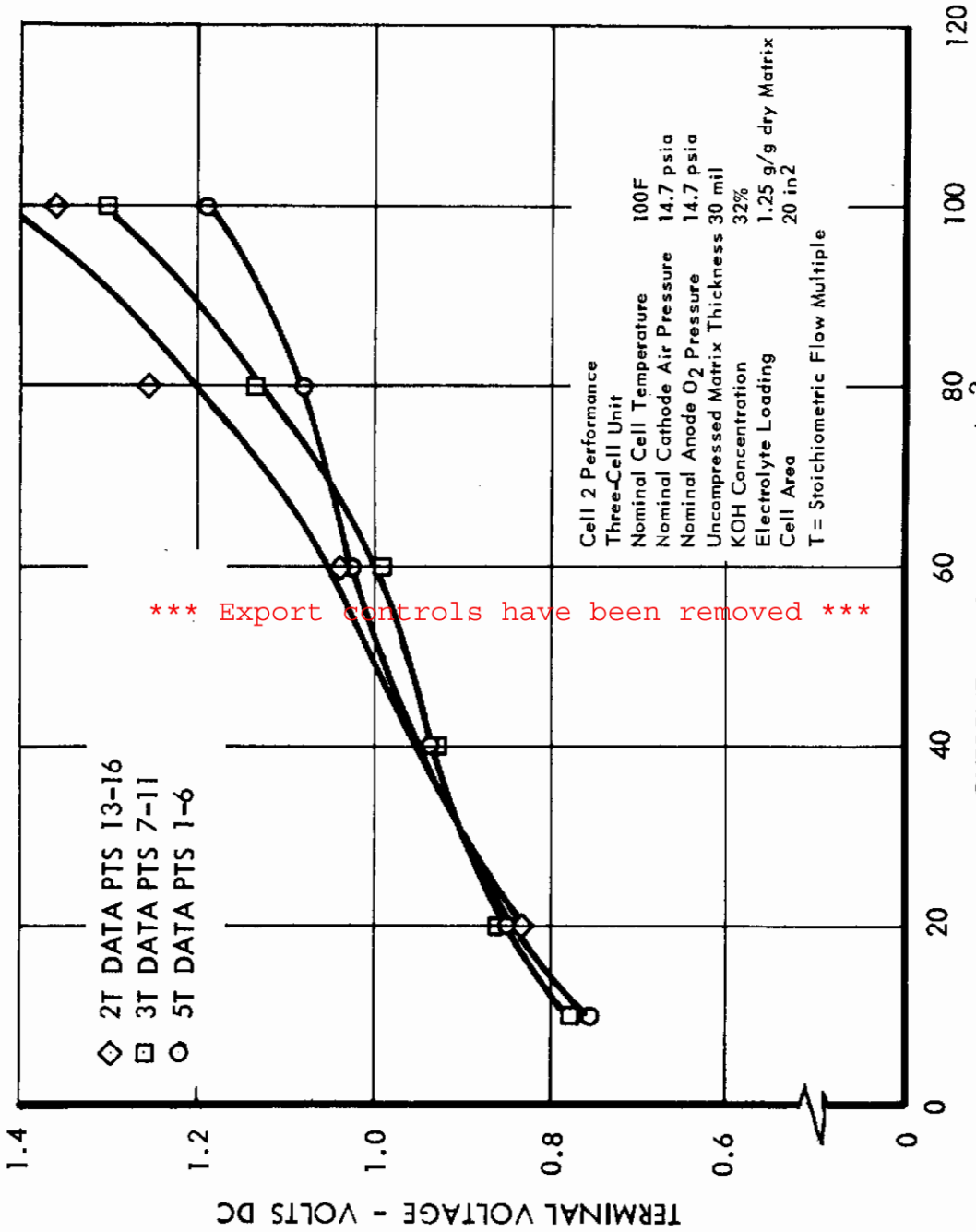

Figure 25 Reduced Data Plot

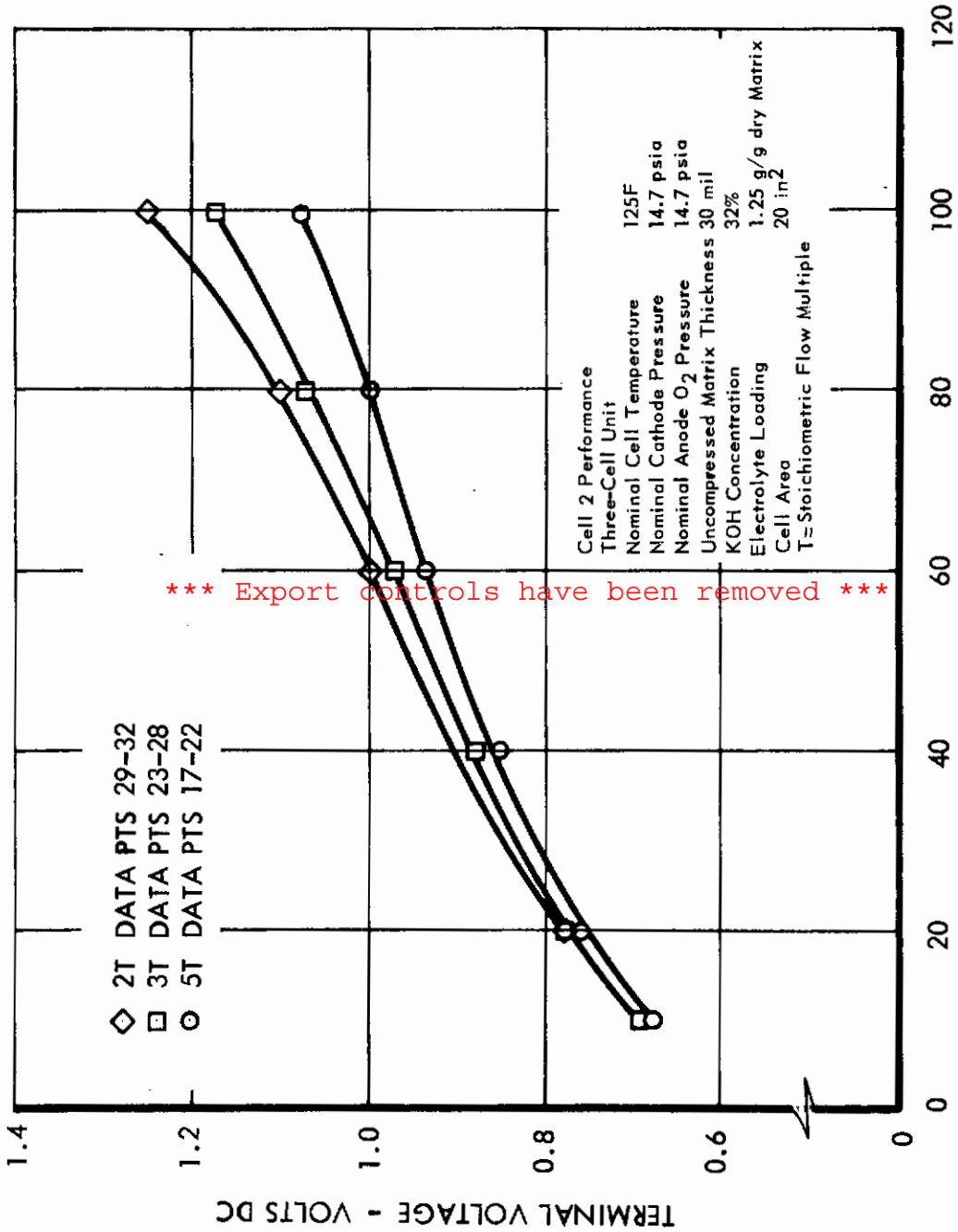

Figure 26 Reduced Data Plot

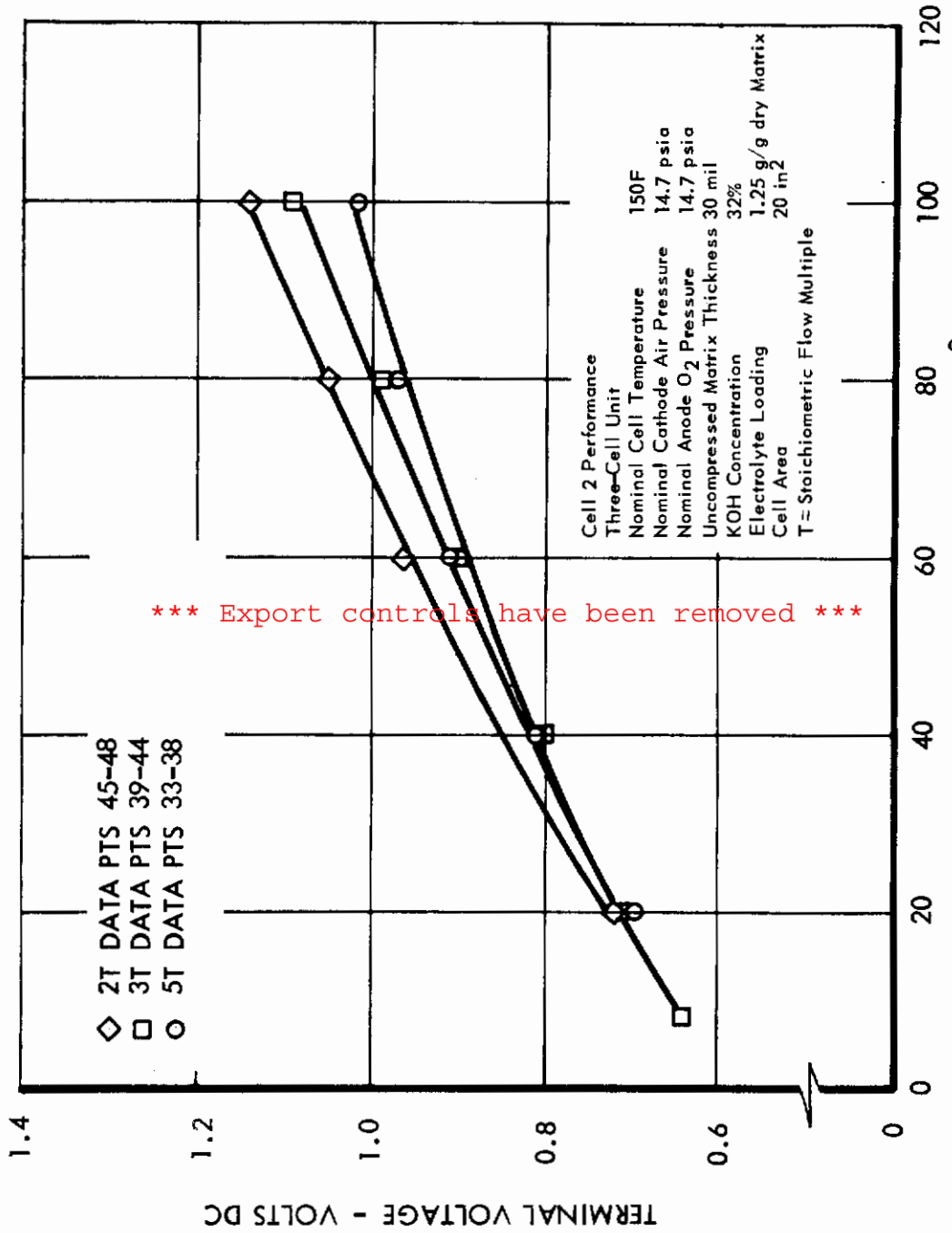

Figure 27 Reduced Data Plot

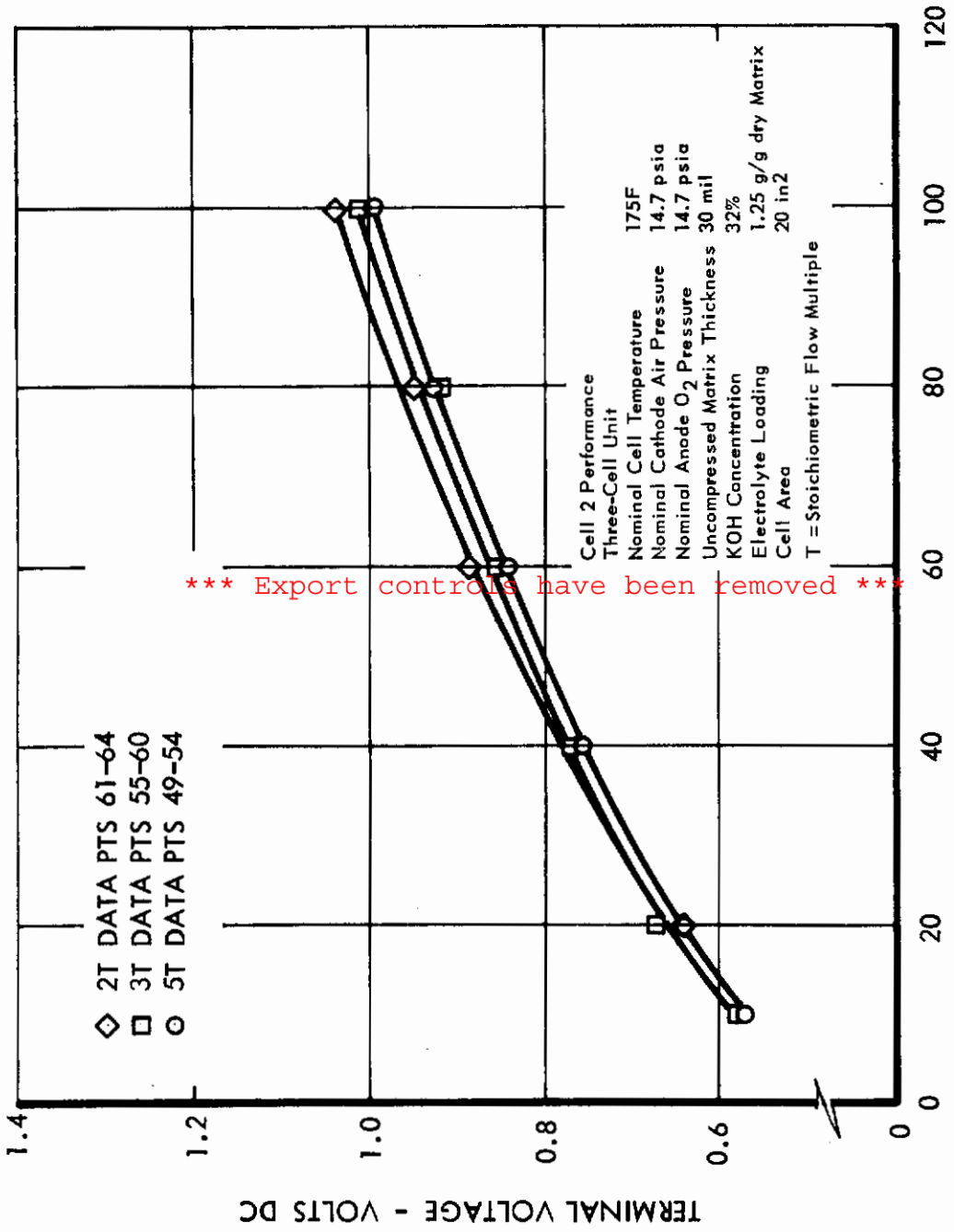

Figure 28 Reduced Data Plot

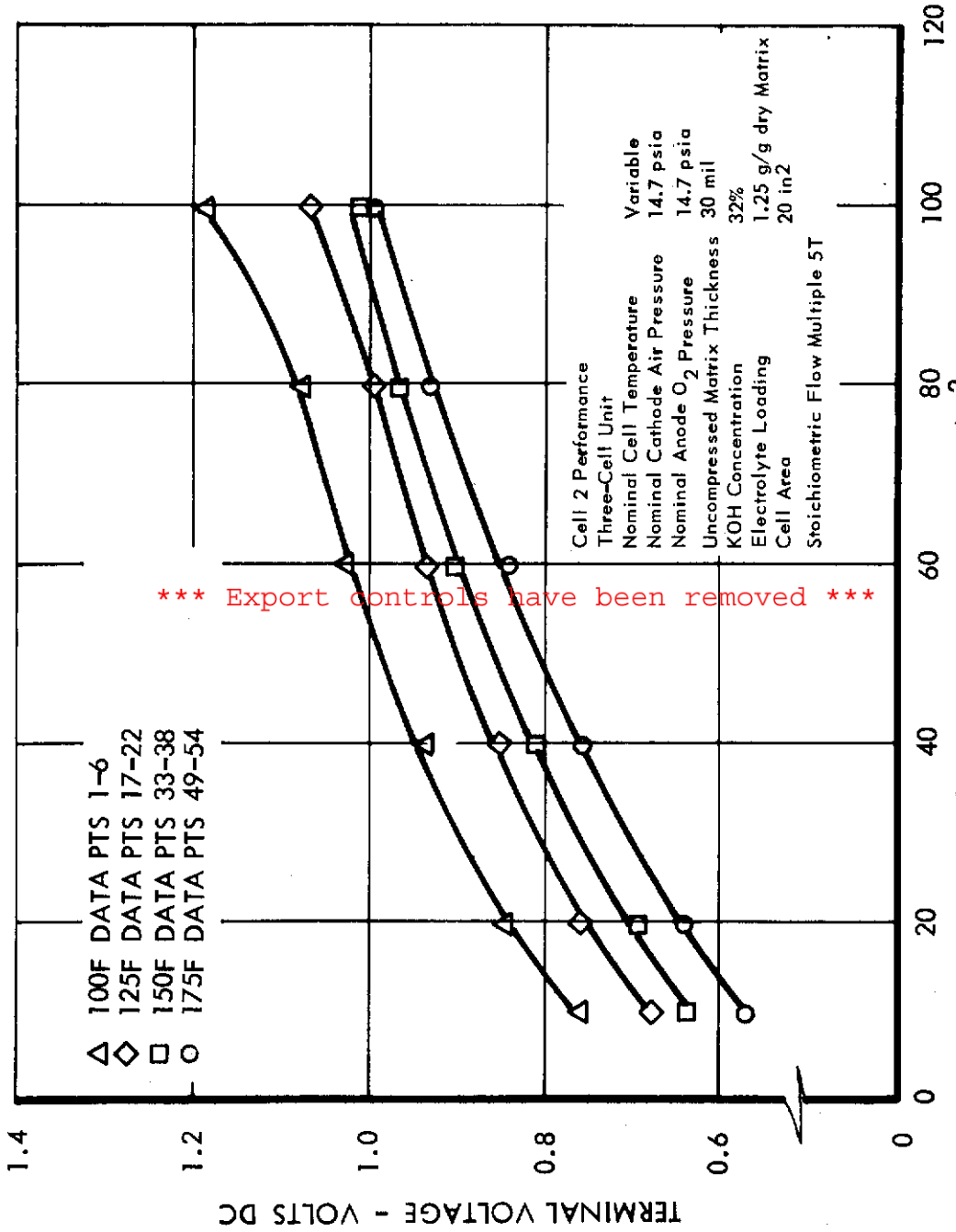

Figure 29 Reduced Data Plot

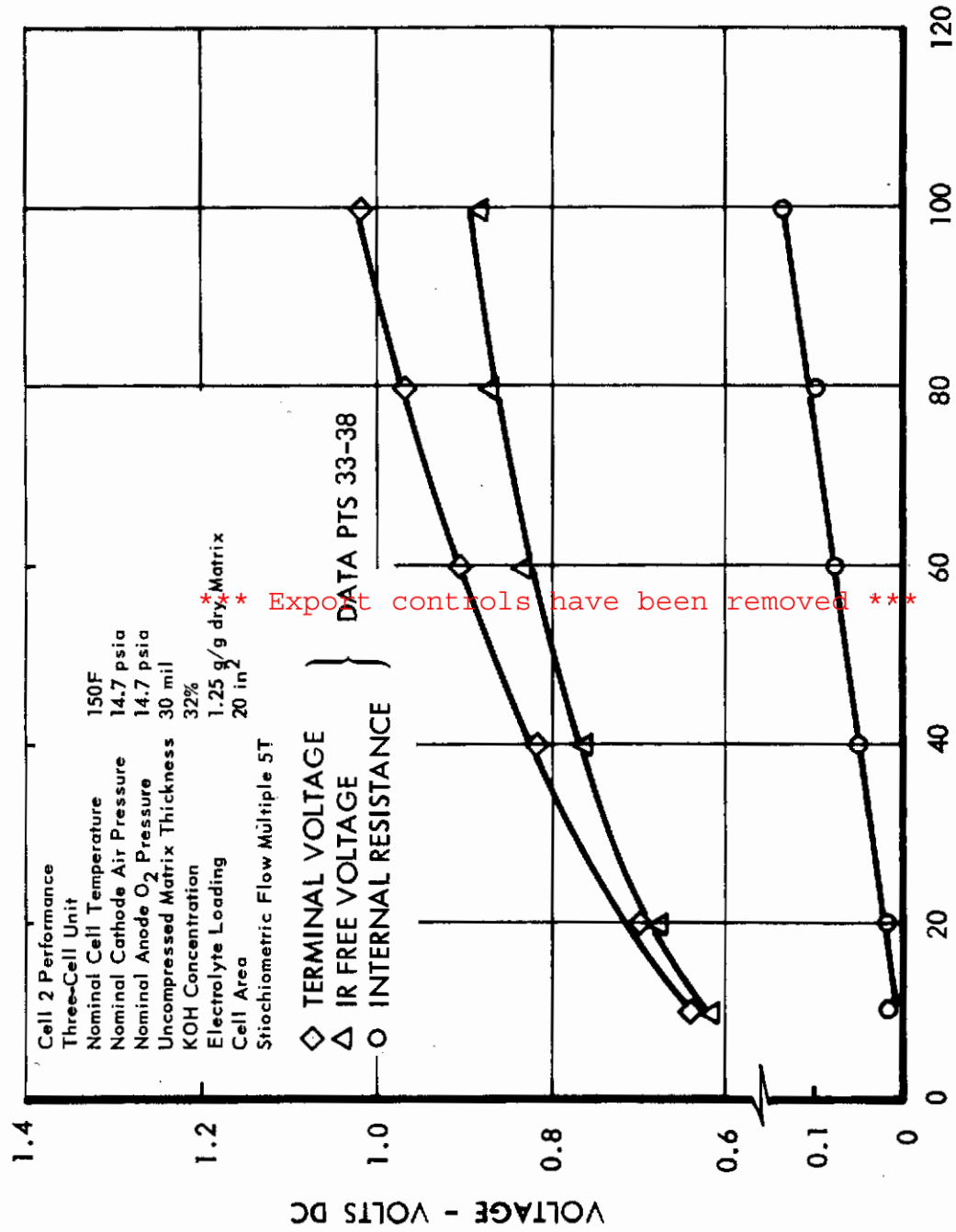

Figure 30 Reduced Data Plot

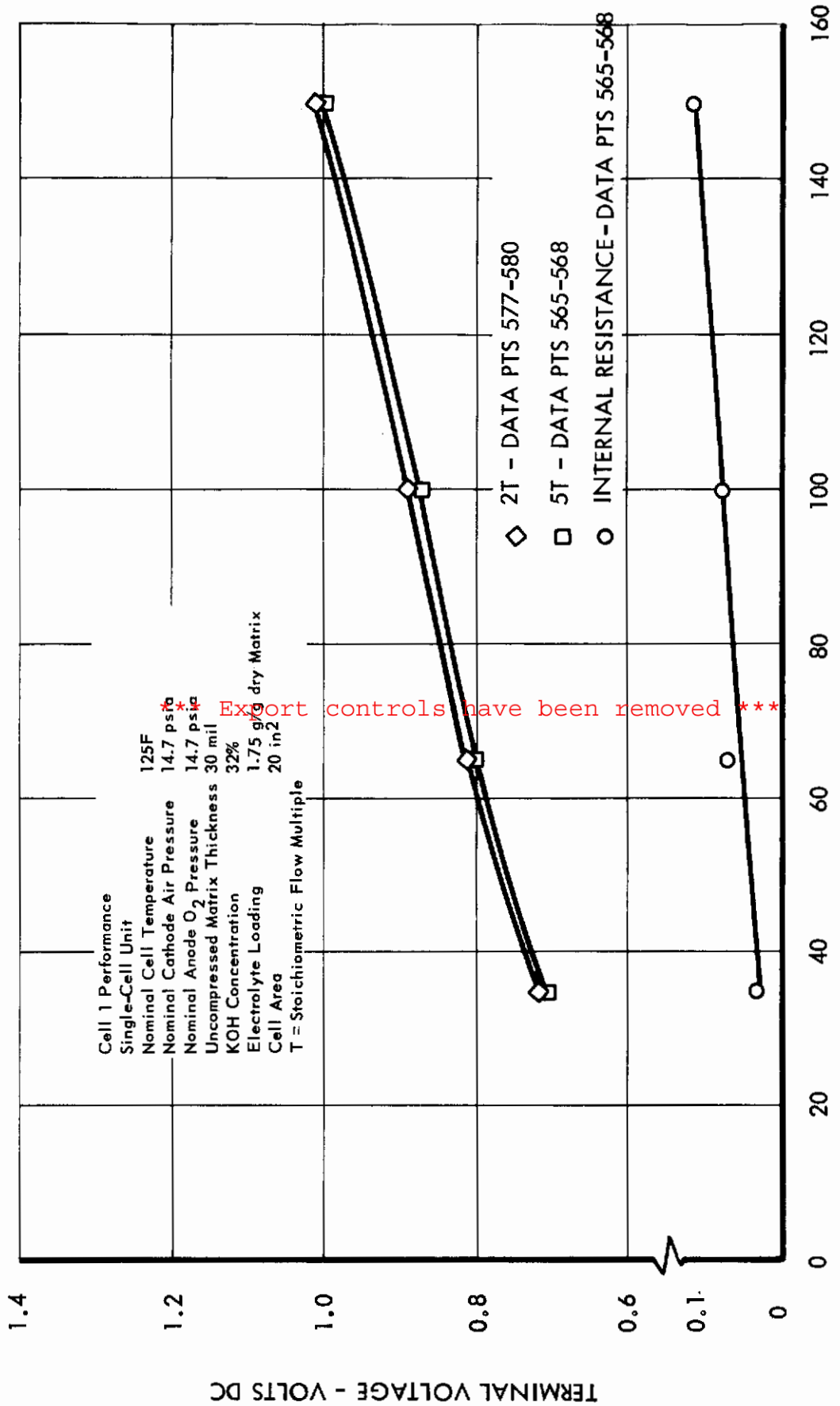

Figure 31 Reduced Data Plot

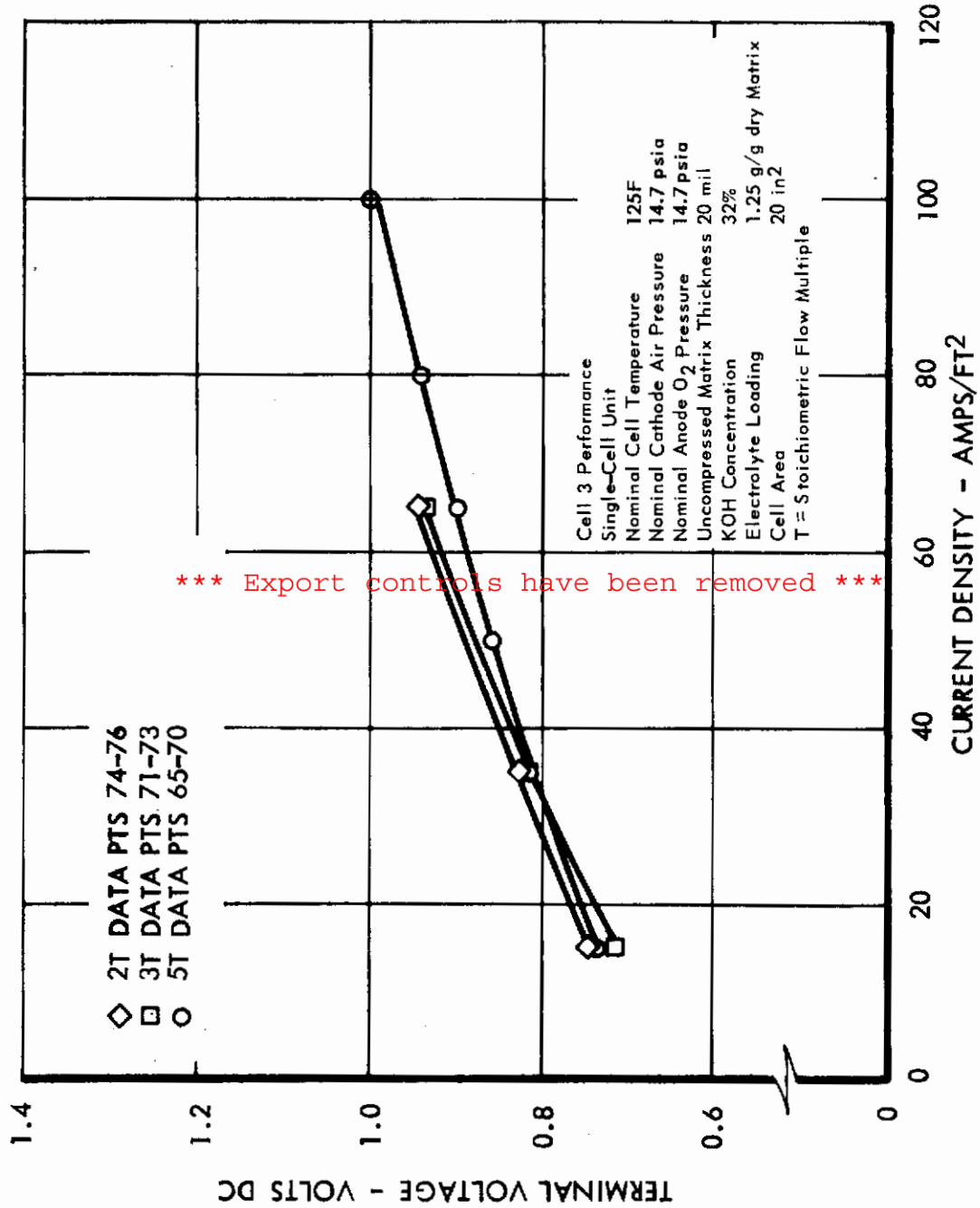

Figure 32 Reduced Data Plot

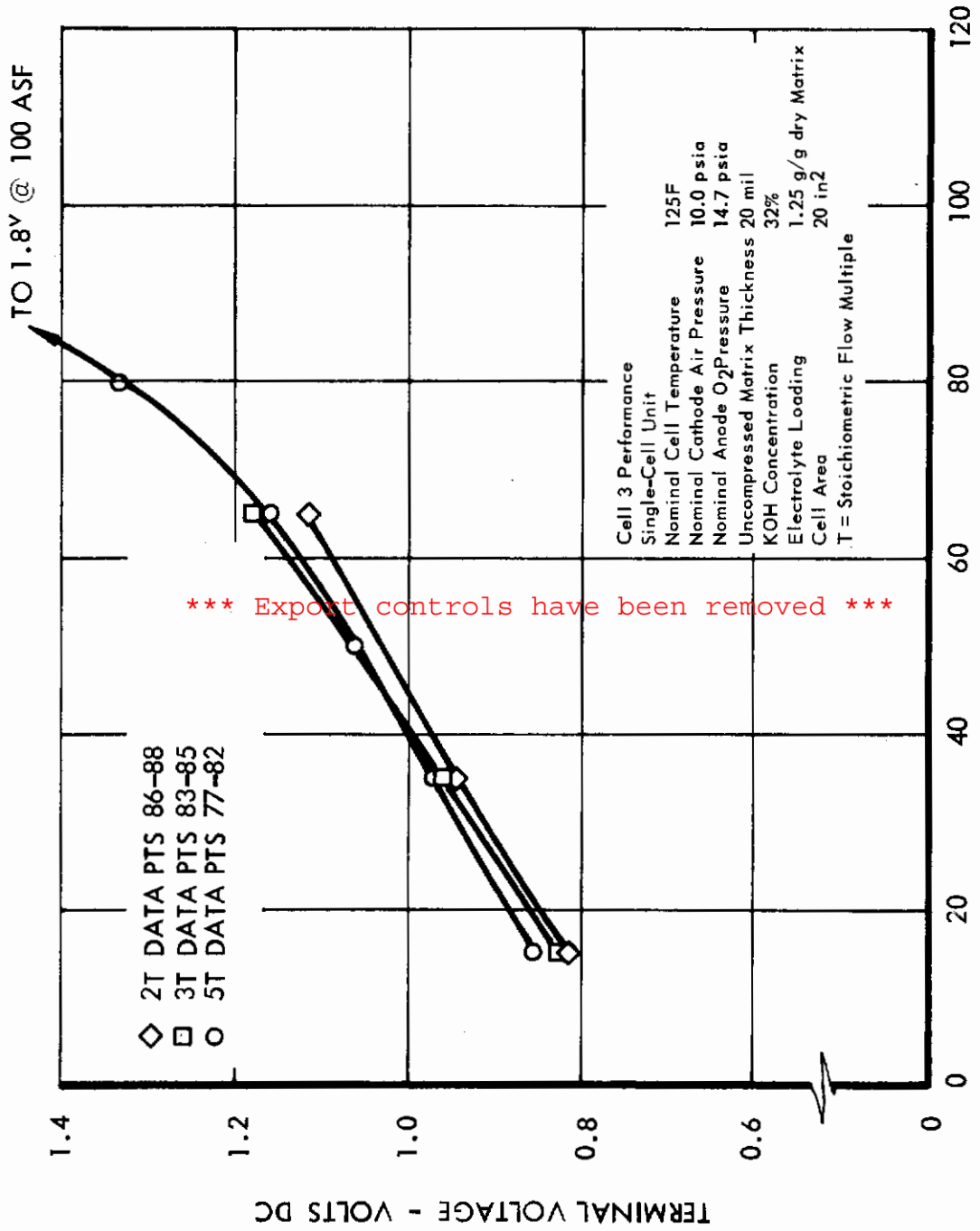

Figure 33 Reduced Data Plot

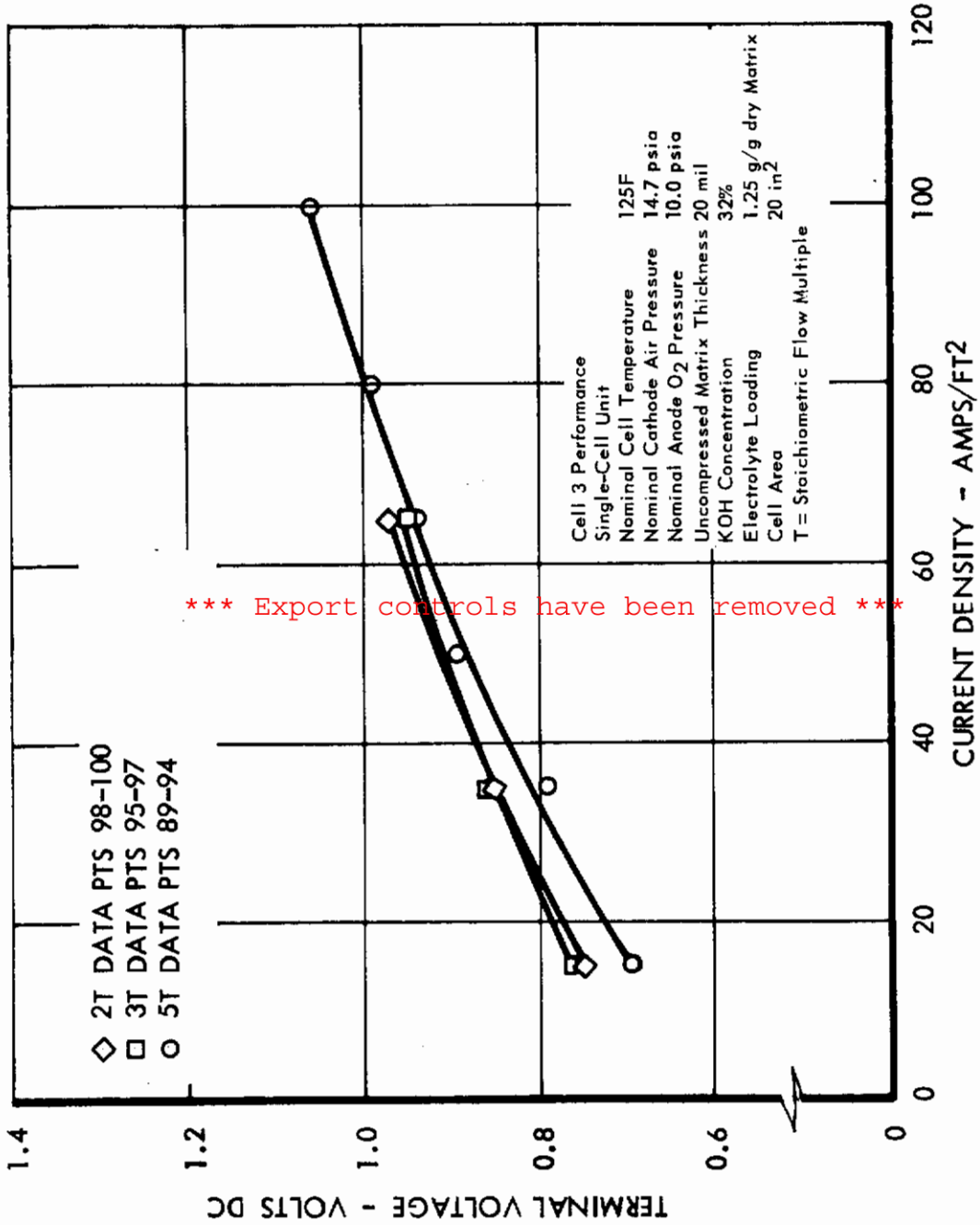

Figure 34 Reduced Data Plot

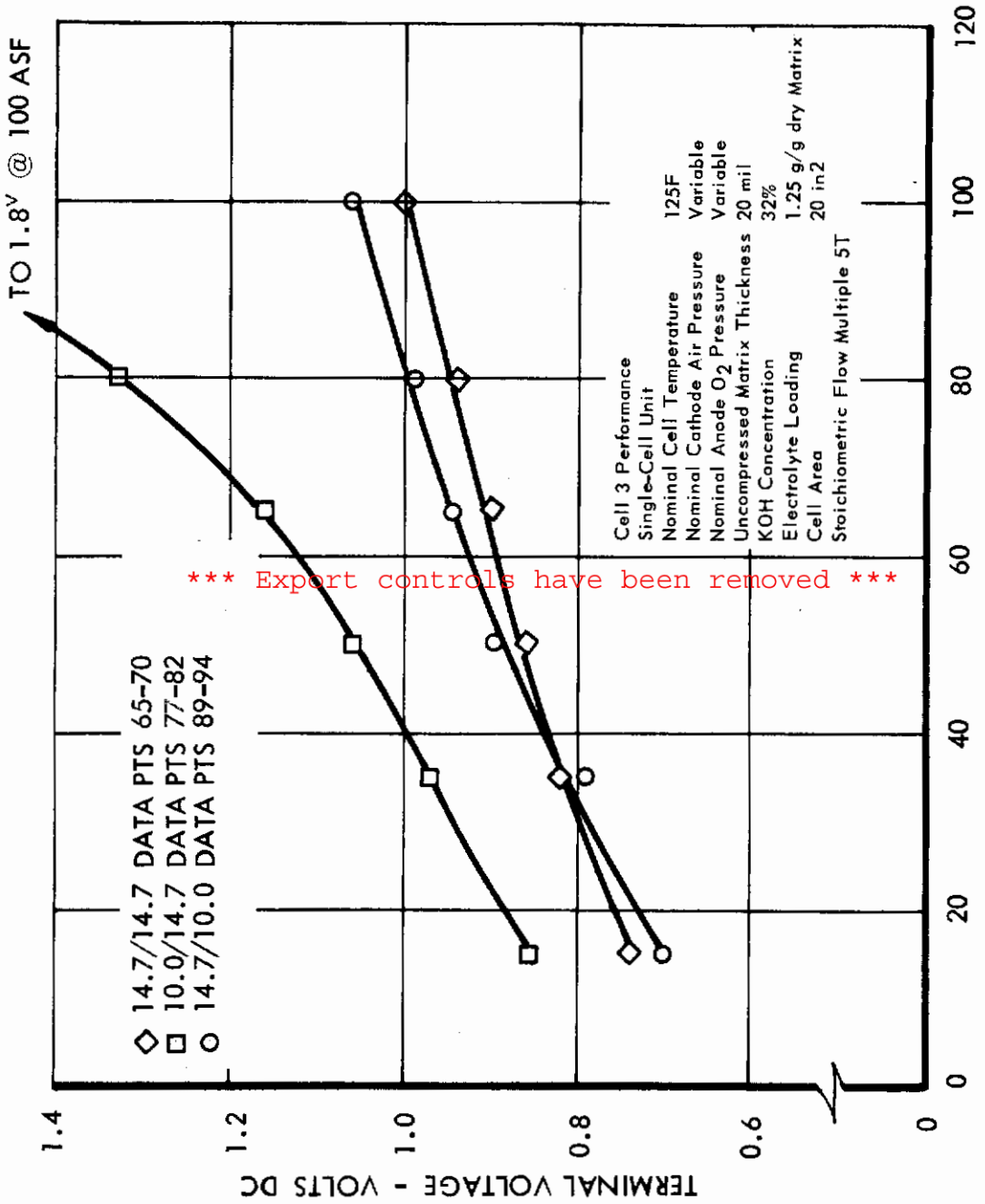

Figure 35 Reduced Data Plot

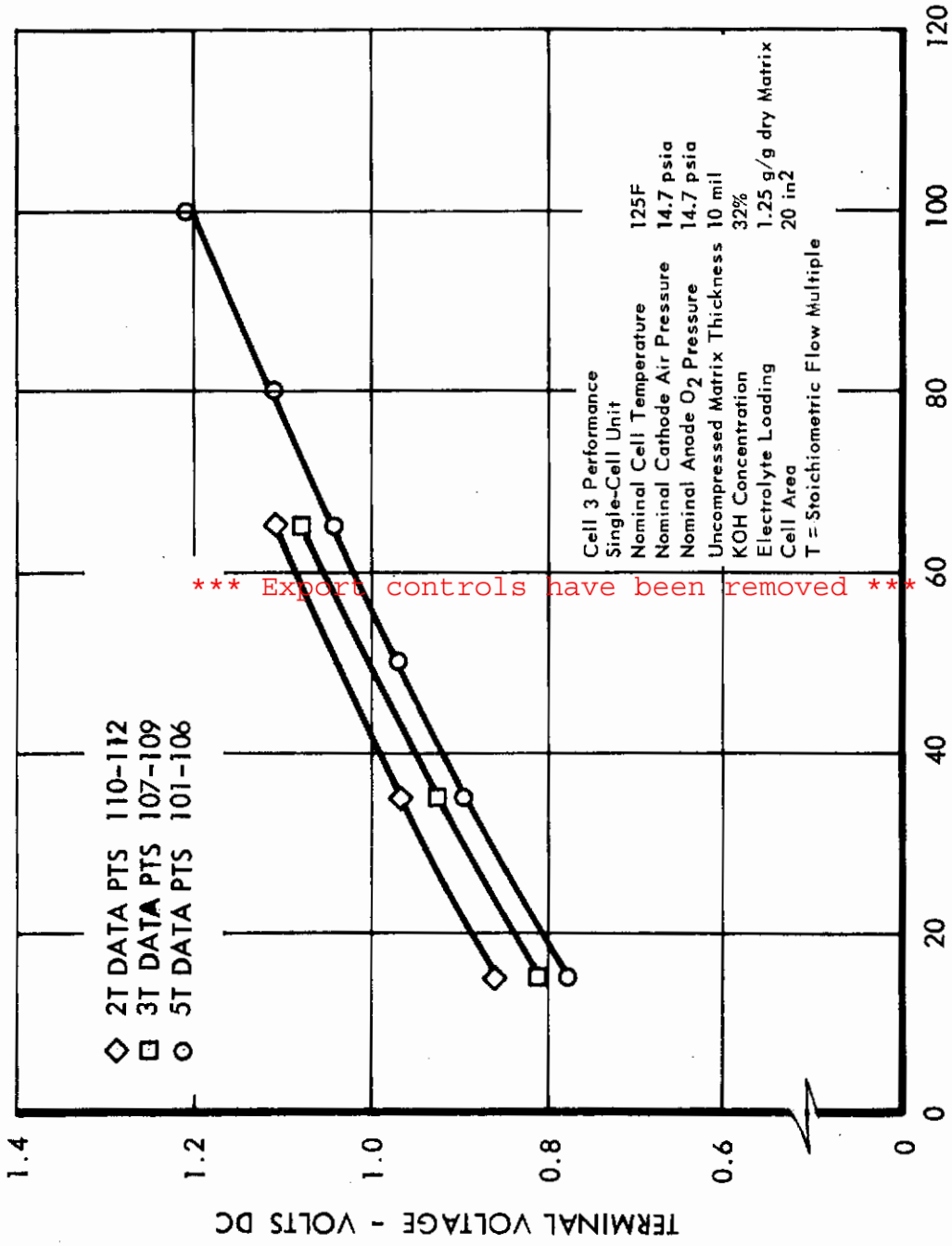

Figure 36 Reduced Data Plot

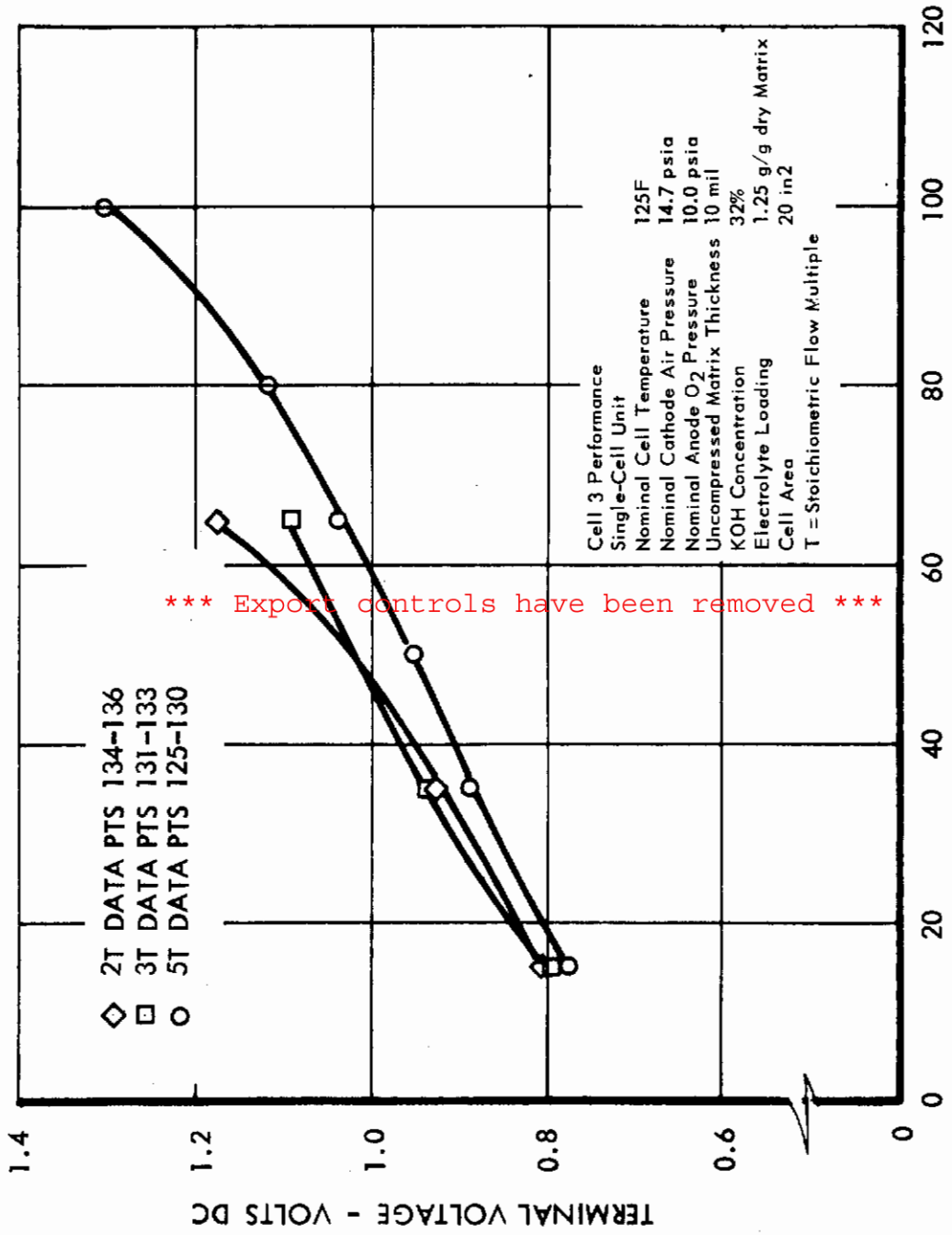

Figure 37 Reduced Data Plot

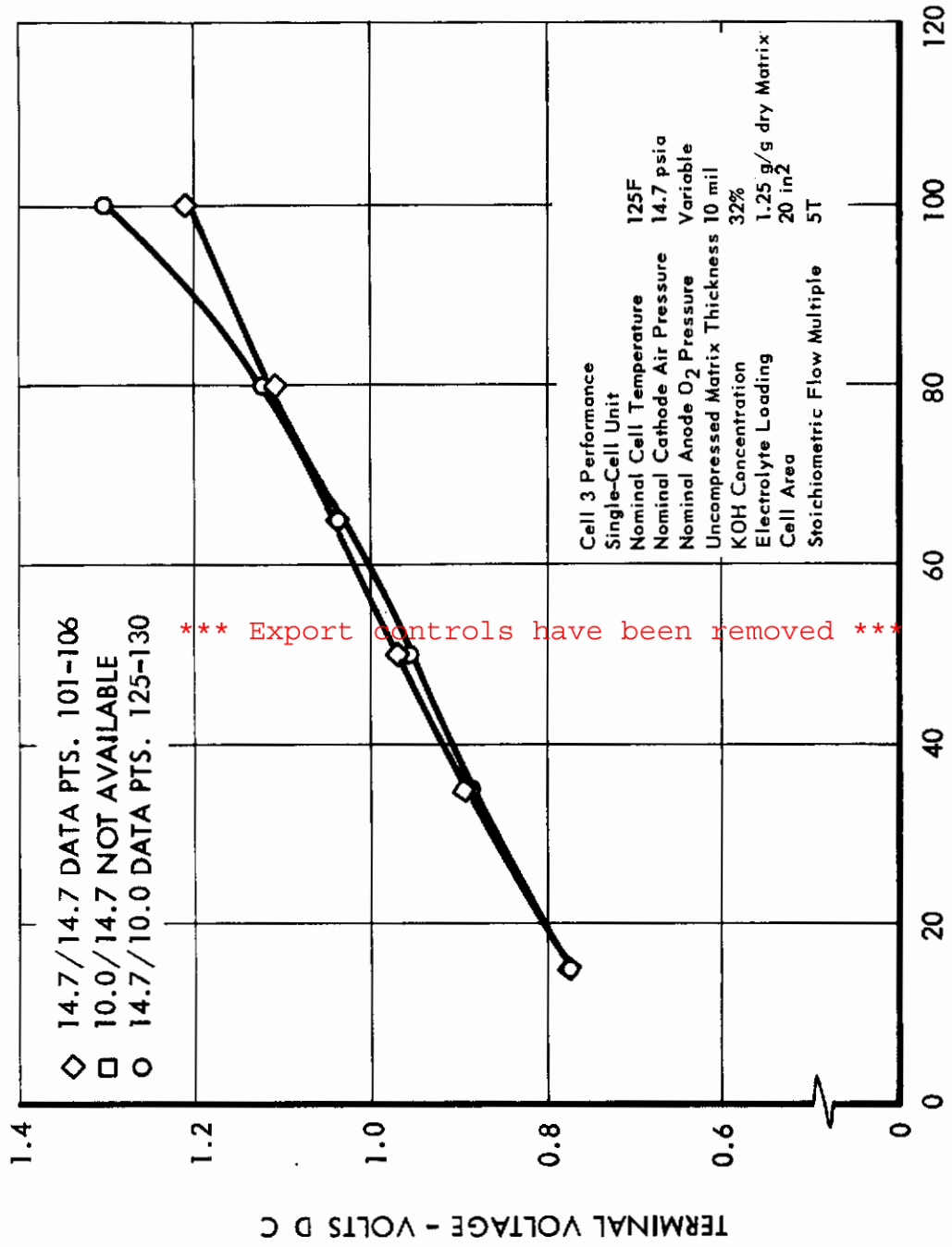

Figure 38 Reduced Data Plot

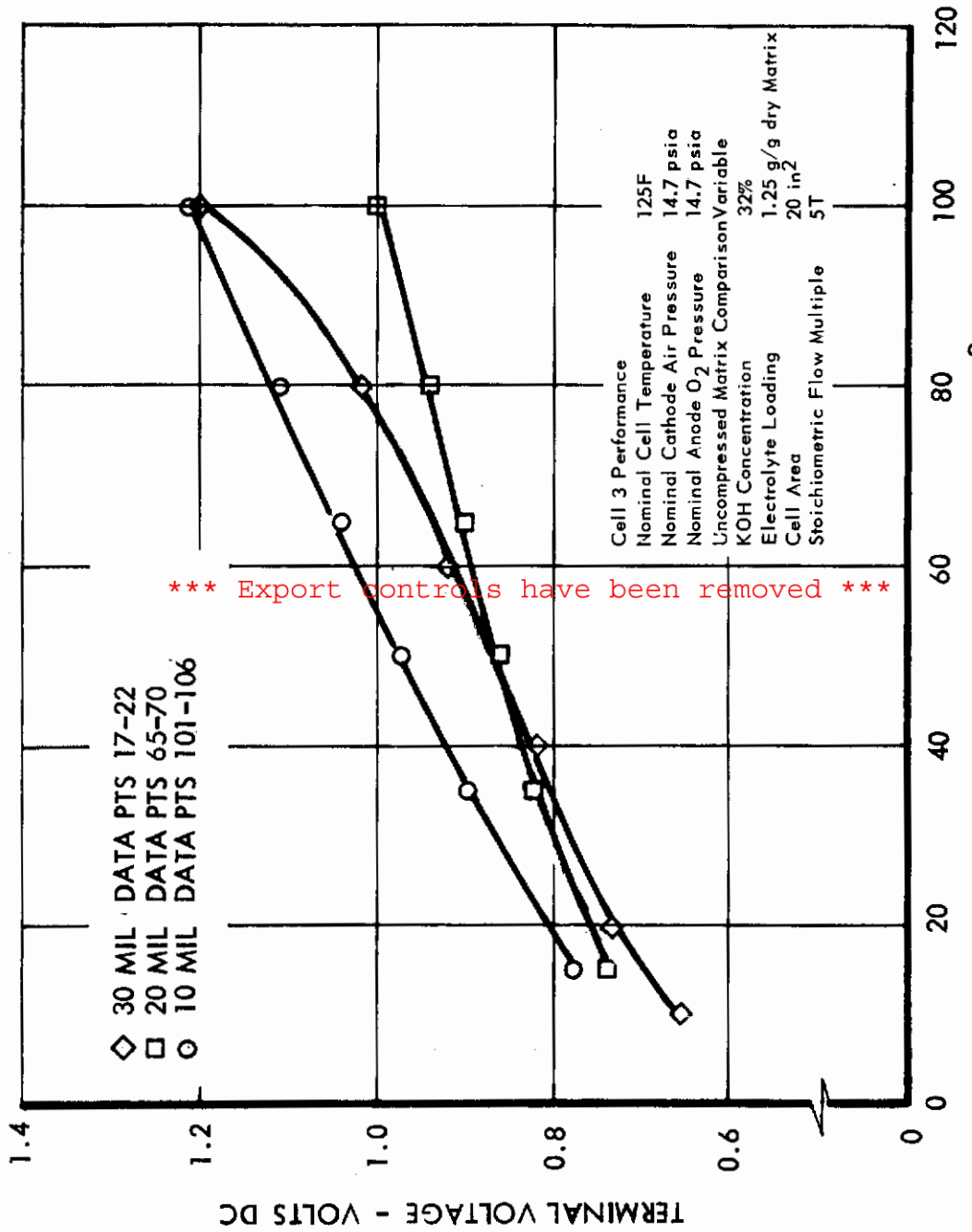

Figure 39 Reduced Data Plot

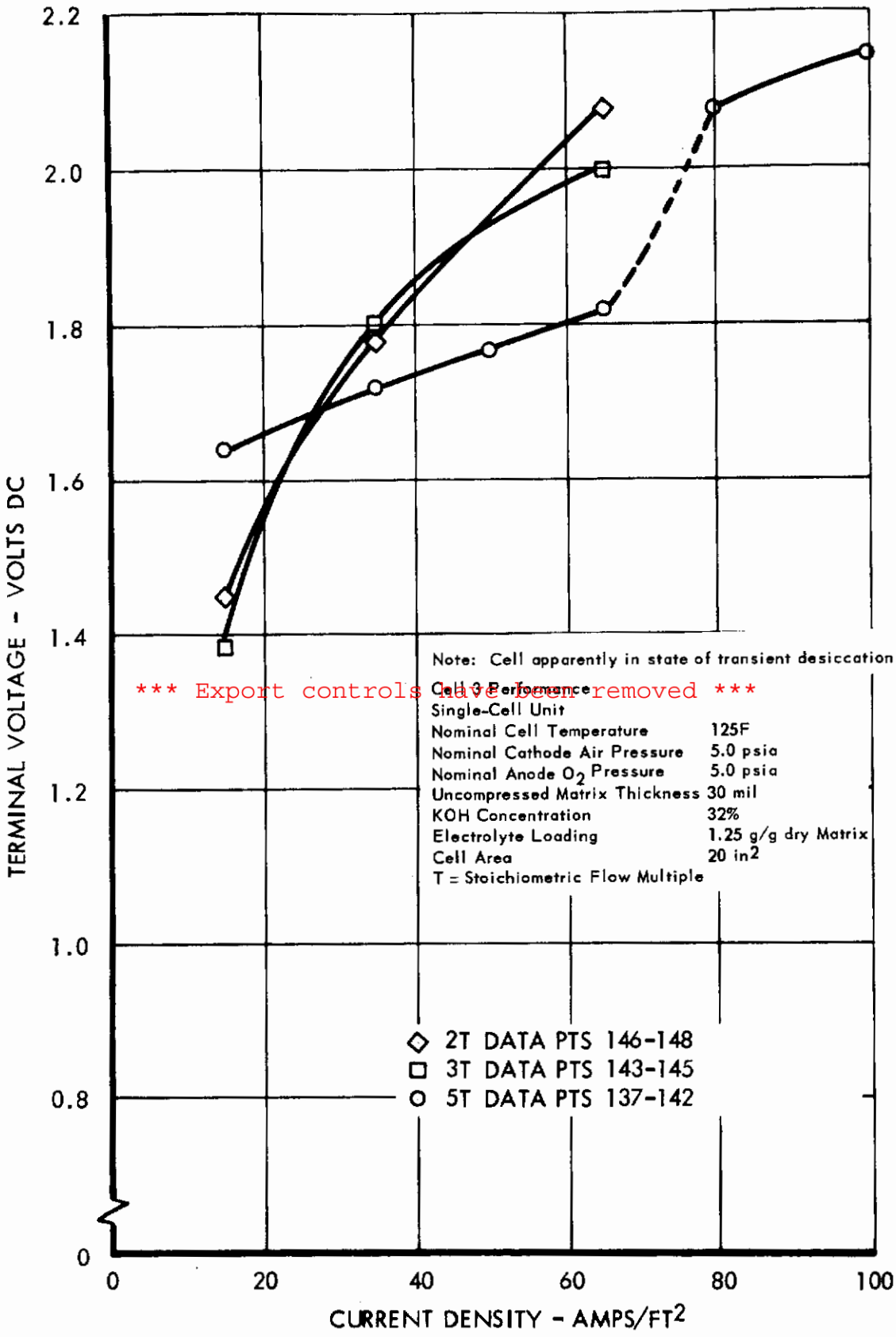

Figure 40 Reduced Data Plot

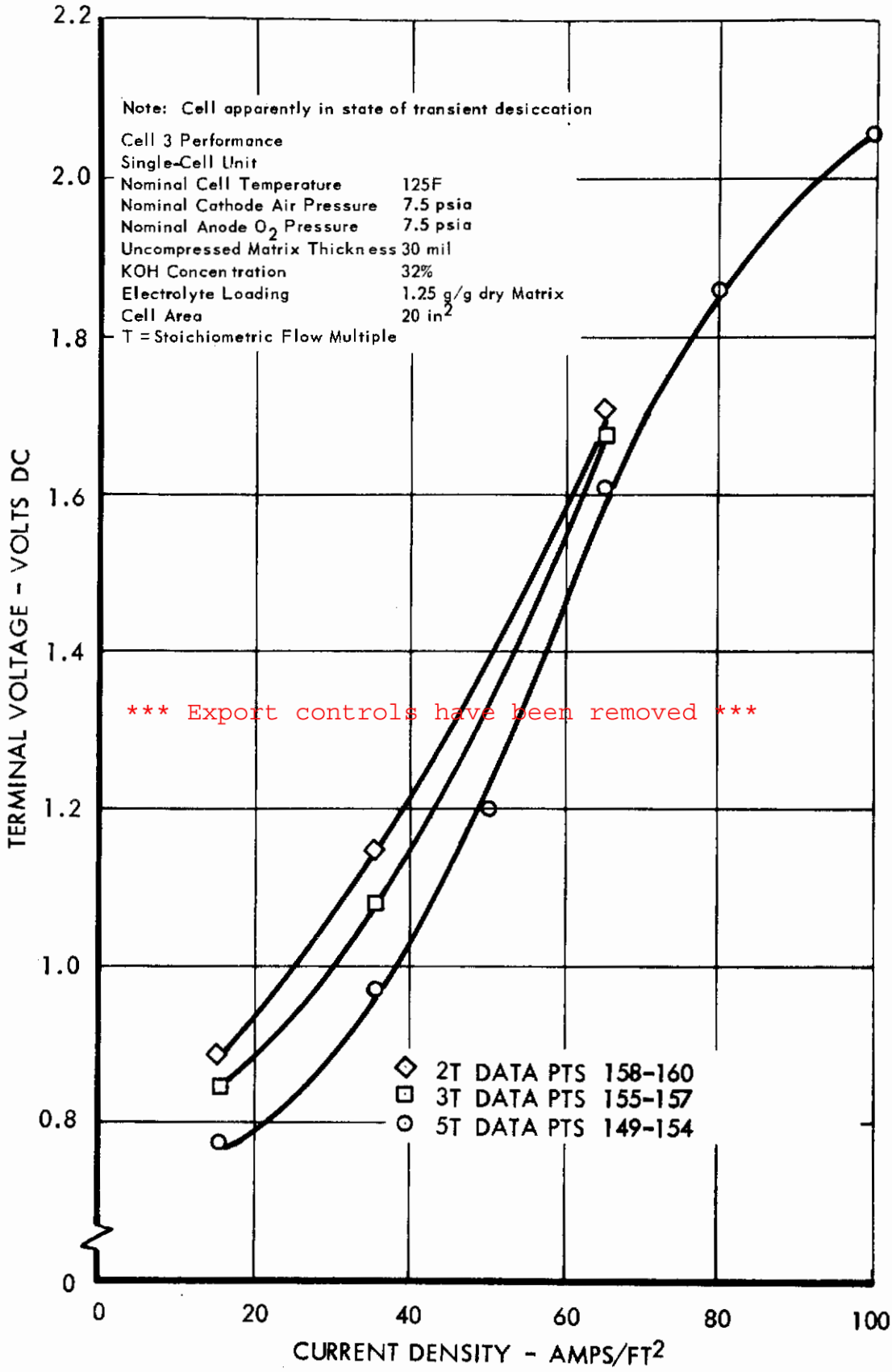

Figure 41 Reduced Data Plot

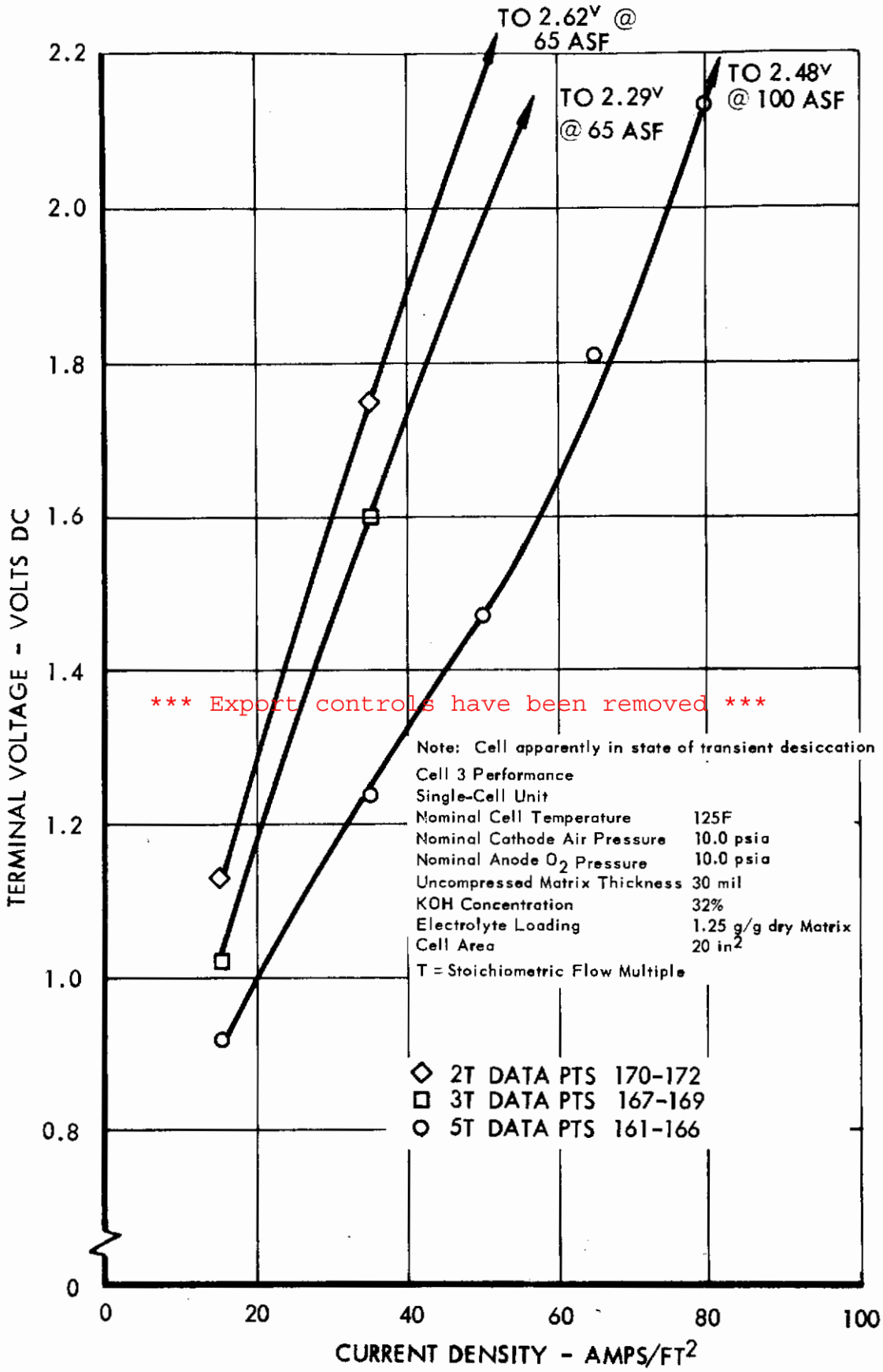

Figure 42 Reduced Data Plot

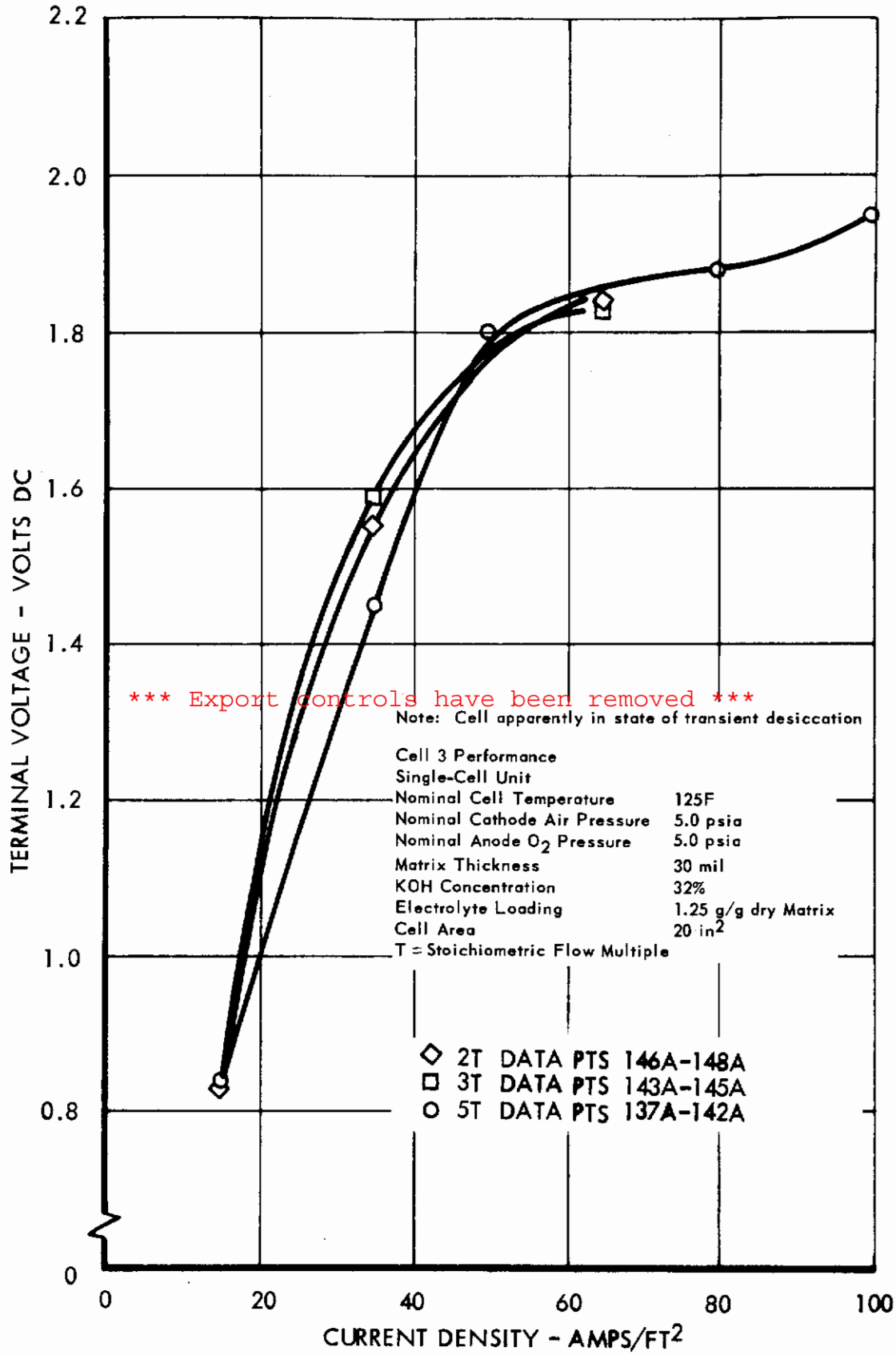

Figure 43 Reduced Data Plot

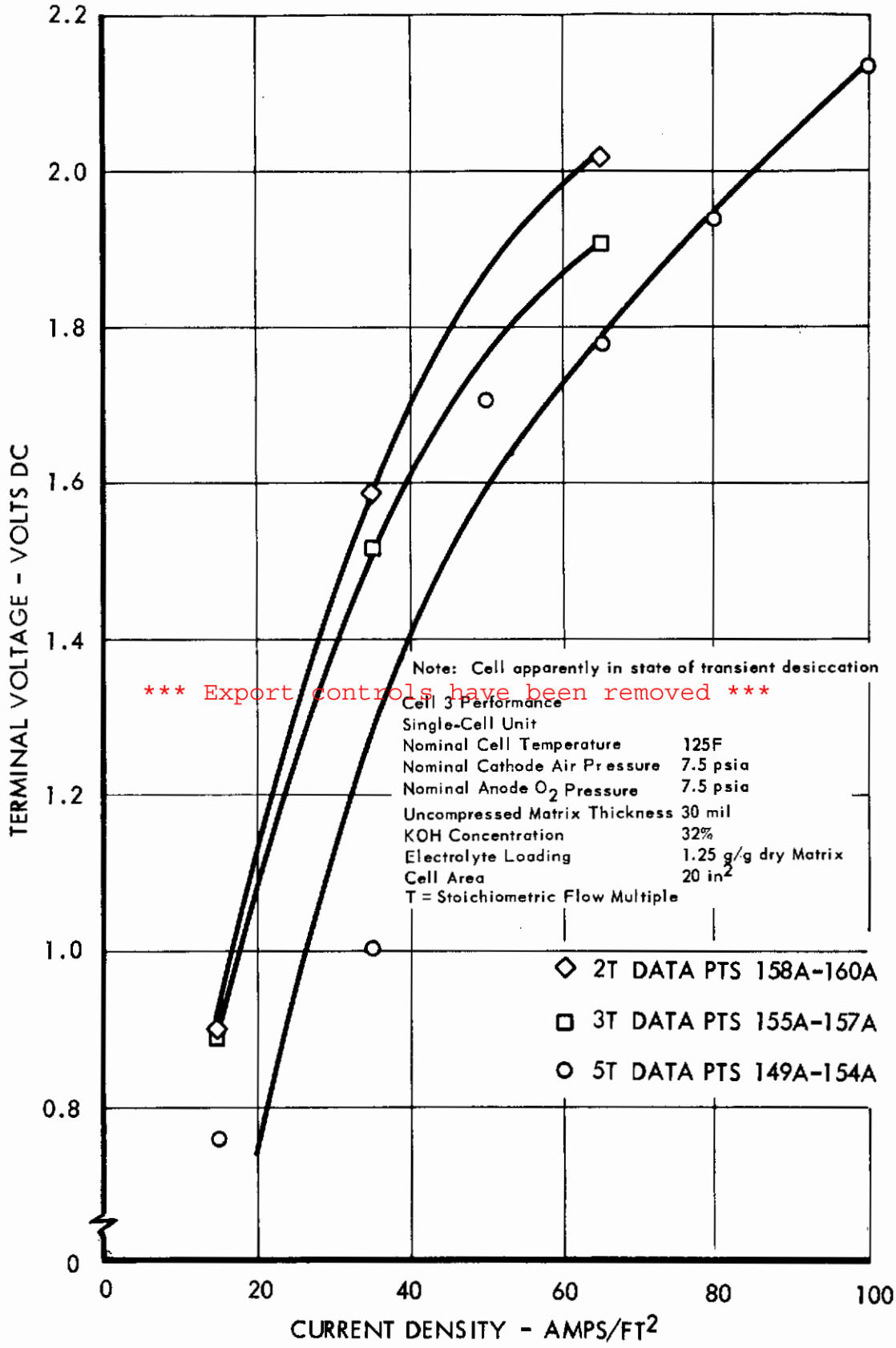

Figure 44 Reduced Data Plot

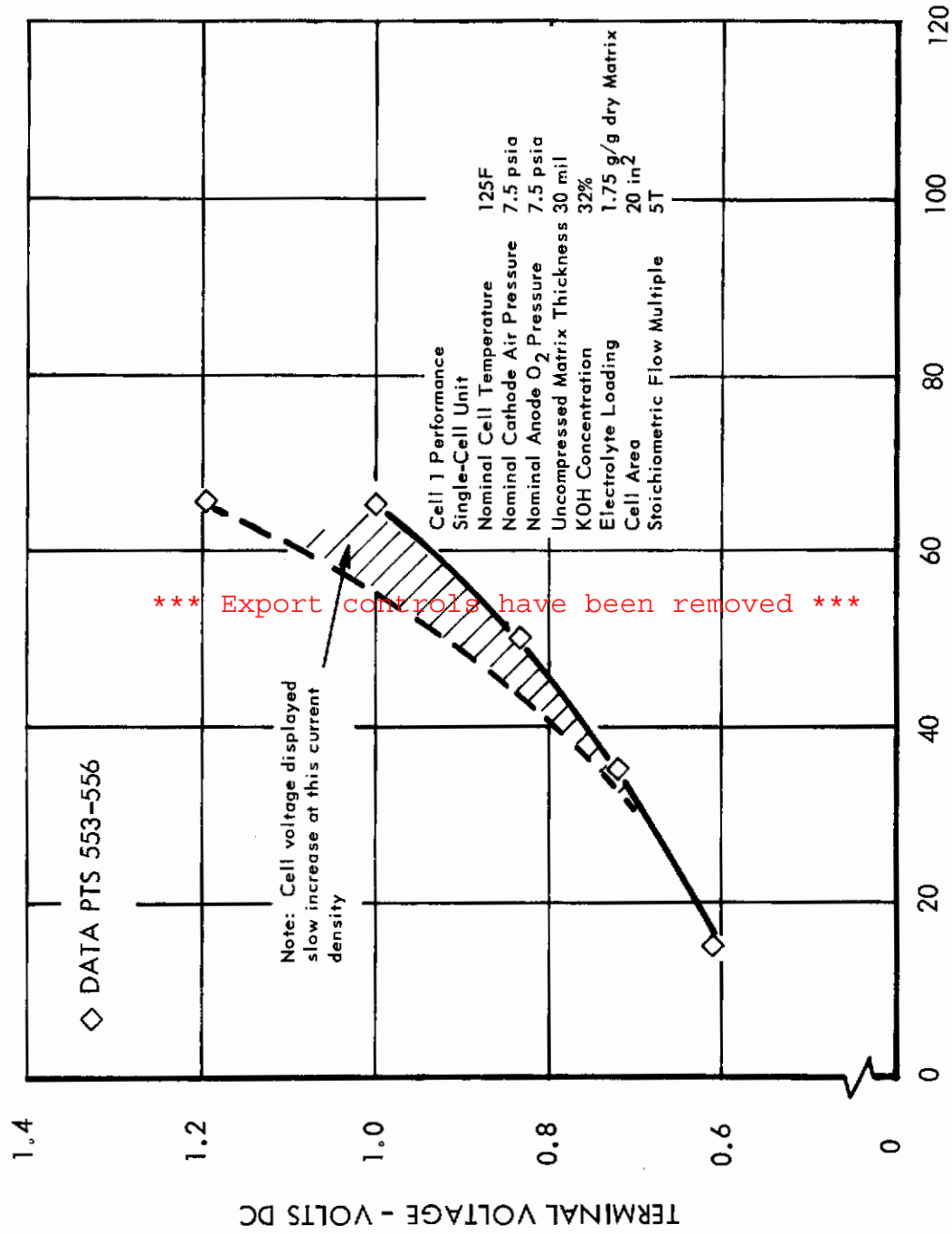

Figure 45 Reduced Data Plot

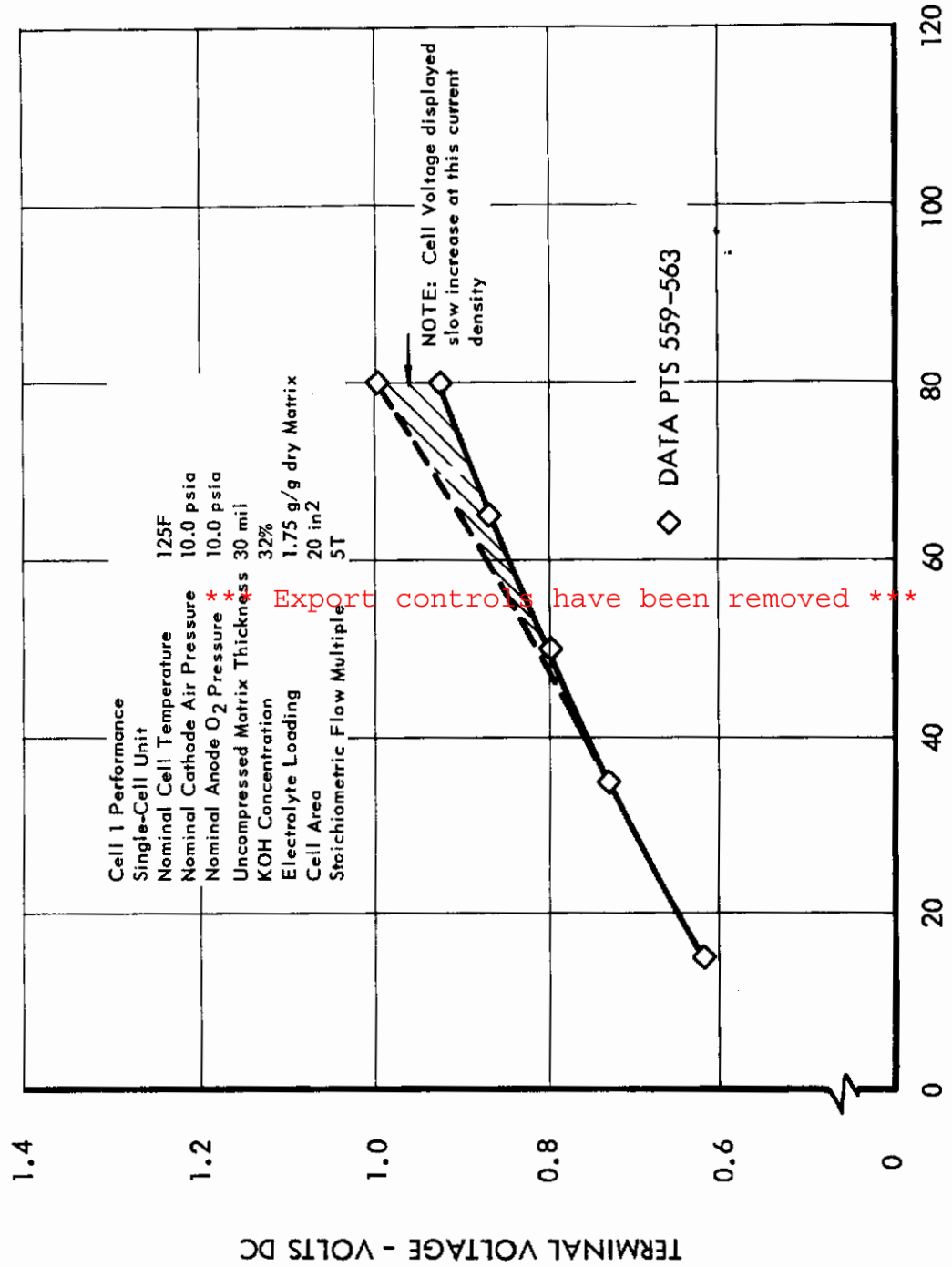

Figure 46 Reduced Data Plot

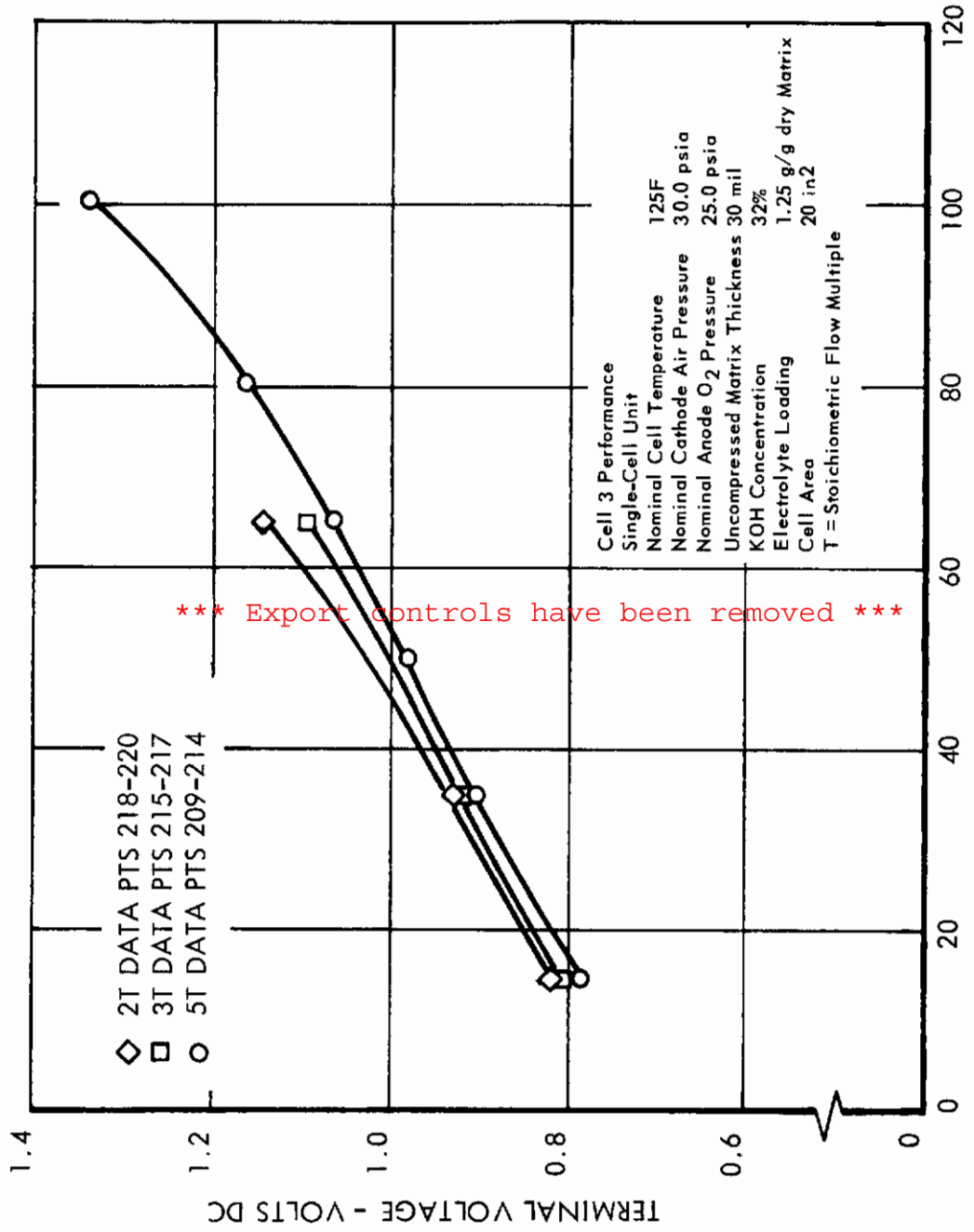

Figure 47 Reduced Data Plot

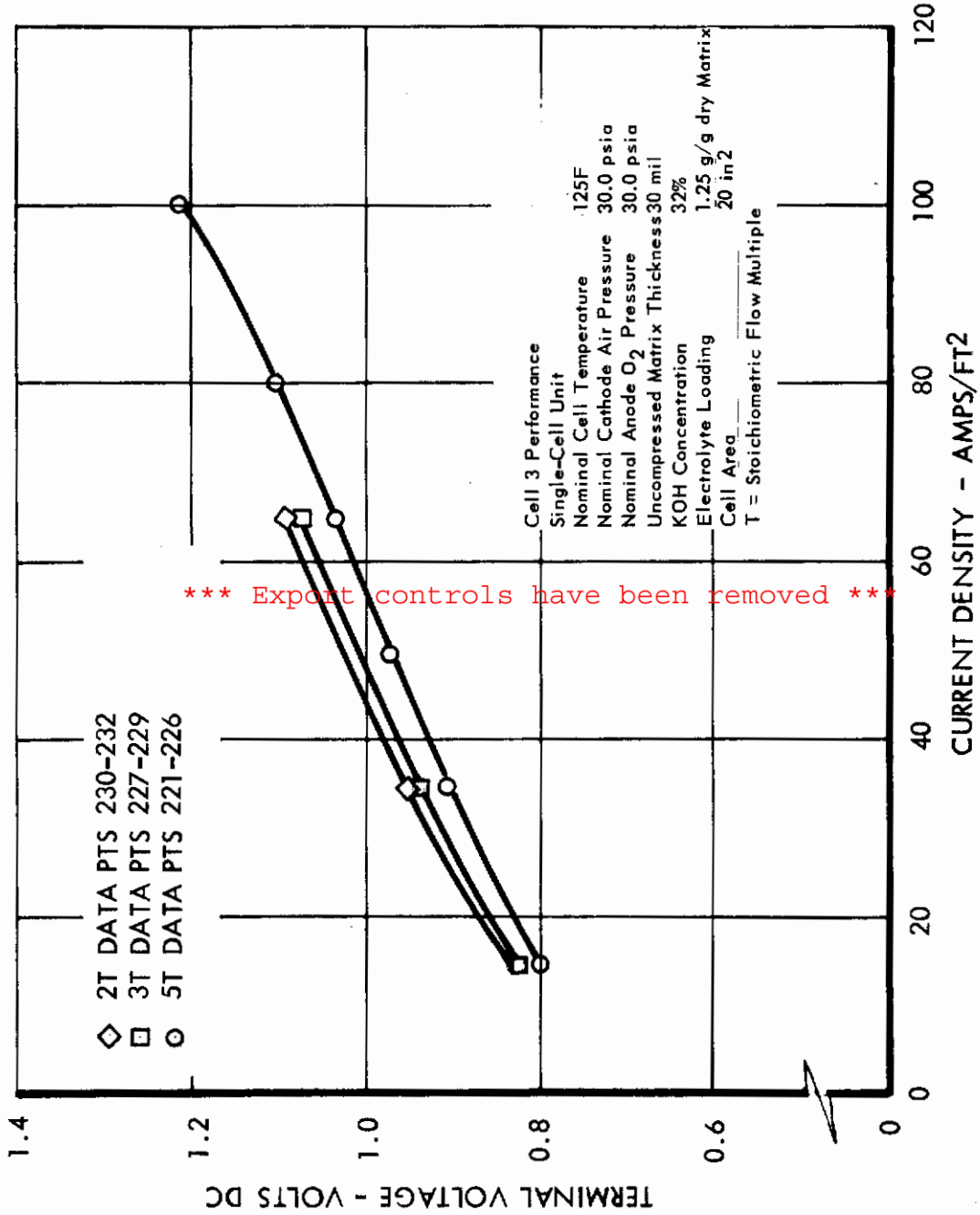

Figure 48 Reduced Data Plot

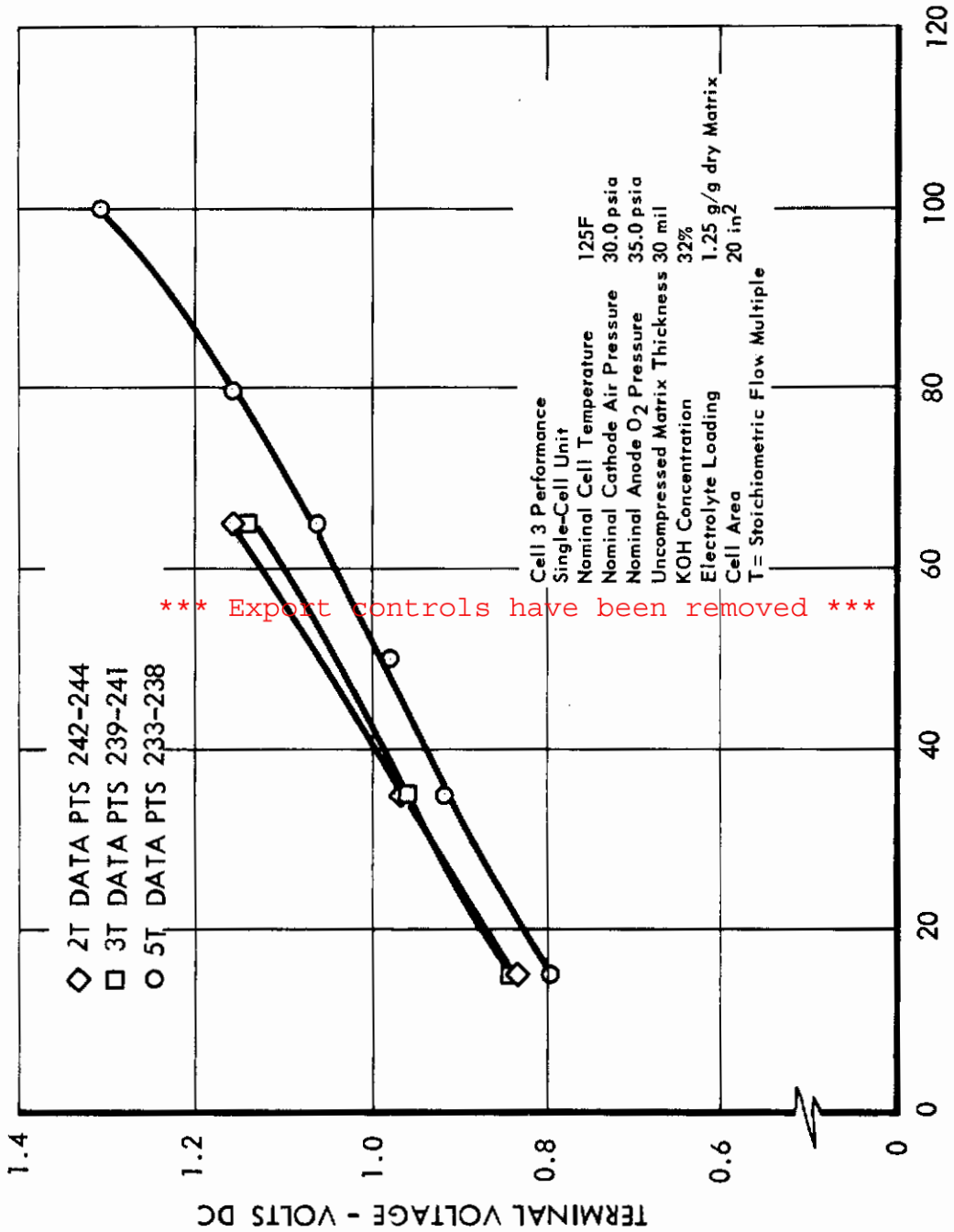

Figure 49 Reduced Data Plot

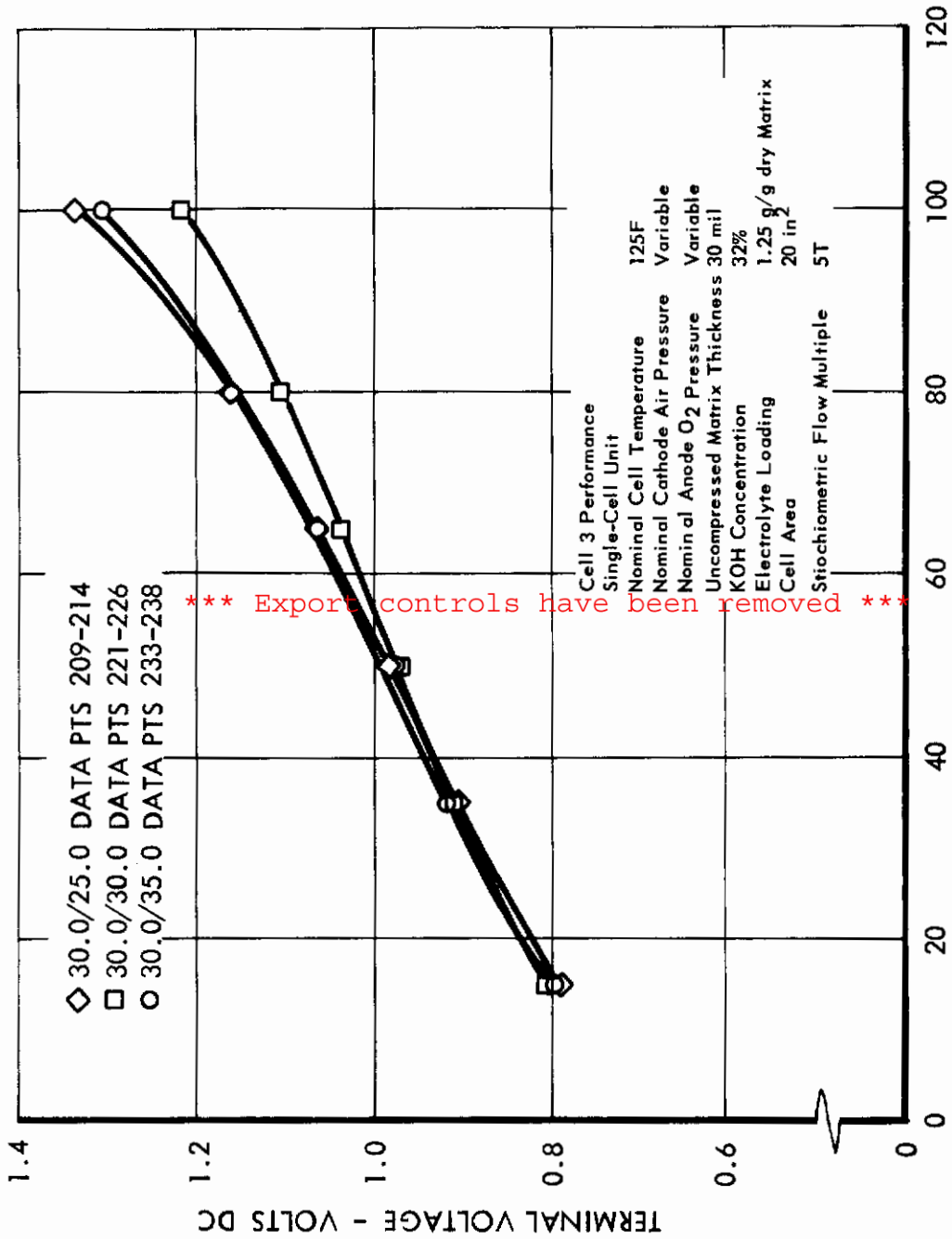

Figure 50 Reduced Data Plot

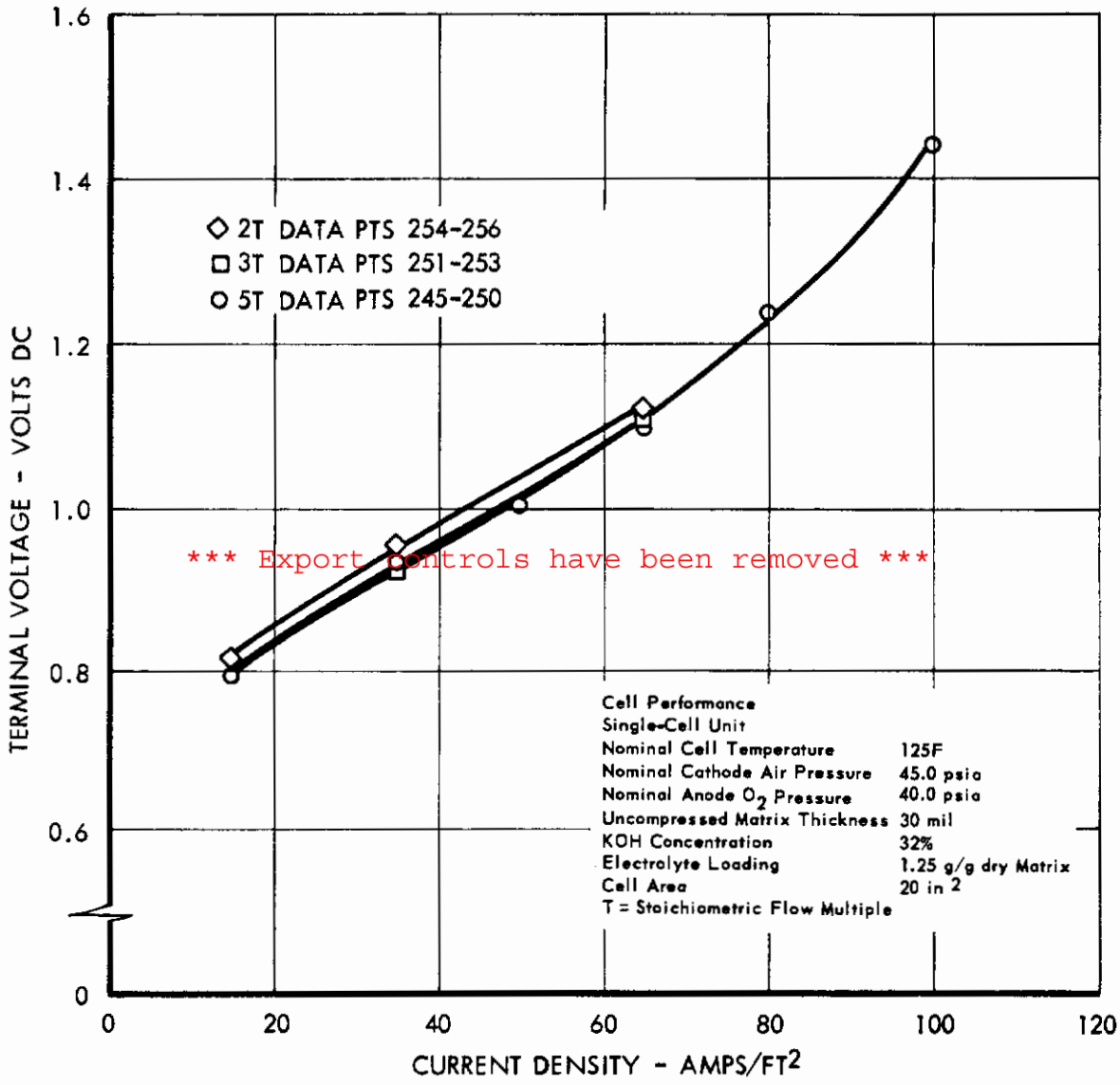

Figure 51 Reduced Data Plot

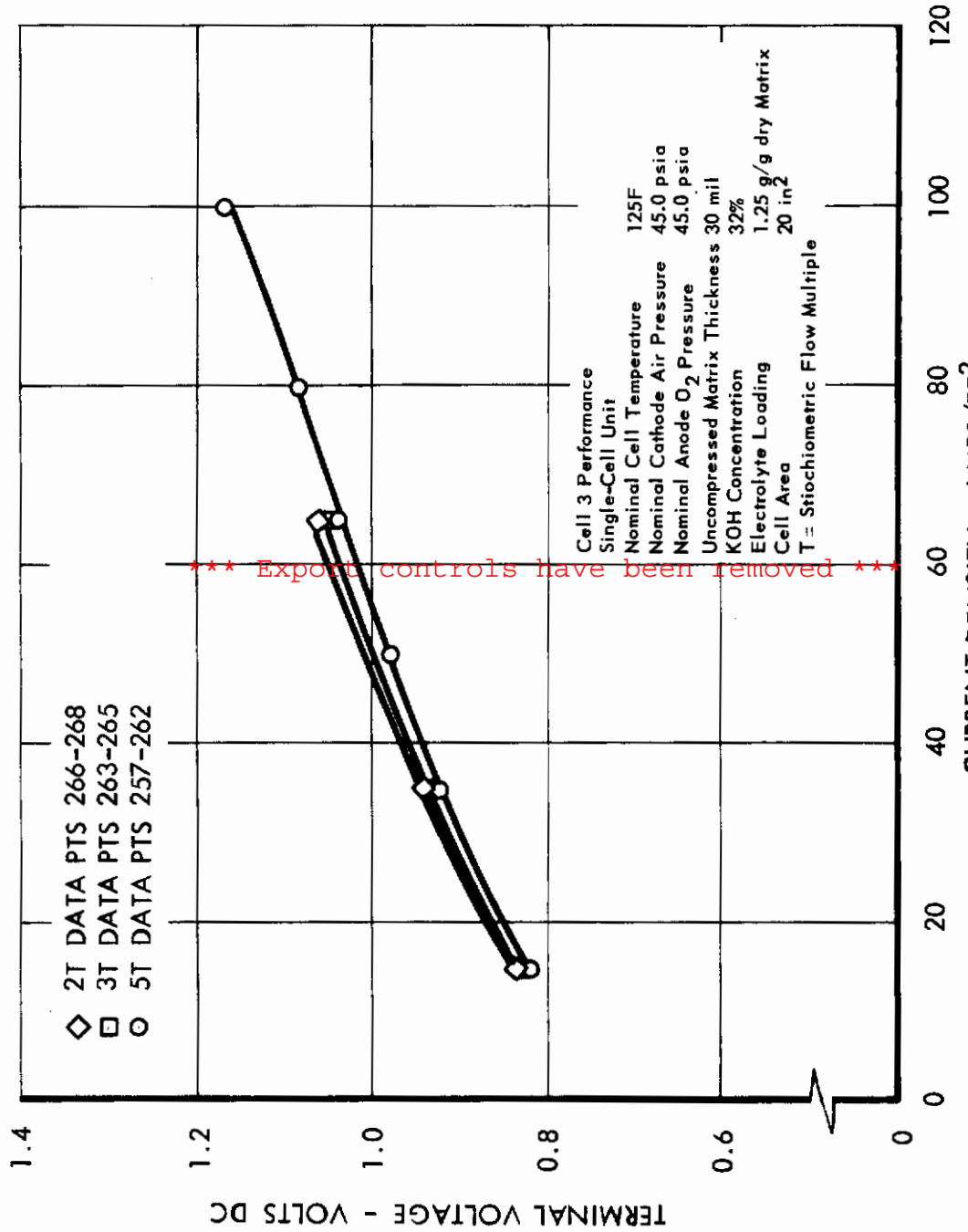

Figure 52 Reduced Data Plot

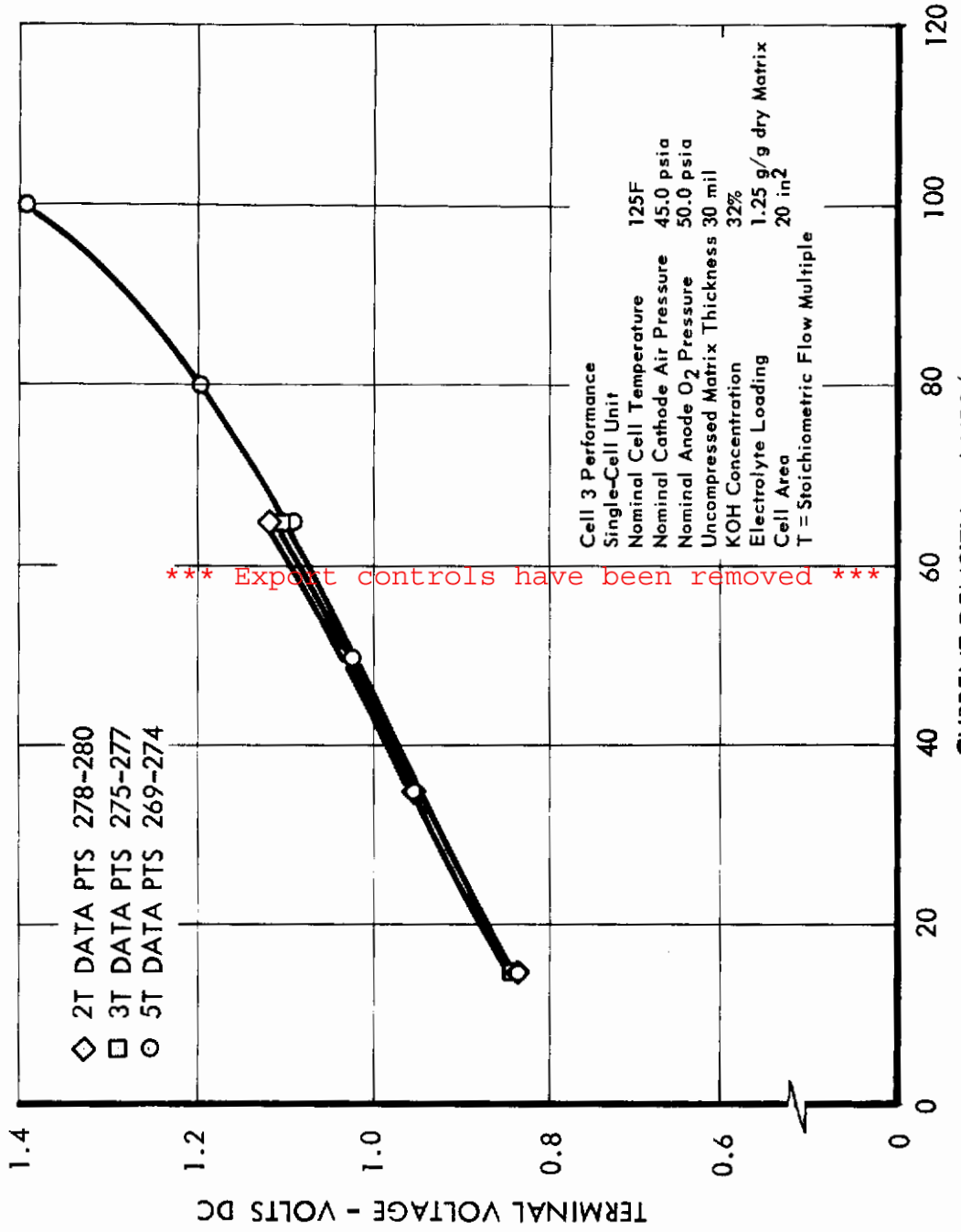

Figure 53 Reduced Data Plot

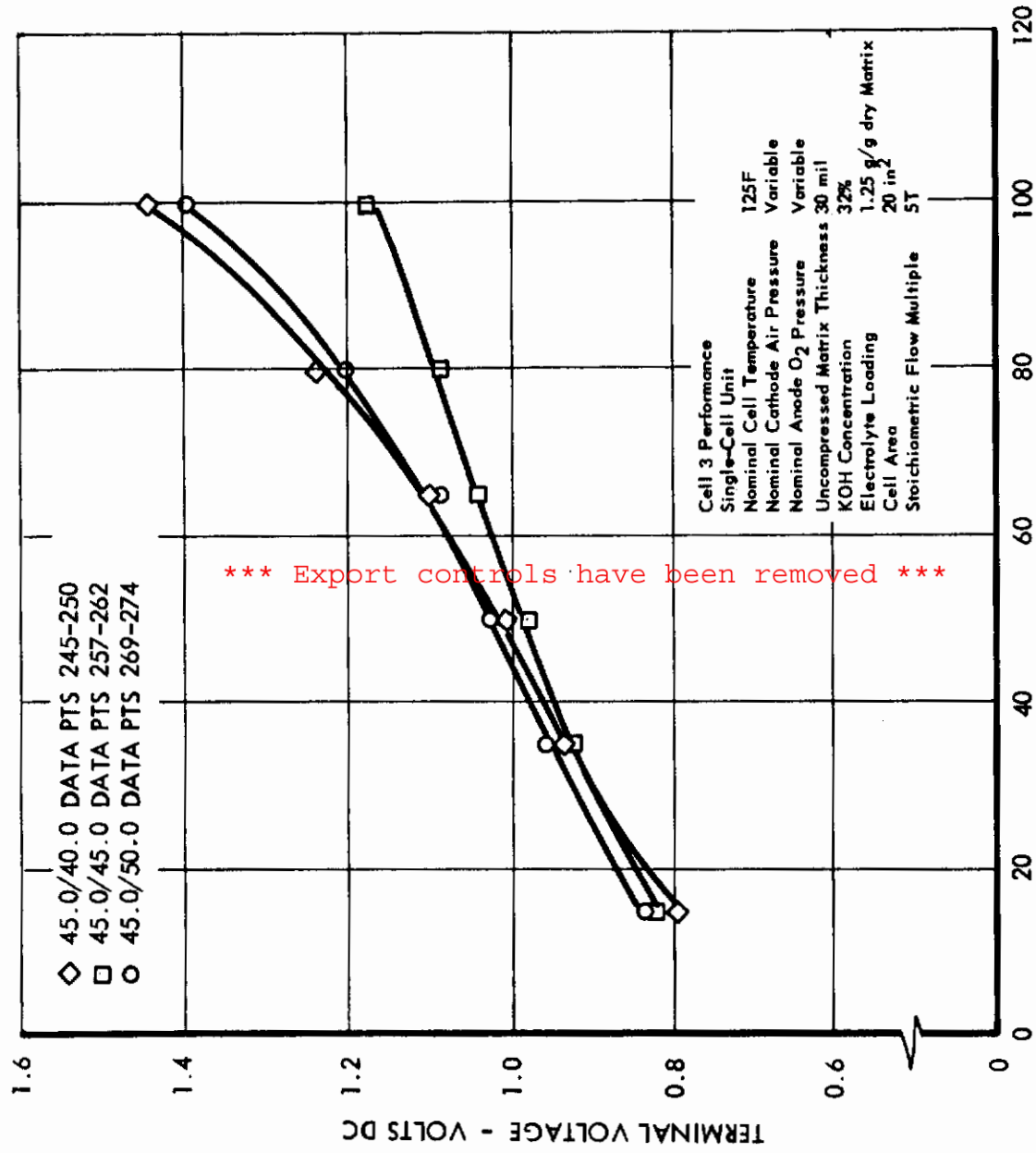

Figure 54 Reduced Data Plot

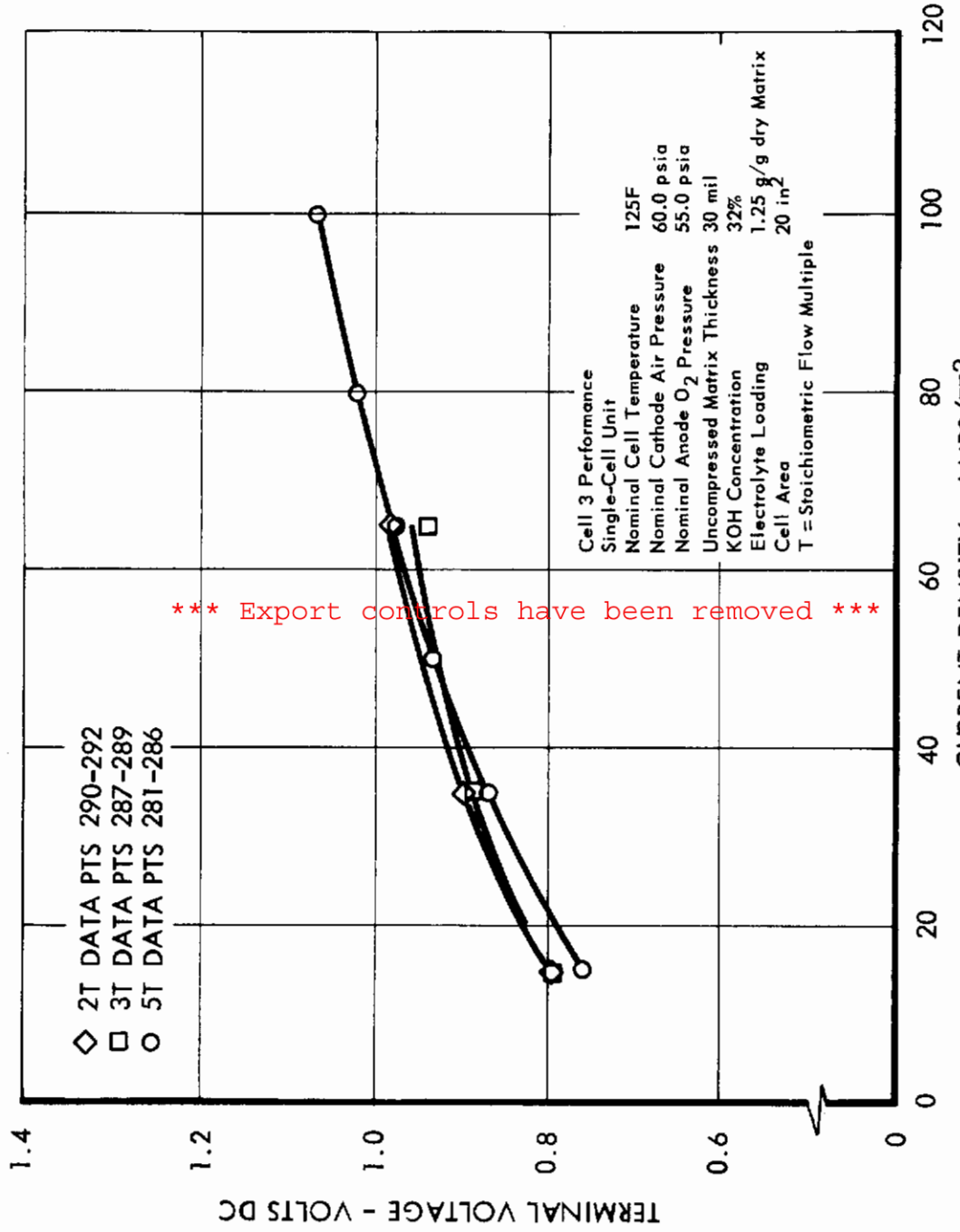

Figure 55 Reduced Data Plot

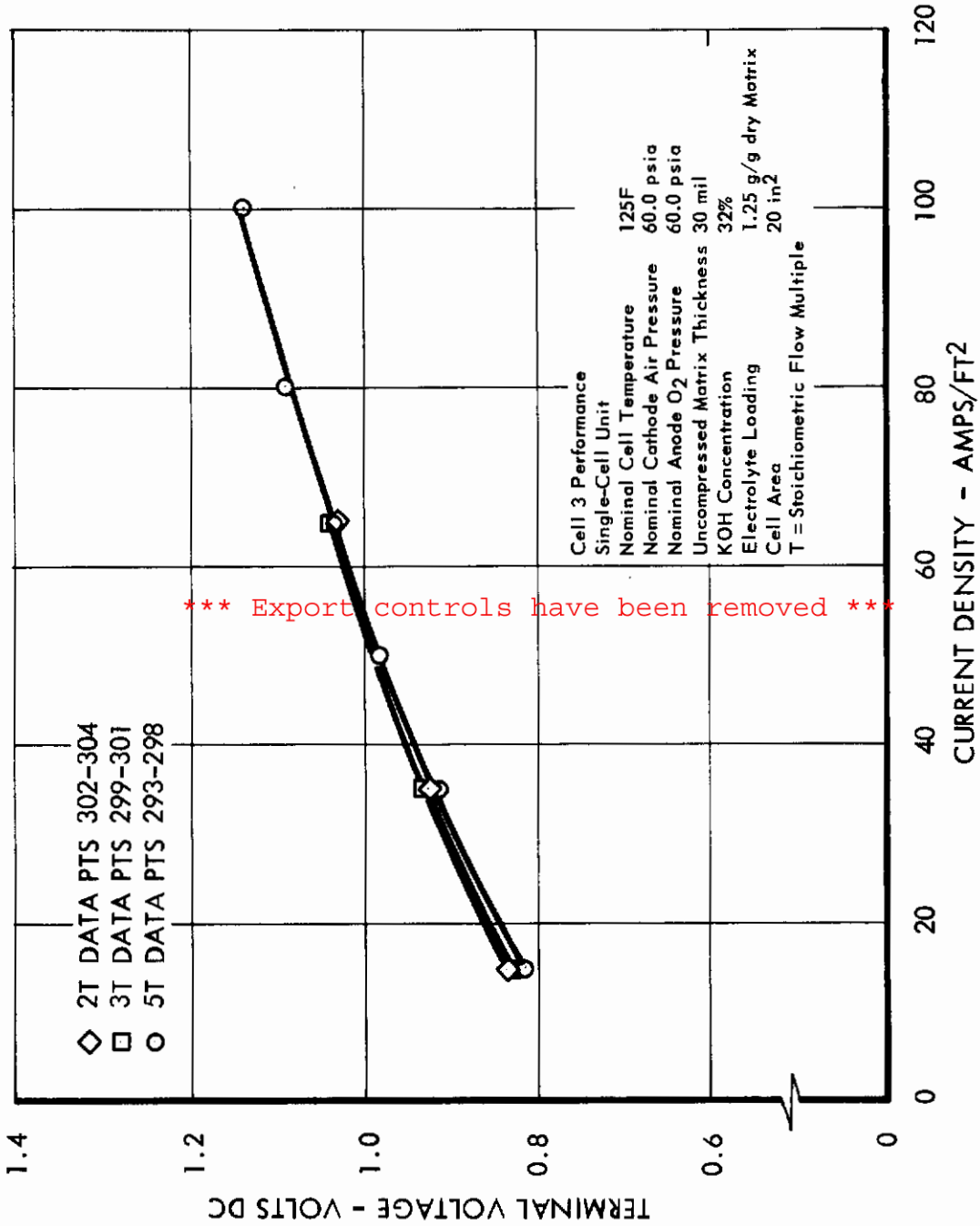

Figure 56 Reduced Data Plot

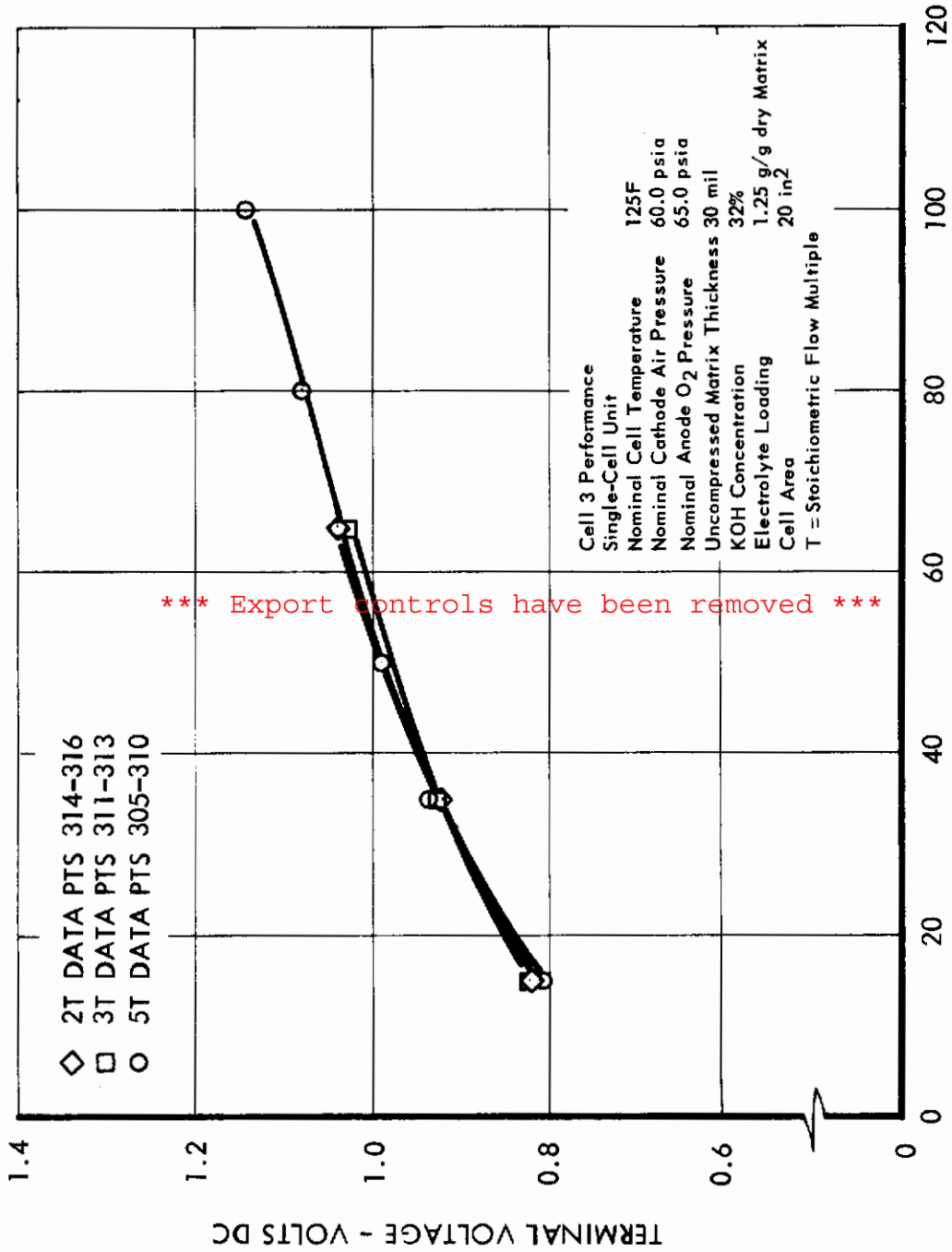

Figure 57 Reduced Data Plot

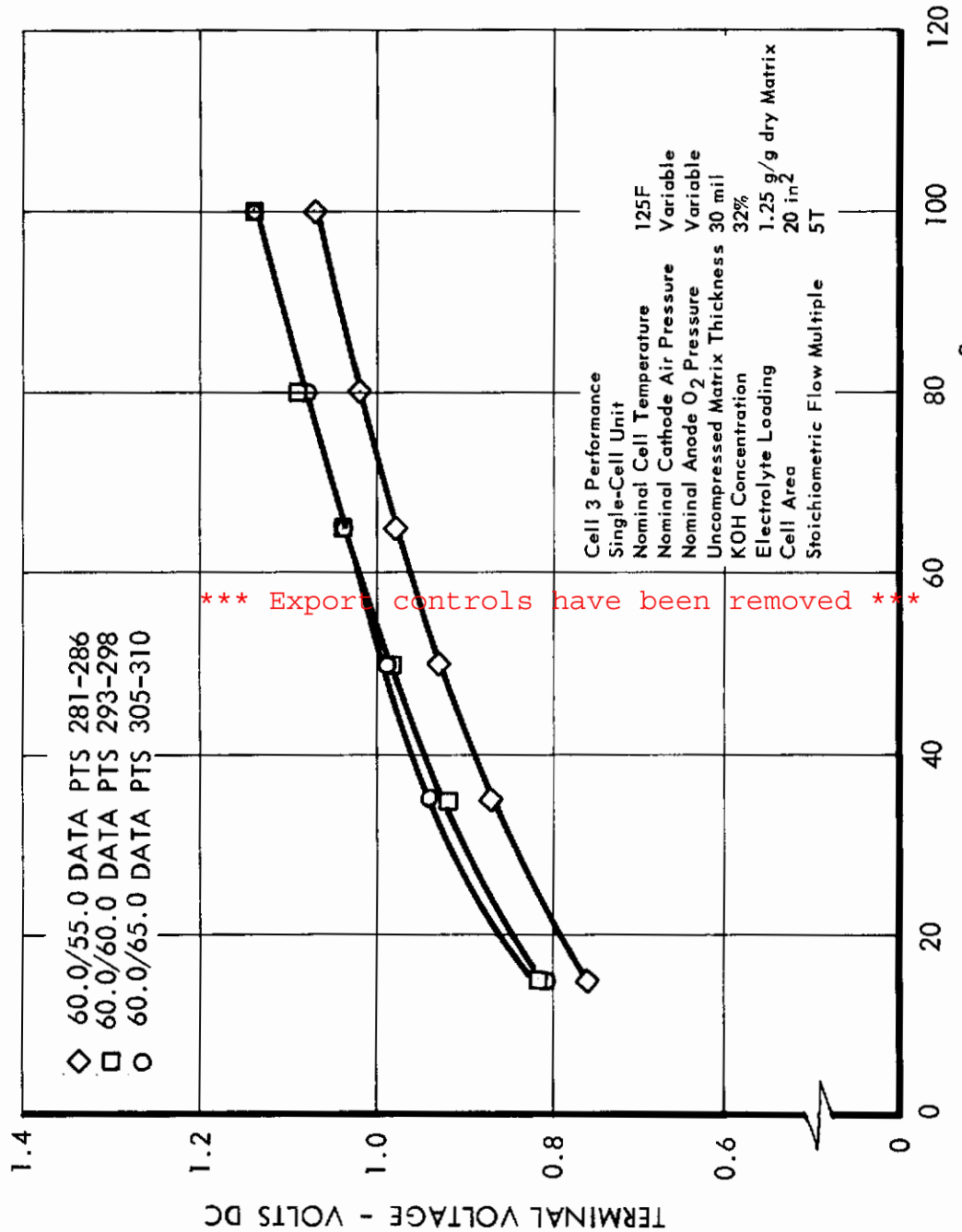

Figure 58 Reduced Data Plot

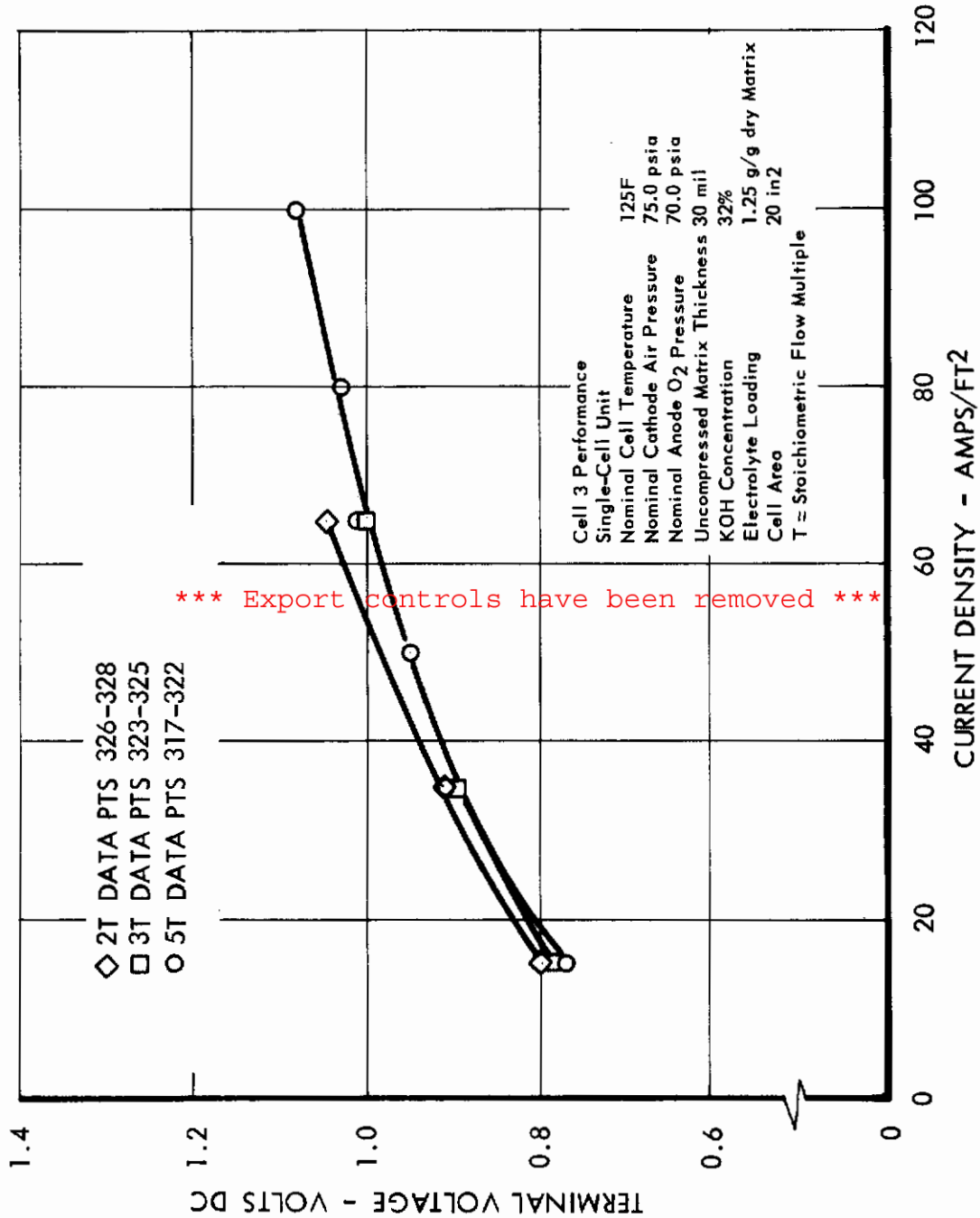

Figure 59 Reduced Data Plot

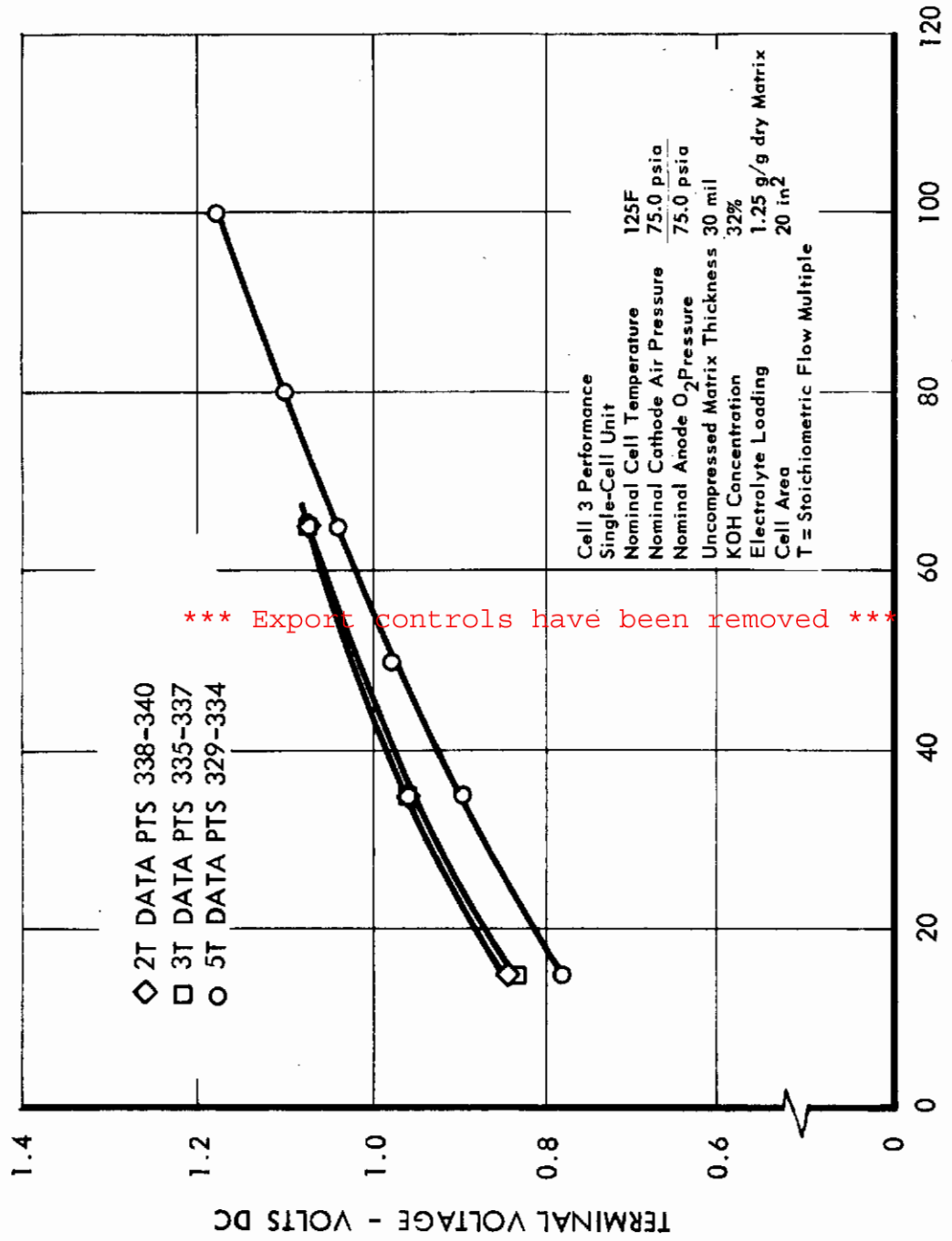

Figure 60 Reduced Data Plot

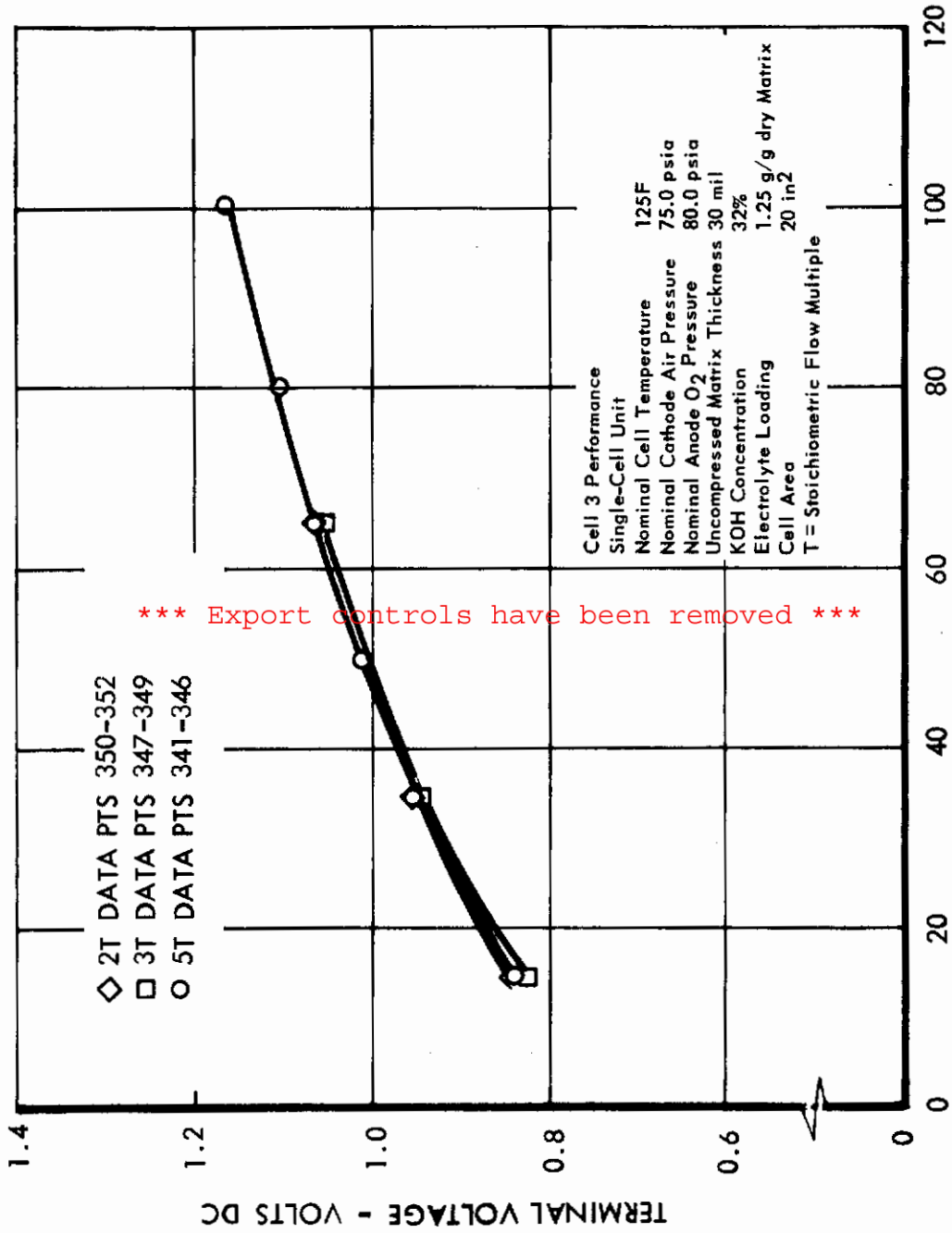

Figure 61 Reduced Data Plot

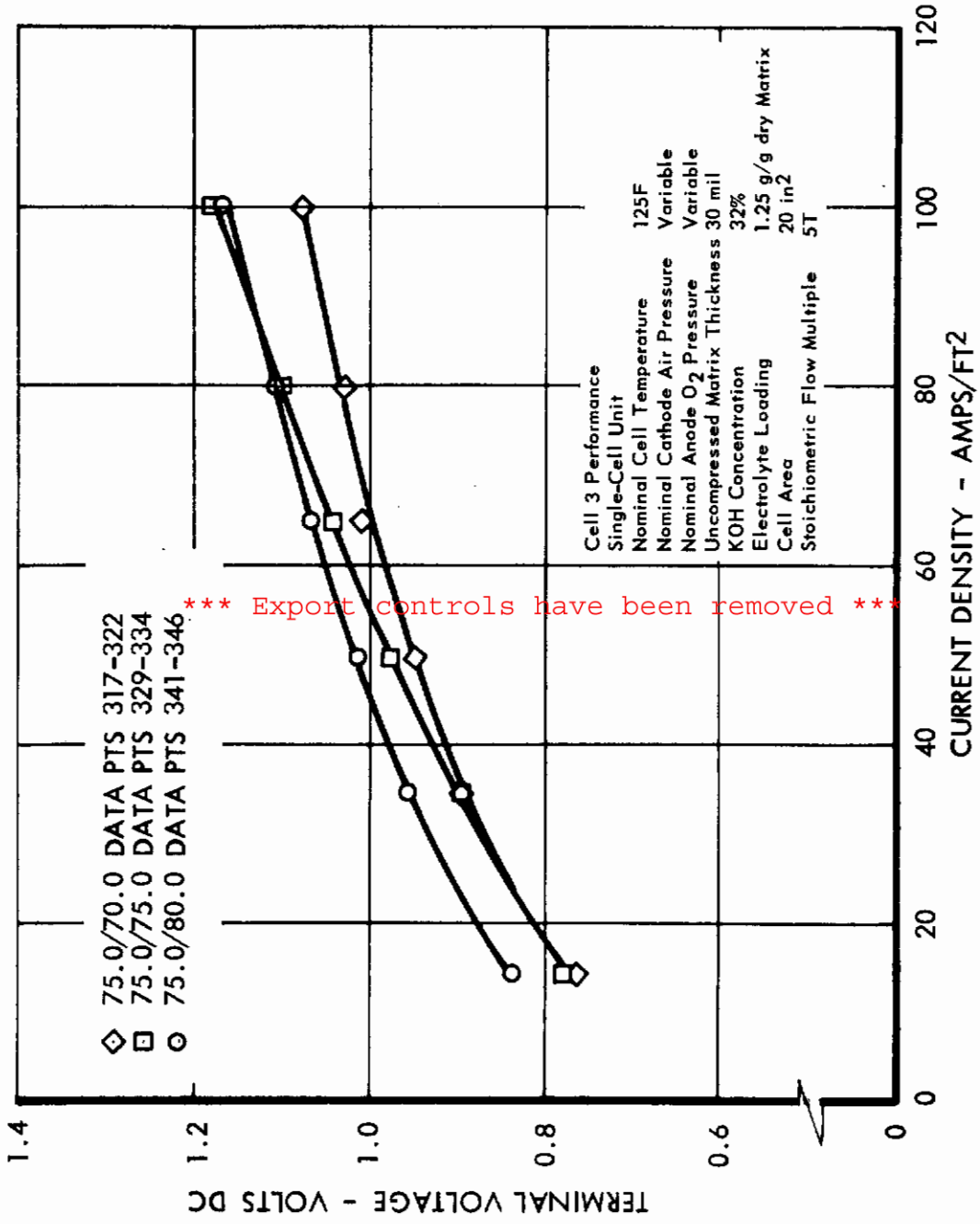

Figure 62 Reduced Data Plot

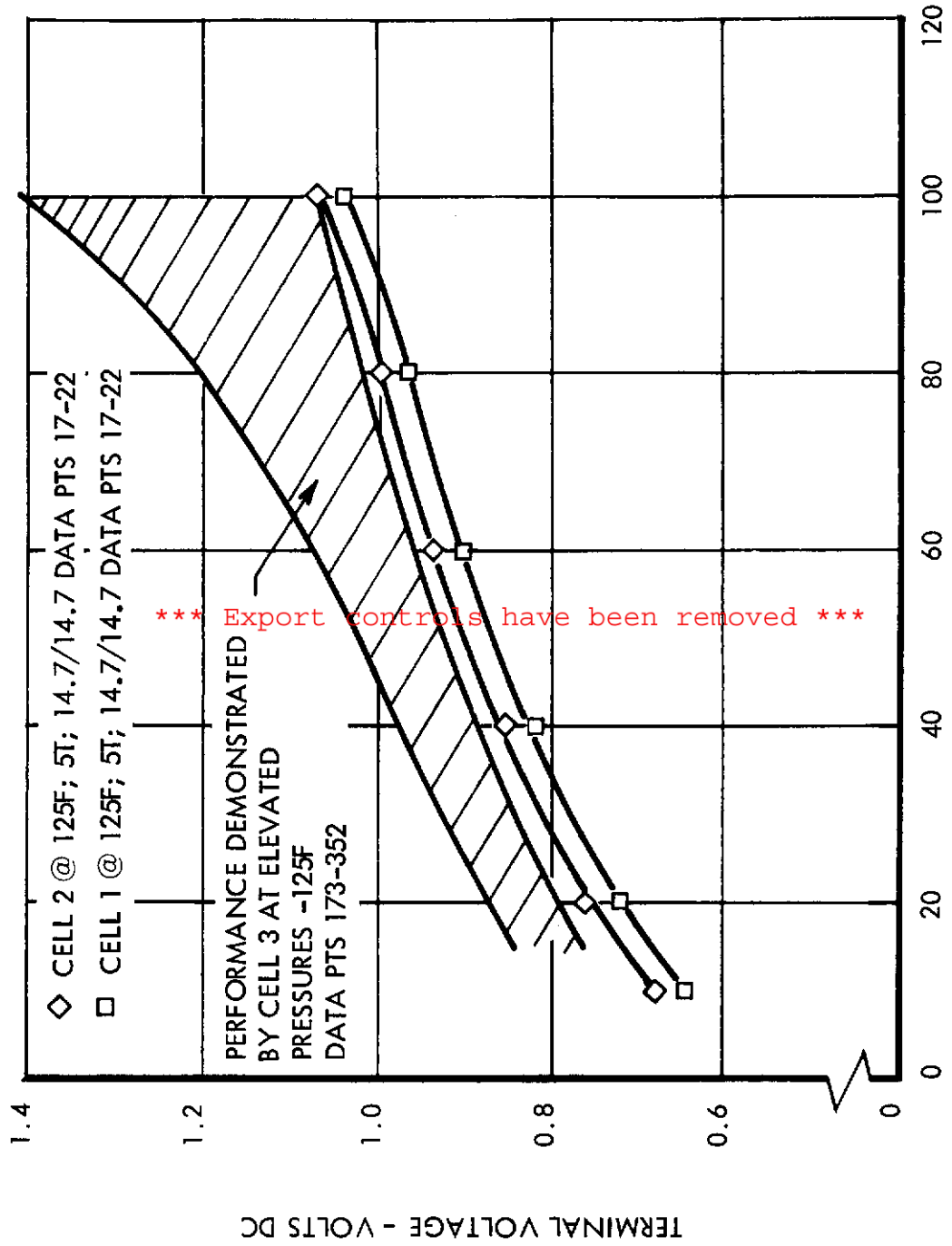

Figure 63 Reduced Data Plot

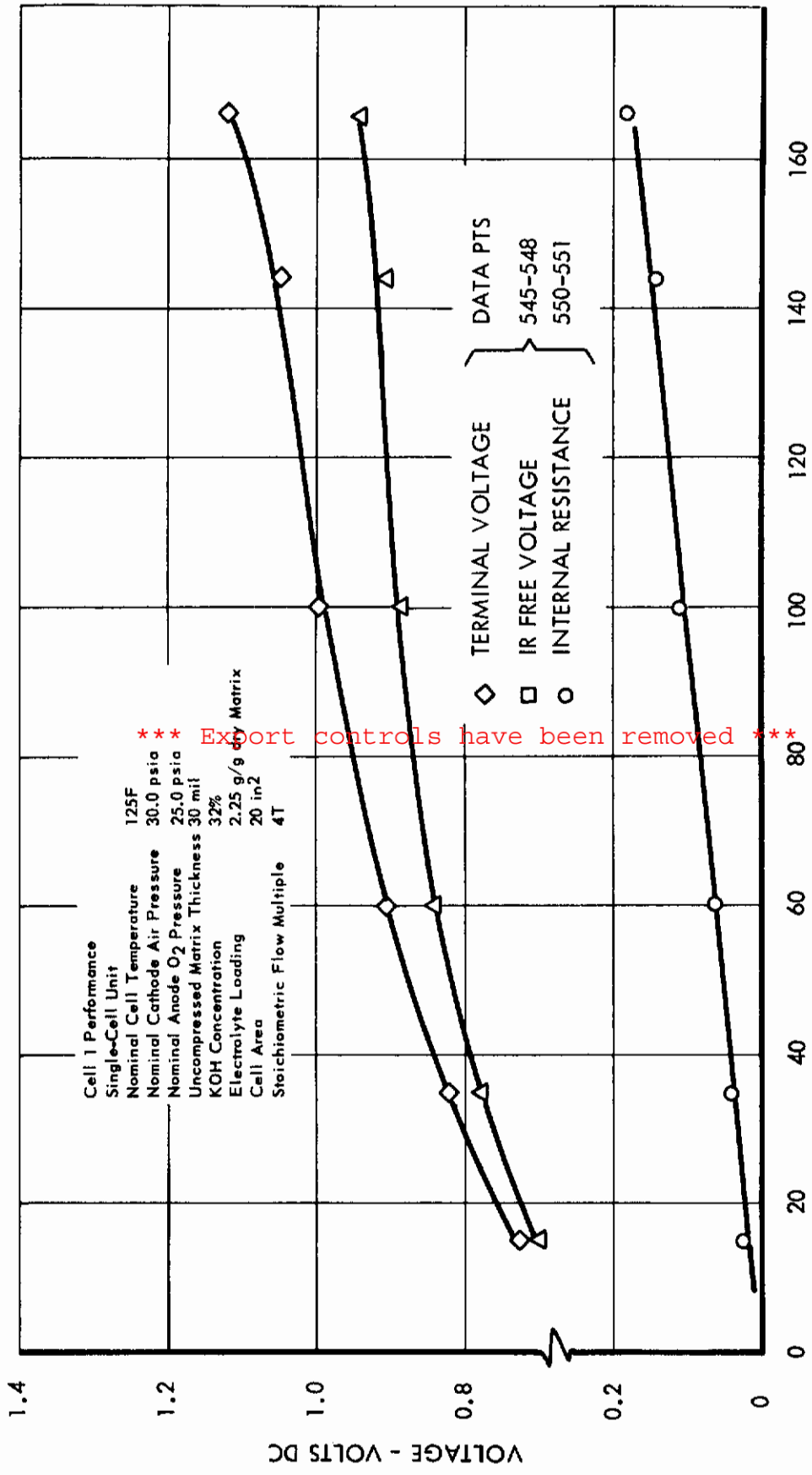

Figure 64 Reduced Data Plot

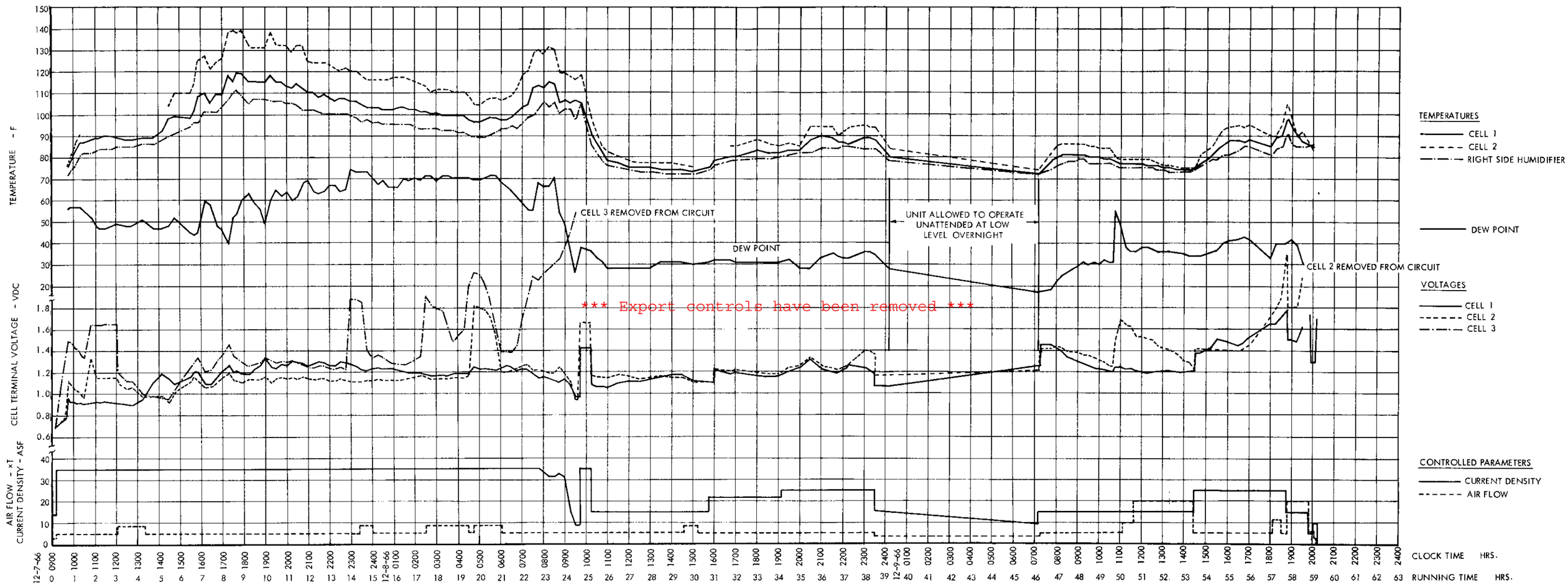

Figure 65 Self-Regulation 59 Hour Run

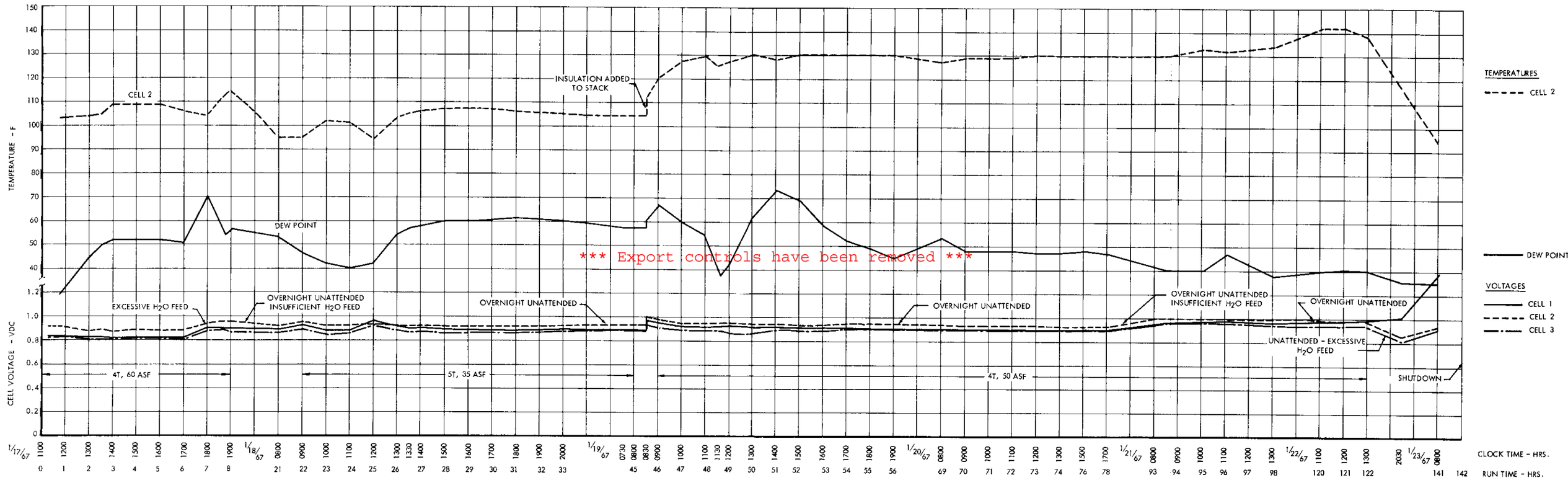

Figure 66 Self-Regulation 142 Hour Run

SECTION V

THE 0.2-LB O_2/HR DESIGN ANALYSIS AND RECOMMENDATIONS

1. DESIGN ANALYSIS

Since initial conception of the oxygen concentrating scheme in 1962, TRW has analytically and experimentally evaluated various approaches to simplifying its operation and control. Applying this concept to the requirement for supplying oxygen to aviators added a new dimension in design criteria, namely, operation independent of gravitational forces and under all degrees of rotation. In addition to self-regulation, many other cell designs were considered, including:

a) circulation of electrolyte between the cell electrodes using (1) dual-porosity electrodes to prevent electrode flooding, and (2) the dual-membrane cell construction;

b) circulation of the electrolyte through the anode compartment followed by external cell separation of the evolved oxygen from the electrolyte;

c) circulation of a liquid coolant through hollow compartments incorporated in the cell bipolar plates;

d) providing each individual cell with its own wick for humidification eliminating the need for a separate humidifier; and

e) use of static water-feed mechanisms based upon the osmotic transfer of water across a water-feed membrane, or water-vapor distillation through a porous feed matrix, with matrix materials consisting of either metal, asbestos or synthetic felts.

Each of these methods had certain advantages making them attractive and certain disadvantages limiting their applicability. In a broad sense all of the above, except (c) encompass the idea of self-regulation since the result of these techniques is a stack thermal equilibrium incorporating air humidification internal to the concentrator. As such, the evaporative cooling load can be applied to remove the heat generated during the oxygen concentrating process.

Selection of the most appropriate design depends upon the time and engineering effort (man-hours) available for its development. The more advanced the design concept, the more difficult the development. For present purposes, the term "advanced design concept" refers to a design capable of handling all environmental conditions experienced by an oxygen concentrator installed aboard actual aircraft.

The self-regulating oxygen concentrator concept, the subject of the present contractual effort, was directed toward the advanced version. It offers the advantage of eliminating

the circulation of coolants or electrolyte and the associated mechanical and electro-mechanical accessories. The design requires only one humidifier for every three cells, is amenable to zero-gravity operation, does not require separation of the generated oxygen from a circulating electrolyte stream and has the optimum design for lightweight packaging.

Designs tested and evaluated by TRW requiring electrolyte or coolant circulation cannot be made as compact and lightweight as cells employing a matrix-held electrolyte and a wick-type humidifier. The former designs had limitations imposed upon their physical size as a result of fluid manifolds allowing for small pressure drops that enabled the auxiliary pump weight and power to be kept at an acceptable level. Systems circulating hot, concentrated potassium hydroxide or an acid solution through the concentrator, seemed to add an unnecessary hazard to the personnel breathing the generated oxygen, although they do allow for ease of control.

As a result of the analysis completed, it was decided that the proposed 0.2-lb/hr oxygen concentrator design should allow for ultimate simplicity in operation and minimization in size (weight, power and volume). As such, the self-regulating design, (subject of the present contract), still appeared most applicable. Before it can be termed ready for field application, however, additional engineering effort must be devoted to further define its mode of operation.

The control concept is inherently simple -- no controls are needed. Air is simply fed into the concentrator. The concentrator, in turn, striving to maintain thermal equilibrium, automatically adjusts its temperature to remove the heat generated in the oxygen concentrating process by the evaporative cooling provided by the water being introduced to the air stream in the humidifiers (see Section II and Appendix I). The air exhaust is then passed through a condenser whereby the concentrator's heat load is rejected to the aircraft cooling system. The water condensed, in turn, is wicked back into the humidifier chambers of the concentrator, and the cycle continues as long as desired. The attractiveness of this control method is that the concentrator inherently corrects itself for variations in such difficult-to-control parameters as temperature of the surroundings and variations in electrode activity over the unit's operational life.

This program provided the following information. First, the idea of self-regulation was proven feasible. A control system can be developed that will be independent of auxiliary heaters, coolers, fluid circulating pumps, thermal controls, etc. Secondly, the program demonstrated where additional effort must be expended. Specifically, additional consideration must be given to (a) a reliable mechanism for feeding water into the humidifier compartments, and (b) a detailed analytical evaluation of the cell's moisture tolerance followed by experimental demonstration.

The water feed system used was too sensitive to fluctuations in the cell operating parameters of air flow rate and air feed pressure. The water reservoir requires a pressure reference in the concentrator, and since the cell responds faster to changes in these

operating parameters than the water feed system, a rapid decrease in air flow rate, or increase in air pressure, resulted in flooding of the humidifier compartment.[a]

Several aspects of the concentrator's moisture tolerance still remain to be considered. Moisture tolerance is important for several reasons. If the cells become too dry, gas crossover is experienced. If the cells become too wet, electrode flooding is first experienced which, in turn, results in aerosol formation.[b] If the flooding becomes excessive, electrolyte accumulation occurs in the cell gas compartments. This leads to two potential problems. First, since electrolyte has been leached from the matrix, the electrolyte concentration will be diluted when the electrolyte volume is returned to design level. Secondly, electrolyte blockage of the gas ducts may occur.

To be determined are the optimum electrolyte volume, electrolyte concentration, and ratio of matrix to electrode pore volume to permit continuous moisture (and thermal) balance over the anticipated range in operating temperatures. Knowledge of these relationships must be integrated with the effects such ranges in temperature have upon the temperature differentials of the three cells located between the humidifiers. The effect these differentials have upon maintaining a balanced moisture level must be tied to the available electrolyte concentration and ratio of total quantity of electrolyte to that available in the electrodes.

Consideration should also be given to the fact that the unit must retain a moisture balance despite the gradual degradation in performance experienced during the operating life. This effect, and any other causes which tend to increase the power required to concentrate the oxygen, means cell moisture tolerance design must be capable of also handling gradual increases in heat loads (increases in operating temperatures).

Before describing the 0.2-lb/hr oxygen concentrator design, it is appropriate to note that several modifications could be made in the design, serving as intermediate steps leading to the ultimate self-regulating design.

2. MODIFIED APPROACHES TO SELF-REGULATION

The concept of self-regulation, from an applications viewpoint, is best adapted to concentrator operation with low-pressure feed air. As noted previously, it was under these conditions that the quantity of water evaporated (cooling capability) was sufficiently high to keep the concentrator operating temperature low. The relationship of the amount of water vapor required to satisfy conditions of equilibrium as a function of cell supply pressure and temperature is readily synthesized by consideration of equation (7) in

---

[a] Experimental results indicate this can be curtailed if a proper amount of resistance is included in the water transport line between the water reservoir and the humidifier within the concentrator.

[b] Fine bubbles (aerosol) of electrolyte being carried out with evolved oxygen.

Appendix I. A low cell operating temperature means that system startup and shutdown processes are simpler, that moisture vented with the evolved oxygen is less[(a)], and that cell tolerances to moisture balance are less critical.

At least three modifications in design concept are possible, wherein supplemental cooling could be used to allow for concentrator operation at high air feed pressures (higher self-regulating cell temperatures). In one case, excess air could be recirculated through the cathode at ten-to-twenty times theoretical. This modification is illustrated in Figure 67. The effect would be to lower cell operating temperature.

In the second case, a liquid auxiliary cooling loop could be added. Thus, when the operating conditions become such that the heat input is greater than the cooling available at a desired self-regulating temperature, the excess heat load would be removed with the auxiliary coolant. This would prevent the cell temperature from exceeding the design temperature.

In the third case, a combination of cooling by water evaporation and auxiliary coolant is made possible when the fluid used to moisturize the feed air is circulated through the humidifier compartments. Excess heat is then removed from the fluid in an external heat exchanger. This approach has been shown to be effective but yields a design with weight and volume penalties.

3. DESCRIPTION OF THE 0.2-LB O_2/HR SELF-REGULATING CONCENTRATOR

In light of the above considerations, the oxygen concentrator model proposed is one using 120-mil magnesium stock for the bipolar plates and will be termed Model 120. The design parameters for the 0.2-lb/hr concentrator are summarized in Table VIII. The design parameters of the unit incorporate the best features based upon TRW's past experience and engineering evaluation of the analyses and testing conducted on this program.

a. Electrical Power Requirements

The current density-voltage point selected was based on performance data obtained during the test program (Figure 29). The effective electrode dimensions were 4x9 inches, selected to match the 4-inch height best suited to wicking technology and the preferred number of cells, in light of the voltage output available from an aircraft's

---

(a) If a concentrator having a 33.3% KOH solution as the electrolyte operates at a temperature of 200F at a design point of 0.2 lb of oxygen per hour, it will vent approximately 0.084 lb of water per hour along with the 0.2 lb of oxygen if the oxygen is being delivered at atmospheric pressure. For a twelve-hour flight, about 1.0 lb of water would be required.

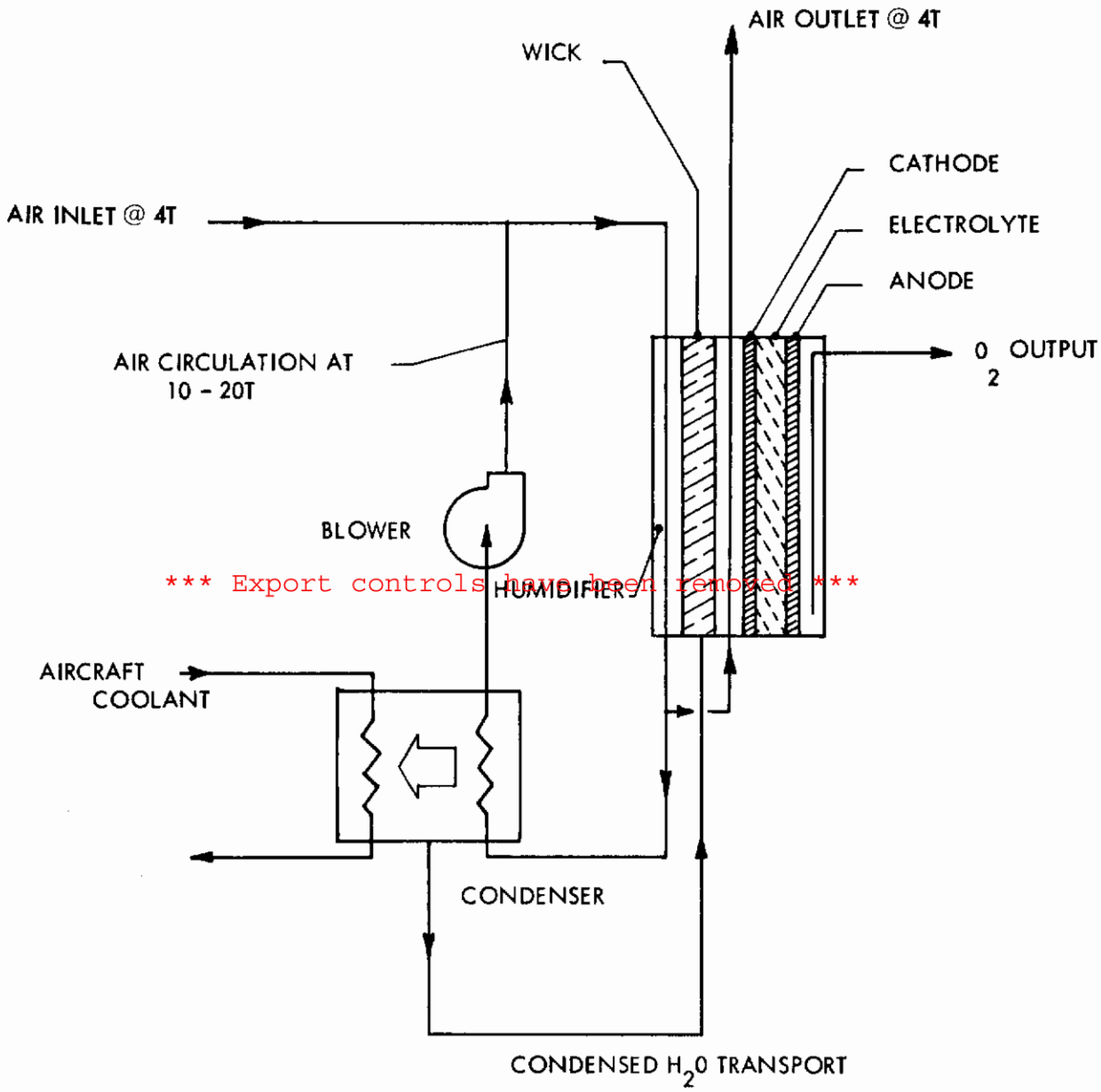

Figure 67 Modified Approach To Self-Regulation

Table VIII Design Parameters for the 0.2 Lb/Hr Oxygen Concentrator

Current Density, ASF	60
Cell Voltage, volts	0.9
Effective Electrode Area (per cell), ft^2	0.25 (4.0 x 9.0 in)
No. Cells, Series Connected	20
Concentrator Current, amps	15
Concentrator Voltage, volts	18
Electrolyte, wt. % KOH	33.3
Air Mass Flow Rate, lb/hr, @ 4T	3.46
Percentage Oxygen Removed, %	25
Operating Temperature, F	180
Operating Pressure, psia	15.7
Specific Humidity, lb H_2O/lb dry air	0.23
Evaporative Cooling Load, watts	270

power supply. The merits of selecting a larger effective area are obvious. For two bipolar plates of a given thickness, the larger one will display a lower ratio of plate weight/effective area. This results in a lighter overall stack assembly. This is caused by the fact that for the smaller plate, there is more flange area/effective area, and hence a relatively heavier plate. This is illustrated when comparing the bipolar plates fabricated on the present contract with those from contract AF 33(615)-1856 (see Table IX). Note that the larger plate, even though thicker, displays a lower weight/area ratio.

Figure 68 illustrates the effect other selections of current density and electrode area would have on the number of cells required to generate 0.2 lb of oxygen per hour.

b. Air Feed Requirements

Two-tenths of a pound of oxygen per hour requires 3.46-pounds of air per hour at a flow of 4T. A definition of the relationship of oxygen output to air flow requirements is presented in Appendix IV.

c. Operating Temperature

Based on an operating air flow rate of 4T (i.e., 25% of the oxygen in the air is being concentrated) and a cell voltage of 0.9 volt, the self-regulating temperature will be 180F when the operating pressure is 15.7 psia. This results from the data presented in Figure 1 for the condition where the cell voltage is 0.9 volt. For a 33.3 weight percent KOH solution as the electrolyte, the specific humidity of the air feed is 0.23-lb water per pound of dry air. Figure 69 aids in obtaining the specific humidity for alternate conditions of total pressure and self-regulation temperatures.

The cell cooling load is approximately 270 watts, the product of stack current (15 amps) times the stack voltage (18 volts). The stack voltage is the product of the individual cell voltage (0.9) times the number of cells (20). The effect of other cell voltages on the cooling load is shown in Figure 70.

d. Design Optimization

During fabrication and test of the concentrator system, consideration was given to various modifications in the design to further optimize and simplify its construction and operation. In carrying out the design analysis, one aspect occurred repeatedly -- should the recommended design improvements be directed toward the ultimate configuration of the concentrator model, or should recommendations be specified for an incremental improvement (optimization) in the model configuration. The particular model selected, intermediate or ultimate, has a decided effect on the approach taken toward design modifications. For example, for an incremental improvement in the model design, the gas ducting technique recommended would be one in which the 42-mil gas ducts are replaced in Model 120 with 32-mil ducts, or a 20x86-mil rectangular slot with 20 mils being the slot height. The ultimate configuration would require a completely new approach to the

Table IX Comparison of Bipolar Plates

	AF 33(615)-1856	Present Contract
Thickness, in	0.188	0.140
Flange Width, in	0.438	0.375
External Dimensions, in	15.0 x 6.5	8.62 x 5.38
Duct Diameter, in	0.042	0.042
Port Diameter, in	0.438	0.375
Air Compartment Height, in	0.063	0.052
Oxygen Compartment Height, in	0.062	0.052
Nickel Plate, mil	1.2	1.3
Gold Plate, mil	0.02	0.03
Effective Electrode Dimensions, in^2	11.8 x 4.2	3.5 x 5.8
Effective Electrode Area, in^2	49.6	20.3
Weight, grams	353	149
Bipolar Plate Weight/Effective Electrode Area, g/in^2	7.1	7.5

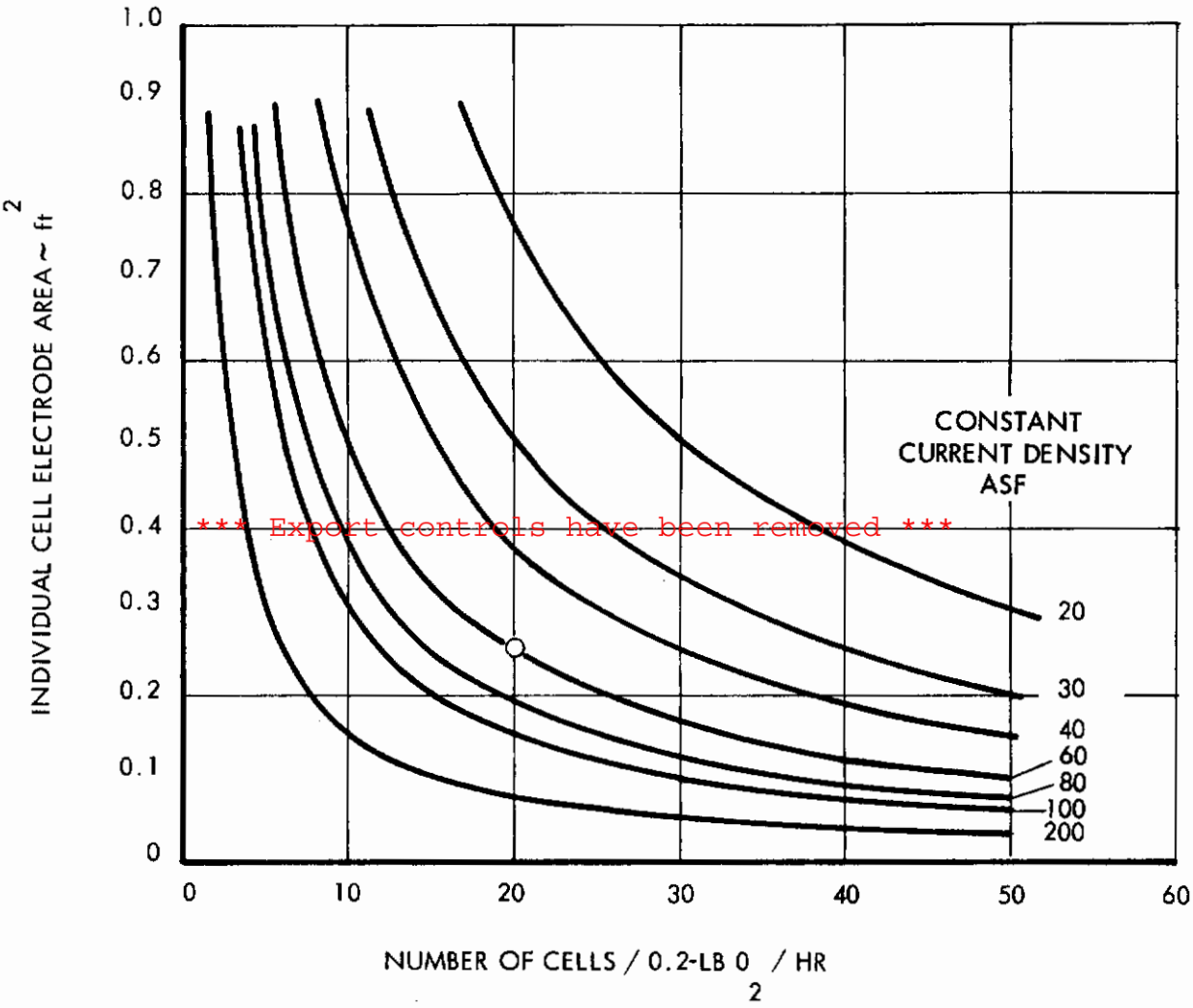

Figure 68 Current Density And Electrode Area Versus No. Cells

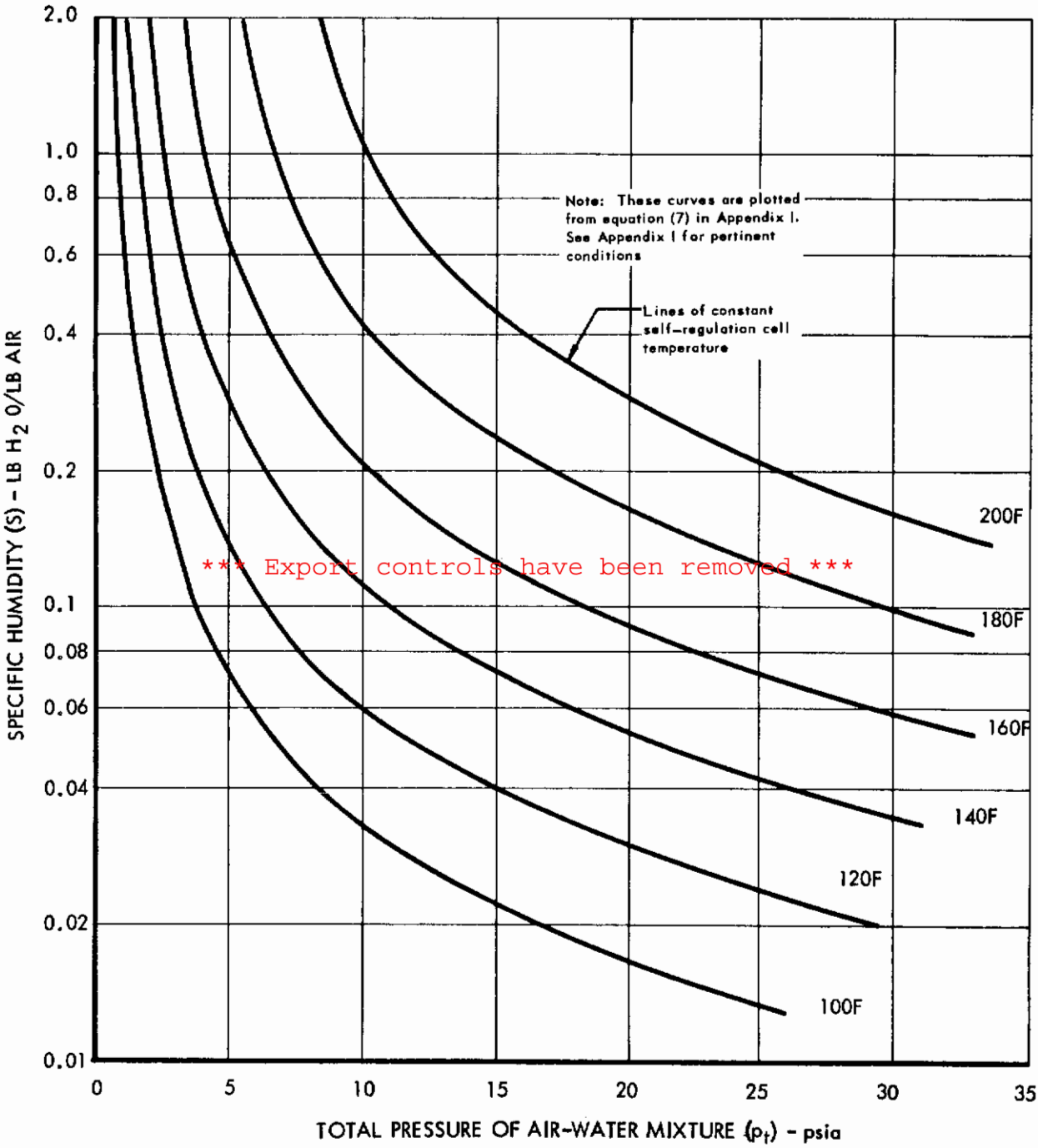

Figure 69 Specific Humidity Versus Pressure And Temperature

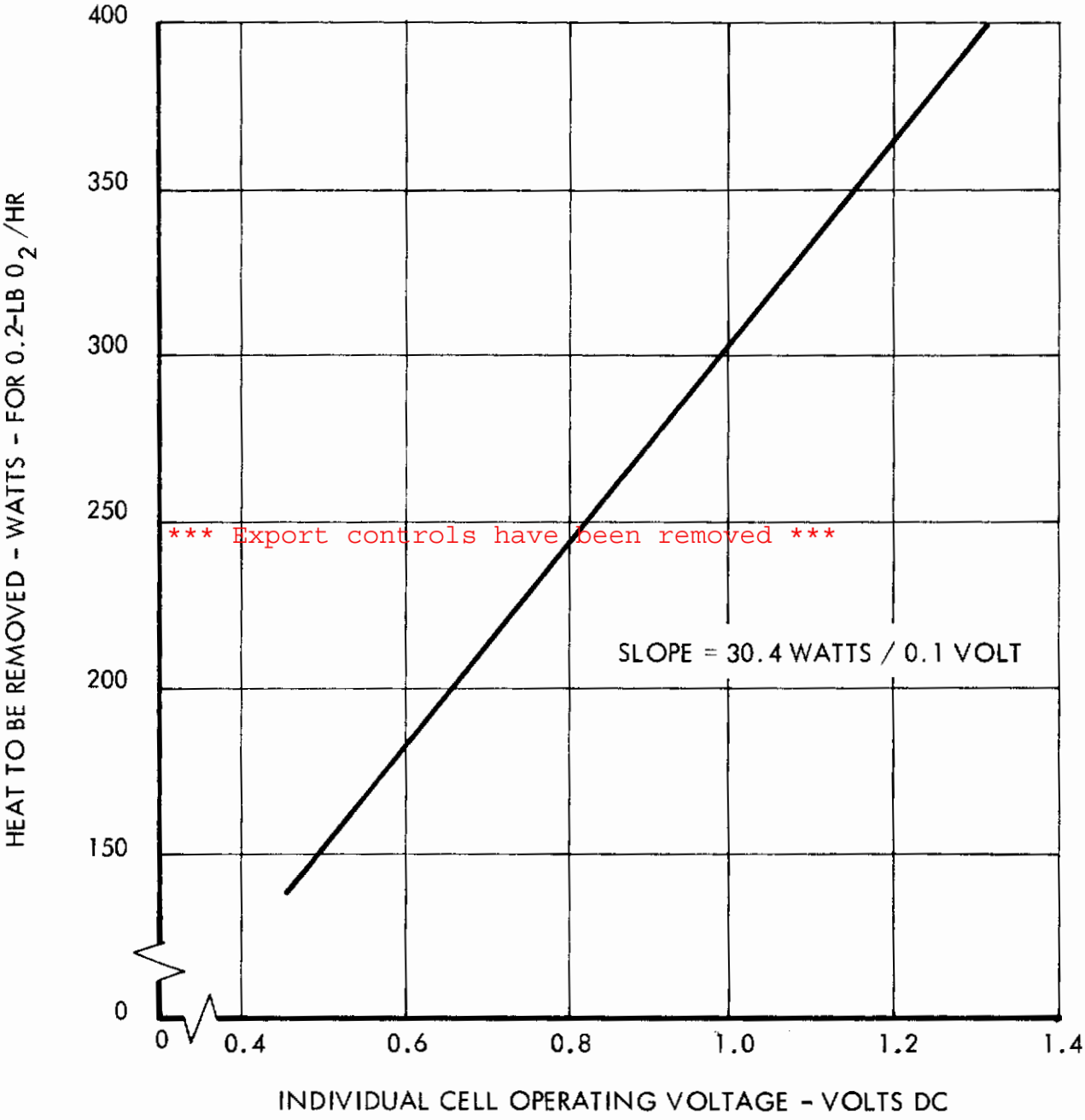

Figure 70 Cooling Load Versus Voltage

gas ducting (manifolding) design. In addition, use of the O-ring edge seal would be eliminated. Going from Model 140 (42-mil ducts) to Model 120 (32-mil ducts) for example, results in a 13% weight savings in the 0.2-lb/hr concentrator stack assembly. Going from Model 140 to Model 75, however, results in a 40% weight reduction.

A description of the recommended component materials and configurations is presented in Table X. The concentrator design is inherently a lightweight, compact configuration because of the thin geometry of the electrode-matrix-electrode "pack ". With the proposed design, the electrode-matrix-electrode "pack" is 40 mils. This could be decreased to 30 or 20 mils if the 20- or 10-mil matrix, respectively, were used.

A trade-off analysis was made between electrode types AB-1 and AB-6.[(a)] Table XI summarizes the comparison between electrode properties. The thicker electrodes, type AB-6, have an electrode density approximately 90% greater than the AB-1 electrodes used in the concentrator delivered under the present contract. For the forty electrodes required in the 0.2-lb/hr design, the total electrode weight is 0.7 lb with the AB-1 type, 0.6 lb less than with the AB-6 type. The AB-6 electrodes would add an additional 0.316 pound to a 0.2-lb/hr unit because of thicker bipolar plate flanges required to accommodate the greather electrode thickness.

The AB-1 electrodes have essentially the same performance characteristics as the AB-6 type. An advantage of the AB-6 electrodes over the AB-1 type is that they are easier to handle during the assembly and disassembly of cells. Since a final prototype unit will not be disassembled once the concentrator is ready for use, this handling advantage in itself does not seem to justify the choice of the AB-6 over the AB-1. Type AB-1 electrodes, therefore, were selected for the design.

4. FABRICATION PROCESSES

To ensure that the bipolar plates do not buckle following fly cutting to size, it is necessary that even amounts of magnesium stock are removed on each side. The 42-mil duct passages were made with specially purchased aircraft extension drills. These drills could not be obtained with a 32-mil diameter except by special purchase. Prior to the time the smaller diameter drills arrived, it was determined that an ordinary 32-mil drill, silver-soldered to a stainless steel welding rod, was a suitable substitute. The 32-mil diameter ducts were drilled into the sample with this "assembled" drill. This technique, therefore, permits fabrication of duct passages of almost any size without the need for purchasing special tools and eliminates the inherently long (six to eight weeks) delivery time associated with the special purchase.

When Model 120, or more compact versions are fabricated, duct diameters of 32 mils or smaller may be necessary. An alternate to drilling these is to use an electrical dis-

---

(a) Electrode designations of the supplier, American Cyanamid Company

Table X Geometrical Design Parameters for 0.2-lb/hr Unit

Cell Matrices	
Material	Johns Manville Fuel Cell Asbestos
Area Dimensions, in	4.6 x 9.6
Uncompressed Thickness, mil	30
Electrolyte	
Weight % KOH	33.3
Loading, g/g dry matrix	1.5
Electrodes*	
Type	American Cyanamid AB-1
Area Dimensions, in	4.2 x 9.2
Effective Area Dimensions, in	4.0 x 9.0
Bipolar Plates	
Material	Magnesium ZE-10
Plating Thickness, mil	
Nickel	1.3
Gold	0.03
Area Dimensions, in	6.1 x 11.8
Pin Height, in	
Air Compartment	0.032
Oxygen Compartment	0.032
Duct Diameter, in	0.032 max. or 0.020 slot
Total Thickness, in	0.120
Insulating Gaskets	
Material	Neoprene
Thickness, in	0.030
O-Rings	
Material	Ethylene-Propylene
Wicks	
Material	Polypropylene
Uncompressed Thickness, in	0.030
Electrolyte, wt % KOH	23
Support Screens	
Material	Nickel
Thickness, in	0.005

*See Table XI for details on electrodes

Table XI Comparison of Concentrator Electrodes

Property	Electrode AB-1	Electrode AB-6
Wetproofing Agent	Teflon	Teflon
Catalytic Material	Platinum Black; 9.0 ± 0.5 mg/cm^2	Platinum Black; 10.2 ± 1.1 mg/cm^2
Screen Material	Nickel	Gold-Plated Nickel
Mesh Size	100	70
Wire Size, mil	2	4.5
Thickness, mil	4-5	8-9
Electrode Weight (nominal), mg/in^2	220	420
Limiting Temperature, F	190	212

charge machining process. By this technique duct passages, in the form of rectangular slits, can be machined into a bipolar plate surface in the manner shown in Figure 71. One opening fabricated by this technique serves the same purpose as several circular duct passages lying side by side. Such ducts would be easier to make and would be more resistant to clogging.

Care must be taken to ensure that if Neoprene gaskets thinner than 30 mils are used that their electrical insulating property is checked. In measuring the resistance of some samples of 15-mil Neoprene, it was observed that not all samples were insulators. Upon checking with the supplier, it was determined that occasional batches of Neoprene can conduct electricity, particularly when the stock is very thin. This results from an electrical bridge of carbon used in its fabrication which extends from one face of the Neoprene to the other.

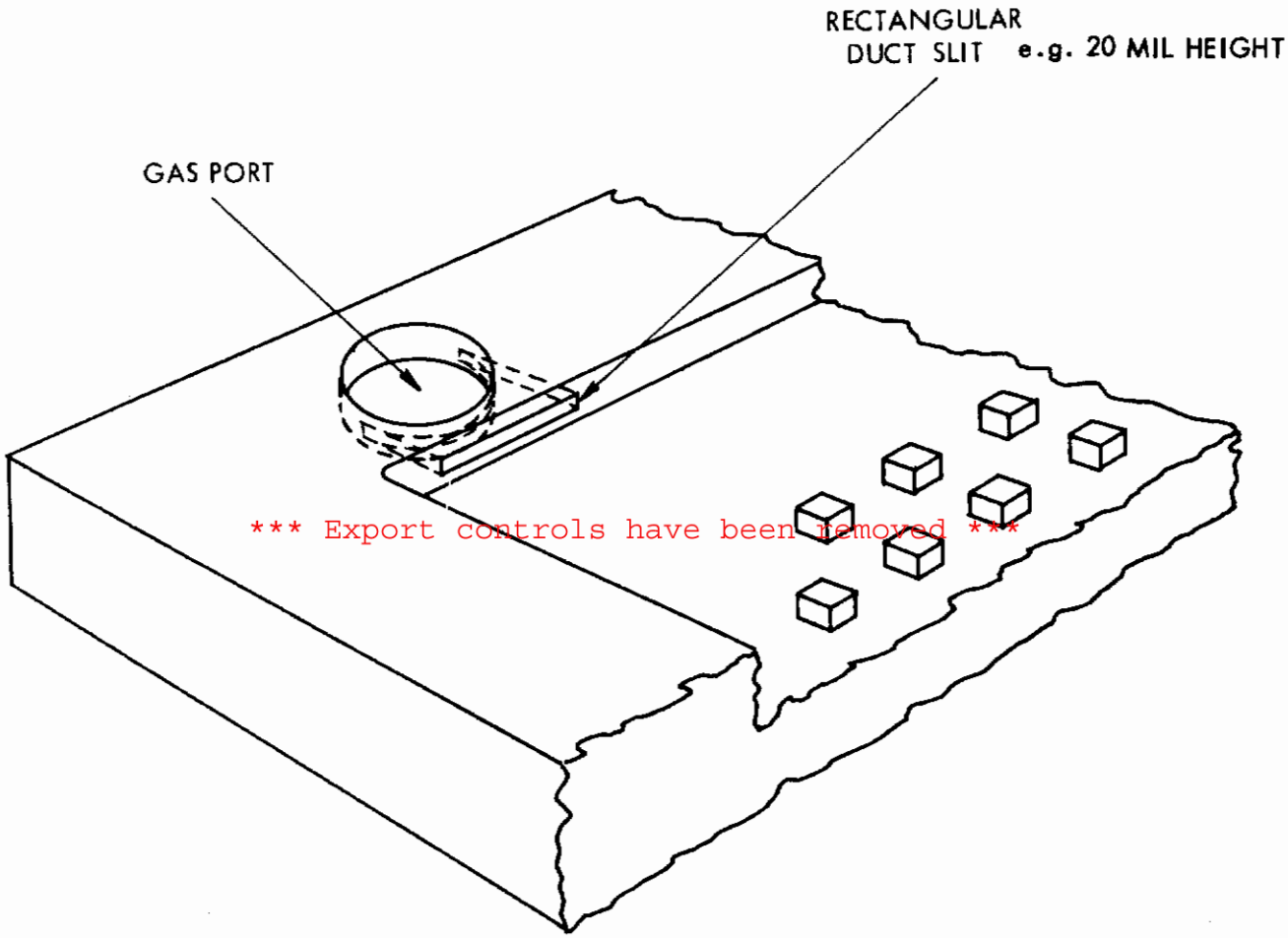

Figure 71 Rectangular Duct

SECTION VI

SUMMARY

A self-regulating, electrochemical oxygen concentrator for separating pure oxygen from air has been designed, fabricated and tested. The unit consists of three cells sandwiched between air humidifiers.

Compared to former models, size and weight have been reduced by minimizing flange dimensions, reducing bipolar plate thickness 25%, and optimizing the end plate configuration to allow for a 7% weight reduction over non ribbed configurations (see Figure 10). Additional size and weight reductions, compared to the unit in reference 1, resulted from the improved design point (a 10% decrease in cell voltage, a 14% increase in current density, and a 25% increase in percentage of oxygen concentrated from the incoming air stream).

Varying configurations were considered in designing the unit such as air distribution patterns, improved gas baffles, alternate gas ducts, an electrode trade-off evaluation, increased nickel-and gold-plate thickness for added corrosion protection and an ability to operate using 10-, 20-, and 30-mil electrolyte holding matrices.

The concentrator utilized 20 sq. in. electrodes, 5 mils thick. A 32% (by weight) KOH solution was held in a porous matrix that is able to retain the electrolyte in proper position regardless of gravity, orientation, or acceleration. The cell stack was constructed of a series of magnesium plates that were in turn plated with 1.3 mils of nickel and 0.03 mils of gold required for corrosion protection and electrical and thermal conductivity. Ethylene-propylene O-rings were used to effect a leak-free construction when operating on internal pressures up to 90 psia, and pressure differentials of up to 10 psia across cell matrices. Although Dacron and polypropylene wicks were used in the self-regulating process, only the polypropylene material proved effective against deterioration by the KOH humidifier fluid. Supplemental heating and cooling, not required of a flight unit, were included in the fabricated unit to allow for testing over a wide range of conditions.

The unit was tested in an instrumented rig at flow rates from two to five times the theoretical stoichiometric air flow rate (denoted at 2T, 5T, etc.) required for the oxygen being separated (concentrated), at current densities to 166 ASF, at cell temperatures from room temperature to 175F and at pressures from 5 to 90 psia. Performance data was taken with and without the cells' internal resistances being included in the terminal voltage measurement. Measurements were made which showed that when the unit was operating at 35 ASF and 5T, the pressure drop across the cells was only 0.4 inch of water. During initial testing the unit's stability to pressure differentials exceeded 10 psi. Early in the program cooling water created an unexpected corrosion problem which prevented further meaningful stability and oxygen purity tests. The problem was a result of the supplimentary cooling system and not, therefore, of direct concern to a

flight system. Prior to the cooling system failure, oxygen purity measurements showed the generated gas to be 100% oxygen when corrected for the water present. Parametric tests demonstrated the improvement possible as a result of high (175F) temperature operation. A 20-mil cell matrix gave better performance than either the 30- or 10-mil matrices. Internal resistance losses were low, 0.2-volt/cell or less (less than 1.8 ohm-cm^2) at the 100 ASF and 175F point. It was unexpectedly observed that the internal resistance fell with decreasing temperature, demonstrating a value of 0.12 volts per cell (1.1 ohm-cm^2) at the 100 ASF and 100F point. Under "dry" cell conditions internal resistances were observed to increase by a factor of two or three times the normal operating level. In general, it appeared as if the cell performance improved as the electrolyte loadings were increased from 1.0-1.25 g 32% KOH/g dry matrix to the 1.75-2.25 g 32% KOH/g dry matrix range. The testing program was culminated in two successful tests under self-regulating conditions, totaling over 200 hours.

A full-scale 0.2-lb/hr concentrator design analysis was carried on simultaneously with the testing program. Incorporated into the design recommendations were the best results obtained from testing and analytical evaluations. A self-regulating design was recommended consisting of 20-series-connected cells containing 7 humidifier units (one unit located between every third cell), with single cells outboard of the last humidifier units at each end of the stack. An exploded view of the unit is shown in Figure 72. The preferred electrode area was 4 x 9 inches, commensurate with the existing wicking technology. The design employs 120-mil-thick magnesium for the bipolar plates and represents an intermediate step toward the ultimate configuration. Note is made of the fact that additional analytical and testing experience must be obtained with the self-regulating system before the concept will reach its full potential of simplicity in control, i.e., no controls required at all. However, some modifications to the self-regulated design will permit its application prior to the time of ultimate development.

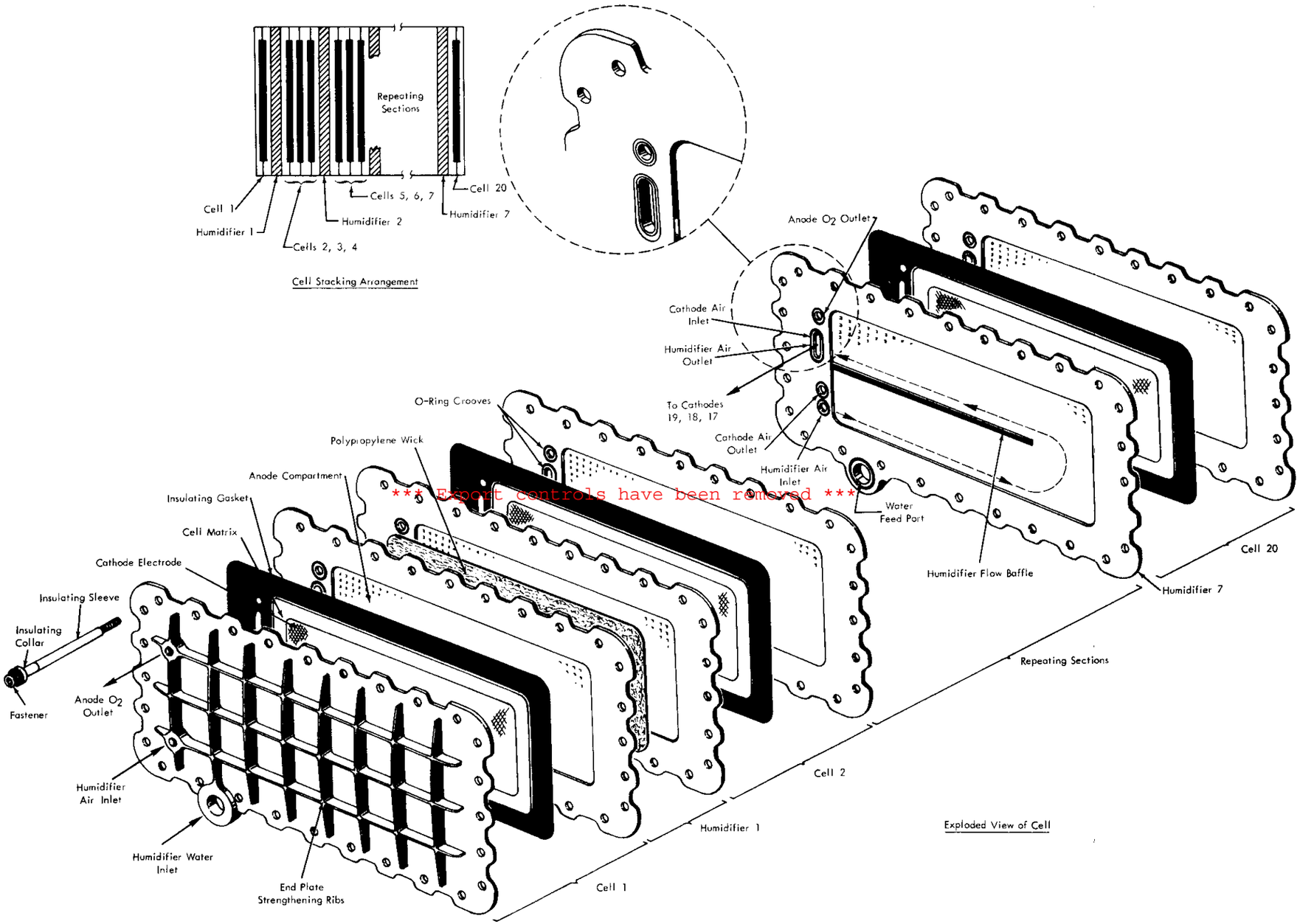

Figure 72 0.2-Lb/Hr Oxygen Concentrator

APPENDIX I

DETERMINATION OF SELF-REGULATION OPERATING EQUILIBRIUM

Determination of the conditions under which the cell self-regulates is concerned with the thermal balance between the heat generated during the oxygen concentrating process resulting from the application of electrical power and the heat removal by various means. The term "self regulation" implies that these means will be natural, i. e., no auxiliary heating or cooling is used. The rate of heat input, or power in, is defined by:

$$P_i = \dot{Q}_i = EIN \tag{1}$$

where:

$\dot{Q}_i$ = rate of heat input, watts

E = individual cell potential requirement, volts

I = current, amps

N = number of cells in the stack

Further, according to Faraday's Law:

$$W_{o_2} = 6.58 \times 10^{-4} IN \tag{2}$$

where:

W_{o_2} = mass flow rate of oxygen generated, lb/hr

Therefore by solving equations (1) and (2), the rate of heat input to the unit can be expressed as:

$$\dot{Q}_i = \frac{E\, W_{o_2}}{6.58} \times 10^4 \tag{3}$$

The resultant cell conditions which balance this heat load then define self-regulation equilibrium. This rate of heat removal is expressed by:

$$\dot{Q}_o = \dot{Q}_1 + \dot{Q}_p + \dot{Q}_a + \dot{Q}_e \tag{4}$$

where:

$\dot{Q}_o$ = total rate of heat removal, watts

$\dot{Q}_1$ = rate of heat lost by conduction, convection, and radiation, watts

$\dot{Q}_p$ = theoretical resistance - free power required to pump oxygen across the cell, watts

$\dot{Q}_a$ = rate of heat required to raise temperature of inlet air, watts

$\dot{Q}_e$ = rate of heat required to humidify incoming air, watts

Thermodynamically, it can be shown that $\dot{Q}_p$ is theoretically quite small since the application of only a small voltage (on the order of 0.01 vdc/cell) is sufficient to pump the oxygen in the air into a compartment of pure oxygen. Therefore, if a nominal cell total potential of 1.0 volt is assumed, the $\dot{Q}_p$ term will be on the order of 1% of the total load and will be neglected for this calculation. Further, in an effort to determine the highest possible self-regulation temperature, the rate of heat loss, $\dot{Q}_1$, will be neglected. The expression for the remaining terms are given by:

$$\dot{Q}_a = W_a \; c_p \; (T_c - T_a)K \tag{5}$$

where:

W_a = mass flow rate of air input, lb/hr

c_p = specific heat of air, 0.242 BTU/lb-F

T_c = cell temperature, F

T_a = ambient temperature, assumed 70F

K = conversion factor, 0.293 watt hr/BTU

and:

$$\dot{Q}_e = W_a S \ (h_g - h_f) K \qquad (6)^{(a)}$$

where:

S = specify humidity required to maintain cell moisture balance, lb $H_2 0$/lb air

h_g = enthalpy of saturated water vapor at cell temperature, T_c, BTU/lb

h_f = enthalpy of subcooled water as supplied to humifidier at ambient temperature, T_a (38 BTU/lb @ 70F)

K = conversion factor, 0.293 watt hr/BTU

and the specific humidity requirements dictated by the cell are:

$$S = \left[\frac{p_v}{p_t - p_v} \right] r \qquad (7)$$

where:

p_v = vapor pressure of cell electrolyte (33.3% KOH), psia

p_t = total pressure of air-water mixture, psia

r = ratio of molecular weights of water/air, 18/29

Since self-regulation, under the conditions specified, is defined by:

$$\dot{Q}_i = \dot{Q}_o = \frac{E \ W_{o_2}}{6.58} \ 10^4 \qquad (8)$$

(a) Values for h_g and h_f used in the calculations noted above were obtained from: Keenan, J. H., and Keyes, F. G., "Thermodynamic Properties of Steam," First Edition, John Wiley and Sons, Inc., New York, p. 28.

combining equations (3), (4), (5), (6), and (7) gives:

$$\frac{E\ W_{o_2}}{6.58}\ 10^4 = W_a K \left[c_p\ (T_c - T_a) + S(h_g - h_f) \right] \qquad (9)$$

Further, in Appendix IV it is shown that the air required to generate a specified amount of oxygen is:

$$W_a = K_1\ W_{o_2}\ xT \qquad (10)$$

where:

K_1 = conversion factor, 4.32 lb air/lb 0_2

xT = stoichiometric multiple

If equations (9) and (10) are solved for W_a and equated and solved for xT, the result is:

*** Export controls have been removed ***

$$xT = \frac{E}{6.58\ K\ K_1 \left[c_p\ (T_c - T_a) + S\ (h_g - h_f) \right]}\ 10^4 \qquad (11)$$

Hence an expression, independent of a specific oxygen generation rate, has been developed which defines conditions of self-regulation. Now, by specifying various total pressures and temperatures, the equation can be evaluated. The Equilibrium Map, presented in Figure 1, Section II, defines performance of self-regulation based on this data. Values for S in equation (7) are plotted in Figure 69 as a function of pressure and temperature.

APPENDIX II

EVALUATION OF THE 32-MIL GAS DUCTS

The three-cell, self-regulating concentrator was initially designed to be a version of concentrator Model 120. This design required 32-mil gas duct diameters. Since the plating subcontractor was unable to guarantee that the interior of these small diameter ducts could be plated, the concentrator model was changed to 140. It was decided that a specially designed test piece would be constructed to determine if bipolar plates having 32-mil diameter ducts can be fabricated and plated. This sample was then to be nickel- and gold-plated to determine if there would be sufficient plating buildup on the inside of the ducts. A copper layer was to be applied as a base for nickel plate, since nickel cannot be plated directly onto magnesium.

Figure 73 shows a sketch of the test piece designed to simulate the 32-mil duct passages that would exist in a bipolar plate of a concentrator having the gas flow rate requirements specified in the contract. A series of 42-mil ducts was also included for comparison purposes. The test piece was designed to test two parameters that affect the thickness of the plating inside duct passages of a given diameter, port diameter and length of the gas ducts leading from the electrode field (gas compartment) to the port.

Leading from the field are duct passages of a constant length (1/4 in.) with port diameters varying from 1/8 to 3/4 inch. A second test, at the opposite end, consisted of constant 1/4-inch gas port diameters. The 32- and 42-mil duct passages of lengths varying from 1/16 to 11/16 inch led from the ports to the simulated field.

The ZE10 magnesium test sample was nickel- and gold-plated according to the normal procedure. After being plated the piece was cross-sectioned at several different points, and the thicknesses of the copper, nickel and gold deposits were determined.

Figure 74 shows the results of the thickness measurements and the positions where the cross-sections were made.

The plating depth on the exterior surface of the sample was iniformly 0.75 mils of copper, 1.75 mils of nickel, and 5-6 microns of gold. The plating thickness in the duct passages, however, varied considerably depending upon the length of the duct, its diameter, and the diameter of the gas port. The following general comments can be made in regard to the results obtained:

a) The smaller duct holes had, for the most part, less plating in them than the larger duct holes. Because of their smaller size, less plating solution circulated through them. The irregularities resulted from gas entrapment in the passages.

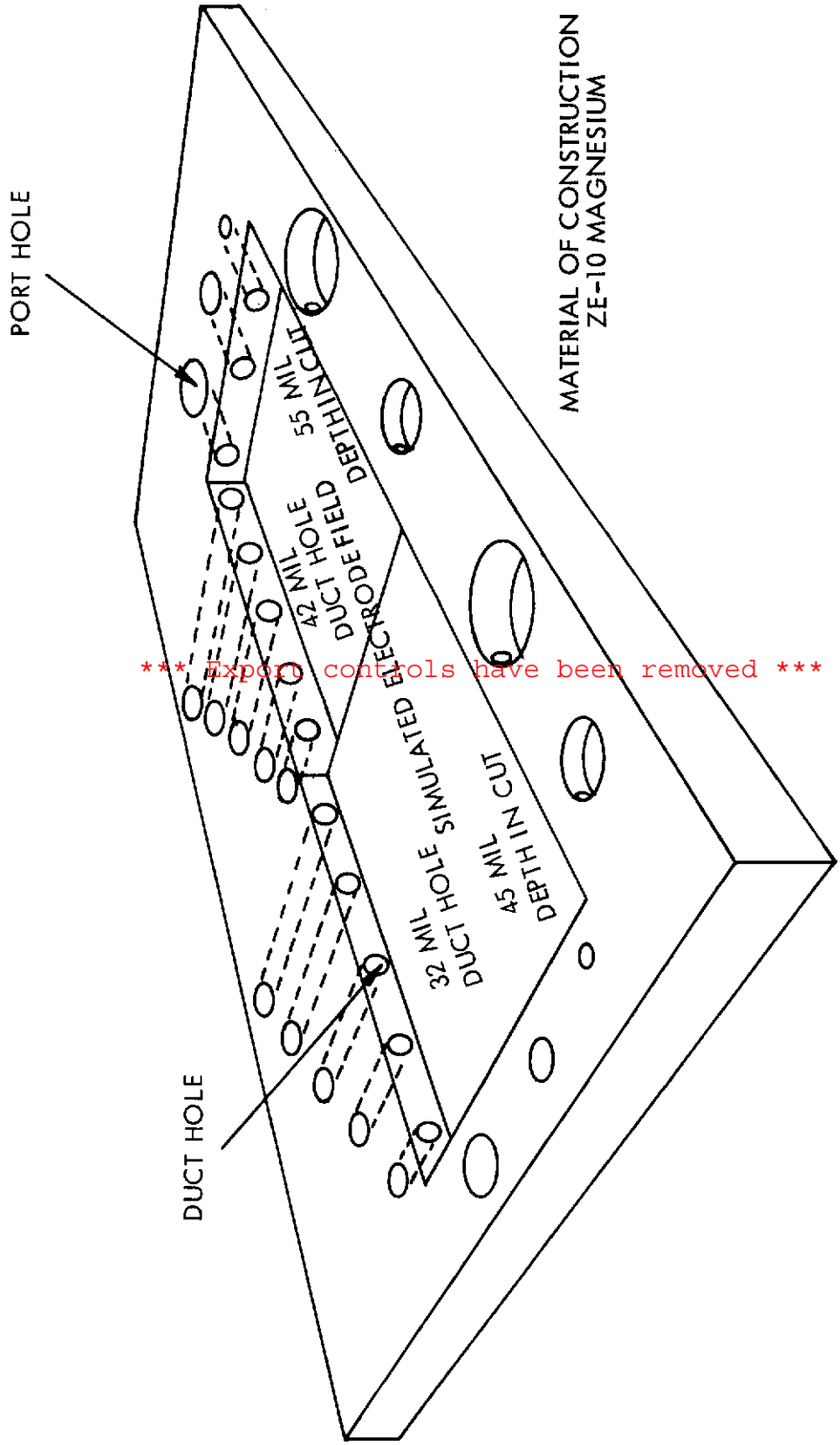

Figure 73 Simulated Port And Duct Hole Bipolar Plate Test Fixture

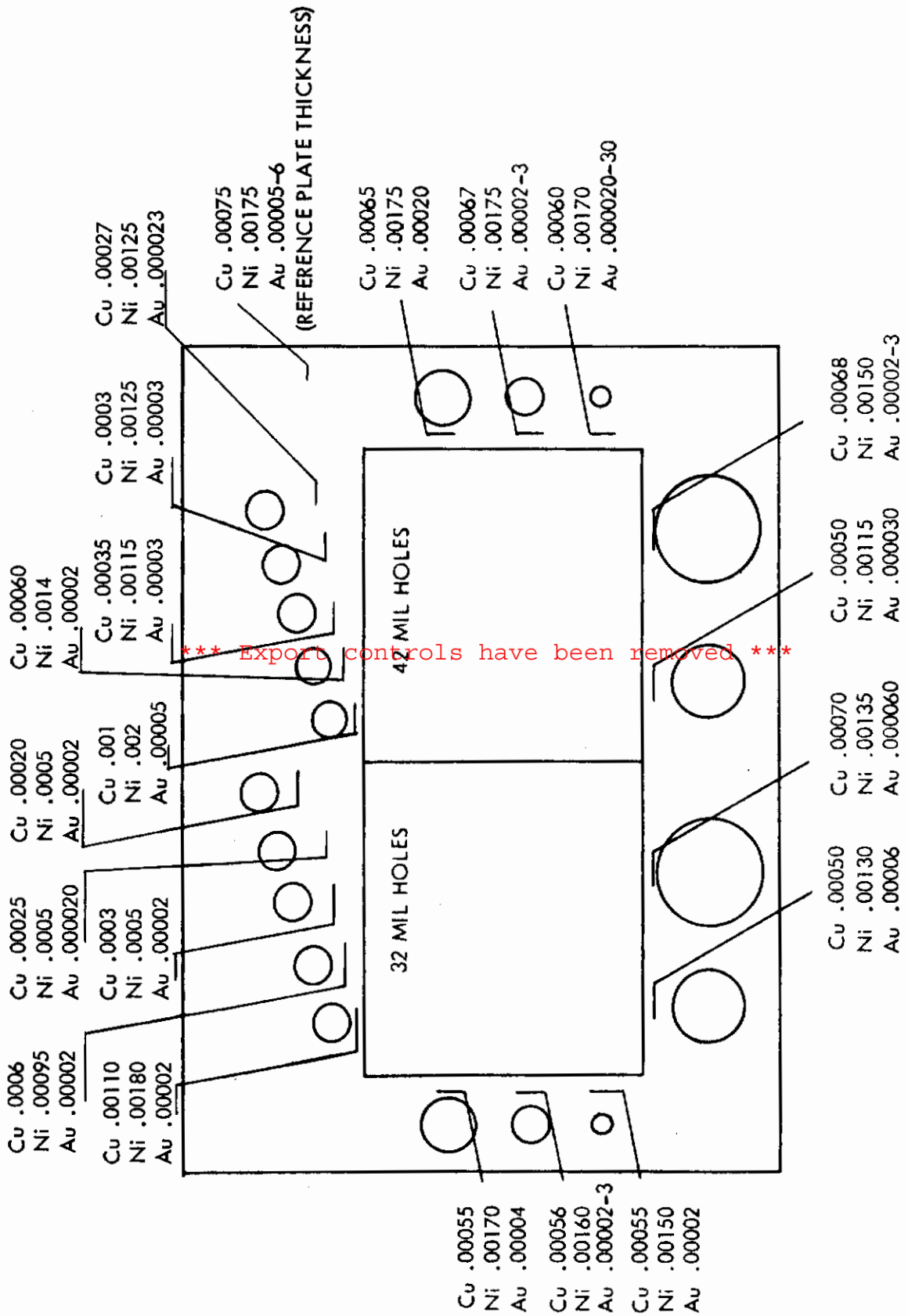

Figure 74 Plating Thickness Results

b) Copper plate thickness varied with duct size, port size and distance from the simulated electrode field. In general, the larger the duct size and the shorter the duct length, the thicker the deposits of copper.

c) Both the nickel and gold deposits varied with change in geometry in the same manner as the copper deposit, but the magnitude of the variation was less.

It can be concluded from these tests that gas ducts having a 32-mil diameter can be successfully plated. For an equivalent plating time, however, there will be less deposit in the 32-mil duct than in the 42-mil duct. In using a 32-mil duct, the length from the port to the electrode field (gas compartment) should be kept as short as possible and the port diameter as large as possible.

APPENDIX III

TEST DATA TABULATION

Included in the following pages are the data taken during the experimental test program discussed in SECTION IV - EXPERIMENTAL RESULTS.

0_2 CONCENTRATOR TEST DATA - PRELIMINARY EVALUATION

Nominal Cell Temp. 110-125
Nominal Cathode Pressure . . . . . 14.7 psia
Nominal Anode Pressure . . . . . 14.7 psia
Uncompressed Matrix Thickness . . . . . 30 mil
KOH Concentration 32%
Electrolyte Loading $_2$ . . . . . 1.0gm/gm dry matrix
No. of Cells @ 20 in^2 Each. 3

Data Pt. No.	Flow xT	Current Density ASF	Cell 1 Temp. F	Cell 3 Temp. F	Voltage - Terminal Cell 1 E_{1t}	Cell 2 E_{2t}	Cell 3 E_{3t}
PE-1	5T	10.8	118	120	0.600	0.600	0.560
PE-2	↓	21.6	118	118	0.640	0.640	0.600
PE-3		31.6	118	118	0.670	0.670	0.640
PE-4		41.0	118	118	0.700	0.700	0.670
PE-5		50.3	120	118	0.730	0.730	0.720
PE-6		59.4	123	120	0.760	0.760	0.760
PE-7		79.0	125	123	0.790	0.790	0.890
PE-8	4T	10.8	110	110	0.570	0.570	0.560
PE-9	↓	21.6	109	110	0.605	0.608	0.608
PE-10		31.6	110	110	0.640	0.640	0.650
PE-11		41.0	111	110	0.660	0.670	0.730
PE-12		50.3	114	113	0.690	0.690	0.890
PE-13		59.4	120	105	0.700	0.703	1.020
PE-14		79.0	123	119	0.715	0.740	1.320
PE-15	3T	10.8	120	123	0.570	0.580	0.550
PE-16	↓	21.6	118	118	0.610	0.630	0.610
PE-17		31.6	118	118	0.645	0.660	0.660

0_2 CONCENTRATOR TEST DATA - PRELIMINARY EVALUATION (Con't.)

Data Pt. No.	Flow xT	Current Density ASF	Cell 1 Temp. F	Cell 3 Temp. F	Voltage - Terminal Cell 1 $E1_t$	Cell 2 E_{2t}	Cell 3 E_{3t}
PE-18	3T	41.0	119	118	0.670	0.680	0.800
PE-19	↓	50.3	120	120	0.700	0.720	1.260
PE-20	↓	59.4	124	120	0.720	0.730	1.280
PE-21	2T	10.8	124	120	0.590	0.590	0.550
PE-22	↓	31.6	124	120	0.660	0.680	0.800
PE-23	↓	50.3	124	120	0.760	0.740	1.400

O_2 CONCENTRATOR TEST DATA

Nominal Cell Temp.	100F
Nominal Cathode Pressure	14.7 psia
Nominal Anode Pressure	14.7 psia
Uncompressed Matrix Thickness	30 mil
No. of Bolts	13
Bolt Torque	40 lb. in.
KOH Concentration	32%
Electrolyte Loading	1.25 g dry Matrix
No. of Cells @ 20 in^2 each	3

Data Pt. No.	Flow xT	Current Amp	Current Density ASF	Humidifier Temp. F	Cell 1 Temp. F	Cell 2 Temp. F	Cell 3 Temp. F	Cell 1 Voltage E_{1t}	Cell 1 IR Free E_{1f}	Cell 2 Voltage E_{2t}	Cell 2 IR Free E_{2f}	Cell 3 Voltage E_{3t}	Cell 3 IR Free E_{3f}
1	5T	1.39	10	82	100	107	100	0.725	0.715	0.760	0.750	0.720	0.705
2	↓	2.78	20	82	100	108	100	0.820	0.784	0.850	0.820	0.815	0.784
3		5.55	40	82	104	105	103	0.920	0.880	0.940	0.900	0.900	0.865
4		8.35	60	82	107	105	107	1.000	0.930	1.030	0.945	0.970	0.910
5		11.1	80	82	107	100	107	1.070	0.970	1.080	0.995	1.040	0.960
6		13.9	100	82	109	95	109	1.160	1.010	1.190	1.050	1.160	1.020
7	3T	1.39	10	82	100	109	100	0.740	0.715	0.780	0.760	0.740	0.720
8		2.78	20	82	101	105	100	0.820	0.800	0.860	0.840	0.824	0.803
9		5.55	40	81	103	105	102	0.910	0.860	0.935	0.880	0.900	0.860
10		8.35	60	80	108	100	108	0.960	0.910	0.990	0.950	0.960	0.900
11		11.1	80	80	110	100	110	1.090	1.020	1.130	1.075	1.060	1.000
12		13.9	100	80	115	100	115	1.260	1.140	1.300	1.190	1.240	1.130
13	2T	2.78	20	80	100	100	100	0.795	0.765	0.835	0.815	0.800	0.780
14		8.35	60	80	106	100	107	1.025	0.950	1.040	0.975	1.005	0.940
15		11.1	80	80	110	100	111	1.195	1.100	1.255	1.170	1.145	1.055
16		13.9	100	80	115	100	116	1.315	1.195	1.360	1.250	1.280	1.180

O_2 CONCENTRATOR TEST DATA

Nominal Cell Temp	125F
Nominal Cathode Pressure	14.7 psia
Nominal Anode Pressure	14.7 psia
Uncompressed Matrix Thickness	30 mil
No. of Bolts	13
Bolt Torque	40 lb. in.
KOH Concentration	32%
Electrolyte Loading	1.25 g/g dry Matrix
No. of Cells @ 20 in^2 each	3

Data Pt. No.	Flow xT	Current Amp	Current Density ASF	Humidifier Temp. F	Cell 1 Temp. F	Cell 2 Temp. F	Cell 3 Temp. F	Cell 1 Voltage E_{1t}	Cell 1 IR Free E_{1f}	Cell 2 Voltage E_{2t}	Cell 2 IR Free E_{2f}	Cell 3 Voltage E_{3t}	Cell 3 IR Free E_{3f}
17	5T	1.39	10	103	126	135	125	0.640	0.635	0.675	0.670	0.655	0.640
18	↓	2.78	20	103	125	135	124	0.720	0.705	0.765	0.745	0.735	0.715
19		5.55	40	104	128	125	128	0.815	0.770	0.850	0.810	0.820	0.780
20		8.35	60	103	127	125	127	0.900	0.830	0.935	0.865	0.925	0.860
21		11.1	80	103	128	125	128	0.965	0.875	0.995	0.910	1.020	0.930
22		13.9	100	104	129	125	130	1.040	0.910	1.070	0.960	1.200	1.080
23	3T	1.39	10	105	127	135	127	0.650	0.640	0.685	0.680	0.660	0.650
24	↓	2.78	20	104	126	135	127	0.730	0.705	0.780	0.755	0.750	0.725
25		5.55	40	104	126	125	126	0.830	0.785	0.880	0.835	0.860	0.810
26		8.35	60	104	126	125	127	0.930	0.855	0.970	0.900	0.990	0.915
27		11.1	80	104	129	130	129	1.030	0.920	1.070	0.970	1.190	1.080
28		13.9	100	104	135	128	136	1.110	0.980	1.170	1.050	1.420	1.270
29	2T	2.78	20	104	124	128	125	0.740	0.708	0.780	0.750	0.750	0.725
30	↓	8.35	60	104	125	128	125	0.960	0.880	1.000	0.930	1.030	0.940
31		11.1	80	104	130	128	130	1.050	0.955	1.100	1.015	1.220	1.110
32		13.9	100	104	133	128	135	1.160	1.050	1.250	1.150	1.540	1.375

0_2 CONCENTRATOR TEST DATA

Nominal Cell Temp.	125F
Nominal Cathode Pressure	14.7 psia
Nominal Anode Pressure	14.7 psia
Uncompressed Matrix Thickness	20 mil
No. of Bolts	19
Bolt Torque	40 lb in
KOH Concentration	32%
Electrolyte Loading	1.25g/g dry matrix
No. of Cells @ 20 in^2 each	1 (No. 3)

Data Pt. No.	Flow xT	Current Amp	Current Density ASF	Humifidier Temp. F	Cell Temp. F	Cell Voltage E_t	Cell E IR Free E_f
65	5T	2.08	15	104	126	0.740	0.730
66	↓	4.86	35	103	125	0.820	0.800
67	↓	6.95	50	103	124	0.860	0.830
68	↓	9.02	65	104	125	0.900	0.860
69	↓	11.1	80	104	125	0.940	0.870
70	↓	13.9	100	104	125	1.000	0.925
71	3T	2.08	15	105	125	0.715	0.705
72	↓	4.86	35	106	125	0.820	0.800
73	↓	9.02	65	105	125	0.940	0.900
74	2T	2.08	15	105	125	0.750	0.745
75	↓	4.86	35	105	125	0.830	0.805
76	↓	9.02	65	104	125	0.950	0.905

O_2 CONCENTRATOR TEST DATA

Nominal Cell Temp	150F
Nominal Cathode Pressure	14.7 psia
Nominal Anode Pressure	14.7 psia
Uncompressed Matrix Thickness	30 mil
No. of Bolts	13
Bolt Torque	40 lb. in.
KOH Concentration	32%
Electrolyte Loading $_2$	1.25 g/g dry Matrix
No. of Cells @ 20 in^2 each	3

Data Pt. No.	Flow xT	Current Amp	Current Density ASF	Humidifier Temp. F	Cell 1 Temp. F	Cell 2 Temp. F	Cell 3 Temp. F	Cell 1 Voltage E_{1t}	Cell 1 IR Free E_{1f}	Cell 2 Voltage E_{2t}	Cell 2 IR Free E_{2f}	Cell 3 Voltage E_{3t}	Cell 3 IR Free E_{3f}
33	5T	1.39	10	126	152	158	150	0.605	0.595	0.640	0.620	0.625	0.605
34	↓	2.78	20	127	152	154	151	0.660	0.645	0.695	0.675	0.685	0.660
35		5.55	40	127	148	154	150	0.770	0.722	0.812	0.764	0.804	0.750
36		8.35	60	127	146	159	147	0.870	0.790	0.905	0.830	0.930	0.840
37		11.1	80	127	153	166	153	0.935	0.830	0.970	0.870	1.050	0.930
38		13.9	100	127	159	160	160	0.965	0.840	1.015	0.880	1.170	1.000
39	3T	1.39	10	127	150	155	150	0.610	0.600	0.640	0.620	0.630	0.610
40	↓	2.78	20	127	147	160	147	0.660	0.640	0.700	0.680	0.690	0.655
41		5.55	40	127	153	165	150	0.760	0.700	0.805	0.745	0.815	0.735
42		8.35	60	127	155	162	155	0.850	0.775	0.900	0.820	0.945	0.835
43		11.1	80	127	155	157	156	0.945	0.830	0.990	0.880	1.130	0.980
44		13.9	100	127	157	157	159	1.040	0.900	1.090	0.950	1.440	1.250
45	2T	2.78	20	127	146	165	145	0.670	0.640	0.720	0.680	0.700	0.650
46	↓	8.35	60	127	154	165	152	0.915	0.815	0.962	0.862	1.040	0.900
47		11.1	80	127	161	155	161	1.000	0.880	1.050	0.930	1.230	1.070
48		13.9	100	127	159	155	162	1.070	0.940	1.140	1.005	1.490	1.300

O_2 CONCENTRATOR TEST DATA

Nominal Cell Temp.	175F
Nominal Cathode Pressure	14.7 psia
Nominal Anode Pressure	14.7 psia
Uncompressed Matrix Thickness	30 mil
No. of Bolts	13
Bolt Torque	40 lb. in.
KOH Concentration	32%
Electrolyte Loading	1.25 g/g dry Matrix
No. of Cells @ 20 in^2 each	3

Data Pt. No.	Flow xT	Current Amp	Current Density ASF	Humidifier Temp. F	Cell 1 Temp. F	Cell 2 Temp. F	Cell 3 Temp. F	Cell 1 Voltage E_{1t}	Cell 1 IR Free E_{1f}	Cell 2 Voltage E_{2t}	Cell 2 IR Free E_{2f}	Cell 3 Voltage E_{3t}	Cell 3 IR Free E_{3f}
49	5T	1.39	10	151	171	185	172	0.560	0.530	0.570	0.550	0.580	0.550
50	↓	2.78	20	151	173	185	173	0.610	0.575	0.640	0.595	0.645	0.580
51		5.55	40	151	175	185	176	0.720	0.650	0.760	0.680	0.780	0.660
52		8.35	60	151	175	185	177	0.815	0.700	0.845	0.730	0.900	0.725
53		11.1	80	151	176	185	179	0.890	0.740	0.930	0.780	1.050	0.815
54		13.9	100	151	177	185	182	0.962	0.780	0.995	0.815	1.170	0.900
55	3T	1.39	10	151	169	185	170	0.565	0.550	0.580	0.560	0.585	0.550
56	↓	2.78	20	151	170	192	171	0.640	0.600	0.670	0.625	0.680	0.610
57		5.55	40	151	175	192	175	0.730	0.650	0.770	0.685	0.800	0.670
58		8.35	60	151	183	192	185	0.805	0.695	0.850	0.725	0.925	0.730
59		11.1	80	151	182	185	185	0.885	0.730	0.925	0.760	1.055	0.795
60		13.9	100	151	182	185	188	0.970	0.770	1.010	0.800	1.230	0.900
61	2T	2.78	20	151	170	192	170	0.620	0.580	0.640	0.605	0.655	0.585
62	↓	8.35	60	151	175	192	177	0.855	0.725	0.890	0.760	0.990	0.770
63		11.1	80	151	182	185	185	0.920	0.750	0.950	0.790	1.100	0.835
64		13.9	100	151	183	185	188	1.000	0.800	1.040	0.830	1.270	0.945

0_2 CONCENTRATOR TEST DATA

Nominal Cell Temp.	125F
Nominal Cathode Pressure	10.0 psia
Nominal Anode Pressure	14.7 psia
Uncompressed Matrix Thickness	20 mil
No. of Bolts	19
Bolt Torque	40 lb in
KOH Concentration	32%
Electrolyte Loading	1.25g/g dry matrix
No. of Cells @ 20 in^2 each	1 (No. 3)

Data Pt. No.	Flow xT	Current Amp	Current Density ASF	Humifidier Temp. F	Cell Temp. F	Cell Voltage E_t	Cell E IR Free E_f
77	5T	2.08	15	105	125	0.855	0.830
78	↓	4.86	35	104	125	0.970	0.940
79	↓	6.95	50	104	125	1.060	1.000
80	↓	9.02	65	104	125	1.160	1.100
81	↓	11.1	80	104	125	1.330	1.230
82	↓	13.9	100	104	125	1.800	1.690
83	3T	2.08	15	104	125	0.825	0.815
84	↓	4.86	35	104	125	0.960	0.920
85	↓	9.02	65	104	125	1.180	1.095
86	2T	2.08	15	104	125	0.815	0.795
87	↓	4.86	35	104	125	0.945	0.905
88	↓	9.02	65	104	125	1.115	1.045

0_2 CONCENTRATOR TEST DATA

Nominal Cell Temp.	125F
Nominal Cathode Pressure	14.7 psia
Nominal Anode Pressure	10.0 psia
Uncompressed Matrix Thickness	20 mil
No. of Bolts	19
Bolt Torque	40 lb in
KOH Concentration	32%
Electrolyte Loading	1.25g/g dry matrix
No. of Cells @ 20 in^2 each	1 (No. 3)

Data Pt. No.	Flow xT	Current Amp	Current Density ASF	Humifidier Temp. F	Cell Temp. F	Cell Voltage E_t	Cell E IR Free E_f
89	5T	2.08	15	103	125	0.695	0.685
90	↓	4.86	35	104	125	0.790	0.765
91	↓	6.95	50	104	125	0.895	0.850
92	↓	9.02	65	105	125	0.945	0.895
93	↓	11.1	80	105	125	0.990	0.930
94	↓	13.9	100	105	125	1.060	0.980
95	3T	2.08	15	104	124	0.755	0.745
96	↓	4.86	35	104	125	0.855	0.820
97	↓	9.02	65	105	125	0.950	0.905
98	2T	2.08	15	105	125	0.750	0.735
99	↓	4.86	35	103	125	0.850	0.830
100	↓	9.02	65	104	125	0.970	0.920

O_2 CONCENTRATOR TEST DATA

Nominal Cell Temp.	125F
Nominal Cathode Pressure	14.7 psia
Nominal Anode Pressure	14.7 psia
Uncompressed Matrix Thickness	10 mil
No. of Bolts	18
Bolt Torque	30 lb in
KOH Concentration	32%
Electrolyte Loading	1.25g/g dry matrix
No. of Cells @ 20 in^2 each	1 (No. 3)

Data Pt. No.	Flow xT	Current Amp	Current Density ASF	Humifidier Temp. F	Cell Temp. F	Cell Voltage E_t	Cell E IR Free E_f
101	5T	2.08	15	104	125	0.775	0.755
102	↓	4.86	35	104	125	0.895	0.840
103	↓	6.95	50	103	125	0.970	0.900
104	↓	9.02	65	103	125	1.040	0.945
105	↓	11.1	80	104	125	1.110	0.995
106	↓	13.9	100	104	125	1.210	1.060
107	3T	2.08	15	104	125	0.810	0.790
108	↓	4.86	35	104	125	0.925	0.875
109	↓	9.02	65	104	125	1.080	0.990
110	2T	2.08	15	104	125	0.860	0.840
111	↓	4.86	35	104	125	0.970	0.910
112	↓	9.02	65	104	125	1.110	1.050
113-124	Not Obtained Due To Malfunction						

0_2 CONCENTRATOR TEST DATA

Nominal Cell Temp.	125F
Nominal Cathode Pressure	14.7 psia
Nominal Anode Pressure	10.0 psia
Uncompressed Matrix Thickness	10 mil
No. of Bolts	18
Bolt Torque	30 lb in
KOH Concentration	32%
Electrolyte Loading	1.25g/g dry matrix
No. of Cells @ 20 in^2 each	1 (No. 3)

Data Pt. No.	Flow xT	Current Amp	Current Density ASF	Humifidier Temp. F	Cell Temp. F	Cell Voltage E_t	Cell E IR Free E_f
125	5T	2.08	15	104	125	0.775	0.765
126	↓	4.86	35	104	125	0.890	0.845
127	↓	6.95	50	104	125	0.955	0.895
128	↓	9.02	65	104	125	1.040	0.945
129	↓	11.1	80	104	125	1.120	1.050
130	↓	13.9	100	104	125	1.305	1.120
131	3T	2.08	15	104	125	0.800	0.780
132	↓	4.86	35	104	125	0.935	0.860
133	↓	9.02	65	104	125	1.095	0.960
134	2T	2.08	15	104	125	0.805	0.780
135	↓	4.86	35	104	125	0.930	0.850
136	↓	9.02	65	104	125	1.180	0.950

O_2 CONCENTRATOR TEST DATA

Nominal Cell Temp.	125F
Nominal Cathode Pressure	5.0 psia
Nominal Anode Pressure	5.0 psia
Uncompressed Matrix Thickness	30 mil
No. of Bolts	18
Bolt Torque	35-40 lb in
KOH Concentration	32%
Electrolyte Loading	1.25g/g dry matrix
No. of Cells @ 20 in^2 each	1 (No. 3)

Data Pt. No.	Flow xT	Current Amp	Current Density ASF	Humifidier Temp. F	Cell Temp. F	Cell Voltage E_t	Cell E IR Free E_f
137	5T	2.08	15	104	125	1.640	1.620
138	↓	4.86	35	104	125	1.720	1.690
139	↓	6.95	50	104	125	1.770	1.720
140	↓	9.02	65	104	125	1.820	1.750
141	↓	11.1	80	104	125	2.080	1.900
142	↓	13.9	100	104	125	2.150	1.940
143	3T	2.08	15	104	125	1.380	1.360
144	↓	4.86	35	104	125	1.800	1.700
145	↓	9.02	65	104	125	2.000	1.880
146	2T	2.08	15	104	125	1.450	1.400
147	↓	4.86	35	104	125	1.780	1.700
148	↓	9.02	65	104	125	2.080	1.900

0_2 CONCENTRATOR TEST DATA

Nominal Cell Temp.	125F
Nominal Cathode Pressure	5.0 psia
Nominal Anode Pressure	5.0 psia
Uncompressed Matrix Thickness	30 mil
No. of Bolts	18
Bolt Torque	35-40 lb in
KOH Concentration	32%
Electrolyte Loading	1.25g/g dry matrix
No. of Cells @ 20 in^2 each	1 (No. 3)

Data Pt. No.	Flow xT	Current Amp	Current Density ASF	Humifidier Temp. F	Cell Temp. F	Cell Voltage E_t	Cell E IR Free E_f
137A	5T	2.08	15	104	125	0.835	0.815
138A	↓	4.86	35	104	125	1.450	1.410
139A	↓	6.95	50	104	125	1.800	1.730
140A	↓	9.02	65	104	125	1.840	1.780
141A	↓	11.1	80	104	125	1.880	1.790
142A	↓	13.9	100	104	125	1.950	1.830
143A	3T	2.08	15	104	121	0.825	0.805
144A	↓	4.86	35	104	125	1.590	1.510
145A	↓	9.02	65	104	125	1.830	1.740
146A	2T	2.08	15	104	124	0.825	0.805
147A	↓	4.86	35	104	125	1.550	1.510
148A	↓	9.02	65	104	125	1.840	1.730

0_2 CONCENTRATOR TEST DATA

Nominal Cell Temp.	125F
Nominal Cathode Pressure	7.5 psia
Nominal Anode Pressure	7.5 psia
Uncompressed Matrix Thickness	30 mil
No. of Bolts	18
Bolt Torque	35-40 lb in
KOH Concentration	32%
Electrolyte Loading	1.25g/g dry matrix
No. of Cells @ 20 in^2 each	1 (No. 3)

Data Pt. No.	Flow xT	Current Amp	Current Density ASF	Humifidier Temp. F	Cell Temp. F	Cell Voltage E_t	Cell E IR Free E_f
149	5T	2.08	15	104	125	0.775	0.740
150	↓	4.86	35	104	125	0.970	0.880
151	↓	6.95	50	104	125	1.200	1.075
152	↓	9.02	65	104	125	1.610	1.360
153	↓	11.1	80	104	125	1.860	1.620
154	↓	13.9	100	104	125	2.060	1.750
155	3T	2.08	15	104	125	0.845	0.780
156	↓	4.86	35	104	125	1.080	0.940
157	↓	9.02	65	104	125	1.680	1.410
158	2T	2.08	15	104	125	0.890	0.825
159	↓	4.86	35	104	125	1.150	1.000
160	↓	9.02	65	104	125	1.710	1.400

O_2 CONCENTRATOR TEST DATA

Nominal Cell Temp.	125F
Nominal Cathode Pressure	7.5 psia
Nominal Anode Pressure	7.5 psia
Uncompressed Matrix Thickness	30 mil
No. of Bolts	18
Bolt Torque	35-40 lb in
KOH Concentration	32%
Electrolyte Loading	1.25g/g dry matrix
No. of Cells @ 20 in^2 each	1 (No. 3)

Data Pt. No.	Flow xT	Current Amp	Current Density ASF	Humifidier Temp. F	Cell Temp. F	Cell Voltage E_t	Cell E IR Free E_f
149A	5T	2.08	15	104	125	0.760	0.740
150A	↓	4.86	35	104	125	1.000	0.930
151A	↓	6.95	50	104	126	1.710	1.600
152A	↓	9.02	65	104	126	1.780	1.640
153A	↓	11.1	80	104	126	1.940	1.780
154A	↓	13.9	100	104	129	2.140	1.910
155A	3T	2.08	15	105	125	0.895	0.840
156A	↓	4.86	35	107	123	1.520	1.430
157A	↓	9.02	65	106	126	1.910	1.700
158A	2T	2.08	15	108	120	0.900	0.850
159A	↓	4.86	35	108	121	1.590	1.470
160A	↓	9.02	65	109	124	2.020	1.790

O_2 CONCENTRATOR TEST DATA

Nominal Cell Temp.	125F
Nominal Cathode Pressure	10.0 psia
Nominal Anode Pressure	10.0 psia
Uncompressed Matrix Thickness	30 mil
No. of Bolts	18
Bolt Torque	35-40 lb in
KOH Concentration	32%
Electrolyte Loading	1.25g/g dry matrix
No. of Cells @ 20 in^2 each	1 (No. 3)

Data Pt. No.	Flow xT	Current Amp	Current Density ASF	Humifidier Temp. F	Cell Temp. F	Cell Voltage E_t	Cell E IR Free E_f
161	5T	2.08	15	104	125	0.920	0.835
162	↓	4.86	35	104	125	1.235	1.020
163	↓	6.95	50	104	125	1.470	1.120
164	↓	9.02	65	104	125	1.810	1.310
165	↓	11.1	80	104	125	2.140	1.450
166	↓	13.9	100	104	125	2.480	1.500
167	3T	2.08	15	104	125	1.020	0.840
168	↓	4.86	35	104	125	1.600	1.120
169	↓	9.02	65	104	130	2.290	1.340
170	2T	2.08	15	104	120	1.130	0.905
171	↓	4.86	35	104	120	1.750	1.150
172	↓	9.02	65	104	120	2.620	1.340
173-196	Not Obtained Due To Malfunction						

0_2 CONCENTRATOR TEST DATA

Nominal Cell Temp.	125F
Nominal Cathode Pressure	14.7 psia
Nominal Anode Pressure	14.7 psia
Uncompressed Matrix Thickness	30 mil
No. of Bolts	18
Bolt Torque	34 lb in
KOH Concentration	32%
Electrolyte Loading	1.25g/g dry matrix
No. of Cells @ 20 in^2 each	1 (No. 3)

Data Pt. No.	Flow xT	Current Amp	Current Density ASF	Humifidier Temp. F	Cell Temp. F	Cell Voltage E_t	Cell E IR Free E_f
197	5T	2.08	15	104	124	0.790	0.775
198	↓	4.86	35	103	124	0.885	0.850
199	↓	6.95	50	103	127	0.945	0.895
200	↓	9.02	65	104	125	1.020	0.960
201	↓	11.1	80	105	126	1.115	1.040
202	↓	13.9	100	104	130	1.305	1.210
203	3T	2.08	15	105	121	0.815	0.785
204	↓	4.86	35	104	122	0.910	0.875
205	↓	9.02	65	104	127	1.060	0.985
206	2T	2.08	15	104	122	0.830	0.815
207	↓	4.86	35	104	124	0.945	0.915
208	↓	9.02	65	104	130	1.320	1.245

0_2 CONCENTRATOR TEST DATA

Nominal Cell Temp.	125F
Nominal Cathode Pressure	30.0 psia
Nominal Anode Pressure	25.0 psia
Uncompressed Matrix Thickness	30 mil
No. of Bolts	18
Bolt Torque	34 lb in
KOH Concentration	32%
Electrolyte Loading	1.25g/g dry matrix
No. of Cells @ 20 in^2 each	1 (No. 3)

Data Pt. No.	Flow xT	Current Amp	Current Density ASF	Humifidier Temp. F	Cell Temp. F	Cell Voltage E_t	Cell E IR Free E_f
209	5T	2.08	15	104	125	0.790	0.765
210	↓	4.86	35	104	123	0.905	0.860
211	↓	6.95	50	104	125	0.985	0.915
212	↓	9.02	65	104	125	1.070	0.980
213	↓	11.1	80	105	127	1.165	1.060
214	↓	13.9	100	104	127	1.340	1.220
215	3T	2.08	15	105	123	0.807	0.780
216	↓	4.86	35	105	124	0.920	0.870
217	↓	9.02	65	104	123	1.095	1.010
218	2T	2.08	15	105	122	0.820	0.795
219	↓	4.86	35	104	124	0.930	0.885
220	↓	9.02	65	104	127	1.150	1.065

0_2 CONCENTRATOR TEST DATA

Nominal Cell Temp.	125F
Nominal Cathode Pressure	30.0 psia
Nominal Anode Pressure	30.0 psia
Uncompressed Matrix Thickness	30 mil
No. of Bolts	18
Bolt Torque	34 lb in
KOH Concentration	32%
Electrolyte Loading	1.25g/g dry matrix
No. of Cells @ 20 in^2 each	1 (No. 3)

Data Pt. No.	Flow xT	Current Amp	Current Density ASF	Humifidier Temp. F	Cell Temp. F	Cell Voltage E_t	Cell E IR Free E_f
221	5T	2.08	15	105	121	0.800	0.780
222	↓	4.86	35	104	124	0.908	0.865
223	↓	6.95	50	105	122	0.978	0.905
224	↓	9.02	65	105	124	1.040	0.960
225	↓	11.1	80	104	125	1.105	1.003
226	↓	13.9	100	104	127	1.215	1.085
227	3T	2.08	15	104	123	0.825	0.808
228	↓	4.86	35	104	123	0.940	0.880
229	↓	9.02	65	105	126	1.075	0.980
230	2T	2.08	15	104	124	0.830	0.805
231	↓	4.86	35	104	126	0.955	0.895
232	↓	9.02	65	105	126	1.095	1.015

O_2 CONCENTRATOR TEST DATA

Nominal Cell Temp.	125F
Nominal Cathode Pressure	30.0 psia
Nominal Anode Pressure	35.0 psia
Uncompressed Matrix Thickness	30 mil
No. of Bolts	18
Bolt Torque	34 lb in
KOH Concentration	32%
Electrolyte Loading	1.25g/g dry matrix
No. of Cells @ 20 in^2 each	1 (No. 3)

Data Pt. No.	Flow xT	Current Amp	Current Density ASF	Humifidier Temp. F *	Cell Temp. F	Cell Voltage E_t	Cell E IR Free E_f
233	5T	2.08	15		125	0.795	0.775
234	↓	4.86	35		124	0.915	0.860
235	↓	6.95	50		126	0.980	0.910
236	↓	9.02	65		126	1.062	0.962
237	↓	11.1	80		127	1.160	1.045
238	↓	13.9	100		127	1.305	1.150
239	3T	2.08	15		125	0.840	0.810
240	↓	4.86	35		127	0.960	0.895
241	↓	9.02	65		125	1.140	1.040
242	2T	2.08	15		125	0.835	0.805
243	↓	4.86	35		125	0.975	0.910
244	↓	9.02	65		126	1.160	1.083

*See Section IV

0_2 CONCENTRATOR TEST DATA

Nominal Cell Temp.	125F
Nominal Cathode Pressure	45.0 psia
Nominal Anode Pressure	40.0 psia
Uncompressed Matrix Thickness	30 mil
No. of Bolts	18
Bolt Torque	34 lb in
KOH Concentration	32%
Electrolyte Loading	1.25g/g dry matrix
No. of Cells @ 20 in^2 each	1 (No. 3)

Data Pt. No.	Flow xT	Current Amp	Current Density ASF	Humifidier Temp. F *	Cell Temp. F	Cell Voltage E_t	Cell E IR Free E_f
245	5T	2.08	15		123	0.795	0.775
246	↓	4.86	35		125	0.935	0.865
247	↓	6.95	50		126	1.002	0.930
248	↓	9.02	65		128	1.100	1.000
249	↓	11.1	80		127	1.235	1.120
250	↓	13.9	100		130	1.440	1.290
251	3T	2.08	15		123	0.795	0.775
252	↓	4.86	35		125	0.925	0.870
253	↓	9.02	65		125	1.105	1.020
254	2T	2.08	15		122	0.815	0.790
255	↓	4.86	35		122	0.955	0.890
256	↓	9.02	65		124	1.120	1.030

*See Section IV

0_2 CONCENTRATOR TEST DATA

Nominal Cell Temp.	125F
Nominal Cathode Pressure	45.0 psia
Nominal Anode Pressure	45.0 psia
Uncompressed Matrix Thickness	30 mil
No. of Bolts	18
Bolt Torque	34 lb in
KOH Concentration	32%
Electrolyte Loading	1.25g/g dry matrix
No. of Cells @ 20 in^2 each	1 (No. 3)

Data Pt. No.	Flow xT	Current Amp	Current Density ASF	Humifidier Temp. F*	Cell Temp. F	Cell Voltage E_t	Cell E IR Free E_f
257	5T	2.08	15		125	0.820	0.795
258	↓	4.86	35		124	0.925	0.865
259		6.95	50		124	0.980	0.905
260		9.02	65		126	1.040	0.955
261		11.1	80		128	1.085	0.980
262		13.9	100		129	1.170	1.040
263	3T	2.08	15		126	0.830	0.800
264	↓	4.86	35		128	0.935	0.880
265		9.02	65		125	1.055	0.960
266	2T	2.08	15		123	0.835	0.815
267	↓	4.86	35		122	0.940	0.895
268		9.02	65		124	1.065	0.970

*See Section IV

O_2 CONCENTRATOR TEST DATA

Nominal Cell Temp.	125F
Nominal Cathode Pressure	45.0 psia
Nominal Anode Pressure	50.0 psia
Uncompressed Matrix Thickness	30 mil
No. of Bolts	18
Bolt Torque	34 lb in
KOH Concentration	32%
Electrolyte Loading	1.25g/g dry matrix
No. of Cells @ 20 in^2 each	1 (No. 3)

Data Pt. No.	Flow xT	Current Amp	Current Density ASF	Humifidier Temp. F*	Cell Temp. F	Cell Voltage E_t	Cell E IR Free E_f
269	5T	2.08	15		124	0.835	0.810
270	↓	4.86	35		122	0.955	0.900
271	↓	6.95	50		122	1.022	0.958
272	↓	9.02	65		125	1.095	1.010
273	↓	11.1	80		126	1.200	1.100
274	↓	13.9	100		128	1.395	1.240
275	3T	2.08	15		123	0.840	0.810
276	↓	4.86	35		125	0.955	0.905
277	↓	9.02	65		126	1.110	1.022
278	2T	2.08	15		124	0.835	0.810
279	↓	4.86	35		124	0.958	0.908
280	↓	9.02	65		125	1.120	1.030

*See Section IV

O_2 CONCENTRATOR TEST DATA

Nominal Cell Temp.	125F
Nominal Cathode Pressure	60.0 psia
Nominal Anode Pressure	55.0 psia
Uncompressed Matrix Thickness	30 mil
No. of Bolts	18
Bolt Torque	34 lb in
KOH Concentration	32%
Electrolyte Loading	1.25g/g dry matrix
No. of Cells @ 20 in^2 each	1 (No. 3)

Data Pt. No.	Flow xT	Current Amp	Current Density ASF	Humifidier Temp. F*	Cell Temp. F	Cell Voltage E_t	Cell E IR Free E_f
281	5T	2.08	15		127	0.760	0.735
282	↓	4.86	35		125	0.870	0.825
283	↓	6.95	50		126	0.935	0.865
284	↓	9.02	65		126	0.980	0.900
285	↓	11.1	80		126	1.020	0.920
286	↓	13.9	100		129	1.070	0.950
287	3T	2.08	15		124	0.795	0.765
288	↓	4.86	35		125	0.890	0.845
289	↓	9.02	65		126	0.945	0.875
290	2T	2.08	15		125	0.795	0.770
291	↓	4.86	35		126	0.895	0.845
292	↓	9.02	65		125	0.965	0.905

*See Section IV

0_2 CONCENTRATOR TEST DATA

Nominal Cell Temp.	125F
Nominal Cathode Pressure	60.0 psia
Nominal Anode Pressure	60.0 psia
Uncompressed Matrix Thickness	30 mil
No. of Bolts	18
Bolt Torque	34 lb in
KOH Concentration	32%
Electrolyte Loading	1.25g/g dry matrix
No. of Cells @ 20 in^2 each	1 (No. 3)

Data Pt. No.	Flow xT	Current Amp	Current Density ASF	Humifidier Temp. F *	Cell Temp. F	Cell Voltage E_t	Cell E IR Free E_f
293	5T	2.08	15		126	0.815	0.790
294	↓	4.86	35		124	0.920	0.870
295	↓	6.95	50		124	0.985	0.920
296	↓	9.02	65		127	1.040	0.960
297	↓	11.1	80		126	1.090	0.985
298	↓	13.9	100		127	1.140	1.030
299	3T	2.08	15		122	0.820	0.795
300	↓	4.86	35		124	0.930	0.890
301	↓	9.02	65		124	1.040	0.960
302	2T	2.08	15		123	0.835	0.805
303	↓	4.86	35		126	0.925	0.880
304	↓	9.02	65		127	1.035	0.950

*See Section IV

0_2 CONCENTRATOR TEST DATA

Nominal Cell Temp.	125F
Nominal Cathode Pressure	60.0 psia
Nominal Anode Pressure	65.0 psia
Uncompressed Matrix Thickness	30 mil
No. of Bolts	18
Bolt Torque	34 lb in
KOH Concentration	32%
Electrolyte Loading	1.25g/g dry matrix
No. of Cells @ 20 in^2 each	1 (No. 3)

Data Pt. No.	Flow xT	Current Amp	Current Density ASF	Humifidier Temp. F *	Cell Temp. F	Cell Voltage E_t	Cell E IR Free E_f
305	5T	2.08	15		123	0.810	0.795
306	↓	4.86	35		127	0.940	0.885
307		6.95	50		123	0.990	0.920
308		9.02	65		124	1.040	0.955
309		11.1	80		122	1.080	0.990
310		13.9	100		125	1.140	1.020
311	3T	2.08	15		123	0.820	0.795
312	↓	4.86	35		124	0.930	0.880
313		9.02	65		125	1.035	0.950
314	2T	2.08	15		125	0.820	0.795
315	↓	4.86	35		123	0.925	0.880
316		9.02	65		125	1.040	0.950

*See Section IV

O_2 CONCENTRATOR TEST DATA

Nominal Cell Temp.	125F
Nominal Cathode Pressure	75.0 psia
Nominal Anode Pressure	70.0 psia
Uncompressed Matrix Thickness	30 mil
No. of Bolts	18
Bolt Torque	34 lb in
KOH Concentration	32%
Electrolyte Loading	1.25g/g dry matrix
No. of Cells @ 20 in^2 each	1 (No. 3)

Data Pt. No.	Flow xT	Current Amp	Current Density ASF	Humifidier Temp. F *	Cell Temp. F	Cell Voltage E_t	Cell E IR Free E_f
317	5T	2.08	15		122	0.770	0.750
318	↓	4.86	35		126	0.895	0.840
319	↓	6.95	50		126	0.950	0.880
320	↓	9.02	65		127	1.010	0.910
321	↓	11.1	80		128	1.030	0.925
322	↓	13.9	100		128	1.080	0.950
323	3T	2.08	15		126	0.775	0.750
324	↓	4.86	35		125	0.895	0.840
325	↓	9.02	65		128	1.000	0.910
326	2T	2.08	15		124	0.800	0.770
327	↓	4.86	35		124	0.910	0.850
328	↓	9.02	65		126	1.050	0.910

*See Section IV

O_2 CONCENTRATOR TEST DATA

Nominal Cell Temp. 125F
Nominal Cathode Pressure . . . . . 75.0 psia
Nominal Anode Pressure . . . . . 75.0 psia
Uncompressed Matrix Thickness . . . . . 30 mil
No. of Bolts 18
Bolt Torque. . . . . 34 lb in
KOH Concentration 32%
Electrolyte Loading $_2$ . . . . . 1.25g/g dry matrix
No. of Cells @ 20 in^2 each . . . . . 1 (No. 3)

Data Pt. No.	Flow xT	Current Amp	Current Density ASF	Humifidier Temp. F *	Cell Temp. F	Cell Voltage E_t	Cell E IR Free E_f
329	5T	2.08	15		124	0.780	0.750
330	↓	4.86	35		120	0.895	0.855
331		6.95	50		125	0.980	0.910
332		9.02	65		126	1.045	0.965
333		11.1	80		123	1.100	1.000
334		13.9	100		126	1.180	1.050
335	3T	2.08	15		123	0.835	0.815
336	↓	4.86	35		125	0.960	0.905
337		9.02	65		125	1.070	0.985
338	2T	2.08	15		123	0.845	0.825
339	↓	4.86	35		123	0.960	0.905
340		9.02	65		123	1.075	0.985

*See Section IV

O_2 CONCENTRATOR TEST DATA

Nominal Cell Temp.	125F
Nominal Cathode Pressure	75.0 psia
Nominal Anode Pressure	80.0 psia
Uncompressed Matrix Thickness	30 mil
No. of Bolts	18
Bolt Torque	34 lb in
KOH Concentration	32%
Electrolyte Loading	1.25g/g dry matrix
No. of Cells @ 20 in^2 each	1 (No. 3)

Data Pt. No.	Flow xT	Current Amp	Current Density ASF	Humifidier Temp. F *	Cell Temp. F	Cell Voltage E_t	Cell E IR Free E_f
341	5T	2.08	15		121	0.840	0.820
342	↓	4.86	35		123	0.960	0.905
343		6.95	50		126	1.015	0.950
344		9.02	65		125	1.070	0.980
345		11.1	80		130	1.110	1.005
346		13.9	100		128	1.170	1.045
347	3T	2.08	15		125	0.830	0.810
348	↓	4.86	35		123	0.955	0.900
349		9.02	65		125	1.060	0.980
350	2T	2.08	15		123	0.845	0.820
351	↓	4.86	35		124	0.960	0.905
352		9.02	65		125	1.070	0.980

*See Section IV

O_2 CONCENTRATOR TEST DATA - 59-HOUR SELF-REGULATION LOG

Nominal Cathode Pressure . . . . . 10.0 psia
Nominal Anode Pressure . . . . . 10.0 psia
Uncompressed Matrix Thickness . . . . . 30 mil
No. of Bolts 22
Bolt Torque . . . . . 30 lb. in.
KOH Concentration (cells) 32%
Electrolyte Loading . . . . . 1.25 g/g dry matrix
KOH Concentration (wicks) 23%
No. of Cells @ 20 in^2 each 3

Thermocouple Locations

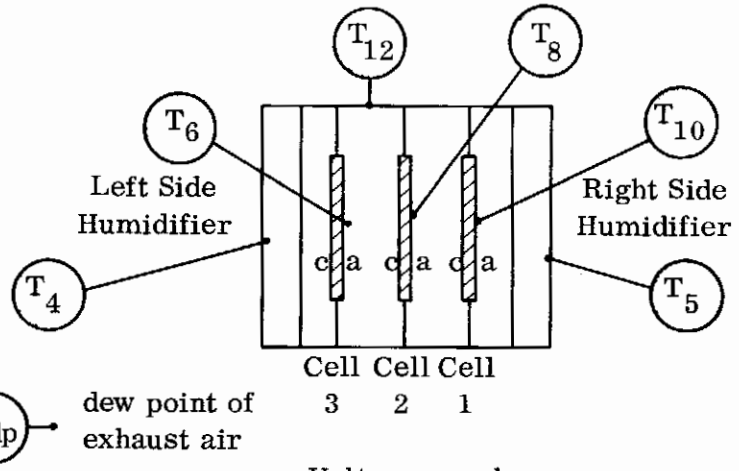

Data Pt. No.	Time After Start Date/Time	Current Density ASF	Flow xT	Temperatures - F T_4	T_5	T_6	T_8	T_{10}	T_{12}	T_{dp}	Voltages - vdc (Terminal - IR Free) Cell 1 E_{1t}	E_{1f}	Cell 2 E_{2t}	E_{2f}	Cell 3 E_{3t}	E_{3f}
12/7/66																
353	0908 hrs.	15	3	Note: s = Shorted Thermocouple							0.700		0.690		0.700	
354	0940	35	"								0.780		0.790		1.360	
355	0945	"	"								0.960		1.130		1.500	
356	0947	"	5	73	72	s	76	76	-	56	0.940		1.130		1.480	
357	0953	"	"	76	74	"	79	78	-	57	0.930	0.915	1.090	1.070	1.480	1.440
358	1003	"	"	78	76	"	83	82	-	57	0.930	0.905	1.050	1.020	1.440	1.430
359	1010	"	"	80	78	"	87	84	-	57	0.920	0.900	1.020	1.000	1.420	1.400
360	1020	"	"	83	81	"	91	87	-	57	0.920	0.890	0.990	0.960	1.370	1.345
361	1030	"	"	84	82	"	s	87	-	55	0.910	0.890	0.970	0.960	1.330	1.315
	1040	Add 10cc H_2O														
362	1050	35	5	84	82	s	s	88	-	52	0.920	0.900	1.330	1.295	1.650	1.620
363	1105	"	"	85	83	"	"	89	-	48	0.925	0.900	1.150	1.140	1.640	1.620

59-HOUR SELF-REGULATION LOG (Cont.)

Data Pt. No.	Time After Start Date/Time	Current Density ASF	Flow xT	Temperatures - F T_4	T_5	T_6	T_8	T_{10}	T_{12}	T_{dp}	Voltages - vdc (Terminal - IR Free) Cell 1 E_{1t}	E_{1f}	Cell 2 E_{2t}	E_{2f}	Cell 3 E_{3t}	E_{3f}
364	1115	35	5	86	84	s	s	89	-	47	0.920	0.895	1.150	1.135	1.640	1.620
365	1130	"	"	86	84	"	"	90	-	47	0.930	0.905	1.150	1.140	1.650	1.620
366	1145	"	"	86	84	"	"	90	-	48	0.920	0.895	1.155	1.140	1.650	1.620
	1200	Cells assumed to be over wet; increase air flow to 8.5T to aid drying														
367	1205	35	8.5	85	86	s	s	89	-	49	0.910	0.890	1.010	0.990	1.195	1.165
368	1230	"	"	84	85	"	"	88	-	48	0.900	0.875	1.045	1.025	1.125	1.110
369	1245	"	"	84	85	"	"	88	-	49	0.895	0.870	1.060	1.040	1.120	1.105
370	1315	"	"	84	86	"	"	89	-	51	0.945	0.910	0.970	0.955	1.000	0.980
	1320	Cells sufficiently recovered; return air flow to 5T; add thermocouple T_{12} to stack; add insulation to stack														
371	1345	35	5	86	86	s	s	89	90	47	1.100	1.040	0.980	0.940	0.980	0.940
372	1410	"	"	88	88	"	"	92	93	47	1.190	1.100	0.980	0.930	0.965	0.920
	1412	Add 15cc H_2O														
373	1430	35	5	91	90	s	108	98	99	48	1.140	1.060	1.025	0.960	1.040	0.970
374	1445	"	"	92	91	"	110	99	101	52	1.090	1.025	1.015	0.950	1.030	0.960
375	1530	"	"	95	94	"	110	98	103	45	1.160	1.065	1.120	1.030	1.250	1.120
376	1540	"	"	97	96	"	114	101	105	44	1.205	1.090	1.165	1.055	1.300	1.120
	1545	Add 15cc H_2O														
377	1550	35	5	100	96	s	125	108	111	45	1.200	1.055	1.125	1.025	1.345	1.125
378	1610	"	"	103	101	"	127	110	116	60	1.090	0.995	1.060	0.970	1.205	1.065
379	1625	"	"	103	101	"	121	106	113	58	1.090	1.000	1.070	0.980	1.220	1.085
	1640	Add 8 cc H_2O														
380	1643	35	5	104	101	s	124	109	114	48	1.155	1.025	1.105	0.980	1.310	1.105
381	1700	"	"	105	103	"	126	109	116	46	1.205	1.045	1.150	1.000	1.365	1.120
	1715	Add 8 cc H_2O														
382	1718	35	5	107	107	s	138	118	121	40	1.265	1.040	1.195	0.990	1.465	1.120
383	1730	"	"	108	110	"	139	115	125	52	1.200	0.995	1.125	0.940	1.360	1.085

59-HOUR SELF-REGULATION LOG (Cont.)

Data Pt. No.	Time After Start Date/Time	Current Density ASF	Flow xT	Temperatures - F T_4	T_5	T_6	T_8	T_{10}	T_{12}	T_{dp}	Voltages - vdc (Terminal - IR Free) Cell 1 E_{1t}	Cell 1 E_{1f}	Cell 2 E_{2t}	Cell 2 E_{2f}	Cell 3 E_{3t}	Cell 3 E_{3f}
384	1739	35	5	108	111	s	138	119	125	54	1.215	1.000	1.120	0.940	1.335	1.095
	1745	Add 18cc H_2O to right side humidifier														
385	1754	35	5	108	109	s	139	119	124	60	1.185	0.985	1.100	0.935	1.300	1.100
386	1813	"	"	105	105	"	132	115	121	63	1.180	1.015	1.130	0.995	1.260	1.100
	1825	Add 12cc H_2O														
387	1828	35	5	104	107	s	131	115	120	59	1.225	1.020	1.125	0.980	1.270	1.115
388	1845	"	"	104	107	"	131	115	119	56	1.265	1.025	1.130	0.975	1.290	1.120
389	1900	"	"	109	107	"	131	115	119	49	1.335	1.030	1.155	0.965	1.335	1.125
	1902	Add 18cc H_2O														
	1913	Add 10cc H_2O														
390	1915	35	5	107	106	s	138	118	123	60	1.250	1.050	1.100	0.935	1.305	1.110
391	1930	"	"	106	106	"	133	115	121	65	1.235	1.035	1.140	0.995	1.290	1.120
	1943	Add 16cc H_2O														
392	1945	35	5	104	106	s	132	115	120	62	1.275	1.050	1.150	1.000	1.300	1.135
393	2000	"	"	104	105	"	132	113	119	64	1.265	1.045	1.140	1.000	1.290	1.130
394	2015	"	"	103	105	"	129	112	118	60	1.305	1.060	1.150	1.000	1.305	1.140
	2020	Add 16cc H_2O														
395	2030	35	5	103	104	s	132	114	118	62	1.290	1.045	1.130	0.980	1.290	1.120
396	2045	"	"	102	102	"	132	112	118	68	1.280	1.080	1.155	1.025	1.275	1.125
397	2100	"	"	101	102	112	125	110	115	69	1.255	1.085	1.135	1.020	1.250	1.120
	2110	Add 16cc H_2O														
398	2115	35	5	101	102	112	124	110	114	64	1.280	1.100	1.130	1.015	1.245	1.120
399	2130	"	"	101	101	110	124	108	114	63	1.300	1.105	1.140	1.020	1.260	1.120
	2131	Add 16cc H_2O														
400	2145	35	5	100	100	110	124	109	113	64	1.290	1.105	1.135	1.020	1.260	1.120
401	2200	"	"	100	100	111	123	108	113	67	1.260	1.100	1.120	1.015	1.240	1.115

59-HOUR SELF-REGULATION LOG (Cont.)

Data Pt. No.	Time After Start Date/Time	Current Density ASF	Flow xT	Temperatures - F T_4	T_5	T_6	T_8	T_{10}	T_{12}	T_{dp}	Voltages - vdc (Terminal - IR Free) Cell 1 E_{1t}	E_{1f}	Cell 2 E_{2t}	E_{2f}	Cell 3 E_{3t}	E_{3f}
	2202	Add 16cc H_2O														
402	2215	35	5	99	100	109	121	106	112	67	1.260	1.105	1.115	1.020	1.230	1.110
	2226	Add 18cc H_2O														
403	2230	35	5	99	100	107	120	107	113	64	1.300	1.140	1.135	1.030	1.245	1.112
404	2245	"	"	99	100	107	121	107	111	65	1.290	1.130	1.125	1.025	1.225	1.115
	2250	Add 16cc H_2O														
405	2300	35	5	99	99	105	120	106	110	74	1.270	1.120	1.105	1.015	1.880	1.710
406	2315	"	"	99	98	121	120	106	110	73	1.250	1.120	1.105	1.030	1.880	1.710
407	2330	"	"	97	96	120	118	104	109	73	1.220	1.115	1.105	1.040	1.860	1.690
	2335	Cell 3 apparently over wet; increase air flow to 8.5T to aid drying														
408	2345	35	8.5	96	97	123	115	103	108	73	1.210	1.110	1.115	1.045	1.410	1.330
	2350	Add 10cc H_2O to right side humidifier														
409	2400	35	8.5	95	96	125	115	103	107	70	1.230	1.120	1.120	1.045	1.325	1.245
12/8/66																
	0001	Cell 3 sufficiently recovered, return air flow to 5T														
	0008	Add 10cc H_2O to right side humidifier														
410	0015	35	5	97	96	125	115	103	107	67	1.245	1.130	1.130	1.050	1.360	1.270
411	0030	"	"	98	95	125	116	102	107	69	1.230	1.120	1.120	1.050	1.330	1.230
	0035	Add 10cc H_2O to right side humidifer														
412	0045	35	5	99	95	115	116	102	107	66	1.230	1.125	1.125	1.045	1.295	1.185
	0050	Add 10cc H_2O to right side humidifier														
413	0100	35	5	99	95	125	117	102	108	66	1.230	1.130	1.120	1.040	1.280	1.160
	0105	Add 16cc H_2O to right side humidifier														
414	0115	35	5	96	95	130	117	103	108	66	1.210	1.120	1.120	1.040	1.270	1.150
415	0130	"	"	97	95	130	117	103	108	70	1.200	1.115	1.130	1.060	1.270	1.155
	0135	Add 18cc H_2O to right side humidifier														

59-HOUR SELF-REGULATION LOG (Cont.)

Data Pt. No.	Time After Start Date/Time	Current Density ASF	Flow xT	Temperatures - F							Voltages - vdc (Terminal - IR Free)					
											Cell 1		Cell 2		Cell 3	
				T_4	T_5	T_6	T_8	T_{10}	T_{12}	T_{dp}	E_{1t}	E_{1f}	E_{2t}	E_{2f}	E_{3t}	E_{3f}
416	0145	35	5	96	95	115	116	102	106	69	1.190	1.110	1.140	1.080	1.275	1.170
417	0200	35	5	96	94	113	115	102	106	70	1.190	1.115	1.155	1.090	1.300	1.200
	0207	Add 14cc H_2O to right side humidifier; 5cc H_2O to left side humidifier														
418	0215	35	5	96	93	110	114	101	105	69	1.190	1.115	1.165	1.100	1.345	1.240
419	0230	"	"	95	93	110	113	101	105	71	1.180	1.110	1.155	1.095	1.900	1.820
	0232	Cell 3 again apparently wet; increase air flow to 8.5T														
	0237	Add 14cc H_2O to right side humidifier														
420	0245	35	8.5	95	93	119	110	100	104	71	1.160	1.095	1.130	1.075	1.820	1.750
	0255	Add 10cc H_2O to right side humidifier														
421	0300	35	8.5	94	93	121	111	100	104	69	1.160	1.090	1.135	1.070	1.790	1.720
422	0315	"	"	95	92	124	111	99	103	71	1.165	1.100	1.135	1.080	1.780	1.700
	0322	Add 10cc H_2O to right side humidifier														
423	0330	35	8.5	95	92	126	111	99	103	71	1.160	1.100	1.130	1.080	1.630	1.550
	0338	Add 10cc H_2O to right side humidifier														
424	0345	35	8.5	95	92	129	110	99	102	70	1.175	1.105	1.140	1.085	1.480	1.400
	0348	Add 14cc H_2O to right side humidifier														
	0350	Reduce air flow to 5T to assess degree of dryness														
	0352	Cell 3 not yet sufficiently dry, return flow to 8.5T														
425	0400	35	8.5	93	91	130	110	99	102	70	1.180	1.110	1.140	1.080	1.540	1.480
426	0415	"	"	93	91	130	110	99	102	70	1.175	1.115	1.135	1.085	1.580	1.510
	0417	Add 18cc H_2O to right side humidifier														
427	0430	35	8.5	92	90	120	108	97	100	70	1.180	1.120	1.160	1.090	1.970	1.900
	0431	Reduce air flow to 5T														
	0432	Add 14cc H_2O to right side humidifier; 10cc H_2O to left side humidifier														
428	0445	35	5	91	89	145	104	96	99	69	1.240	1.180	1.810	1.640	2.120	2.020
	0447	Cell 3 appears wet again, increase air flow to 8.5T														
429	0500	35	8.5	91	89	146	104	96	99	69	1.220	1.160	1.790	1.640	2.100	2.010

*** Experiment controls have been removed ***

59-HOUR SELF-REGULATION LOG (Cont.)

Data Pt. No.	Time After Start Date/Time	Current Density ASF	Flow xT	Temperatures - F T_4	T_5	T_6	T_8	T_{10}	T_{12}	T_{dp}	Voltages - vdc (Terminal - IR Free) Cell 1 E_{1t}	E_{1f}	Cell 2 E_{2t}	E_{2f}	Cell 3 E_{3t}	E_{3f}
430	0515	35	8.5	92	89	150	106	97	100	70	1.225	1.160	1.770	1.700	2.020	1.940
431	0530	"	"	93	90	156	107	98	101	71	1.220	1.150	1.700	1.640	1.860	1.790
432	0545	"	"	92	91	155	107	98	101	71	1.210	1.145	1.550	1.500	1.590	1.500
433	0600	"	"	91	93	132	106	97	101	68	1.225	1.145	1.200	1.120	1.395	1.290
	0605	Cell moisture apparently in balance, return flow to 5T														
434	0615	35	5	91	93	132	107	97	101	66	1.260	1.170	1.195	1.120	1.380	1.260
	0620	Add 8cc H_2O to right side humidifier														
435	0630	35	5	95	94	121	108	98	103	64	1.240	1.150	1.210	1.120	1.380	1.220
	0632	Add 12cc H_2O to right side humidifier														
436	0645	35	5	98	93	126	112	101	105	61	1.210	1.110	1.230	1.110	1.440	1.220
437	0700	"	"	102	95	140	118	103	109	58	1.220	1.110	1.250	1.110	1.700	1.260
438	0715	"	"	103	98	139	120	104	111	55	1.220	1.110	1.260	1.105	1.850	1.270
	0718	Add 8cc H_2O to right side humidifier														
	0725	Add 8cc H_2O to left side humidifier														
439	0730	35	5	105	98	142	128	112	117	55	1.180	1.080	1.220	1.070	2.080	1.380
440	0745	"	"	106	102	146	130	113	119	68	1.140	1.070	1.220	1.100	2.050	1.730
441	0800	33	"	107	106	141	128	112	121	66	1.150	1.060	1.210	1.105	2.110	1.780
	0801	Add 8cc H_2O to left side humidifier														
	0809	Add 10cc H_2O to right side humidifier														
442	0815	31	5	107	103	140	131	115	121	66	1.140	1.060	1.190	1.050	2.150	1.780
443	0830	31	"	108	105	141	130	114	121	70	1.120	1.080	1.190	1.050	2.200	1.840
444	0845	32.4	"	100	100	130	119	105	112	54	1.100	1.025	1.240	1.115	2.250	1.850
445	0900	31	"	105	102	126	119	106	114	49	1.130	1.065	1.185	1.075	2.350	1.900
446	0915	14.4	"	105	102	119	117	105	114	36	1.080	0.965	1.100	0.945	2.500	2.000
	0925	Add 10cc H_2O to right side humidifier; 13cc H_2O to left side humidifier														
447	0930	8.2	5	102	97	114	116	106	111	26	0.965	0.885	0.940	0.840	2.680	2.080

59-HOUR SELF-REGULATION LOG (Cont.)

Data Pt. No.	Time After Start Date/Time	Current Density ASF	Flow xT	Temperatures - F T_4	T_5	T_6	T_8	T_{10}	T_{12}	T_{dp}	Voltages - vdc (Terminal - IR Free) Cell 1 E_{1t}	E_{1f}	Cell 2 E_{2t}	E_{2f}	Cell 3 E_{3t}	E_{3f}
	0943	Cell 3 not responding, remove from circuit														
448	0945	35	5	97	105	94	118	105	107	38	1.420	1.170	1.650	1.180	-	-
	0950	Add 12cc H_2O to right side humidifier; 6cc H_2O to left side humidifier														
	0955	Remove insulation from cell														
	1015	Reduce current density to 15 ASF														
449	1015	15	5	86	85	90	97	90	88	36	1.080	1.050	1.170	1.010	-	-
450	1030	"	"	83	82	85	91	86	84	33	1.060	1.000	1.150	1.040	-	-
	1040	Add 12cc H_2O														
451	1045	15	5	78	78	81	85	82	79	31	1.060	1.000	1.150	1.050	-	-
452	1100	"	"	76	76	78	82	78	77	28	1.050	1.005	1.140	1.050	-	-
453	1130	"	"	75	75	77	80	77	76	28	1.090	1.040	1.170	1.070	-	-
454	1200	"	"	74	74	75	78	75	75	28	1.110	1.060	1.160	1.060	-	-
455	1230	"	"	73	73	75	77	75	74	28	1.110	1.060	1.130	1.055	-	-
456	1300	"	"	72	73	75	77	75	74	28	1.130	1.090	1.140	1.060	-	-
457	1330	"	"	73	72	75	77	74	73	31	1.150	1.120	1.160	1.090	-	-
458	1400	"	"	73	72	75	77	74	73	31	1.170	1.130	1.150	1.080	-	-
459	1430	"	"	73	72	74	76	74	73	31	1.170	1.130	1.150	1.080	-	-
	1436	Increase air flow to 8.5T														
460	1500	15	8.5	71	72	72	75	73	73	30	1.117	1.080	1.115	1.050	-	-
	1503	Add 10cc H_2O														
	1515	Reduce air flow to 5T														
461	1545	15	5	73	74	75	s	75	75	31	1.105	1.065	1.105	1.045	-	-
	1545	Increase current density to 21.6 ASF														
462	1600	21.6	5	75	76	77	s	78	78	32	1.220	1.160	1.225	1.130	-	-
463	1645	"	"	76	78	79	85	80	80	32	1.180	1.125	1.205	1.110	-	-
464	1700	"	"	77	78	80	85	80	81	31	1.190	1.125	1.220	1.115	-	-

59-HOUR SELF-REGULATION LOG (Cont.)

Data Pt. No.	Time After Start Date/Time	Current Density ASF	Flow xT	Temperatures - F T_4	T_5	T_6	T_8	T_{10}	T_{12}	T_{dp}	Voltages - vdc (Terminal - IR Free) Cell 1 E_{1t}	E_{1f}	Cell 2 E_{2t}	E_{2f}	Cell 3 E_{3t}	E_{3f}
	1706	Add 10cc H_2O														
465	1800	21.6	5	79	79	83	88	83	83	31	1.165	1.120	1.195	1.105	-	-
466	1830	"	"	79	79	82	86	82	82	31	1.155	1.105	1.185	1.090	-	-
467	1900	"	"	79	80	82	85	82	83	31	1.160	1.105	1.180	1.100	-	-
	1910	Increase current density to 25 ASF														
468	1930	25	5	80	81	82	86	83	85	32	1.200	1.140	1.240	1.140	-	-
469	2000	"	"	82	82	83	85	83	85	28	1.240	1.165	1.260	1.140	-	-
	2010	Add 27cc H_2O														
470	2030	25	5	83	82	87	94	88	87	28	1.320	1.205	1.330	1.170	-	-
471	2100	"	"	84	84	88	94	90	90	33	1.235	1.150	1.265	1.135	-	-
472	2130	"	"	84	84	88	94	89	90	35	1.200	1.130	1.240	1.110	-	-
473	2145	"	"	83	84	86	90	87	88	34	1.195	1.135	1.220	1.110	-	-
474	2200	"	"	83	85	85	92	87	88	33	1.220	1.140	1.235	1.115	-	-
475	2210	"	"	83	85	86	93	86	88	33	1.240	1.155	1.250	1.120	-	-
476	2215	"	"	83	85	86	94	86	88	33	1.270	1.175	1.270	1.140	-	-
	2235	Add 40cc H_2O														
477	2303	25	5	84	84	87	95	89	89	36	1.240	1.165	1.400	1.310	-	-
478	2315	"	"	84	84	87	94	89	89	36	1.220	1.135	1.400	1.305	-	-
479	2330	"	"	84	84	86	94	88	88	35	1.185	1.120	1.375	1.285	-	-
	2330	Reduce current density to 15 ASF; air flow to 3.5T														
12/9/66																
	0010	Add 13cc H_2O														
480	0010	15	3.5	78	78	80	84	80	80	28	1.070	1.040	1.170	1.120	-	-
481	0710	9.4	"	72	72	72	74	72	72	17	1.260	1.190	1.220	1.140	-	-
	0715	Increase air flow to 5T; increase current density to 15 ASF														
	0730	Add 25cc H_2O														

59-HOUR SELF-REGULATION LOG (Cont.)

Data Pt. No.	Time After Start Date/Time	Current Density ASF	Flow xT	Temperatures - F T_4	T_5	T_6	T_8	T_{10}	T_{12}	T_{dp}	Voltages - vdc (Terminal - IR Free) Cell 1 E_{1t}	E_{1f}	Cell 2 E_{2t}	E_{2f}	Cell 3 E_{3t}	E_{3f}
482	0745	15	5	74	74	76	82	78	76	18	1.450	1.290	1.420	1.260	-	-
483	0800	"	"	76	76	79	85	80	79	22	1.430	1.280	1.440	1.260	-	-
484	0815	"	"	77	77	80	86	81	80	25	1.395	1.255	1.430	1.250	-	-
485	0830	"	"	78	78	80	86	81	80	26	1.340	1.220	1.400	1.230	-	-
486	0845	"	"	78	78	81	86	81	81	28	1.320	1.210	1.390	1.240	-	-
487	0900	"	"	79	79	81	86	81	81	29	1.300	1.200	1.390	1.235	-	-
	0904	Add 18cc H_2O														
488	0915	15	5	79	79	80	86	81	81	31	1.270	1.180	1.360	1.220	-	-
489	0930	"	"	78	77	80	85	80	80	30	1.260	1.180	1.360	1.225	-	-
490	0945	"	"	78	77	80	85	80	80	31	1.235	1.160	1.340	1.210	-	-
	0950	Add 22cc H_2O														
491	1000	15	5	78	77	80	84	80	80	30	1.230	1.150	1.320	1.200	-	-
492	1015	"	"	77	77	79	84	79	80	32	1.220	1.145	1.295	1.200	-	-
493	1030	"	"	77	77	79	84	79	80	31	1.200	1.130	1.255	1.170	-	-
	1040	Add 22cc H_2O														
494	1045	15	5	76	76	77	80	78	77	55	1.240	1.180	1.470	1.410	-	-
495	1100	"	"	75	75	77	79	77	76	47	1.250	1.210	1.690	1.600	-	-
	1108	Cells apparently too wet, increase air flow to 10T														
496	1115	15	10	75	75	77	79	77	77	38	1.230	1.190	1.640	1.580	-	-
497	1130	"	"	75	75	77	79	77	77	36	1.230	1.180	1.630	1.550	-	-
	1140	Increase air flow to 20T														
498	1145	15	20	75	75	77	79	77	77	36	1.210	1.160	1.530	1.490	-	-
499	1200	"	"	75	75	77	79	77	77	38	1.200	1.160	1.530	1.480	-	-
500	1215	"	"	75	75	76	79	76	76	38	1.190	1.155	1.510	1.470	-	-
501	1230	"	"	75	75	76	78	76	76	37	1.195	1.150	1.500	1.440	-	-
502	1245	"	"	74	74	75	77	76	75	36	1.200	1.160	1.450	1.390	-	-

*** Export controls have been removed ***

59-HOUR SELF-REGULATION LOG (Cont.)

Data Pt. No.	Time After Start Date/Time	Current Density ASF	Flow xT	Temperatures - F							Voltages - vdc (Terminal - IR Free)					
											Cell 1		Cell 2		Cell 3	
				T_4	T_5	T_6	T_8	T_{10}	T_{12}	T_{dp}	E_{1t}	E_{1f}	E_{2t}	E_{2f}	E_{3t}	E_{3f}
503	1300	15	20	74	74	75	76	*75	75	36	1.205	1.170	1.430	1.370	-	-
504	1315	"	"	73	73	75	76	*75	75	36	1.210	1.190	1.420	1.355	-	-
505	1345	"	"	73	73	74	75	74	74	35	1.200	1.160	1.360	1.300	-	-
506	1400	"	"	72	73	74	75	74	74	35	1.200	1.160	1.310	1.250	-	-
507	1415	"	"	72	73	74	75	74	74	34	1.205	1.165	1.295	1.235	-	-
508	1430	"	"	72	74	74	75	75	74	34	1.210	1.117	1.215	1.155	-	-
	1430	Increase current density to 25 ASF; reduce air flow to 5T														
509	1445	25	5	74	76	77	81	77	76	34	1.375	1.300	1.415	1.320	-	-
510	1515	"	"	77	79	80	85	81	81	36	1.435	1.310	1.410	1.280	-	-
	1523	Add 21cc H_2O to right side humidifier														
511	1530	25	5	80	79	83	89	84	84	37	1.510	1.340	1.410	1.275	-	-
512	1545	"	"	81	81	85	93	86	86	40	1.500	1.330	1.405	1.260	-	-
513	1600	"	"	82	81	87	94	88	88	41	1.490	1.315	1.405	1.260	-	-
514	1630	"	"	84	83	88	95	88	89	42	1.450	1.310	1.400	1.260	-	-
515	1645	"	"	85	85	86	94	87	89	43	1.480	1.330	1.430	1.280	-	-
516	1700	"	"	85	85	88	95	88	90	42	1.520	1.380	1.460	1.320	-	-
	1745	Automatic H_2O feed system connected; feeding at the rate of approximately 10cc H_2O/hour														
517	1800	25	5	84	81	86	90	85	87	33	1.650	1.420	1.710	1.420	-	-
	1808	Cells not responding to H_2O; assume over wet condition; stop H_2O feed; increase air flow to 11.5T														
518	1815	25	11.5	86	84	90	90	89	90	40	1.660	1.410	1.790	1.480	-	-
519	1830	"	"	89	85	90	95	*90	91	40	1.710	1.410	1.910	1.500	-	-
	1831	Cells voltages increasing, rapidly; sign of desiccation; add 15cc H_2O; reduce air flow to 5T														
520	1845	25	5	91	90	96	105	97	98	40	1.790	1.440	2.280	1.650	-	-
	1850	Again cells not responding to H_2O; reduce current density to 15 ASF; increase air flow to 20T														
521	1900	15	20	90	86	93	97	94	97	42	1.500	1.270	1.800	1.450	-	-
522	1915	"	"	87	85	90	90	90	93	39	1.490	1.300	1.810	1.470	-	-

59-HOUR SELF-REGULATION LOG (Cont.)

Data Pt. No.	Time After Start Date/Time	Current Density ASF	Flow xT	Temperatures - F T_4	T_5	T_6	T_8	T_{10}	T_{12}	T_{dp}	Voltages - vdc (Terminal - IR Free) Cell 1 E_{1t}	E_{1f}	Cell 2 E_{2t}	E_{2f}	Cell 3 E_{3t}	E_{3f}
523	1930	15	20	85	85	88	92	87	90	31	1.620	1.360	2.080	1.640	-	-
	1955	Cells again show signs of being too dry; add 25cc H_2O; reduce flow to 6T; reduce current density to 5 ASF														
524	2000	5	6	83	86	84	84	85	88	18	1.290	-	3.250	2.600	-	-
	2005	Cell 2 removed from circuit due to high voltage; cell not performing properly														
525	2010	10	3	-	-	-	-	-	-	-	1.700	1.300	-	-	-	-
	2010	System shut down after 59 hours 10 minutes of operation														

O_2 CONCENTRATOR TEST DATA

Nominal Cell Temp. 125F
Uncompressed Matrix Thickness . . . . . 30 mil
No. of Bolts 22
Bolt Torque . . . . . 30 lb in
KOH Concentration 32%
Electrolyte Loading . . . . . 2.25g/g dry matrix
No. of Cells @ 20 in_2 each . . . . . 1 (No. 1)
Stoichiometric Flow Multiple 4T

Data Pt. No.	Current Amp	Current Density ASF	Cell Pressure psia Cathode/Anode	Cell Temp. F	Cell Voltage E_t	Cell E IR Free E_f
526	8.35	60	14.7/14.7	124	0.835	0.790
527	↓	↓	20.0/14.7	123	0.820	0.775
528			20.0/20.0	125	0.880	0.835
529			30.0/30.0	130	0.960	0.920
530			45.0/45.0	125	0.950	0.930
531			60.0/55.0	120	0.845	0.795
532			60.0/60.0	125	1.100	0.950
533			60.0/65.0	122	1.110	1.000
534			75.0/70.0	120	0.880	0.820
535			75.0/75.0	125	1.055	0.980
536			75.0/80.0	125	1.110	1.000
537			90.0/85.0	120	0.880	0.810
538			90.0/90.0	124	0.970	0.885
539			75.0/75.0	124	1.050	0.980
540			75.0/70.0	120	0.900	0.830

O_2 CONCENTRATOR TEST DATA

Data Pt No.	Current Amp	Current Density ASF	Cell Pressure psia Cathode/Anode	Cell Temp. F	Cell Voltage E_t	Cell E IR Free E_f
541	8.35	60	60.0/60.0	125	1.065	1.005
542	↓	↓	60.0/55.0	123	0.900	0.830
543			45.0/45.0	126	1.110	1.040
544			30.0/25.0	118	0.925	0.865
545	13.9	100	30.0/25.0	117	0.995	0.885
546	4.86	35	30.0/25.0	129	0.820	0.780
547	8.35	60	30.0/25.0	123	0.905	0.840
548	20.0	144	30.0/25.0	125	1.050	0.905
549	20.0	144	30.0/25.0	135	1.040	0.900
550	23.5	166	30.0/25.0	125	1.120	0.940
551	2.08	15	30.0/25.0	128	0.725	0.700
552	8.35	60	14.7/14.7	125	0.960	0.890

Note: Controlled parameters (temp., matrix thickness, etc.) identical to those on page 168.

O_2 CONCENTRATOR TEST DATA

Nominal Cell Temp.	125F
Uncompressed Matrix Thickness	30 mil
No. of Bolts	22
Bolt Torque	30 lb in
KOH Concentration	32%
Electrolyte Loading	1.75g/g dry matrix
No. of Cells @ 20 in^2 each	1 (No. 1)
Stoichiometric Flow Multiple	5T

Data Pt. No.	Current Amp	Current Density ASF	Cell Pressure psia Cathode/Anode	Cell Temp. F	Cell Voltage E_t	Cell E IR Free E_f
553	2.08	15	7.5/7.5	128	0.610	0.600
554	4.86	35	↓	126	0.720	0.690
555	6.95	50	↓	127	0.830	0.800
556	9.02	65	↓	125	1.0 → 1.2	0.980
557	11.1	80	↓	-	>1.2	-
558	13.9	100	↓	-	>1.2	-
559	2.08	15	10.0/10.0	125	0.615	0.605
560	4.86	35	↓	124	0.730	0.700
561	6.95	50	↓	126	0.800	0.750
562	9.02	65	↓	127	0.870	0.820
563	11.1	80	↓	126	0.92 → 1.0	0.870
564	13.9	100	↓		>1.0	-

0_2 CONCENTRATOR TEST DATA

Nominal Cell Temp 125F
Nominal Cathode Pressure . . . . 14.7 psia
Nominal Anode Pressure . . . . . 14.7 psia
Uncompressed Matrix Thickness . . 30 mil
No. of Bolts 22
Bolt Torque . . . . . 30 lb in
KOH Concentration 32%
Electrolyte Loading . . . . . 1.75g/g dry matrix
No. of Cells @ 20 in^2 each . . . . . 1 (No. 1)

Data Pt. No.	Flow xT	Current Amp	Current Density ASF	Cell Voltage E_t	Cell E IR Free E_f
565	5T	4.86	35	0.710	0.680
566	↓	9.02	65	0.800	0.730
567	↓	13.9	100	0.870	0.795
568	↓	20.85	150	1.000	0.890
569	4T	4.86	35	0.710	0.680
570	↓	9.02	65	0.780	0.735
571	↓	13.9	100	0.880	0.795
572	↓	20.85	150	0.990	0.870
573	3T	4.86	35	0.720	0.690
574	↓	9.02	65	0.805	0.755
575	↓	13.9	100	0.880	0.810
576	↓	20.85	150	1.000	0.890
577	2T	4.86	35	0.720	0.680
578	↓	9.02	65	0.810	0.760
579	↓	13.9	100	0.890	0.810
580	↓	20.85	150	1.000	0.880

O_2 CONCENTRATOR TEST DATA-142-HOUR SELF-REGULATION LOG

Nominal Cathode Pressure . . . . . 14.7 psia
Nominal Anode Pressure . . . . . 14.7 psia
Uncompressed Matrix Thickness . . . . . 30 mil
No. of Bolts 22
Bolt Torque . . . . . 30 lb in
KOH Concentration (cells) 32%
Electrolyte Loading . . . . . 1.75g/g dry matrix
KOH Concentration (wicks) 23%
No. of Cells @ 20 in^2 each 3

*Thermocouple Locations - same as 59-hour run

Date Pt. No.	Time After Start Date/Time	Current Density ASF	Flow xT	Temperatures*-F T_4	T_5	T_6	T_8	T_{10}	T_{12}	T_{dp}	Voltage - vdc (Terminal - IR Free) Cell 1 E_{1t}	E_{1f}	Cell 2 E_{2t}	E_{2f}	Cell 3 E_{3t}	E_{3f}
1/17/67																
	1100 Start															
581	1117	60	4	90	72	88	s	91	91	1	0.840	0.770	0.920	0.820	0.830	0.750
582	1150	"	"	105	88	98	103	103	103	29	0.840	0.810	0.920	0.860	0.840	0.795
583	1300	"	"	120	102	105	104	118	117	45	0.830	0.790	0.880	0.830	0.815	0.775
584	1330	"	"	120	104	102	105	117	118	50	0.830	0.790	0.890	0.830	0.810	0.770
585	1400	"	"	123	105	106	109	120	120	52	0.820	0.780	0.870	0.820	0.810	0.770
586	1500	"	"	123	105	106	109	120	120	52	0.830	0.795	0.885	0.830	0.820	0.780
587	1600	"	"	118	106	107	109	98	98	52	0.825	0.790	0.880	0.830	0.818	0.780
588	1700	"	"	122	103	111	106	120	120	51	0.825	0.800	0.885	0.820	0.810	0.775
589	1800	"	"	116	95	109	104	114	113	71	0.905	0.845	0.935	0.865	0.880	0.820
590	1845	"	"	114	95	113	113	116	111	54	0.905	0.850	0.960	0.890	0.890	0.830
591	1900	"	"	121	96	115	115	119	115	56	0.900	0.845	0.960	0.895	0.875	0.830
1/18/67																
592	0800	35	4	95	78	94	95	95	91	53	0.890	0.800	0.920	0.800	0.865	0.795
593	0900	"	5	96	77	94	95	94	91	46	0.930	0.830	0.950	0.850	0.890	0.810

142-HOUR SELF-REGULATION LOG (Con't.)

Date Pt. No.	Time After Start Date/Time	Current Density ASF	Flow xT	Temperatures*-F T_4	T_5	T_6	T_8	T_{10}	T_{12}	T_{dp}	Voltage - vdc (Terminal - IR Free) Cell 1 E_{1t}	E_{1f}	Cell 2 E_{2t}	E_{2f}	Cell 3 E_{3t}	E_{3f}
594	1000	35	5	103	85	100	102	101	97	42	0.880	0.805	0.920	0.830	0.845	0.790
595	1100	"	"	101	85	100	101	100	100	40	0.885	0.810	0.925	0.820	0.860	0.795
596	1200	"	"	94	77	93	93	92	92	42	0.960	0.855	0.935	0.825	0.920	0.825
597	1300	"	"	101	85	101	103	102	103	54	0.915	0.820	0.920	0.820	0.880	0.800
598	1330	"	"	105	88	103	105	104	105	57	0.900	0.810	0.915	0.810	0.870	0.795
599	1400	"	"	105	88	105	106	105	106	58	0.905	0.820	0.920	0.820	0.870	0.800
600	1500	"	"	107	90	105	107	106	107	60	0.890	0.815	0.910	0.820	0.865	0.800
601	1600	"	"	105	90	105	107	106	107	60	0.890	0.810	0.910	0.820	0.865	0.800
602	1630	"	"	106	90	105	107	106	106	60	0.890	0.810	0.915	0.820	0.865	0.800
603	1810	"	"	106	90	104	106	105	106	61	0.880	0.815	0.915	0.825	0.860	0.800
604	2000	"	"	103	89	102	105	105	105	60	0.890	0.820	0.920	0.835	0.875	0.815
1/19/67																
605	0730	35	5	101	86	103	104	102	101	57	0.890	0.820	0.925	0 840	0.875	0.815
606	0800	"	"	102	87	103	104	102	102	57	0.890	0.815	0.925	0.840	0.870	0.820
607	0830	50	4	111	92	111	112	110	112	59	0.975	0.870	1.000	0.880	0.935	0.860
608	0900	"	"	119	100	119	120	118	123	66	0.950	0.830	0.970	0.835	0.910	0.835
609	1000	"	"	127	107	125	127	125	132	59	0.915	0.820	0.940	0.830	0.880	0.810
610	1100	"	"	128	107	127	129	125	133	54	0.910	0.820	0.940	0.825	0.875	0.810
611	1130	"	"	121	103	121	124	120	125	37	0.910	0.820	0.950	0.830	0.885	0.810
612	1200	"	"	125	106	125	127	124	129	42	0.920	0.820	0.950	0.835	0.880	0.820
613	1300	"	"	128	110	128	130	126	132	62	0.915	0.820	0.940	0.820	0.875	0.810
614	1400	"	"	128	108	127	128	125	132	73	0.920	0.825	0.940	0.820	0.895	0.815
615	1500	"	"	130	111	127	130	129	137	69	0.910	0.810	0.930	0.815	0.890	0.805
616	1600	"	"	131	110	127	130	129	134	58	0.910	0.810	0.930	0.820	0.890	0.805
617	1700	"	"	130	110	126	130	129	133	52	0.910	0.820	0.940	0.830	0.900	0.820
618	1800	"	"	131	111	126	130	129	134	49	0.910	0.825	0.950	0.830	0.910	0.825
619	1900	"	"	129	110	125	130	129	132	45	0.910	0.825	0.940	0.835	0.905	0.825

*** Export controls have been removed ***

142-HOUR SELF-REGULATION LOG (Con't.)

Date Pt.	Time After Start	Current Density	Flow	Temperatures*-F T_4	T_5	T_6	T_8	T_{10}	T_{12}	T_{dp}	Voltage (Terminal - IR Free) Cell 1 E_{it}	Cell 1 E_{1f}	Cell 2 E_{2t}	Cell 2 E_{2f}	Cell 3 E_{3t}	Cell 3 E_{3f}
1/20/67																
620	0800	50	4	128	110	115	127	125	129	53	0.900	0.810	0.935	0.820	0.900	0.820
621	0900	"	"	130	110	116	129	127	113	48	0.895	0.810	0.930	0.810	0.900	0.815
622	1000	"	"	130	110	117	129	127	-	48	0.895	0.810	0.930	0.810	0.900	0.820
623	1100	"	"	129	110	117	129	127	-	48	0.895	0.810	0.930	0.810	0.895	0.820
624	1200	"	"	129	111	117	130	128	-	47	0.900	0.810	0.930	0.810	0.900	0.810
625	1300	"	"	129	110	117	130	127	-	47	0.900	0.810	0.930	0.810	0.900	0.820
626	1500	"	"	130	112	118	130	128	-	48	0.900	0.815	0.930	0.810	0.900	0.820
627	1700	"	"	130	110	118	130	128	-	47	0.900	0.820	0.930	0.815	0.900	0.830
1/21/67																
628	0830	50	4	130	118	125	130	128	-	40	0.965	0.885	1.010	0.890	0.965	0.885
629	1000	"	"	134	123	130	133	130	-	40	0.970	0.880	1.005	0.890	0.965	0.880
630	1100	"	"	133	122	130	132	130	-	47	0.980	0.880	1.000	0.885	0.965	0.880
631	1300	"	"	135	125	133	134	130	-	38	0.965	0.875	0.995	0.880	0.950	0.870
1/22/67																
632	1100	50	4	142	130	145	142	140	-	40	0.980	0.895	0.980	0.880	0.945	0.870
633	1200	"	"	141	126	144	142	140	-	41	0.975	0.880	0.975	0.860	0.935	0.845
634	1300	"	"	130	130	140	138	135	-	40	0.980	0.870	0.950	0.860	0.940	0.850
635	2030	15	13	113	110	115	115	85	-	24	1.050	0.850	0.840	0.790	0.815	0.780
1/23/67																
636	0800	15	13	91	83	93	93	72	-	2	1.380	1.030	0.940	0.885	0.900	0.850
	0900	Systems Shutdown After 142 Hours of Operation														

*** Export controls have been removed ***

APPENDIX IV

AIR-OXYGEN FLOW RELATIONSHIP

Consider an oxygen concentrator where the oxygen output, W_{o_2}, is specified in lb/hr. It is desirable to readily determine the air flow rate $^{o}2$ required to produce the specified amount of oxygen. First, it is necessary to convert the specified oxygen mass flow rate to a volume flow:

$$Q_{o_2} = W_{o_2} \quad V_{o_2} \tag{1}$$

where:

Q_{o_2} = volumetric flow rate of oxygen, ft^3/hr

W_{o_2} = mass flow rate of oxygen, lb/hr

V_{o_2} = specific volume of oxygen, ft^3/lb

Where the specific volume of oxygen is determined by the perfect gas equation:

$$V_{o_2} = \frac{R\ T_{o_2}}{32 P_{o_2}} \tag{2}$$

Now, the volume flow rate of air containing the oxygen, as specified, can be determined by knowing that 21% of air, by volume, is oxygen. Therefore:

$$Q_a = \frac{W_{o_2}\ V_{o_2}}{0.21} \tag{3}$$

or

$$Q_a = \frac{W_{o_2}\ R\ T_{o_2}}{32\ P_{o_2}} \quad \frac{1}{0.21} \tag{4}$$

This volume flow rate of air is converted to mass flow by again considering the perfect gas equation:

$$W_a = W_{o_2} \frac{R\,T_{o_2}}{32\,P_{o_2}} \quad \frac{1}{0.21} \quad \cdot \quad \frac{29\,P_a}{R\,T_a} \qquad (5)$$

where:

W_a = mass flow rate of air, lb/hr

If the temperature and pressure of the oxygen are equal to that of the entering air, the equation can be reduced to:

$$W_a = \frac{29}{32} \cdot \frac{1}{0.21} \; W_{o_2} \qquad (6)$$

or

$$W_a = 4.32\, W_{o_2} \qquad (7)$$

This is the air mass flow rate that contains the amount of oxygen, W_{o_2}, or one times theoretical (IT). Therefore, the factor xT can be added to the *** Export controls have been removed ***, equation which allows evaluation of the air flow rate as a function of the anticipated theoretical air flow rate that is desired, as shown in equation (8).

$$W_a = 4.32\, W_{o_2}\, xT \qquad (8)$$

REFERENCES

(1) Wynveen, R. A., and Montgomery, K. M., Experimental Oxygen Concentrating System, AFFDL-TR-65-32, USAF Contract No. 33(615)-1856, April, 1965.

(2) Richardson, D. R., "How to Design Fluid-Flow Distributors," Chemical Engineering, May 1, 1961, p. 83.

(3) Hepfer, I. C., "Plated Finishes for Magnesium," Products Finishing, June, 1965, p. 51.

(4) Kordesch, K. V., and Marko, A., "Sine Wave Pulse Current Tester for Batteries," Journal of the Electrochemical Society, 107, 1960, p. 480.

(5) Pollnow, G. F., and Kay, R. M., "A Transistorized 60 CPS Sine Wave Commutator for Resistance and Potential Measurements," Journal of the Electrochemical Society, 109, 1962, p. 648.

(6) Haldeman, R. G., et al, Research and Development of High-Performance Light-Weight Fuel Cell Electrodes, NASA CR-54171, NASA Contract NAS 3-2786, Third Quarterly Report, May 1 - July 31, 1964, American Cyanamid Company.

(7) Mitchell, Jr., W., Fuel Cells, Academic Press, 1963, p. 35-40.

(8) Young, G. J., Fuel Cells, Reinhold, 1960, p. 67-69.

*** Export controls have been removed ***

UNCLASSIFIED
Security Classification

DOCUMENT CONTROL DATA - R&D
(Security classification of title, body of abstract and indexing annotation must be entered when the overall report is classified)

1. ORIGINATING ACTIVITY (Corporate author) TRW Equipment Laboratories TRW, Inc. 23555 Euclid Ave., Cleveland, Ohio 44117	2a. REPORT SECURITY CLASSIFICATION UNCLASSIFIED 2b. GROUP

3. REPORT TITLE

Self-Regulated Oxygen Concentrator

4. DESCRIPTIVE NOTES (Type of report and inclusive dates)

Final Technical Report, January 1966 through January 1967

5. AUTHOR(S) (Last name, first name, initial)

Wynveen, Dr. Richard A.
Mrava, Gene L.

6. REPORT DATE	7a. TOTAL NO. OF PAGES	7b. NO. OF REFS
March 1967	177	8

8a. CONTRACT OR GRANT NO.	9a. ORIGINATOR'S REPORT NUMBER(S)
AF 33(615)-3392 b. PROJECT NO. 6146 c. Task No. 614614 d.	TRW ER-7043 9b. OTHER REPORT NO(S) (Any other numbers that may be assigned this report) AFFDL-TR-67-6

10. AVAILABILITY/LIMITATION NOTICES - This document is subject to special export controls and each transmittal to foreign governments or foreign nationals may be made only with prior approval of the Air Force Flight Dynamics Laboratory (FDFE), Wright-Patterson Air Force Base, Ohio 45433.

11. SUPPLEMENTARY NOTES	12. SPONSORING MILITARY ACTIVITY
	Air Force Flight Dynamics Laboratory Wright-Patterson Air Force Base, Ohio

13. ABSTRACT - A program to design, fabricate and test a model of an oxygen concentrator employing a method of control termed "self regulation" was successfully conducted. The stack assembly consists of three cells, where the oxygen is electrochemically separated from the air, sandwiched between two humidifier chambers. The self-regulation of the unit results from the thermal equilibrium that exists between the heat generated in the electrochemical cells during the O_2 concentrating process and the evaporative cooling in the himidifiers due to the air humidification process. This mode of operation eliminates external humidifiers and associated thermal controls previously used on apparatus of this type. As a laboratory model, the three-cell unit demonstrated oxygen delivery rates up to 0.045 lb/hr while displaying oxygen purities at a level of 100%. Wide-range parametric testing conducted on the unit covered cell operating temperatures of 100-175F, air inlet pressures from 5-90 psia, air flow rates from 2-5 times theoretical, and current densities up to 166 amps/ft^2. The testing program was culminated with 200 hours of testing which successfully demonstrated the self-regulating characteristics of the unit. As a final conclusion, the data and analyses are used to specify an advanced 0.2-lb/hr oxygen concentrator utilizing self-regulation in addition to size optimization. With additional development the design will be capable of being incorporated into an aviator's oxygen supply system.

This abstract is subject to special export controls and each transmittal to foreign governments or foreign nationals may be made only with prior approval of the Air Force Flight Dynamics Laboratory (FDFE), Wright-Patterson Air Force Base, Ohio 45433.

DD FORM 1 JAN 64 1473

UNCLASSIFIED
Security Classification

14 KEY WORDS	LINK A		LINK B		LINK C	
	ROLE	WT	ROLE	WT	ROLE	WT
Electrochemistry Electrochemical Cells Oxygen generation, Oxygen concentration Oxygen supply systems Aviator's oxygen						

INSTRUCTIONS

1. ORIGINATING ACTIVITY: Enter the name and address of the contractor, subcontractor, grantee, Department of Defense activity or other organization *(corporate author)* issuing the report.

2a. REPORT SECURITY CLASSIFICATION: Enter the overall security classification of the report. Indicate whether "Restricted Data" is included. Marking is to be in accordance with appropriate security regulations.

2b. GROUP: Automatic downgrading is specified in DoD Directive 5200.10 and Armed Forces Industrial Manual. Enter the group number. Also, when applicable, show that optional markings have been used for Group 3 and Group 4 as authorized.

3. REPORT TITLE: Enter the complete report title in all capital letters. Titles in all cases should be unclassified. If a meaningful title cannot be selected without classification, show title classification in all capitals in parenthesis immediately following the title.

4. DESCRIPTIVE NOTES: If appropriate, enter the type of report, e.g., interim, progress, summary, annual, or final. Give the inclusive dates when a specific reporting period is covered.

5. AUTHOR(S): Enter the name(s) of author(s) as shown on or in the report. Enter last name, first name, middle initial. If military, show rank and branch of service. The name of the principal author is an absolute minimum requirement.

6. REPORT DATE: Enter the date of the report as day, month, year; or month, year. If more than one date appears on the report, use date of publication.

7a. TOTAL NUMBER OF PAGES: The total page count should follow normal pagination procedures, i.e., enter the number of pages containing information.

7b. NUMBER OF REFERENCES: Enter the total number of references cited in the report.

8a. CONTRACT OR GRANT NUMBER: If appropriate, enter the applicable number of the contract or grant under which the report was written.

8b, 8c, & 8d. PROJECT NUMBER: Enter the appropriate military department identification, such as project number, subproject number, system numbers, task number, etc.

9a. ORIGINATOR'S REPORT NUMBER(S): Enter the official report number by which the document will be identified and controlled by the originating activity. This number must be unique to this report.

9b. OTHER REPORT NUMBER(S): If the report has been assigned any other report numbers *(either by the originator or by the sponsor)*, also enter this number(s).

10. AVAILABILITY/LIMITATION NOTICES: Enter any limitations on further dissemination of the report, other than those imposed by security classification, using standard statements such as:

(1) "Qualified requesters may obtain copies of this report from DDC."

(2) "Foreign announcement and dissemination of this report by DDC is not authorized."

(3) "U. S. Government agencies may obtain copies of this report directly from DDC. Other qualified DDC users shall request through

_____."

(4) "U. S. military agencies may obtain copies of this report directly from DDC. Other qualified users shall request through

_____."

(5) "All distribution of this report is controlled. Qualified DDC users shall request through

_____."

If the report has been furnished to the Office of Technical Services, Department of Commerce, for sale to the public, indicate this fact and enter the price, if known.

11. SUPPLEMENTARY NOTES: Use for additional explanatory notes.

12. SPONSORING MILITARY ACTIVITY: Enter the name of the departmental project office or laboratory sponsoring *(paying for)* the research and development. Include address.

13. ABSTRACT: Enter an abstract giving a brief and factual summary of the document indicative of the report, even though it may also appear elsewhere in the body of the technical report. If additional space is required, a continuation sheet shall be attached.

It is highly desirable that the abstract of classified reports be unclassified. Each paragraph of the abstract shall end with an indication of the military security classification of the information in the paragraph, represented as *(TS)*, *(S)*, *(C)*, or *(U)*.

There is no limitation on the length of the abstract. However, the suggested length is from 150 to 225 words.

14. KEY WORDS: Key words are technically meaningful terms or short phrases that characterize a report and may be used as index entries for cataloging the report. Key words must be selected so that no security classification is required. Identifiers, such as equipment model designation, trade name, military project code name, geographic location, may be used as key words but will be followed by an indication of technical context. The assignment of links, rules, and weights is optional.